UNIVERSITÀ DI PISA

Scuola di Dottorato in Ingegneria "Leonardo da Vinci"

Corso di Dottorato di Ricerca in
INGEGNERIA NUCLEARE

Tesi di Dottorato di Ricerca

METHODOLOGY FOR THE ANALYSIS OF FUEL BEHAVIOR DURING LOCA AND RIA

Autore:

Martina Adorni _____

Relatori:

Prof. Francesco D'Auria _____

Prof. Francesco Oriolo _____

Dr. Carlo Vitanza _____

Dr. Alessandro Del Nevo _____

Anno 2011

(This page has been intentionally left blank)

Alla mia famiglia, animali compresi, e ad Alessio

Courtesy of C. Lopresti, A.R: 06h 31m 54s - DEC +04° 57' 00"

AKNOWLEDGMENTS

At first, I express my gratitude to *Prof. Francesco D'Auria* (UNIPI-GRNSPG), for the invaluable possibility he gave me to learn.

Special thanks are for *Dr. Carlo Vitanza* (HRP) for his invaluable contribution in the advancement in experiments and modeling in the field of nuclear fuel and his expert supervision.

I express also special thanks to my supervisors *Prof. Francesco Oriolo* (UNIP) and *Alessandro Del Nevo* (ENEA) for the support in carrying out this work.

I wish to express thanks to *Enrico Sartori* (OECD), for his effort in creating, maintaining and making available the OECD/NEA/NSC International Fuel Performance Experiments database and to *John Kjillen* (IAEA) for the FUMEX-III Coordinate Research Project containing a challenging selection of experiments to test the codes.

I wish to express gratitude also to *Wolfgang Wiesenak* (HRP), for the much valuable information for the design of the fuel experiment.

I gratefully acknowledge the support of the fuel modeling team at ITU and the possibility they gave to the me to be part of the TRANSURANUS User Group: *Paul Van Uffeln, Arndt Shcubert, Juacques Van Der Laar and Csaba Gyory* (ITU) and to *Prof. Lelio Luzzi* (POLIMI), for the initial help in entering in the fuel field.

I'd like to acknowledge as well *Oscar Mazzantini* (NA-SA), for the invaluable possibility of learning from a real nuclear power plant under construction, and for the fantastic period that I spent in Argentina working at the power plant.

Patricia Pla Freixa (EC) and *Anis Bousbia-Salah* (BelV) should be acknowledged as well, for the always helpful discussions and much valuable availability and updating.

I'd like to thank also all the person that at various title contributed to my scientific and professional advancement, among with, but not limited at (alphabetic order): *Dino Araneo* (UNIPI-GRNSPG), *Claudio Carbone* (ENEL), *Juan Calos Ferreri* (ARN), *Giorgio Galassi* (Reg. Toscana), *Massimo Sepielli* (ENEA).

Last but not least, huge thanks go to all the people of the GRNSPG!!!

SOMMARIO

Gli incidenti di perdita di refrigerante (LOCA) riguardano la perdita di liquido di raffreddamento del reattore ad un tasso superiore alla capacità del sistema di reintegro, dovuti ad una rottura nel confine in pressione del liquido stesso, fino ad includere una rottura equivalente per dimensioni alla rottura della più grande tubazione del sistema di refrigerazione del reattore con area equivalente pari a due volte quella della tubazione.

Una particolarità del progetto dell'impianto Atucha-II è il coefficiente di reattività per i vuoti positivo. Questa è una caratteristica in comune con altri reattori moderati ad acqua pesante che utilizzano uranio naturale come combustibile. Ciò implica che a seguito di un evento di perdita di refrigerante, il picco di potenza di fissione all'inizio del transitorio è controllato dalla formazione vuoto nei canali del nocciolo, e quindi è determinato dalla propagazione delle onde di pressione dalla rottura. Infatti, il moderatore è ancora liquido ed evapora in ritardo rispetto al liquido refrigerante, così l'evento di perdita di refrigerante (LOCA) è anche un evento di inserzione di reattività (RIA).

A seconda dello specifico scenario e dello scopo delle analisi, potrebbe essere richiesta la disponibilità di metodi di calcolo che non sono implementati nei codici standard di analisi di sistema termoidraulica, come per esempio la temperatura di rottura, la deformazione alla rottura e il possibile bloccaggio della refrigerazione canale. Ciò può richiedere l'uso di un apposito codice per il calcolo del comportamento e delle performance del combustibile nucleare quale il TRANSURANUS.

Questa tesi riporta la descrizione dello sviluppo della metodologia utilizzata per l'analisi dello scenario 2A LB-LOCA per l'impianto nucleare Atucha-2, concentrandosi sulla procedura adottata per l'utilizzo del codice di analisi del combustibile e la sua applicazione per l'analisi della sicurezza dell'impianto stesso (Capitolo 15 FSAR). La procedura comporta l'applicazione della metodologia "best estimate" per la termoidraulica, la neutronica e le analisi del combustibile, con l'obiettivo di verificare la conformità con i criteri di accettazione specifici. Il codice utilizzato per valutare le prestazioni ed il comportamento del combustibile, viene applicato con l'obiettivo primario di valutare l'entità delle rotture della camicia del combustibile durante il transitorio.

La procedura consiste in un calcolo deterministico, tramite il codice di analisi del combustibile, effettuato per ogni singola barretta, della vita della barretta stessa e il calcolo seguente relativo all'incidente di perdita di refrigerante. Le condizioni al bordo ed iniziali (BIC) (ad esempio la potenza lineare) sono forniti dalla fisica del nocciolo e dalla cinetica neutronica tri-dimensionale accoppiata alla termoidraulica di sistema. La procedura si completa con i calcoli sensibilità e l'applicazione del metodo probabilistico.

ABSTRACT

Loss of coolant accidents (LOCA) mean those postulated accidents that result from the loss of reactor coolant at a rate in excess of the capability of the reactor coolant makeup system from breaks in the reactor coolant pressure boundary, up to and including a break equivalent in size to the double-ended rupture of the largest pipe of the reactor coolant system (DEGB LB-LOCA).

A peculiarity of the Atucha-2 design is the positive void reactivity coefficient. This is a characteristic in common to other heavy water moderated reactors that utilize natural uranium as fuel. This implies that after a LB-LOCA event, the fission power peak at the very beginning of the transient is controlled by the void formation in the core channels, and then it is determined by the pressure wave propagation from the break. Indeed, the moderator is still liquid and flashes delayed with respect to the coolant, thus the LOCA event is also a RIA (reactivity insertion accident) event.

Licensing requirements vary by country in terms of their scope, range of applicability and numerical values and in general imply the use of complex system thermal hydraulic computer.

Depending on the specific event scenario and on the purpose of the analysis, it might be required the availability of calculation methods that are not implemented in the standard system thermal hydraulic codes, as for burst temperature, burst strain and flow blockage calculations. This may imply the use of a dedicated fuel rod thermo-mechanical computer code such as TRANSURANUS, which can be coupled with thermal-hydraulic system codes to be used for the safety analysis.

This thesis consists in the development and application of a methodology for the analysis of the 2A LB-LOCA scenario in Atucha-2 nuclear power plant (NPP), focusing on the procedure adopted for the use of the fuel rod thermo-mechanical code and its application for the safety analysis of Atucha-II NPP (Chapter 15 FSAR). The methodology implies the application of best estimate thermal-hydraulic, neutron physics and fuel pin performance computer codes, with the objective to verify the compliance with the specific acceptance criteria. The fuel pin performance code is applied with the main objective to evaluate the extent of cladding failures during the transient.

The procedure consists of a deterministic calculation by the fuel performance code of each individual fuel rod during its lifetime and in the subsequent LB-LOCA transient calculations. The boundary and initial conditions (BIC) (e.g. pin power axial profiles) are provided by core physics and three dimensional neutron kinetic coupled thermal-hydraulic system codes calculations. The procedure is completed by the sensitivity calculations and the application of the probabilistic method.

Validation activities are performed to enhance the TRANSURANUS code capabilities and to improve the reliability of the code results. They relies on the two main sources of data, namely, specific data on Atucha-1 and/or 2, experiments or independent calculations and other data which are representative of the Atucha-2

fuel, in particular for the analysis of the normal operation and power ramp during normal operation and severe transients like LOCA and RIA.

INDEX

ABBREVIATIONS

ACC	Accumulator
AM	Accident Management
ARN	Autoridad Regulatoria Nuclear
BDBA	Beyond Design Basis Accident
BEPU	Best Estimate Plus Uncertainty
BEQ	Burnup Equilibrium
BIC	Boundary and Initial Conditions
BOT	Break Opening Time
BWR	Boiling Water Reactor
CAL	Calculation
CFD	Computational Fluid Dynamics
CFR	Code of Federal Regulation (US)
CHF	Critical Heat Flux
CIAU	Code with capability of Internal Assessment of Uncertainty
CL	Cold Leg
CNA	Central Nuclear Atucha (CNA-2 or CNA-II is Atucha-2 or Atucha-II)
CR	Control Rod
CSAU	Code, Scaling Applicability and Uncertainty
CSNI	Committee on the Safety of Nuclear Installations
DBA	Design Basis Accident
DC	Down-comer
DEGB	Double Ended Guillotine Break
DIMNP	Dipartimento di Ingegneria Meccanica Nucleare e della Produzione
DOE	Department of Energy (US)
EC	European Commission
ECC	Emergency Core Cooling
ECR	Equivalent Cladding Reacted
ENACE	Empresa Nuclear Argentina de Centrales Electricas
EPM	Emergency Power Mode
EXP	Experiment
FDM	Finite Difference Method
FC	Fuel Channel
FPP	Fission Power Peak
FSAR	Final Safety Analysis Report
FW	Feed-water
GRNSPG	San Piero a Grado Nuclear Research Group (of DIMNP)
HL	Hot Leg
HWR	Heavy Water Reactor
IAEA	International Atomic Energy Agency
IFPE	International Fuel Performance Experiments
INEEL	Idaho National Engineering and Environment Laboratory (now INL)
JRC	Joint Research Centre
KWU	Kraftwerk Union AG
LB-LOCA	Large Break LOCA
LHGR	Linear Heat Generation Rate
LHR	Linear Heat Rate

LOCA	Loss Of Coolant Accident
LP	Lower Plenum
LPIS	Low Pressure Injection System
LWR	Light Water Reactor
MCP	Main Coolant Pumps
M-	Matlab
MT	Moderator Tank
MT-	Material Test
NA-SA	Nucleoélectrica Argentina S.A.
NDE	Non Destructive Examination
NEA	Nuclear Energy Agency
NEM	Nodal Expansion Method
NF	Non-Failed
NK	Neutron Kinetic
NPP	Nuclear Power Plant
NRC	Nuclear Regulatory Commission
NRU	National Research Universal
NSC	Nuclear Science Committee
OECD	Organization for Economic Cooperation and Development
Ph.W	Phenomenological Window
PCI	Pellet-Clad l Interaction
PCT	Peak Cladding Temperature
PHWR	Pressurized Heavy Water Reactor
PIE	Post Irradiation Examination
PRZ	Pressurizer
PS	Primary System
PWR	Pressurized Water Reactor
RBMK	Reactor Bolshoy Moshchnosty Kipyashiy
RG	Regulatory Guide
RIA	Reactivity Initiated Accident
RPV	Reactor Pressure Vessel
S	Statistic calculation
SBDBA	Selected Beyond Design Basis Accident
SCC	Stress Corrosion Cracking
SG	Steam Generator
SIP	Safety Injection Pump
SoT	Start of Transient
SYS TH	System Thermal-Hydraulics
T	Temperature
TH	Thermal-hydraulics
TMI	Three Mile Island
TU	TRANSURANUS
TPCF	Two-Phase Critical Flow Model
UNIPI	University of Pisa
U	Uranium
UO2	Uranium Oxide
UP	Upper Plenum
U.S. NRC	United Stated Nuclear Regulatory Commission
VVER	Water Cooled Water Moderated Energy Reactor

XSEC	Macroscopic Cross Sections
3D NK-TH	Three-Dimensional Neutron Kinetics Thermal-Hydraulics

LIST OF FIGURES

LIST OF TABLES

1. INTRODUCTION

Loss of coolant accidents (LOCA) mean those postulated accidents that result from the loss of reactor coolant at a rate in excess of the capability of the reactor coolant makeup system from breaks in the reactor coolant pressure boundary, up to and including a break equivalent in size to the double-ended rupture of the largest pipe of the reactor coolant system (DEGB LB-LOCA).

A peculiarity of the Atucha-2 design is the positive void reactivity coefficient. This is a characteristic in common to other heavy water moderated reactors that utilize natural uranium as fuel. This implies that after a LB-LOCA event, the fission power peak at the very beginning of the transient is controlled by the void formation in the core channels, and then it is determined by the pressure wave propagation from the break. Indeed, the moderator is still liquid and flashes delayed with respect to the coolant, thus the LOCA event is also a RIA (reactivity insertion accident) event.

Licensing requirements vary by country in terms of their scope, range of applicability and numerical values and in general imply the use of complex system thermal hydraulic computer.

Depending on the specific event scenario and on the purpose of the analysis, it might be required the availability of calculation methods that are not implemented in the standard system thermal hydraulic codes, as for burst temperature, burst strain and flow blockage calculations. This may imply the use of a dedicated fuel rod thermo-mechanical computer code such as TRANSURANUS.

1.1 Objectives of the research

The fuel rod constitutes the first barrier against the release of fission products. The accurate description of the fuel rod's performance is an interdisciplinary field. The fuel rod is operated under varying conditions, and it changes the physical and thermodynamic properties during irradiation, e.g. see Fig. 1. The capability of predicting its behavior and life-time, for a wide range of normal, off-normal and accident conditions (including limiting conditions, such as LOCA and RIA) constitutes an achievement in ensuring the safe and economic operation of nuclear power plants. The prediction of the fuel performance in safety analysis requires the use of "*ad hoc*" codes, well defined boundary and initial conditions (connections with thermal hydraulics, three dimensional neutron kinetics, and depletion codes) as well as appropriated and validated models, belonging to different physics' fields.

Investigations of fuel behavior are carried out in close connection with experimental research, operation feedback and computational analyses. In the last decades, a considerable world wide effort has been expended in experimental and numerical modeling of fuel rods behavior in accident conditions, which has led to a broader and deeper understanding of LOCA and RIA related phenomena. In this regard, a complementary, but not less important, activity is the validation of the fuel pin mechanics codes (i.e. TRANSURANUS) against experimental data available, to demonstrate the reliability of their predictions.

The aim of the current PhD program is the development and the application of a methodology for the analysis of the fuel behavior during accident conditions, such as LOCA and RIA in nuclear power plants and the demonstration of the reliability of their prediction , Fig. 2. TRANSURANUS is the fuel performance code, selected for the research activity. The methodology implies the application of best estimate thermal-hydraulic, neutron physics and fuel pin performance computer codes, with the objective to verify the compliance with the specific acceptance criteria. The fuel pin performance code is applied with the main objective to evaluate the extent of cladding failures during the transient.

The procedure consists of a deterministic calculation by the fuel performance code of each individual fuel rod during its lifetime and in the subsequent LB-LOCA transient calculations. The boundary and initial conditions (BIC) (e.g. pin power axial profiles) are provided by core physics and three dimensional neutron kinetic coupled thermal-hydraulic system codes calculations. The procedure is completed by the sensitivity calculations and the application of the probabilistic method.

Validation activities are performed to enhance the TRANSURANUS code capabilities and to improve the reliability of the code results. Verification relies on the two main sources of data, namely, specific data on Atucha-1 and/or 2, experiments or independent calculations and other data which are representative of the Atucha-2 fuel, in particular for the analysis of the normal operation and power ramp during normal operation and severe transients like LOCA and RIA.

1.2 Description of the preformed activity

The activity performed for fulfilling the objectives of the research is outlined in Fig. 2. The steps below are executed to fulfill the objectives:

- acquisition of expertise in the nuclear fuel field, taking advantage from the participation in international activities;
- investigation of issues related to the use of the fuel pin mechanics codes;
- development of a methodology/procedure for predicting the fuel performance in safety analysis (including the connection with the FSAR) by means of fuel pin mechanics code;
- application of the methodology/procedure in case of combined LOCA and RIA transient (selected BDBA in the Chapter 15 of the FSAR of Atucha-2 NPP) for evaluating the number of failed rods and the release of the fission products;
- validation activities to support the reliability of the analyses.
- completion of the activity considering the environmental release.

Finally, the Candidate is also taking part in international activities related to the PhD program.

- Membership to the OECD-NEA “Working Group on Fuel Safety” (WGFS) with the mission to advance the current understanding and address safety issues related to fuel safety.
- Participation to the IAEA Coordinated Research Project on Fuel Modeling at Extended Burnup (CRP FUMEX-III) “Improvement of Computer Codes

used for Fuel Behavior Simulation" (2008-2012), in cooperation to the code developers.
- Participation to ATUCHA-2 Project, commissioned by the Argentinean NA-SA, for the analyses of the fuel behavior in the framework of the preparation of the FSAR (Chapters 4 and 15).
- Participation to the EC Project "Support to VATESI in Assessment Safety of Ignalina NPP" in cooperation with the "Lithuanian Energy Institute" (LEI): tasks related to fuel.
- Participation to the OECD Sandia Fuel Project "Thermal-Hydraulic and Ignition Phenomena Characterization of Prototypic Pressurized Water Reactor Assemblies".

1.3 Structure of the document

The thesis is divided in eight sections and six appendixes.

The Introduction contains the background information and the objective of the activity.

Section 2 describes the Atucha-II NPP, highlighting the peculiarities of the plant with focus on the fuel and refueling strategy.

Section 3 reports the peculiarities of the LB-LOCA: i.e. combined LOCA and RIA. From this section it results clear that there is the need for the analysis of the availability of calculation methods that are not implemented in the standard system thermal hydraulic codes. In the same section, an outline of the specificity of the licensing is reported. Due to the peculiarities of the plant, even setup licensing criteria for normal operation and transient had been challenging (reference to the need of creation of a special category for the LB-LOCA).

Section 4 contains the description of the codes and models, with emphasis given to the interfaces between the different codes. The work of the thesis needed an effort in reviewing the work performed in the framework of the licensing of Atucha-II. The detailed motivation of the selection of the model used for the analysis is highlighted as well.

A strong effort had been performed in order to enhance the TRANSURANUS code capabilities and to improve the reliability of the code results. Section 5 is focused on the applicability of the TRANSURANUS code and of the methodology to CNA-2, and does not want to be related to the general applicability of TRANSURANUS code, whether it results useful for the application of the code itself.

Section 6 contains the description of the developed methodology for the application of the fuel performance code to the safety analysis of Atucha-II NPP.

Finally, the results of the application of the developed methodology are reported in Section 7.

Conclusions are drawn in Section 8, focusing on innovations together with hints for future developments.

1.4 Innovations

The application of the methodology helps to assess the number of the fuel element that can fail in case of the selected accident, identification of the failed fuel rods for the subsequent evaluation of the radiological release. Analysis were performed to support the study of normal operation for the simulation of irradiation fuel rods during normal operation as it defines the status of fuel at the beginning of transient; In addition to this, the activities performed to support the reliability of the code results and constitute an enlargement of the TU validation domain (an example of non standard application is analyzed as well).

Within the overall objective of the research, the following relevant results may be highlighted:

1. Application of the methodology developed, to the FSAR Chapter 15 of Atucha NPP in construction in Argentina.
2. Demonstration that the application of the proposed methodology allows evaluating the performance of the fuel and to the required level of safety (including the review and selection of these criteria, for normal operation (design review) and for the selected accident conditions (LOCA and RIA combined)).
3. Identification and extension of the "validation domain" of the TRANSURANUS code. to enhance the code capabilities and to improve the reliability of the code results.
4. Feasibility study of an experiment to be conducted in a research reactor, including the preparation of the technical specifications and cost analysis, extremely challenging from the scientific point of view.

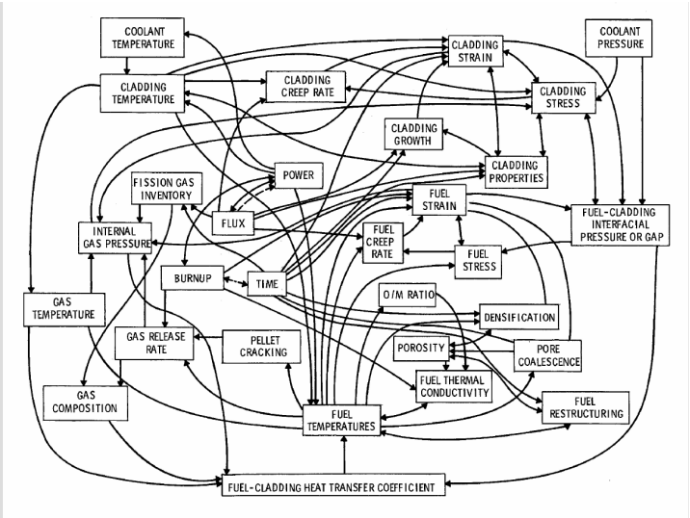

Fig. 1 – Parameters influencing the gap conductance according to G.R. Horn, quoted by Beyer et al. (Horn 1973).

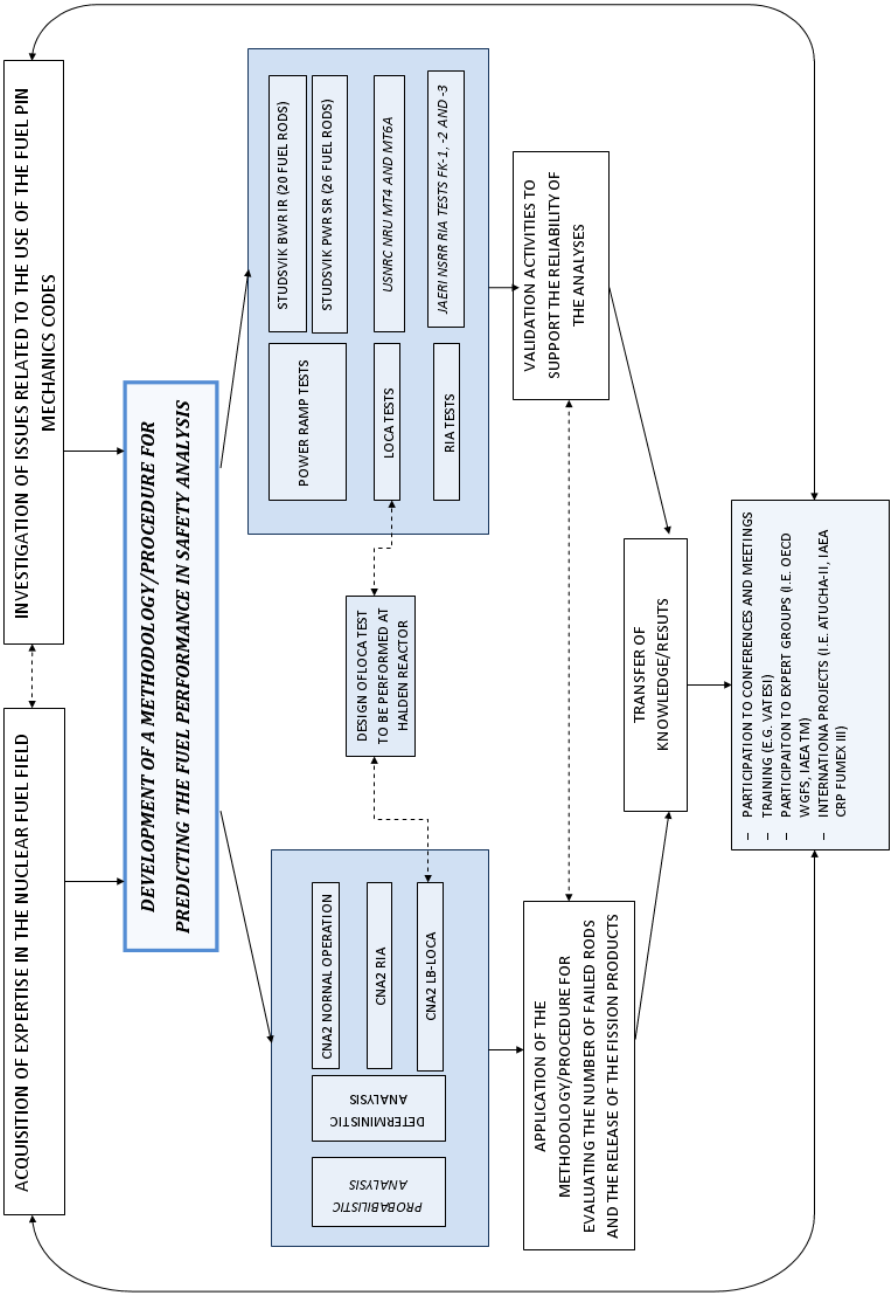

Fig. 2 – Scheme of the activity.

2. ATUCHA-II NPP

2.1 Layout

Atucha II (CNA-2) NPP is a 745 MW(e) reactor constructed by ENACE S.A., Nuclear Argentine Company for Electrical Power Generation and SIEMENS AG KWU, Erlangen, Germany. It belongs to a second generation reactor type PHWR. All the nuclear area is based on the prototype reactor MZFR 56 MW (e) which was placed in operation at the Nuclear Research Center in Karlsruhe (West Germany) in 1966. Also it was designed on the bases of Atucha I NPP with 354 MW (e) (1969). The secondary and auxiliary systems were designed in a similar way as Konvoi PWR plants, from Germany (around 1989). In Tab. 1 the main features of the nuclear island of the plant are showed. Atucha-II reactor employs heavy water (D2O) as moderator and as coolant. Nevertheless moderator and coolant are kept separated, so that the Reactor Coolant System does not handle the large amount of moderator necessary in this kind of reactor, owing to the relatively low moderating power ($\xi\Sigma s$) of D2O. Moreover, maintaining coolant and moderator separated allows keeping them at different temperatures (*Mayers 1985*). In Tab. 2 the comparison of CNA-2 and other type of NPP is reported.

2.2 Primary system

2.2.1 Reactor system (JA)

The reactor system consists of the reactor pressure vessel (JAA), its internals and the control shutdown equipment. Its function is to generate thermal power. In Fig. 3, a schematic view of the RPV is given, the figure shows also coolant and moderator inlet / outlet points and inlet points designed for core safety injection. The reactor core of Atucha-II NPP is built up of 451 fuel assemblies. Each fuel assembly is placed in a shroud type tube which serves as coolant channel. The tubes are arranged in a vertical triangular lattice within the moderator tank. The lattice pitch is 27.24 cm. The fuel assemblies are bundles of 37 closely packed fuel rods, which are arranged in 3 concentric circles with 6, 12 and 18 fuel rods around a central fuel rod. This arrangement is shown in Fig. 4.

At normal moderator temperature the coolant absorbs approx. 90% of the generated power; the moderator absorbs the remaining part. Therefore it is necessary to cool down both of them: the thermal power removed by the coolant is exploited in two steam generators to produce steam destined to the turbines, whereas the remainder is transferred from the moderator to the feed-water (secondary side) in 4 “moderator coolers” upstream the inlet of the steam generators.

A thermal power of approx. 2160 MW is generated in the core, while a thermal power of 15 MW is generated inside the reactor coolant pumps. Therefore the total thermal power transferred to the secondary fluid both in the steam generators and in the moderator coolers is about 2175 MW.

CNA-2 PRIMARY SIDE	
Reactor type	**Thermal PHWR**
Generated power	**2175 [MWth]**
Control rods	**Materials/n°:** hafnium / 9 rods, steel / 9 rods
Cladding	**Material**: Zr-4
Fuel	**Type**: 451 fuel assemblies with 37 fuel rods
	Material / core position: natural UO_2 / vertical
	Equilibrium burnup at fuel discharge [MWd/tonU]: 7800
	Refueling: online with one refueling machine
Coolant data at full load	**Material**: D_2O
	RPV inlet / outlet temperatures [°C]: 277.9 (278.1)* **/** 312.5 (313.5)
	D_2O volume (without pressurizer and surgeline) [m^3]: 211
	Total core mass flow [kg/s]: 10344
	N° of loop: 2
Moderator data at full load	**Material**: D_2O
	Normal / Max average temperatures [°C]: $T_{av.normal}$=170 **/ $T_{av.max}$**=220
	RPV inlet / outlet temperatures [°C]: 141.4 (197) **/** 201 (243.3)
	D_2O volume [m^3]: 234.5
	Total core mass flow [kg/s]: 891.6 (835.6)
	N° of loop: 4
Primary side pressures	**Pressure at reactor outlet [MPa]:** 11.4
	Overall pressure loss in reactor coolant system [MPa]: 1.07
	Overall pressure loss in moderator system [MPa]: 0.65
Pressurizer	**Pressurizer pressure[MPa]:**11.35
	Pressurizer temperature [°C]:320
	Pressurizer total volume [m^3]:
Steam Generator primary side	**N°/Type**: 2 / U-tube heat exchanger
	Heat transferred by each SG at full load [MW]: 1000
	D_2O volume [m^3]: 35.3
	SG inlet / drop temperatures [°C]: 312 (313.5) **/** 34.9 (35.7)
	N° of tubes per each SG: 6524
Moderator coolers Primary side	**Inlet temperature [°C]:** 201.5
	Outlet temperature [°C]: 141.4
	Heat transfer per moderator cooler [MW]: 55.7
	Mass flow rate per Moderator Cooler [kg/s]: 220.9 (207.1)

*: Data stated in brackets refer to the average max. moderator temperature under full load conditions

Tab. 1 – CNA-2 NPP: main features.

Item	CNA-2	CNA-1	BWR	PWR	CANDU	RBMK
Fuel Assembly	**--**	--	8 x 8	17 x 17	--	18 x 2
Fuel Rod per Assembly	**37**	36	63	264	37	36
No of Assemblies	**451**	253	592	193	456	1661
Core Active Length [m]	**5.3**	5.3	3.6	3.6	6.06	6.92
Bundle Length [m]	**5.3**	5.3	3.6	3.6	0.5	3.46
Fuel Weight [kgU]	**89,400**	61,000	126,700	118,00	87,500	192,000
Maximum T Clad [°C]	**325**	324	293	335	326	325
Maximum T Centerline [°C]	**2250**	2250	2100	2260	1900	1400
Discharge Burnup [MWd/tU]	**7,500**	6,000	>25,000	>35,000	7,000	22,200
Refueling (Reactor State)	**On power**	On power	Shut down	Shut down	On power	On power
Cladding Diameter [mm]	**12.9**	11.9	12.3	9.5	13.08	13.6
Cladding Thickness [mm]	**0.57**	0.55	0.81	0.57	0.38	0.9
Fuel Pellet Diameter [mm]	**11.57**	10.62	10.4	8.19	12.15	11.50
Fuel Pellet Height [mm]	**14**	12.0	10.4	8.30	16.04	15.00
Enrichment [%]	**Natural Uranium**	Natural Uranium	~3%	~3 %	Natural Uranium	~ 2.4%
Fill Gas	**Helium**	Helium	Helium	Helium	--	Helium
Fill Gas Press. (absolute) [bar]	**22.5**	22.5	3 – 7	20-30	--	5
Fuel Material	**UO2**	UO2	UO2	UO2	UO2	UO2
Cladding Material	**Zr-4**	Zr-4	Zr-2	Zr-4	Zr-4	ZrNb

Tab. 2 – Comparison of CNA-2 and other NPP: main features.

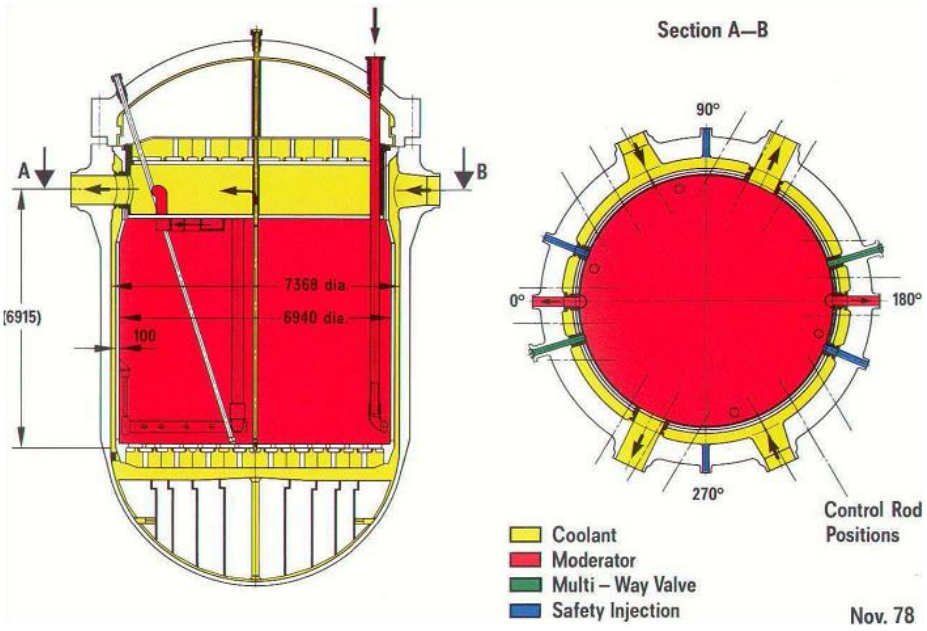

Fig. 3 – CNA-2 NPP: Reactor Pressure Vessel (RPV).

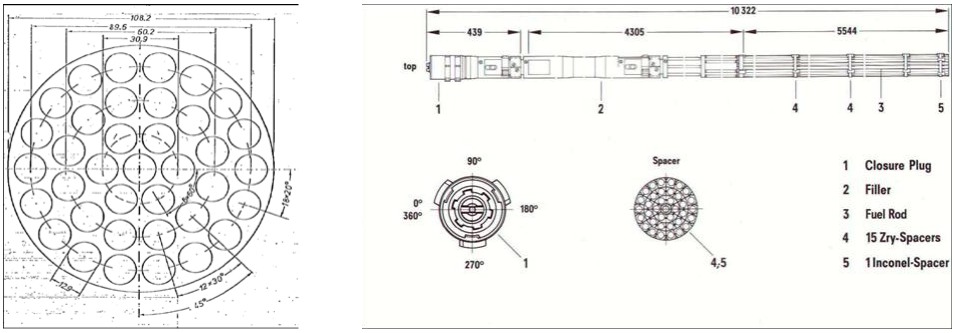

(a) Fuel assembly cross sections

(b) Views of fuel assembly

Fig. 4 – CNA-2 NPP: fuel assembly.

2.2.2 Reactor coolant system (JF)

It consists of two identical loops each comprising one steam generator, one reactor coolant pump and the interconnecting reactor coolant piping together with the pressurizing and pressurizer relief system.

Atucha-II Reactor Coolant System is very similar to the traditional primary system of a PWR with two coolant loops. For each loop, the coolant from the RPV outlet is send toward a U-tube steam generator, where it transfers its thermal energy to the secondary fluid to produce steam. Thereafter, a reactor coolant pump receives the fluid from the SG outlet, increases its pressure and pumps it toward the reactor. After entering the reactor pressure vessel, the coolant, with exception of 1%

bypassed to the RPV closure head, flows downward through the downcomer (between inner vessel wall and moderator tank outer wall), reaches the lower plenum and splits up into the 451 coolant channels (a minor part flows also in the gap between the FCs). The coolant cools down the fuel rods during its flowing upward and then it reaches the upper plenum above the moderator tank. Here the total coolant flow rate gathers again and reaches the reactor vessel outlet (Fig. 3, Fig. 5 and Fig. 6).

In order to impose coolant and moderator pressure and to damp pressure oscillations, a pressurizer is connected to one of the two coolant loops by mean of the surge line that connects hot leg to the pressurizer.

In Fig. 6, the pressurizer relief system (JEG) and pressurizer spray line (JEF) are also shown: JEG consists in essence of the pressurizer valves and the relief tank it and is connected to the pressurizing system by the safety valves flanged on to the relief tank dome. JEF connects the two cold lines (after MCP) to the pressurizer sprays. The pressurizer relief system serves to condense and remove the steam blown down via the pressurizer safety valves while the spray system serves to condense steam and to reduce primary pressure by mean of cold water, each spray line split into two lines connected to the pressurizer dome.

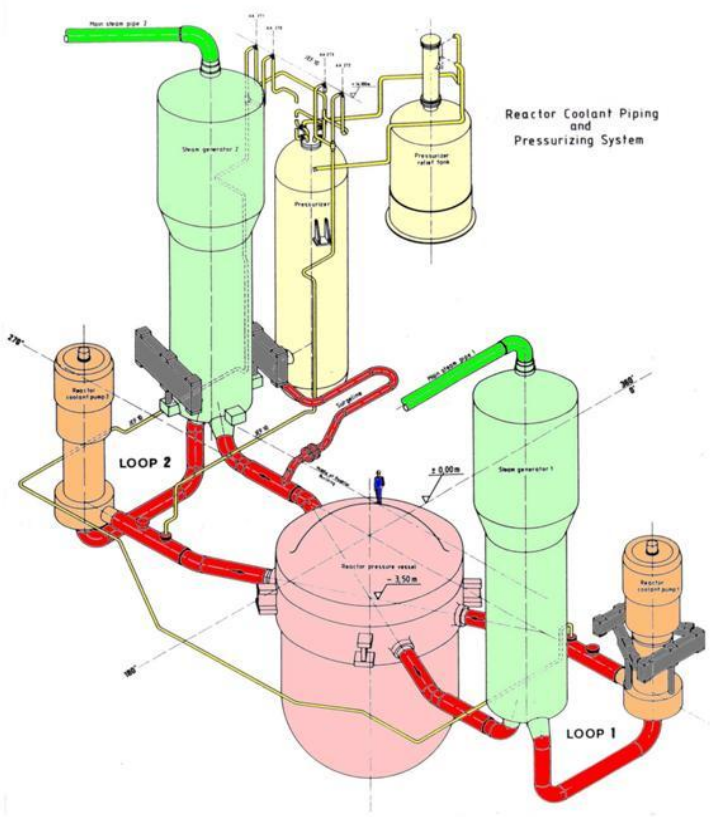

Fig. 5 – CNA-2 NPP: reactor coolant piping and pressurizing systems.

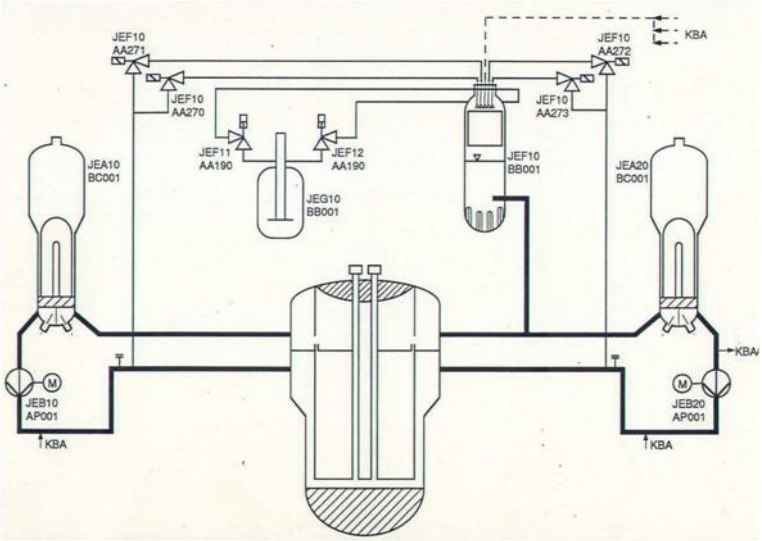

Fig. 6 – CNA-2 NPP: Reactor coolant system logical layout.

2.2.3 Reactor moderator system

The particular aspect of Atucha-II is the Moderator System. This system (Fig. 7) consists of four identical loops each comprising one moderator cooler, one moderator pump, the interconnecting piping and the valves necessary for isolation and changeover. Considering one of the 4 loops, the moderator from the RPV outlet is send toward an horizontal countercurrent U-tube heat exchanger, the so-called “moderator cooler”, where it transfers its thermal energy to the main feedwater, in order to preheat this before entering the steam generator. The moderator at the outlet of the moderator cooler is then pumped toward the reactor pressure vessel by means of a “moderator pump”. The moderator enters into the reactor pressure vessel by means of 4 vertical tubes, which penetrate into the vessel closure head and reach the bottom of the moderator tank. At the end of the 4 tubes, a ring header receives the moderator and distributes it to the tank. The moderator is then collected in the upper part of the tank and flows out of the vessel by means of 2 outlet tubes at the same level of the coolant nozzles. Out of the vessel, the moderator flow rate from these 2 tubes is split up to the 4 moderator loops. By this way there is no direct contact between moderator and coolant in the “active region”.

Although the moderator is maintained at a lower temperature than the coolant, they are maintained at the same pressure of nearly 11.5 MPa during normal operations. This task is achieved with the pressurizer so coolant and moderator are not completely separate, since a small and controlled mass exchange takes place in special equalization ports inside the reactor pressure vessel but far from the active part (in the moderator tank closure head).

In addition to maintaining the average moderator temperature during power operation irrespective of the coolant temperature, the moderator has the following tasks:

- Removal of residual heat from the shutdown reactor and of the heat stored in the primary system during cooldown and when the plant is in the cold condition.
- Use of the moderator loops for emergency core cooling (ECC) and residual heat removal (RHR) by cooling and injection of moderator into the coolant, and cooling of the water injected by the safety injection pumps from the containment sump.

2.2.4 Steam generators and main pumps

The two steam generators are natural circulation, U-tubes bundle heat exchangers. The reactor coolant enters the hot leg U-tubes to transfer the power it has absorbed to the secondary side. After releasing his heat, the reactor coolant passes through the cold out-let plenum to the cold leg reactor coolant line.

The feedwater (secondary side) is preheated in the moderator coolers, and then enters the SG by mean of a nozzle located in the steam plenum. A ring header below the nozzle distributes the feedwater in the down comer where it is mixed with the water separated out in the SG cyclones and driers. In the riser it evaporates on the U-tubes and leaves the SG via the cyclones and driers as saturated steam (dryness: 99.75%).

2.2.5 Residual Heat Removal (KAG) and Safety injection system (JND)

The most important conditions of the plant are three: normal operation depicted in Fig. 8, residual heat removal configuration (Fig. 9), emergency core cooling configuration (Fig. 10). The tasks involved in JND and RHR are performed by changing over the moderator system to the RHR configuration: the isolating gate valves in the RHR suction lines are opened and the normal configuration valves are closed.

In RHR configuration (Fig. 9) the moderator system is of four-train redundancy, as required. The RHR injection lines by mean of the bypass valves inject can inject: in hot and cold leg (circuits 1 and 4), in upper and lower plenum of RPV (circuits 2 and 3 respectively). Two out of the four loops are capable of removing the power generated.

The safety injection system (or ECC system) serves to mitigate consequences of loss of coolant accidents. It is subdivided in two subsystems each of four redundant train configuration (Fig. 10):

- Accumulator injection system consists of pneumatic accumulators (20 m3, 6.6 MPa) and water (H2O) tanks (60 m3). The system is connected to the RHR injection lines by means of rupture discs which open at a differential pressure of more than 0.5 MPa. It is required for core reflooding in the event of large and medium breaks.
- The sump injection system is connected to the moderator coolers by mean of rupture discs that open at differential pressure of over 1 MPa. It is capable of injecting at 7.8 MPa. The system is constituted by H2O flooding tanks (70 m3). It serves core reflooding and for long term emergency RHR system.

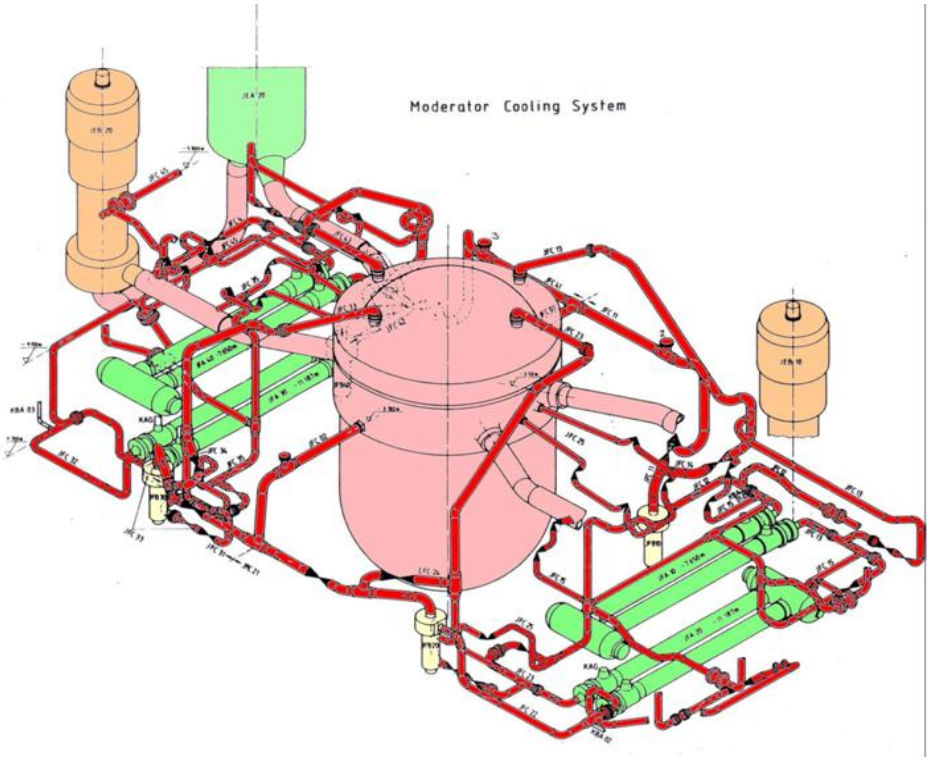

Fig. 7 – CNA-2 NPP: moderator system layout.

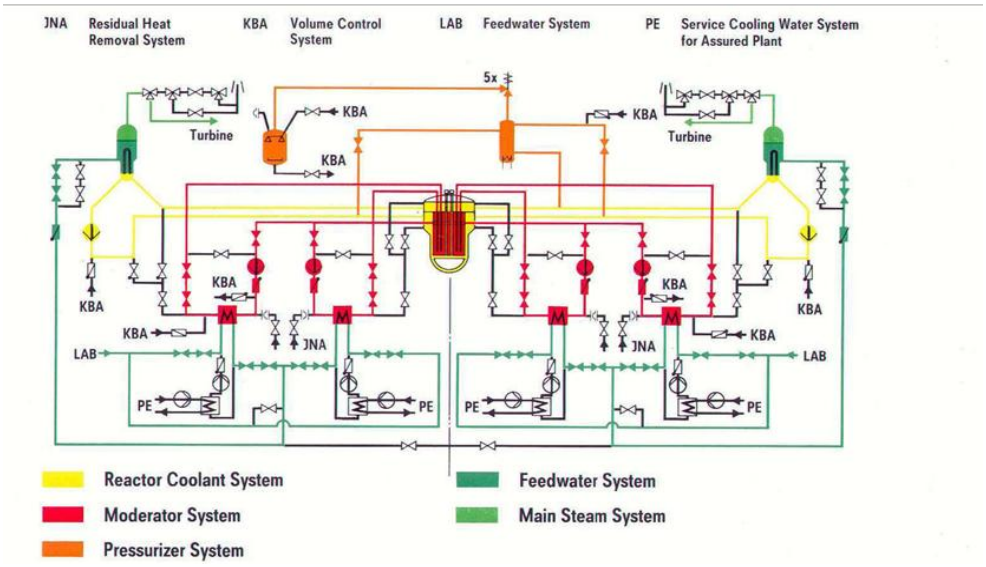

Fig. 8 – CNA-2 NPP primary system in normal operation.

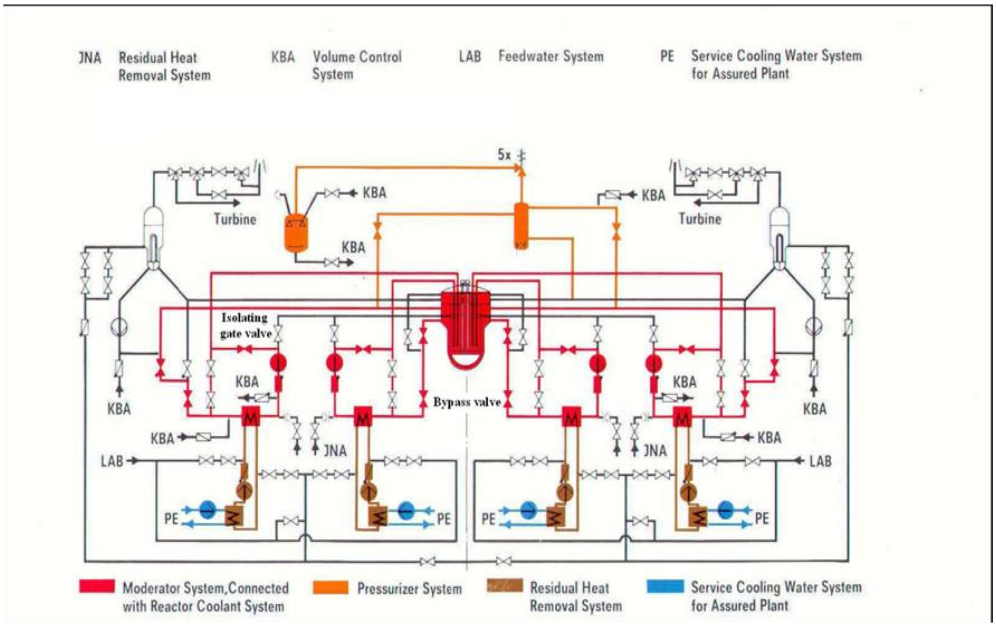

Fig. 9 – CNA-2 NPP: primary system in RHR configuration.

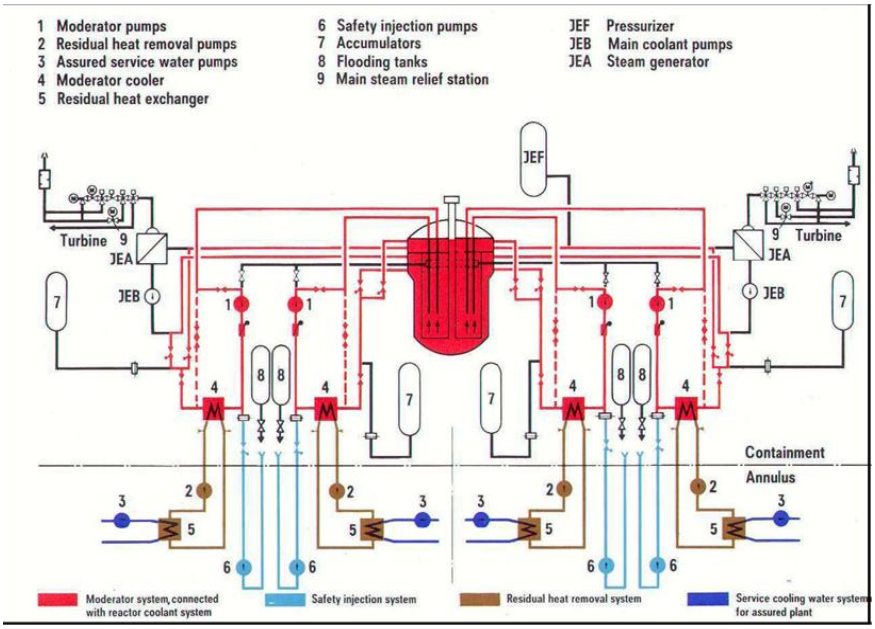

Fig. 10 – CNA-2 NPP: ECC configuration.

2.2.6 Boron injection system (JDJ)

The Fast Boron Injection system is the back shutdown system. It is based on four injection lances which penetrate the RPV and reach the moderator tank interior, and through which a highly borated solution is injected, driven by pressurized air upstream of the tanks containing the boron solution. Each line contains:

A: Pressurized air tank; B: 2 boron tanks; C: Injection lance; D: Valve on piping between A and B; E: Rupture device on piping between B and C.

In detail the primary system places the following requirements on this system:

- Shutdown and maintenance of subcriticality of the reactor on loss of CR function. Should a given number of CR not reached their end position three seconds after reactor shutdown signal, boron injection is started by the reactor protection system.
- This function is actuated when limits such as primary pressure too high or reactor power too high are reached. The JDJ has been designed with the strict regard to safety aspect.
- Shutdown and maintenance of sub-criticality of the reactor in the event of a LOCA. (Boric acid is injected immediately into the moderator system).
- Maintenance of reactor sub-criticality by slow metered boric acid injection by the JDJ via throttling valves after Xenon reduction and unavailability of the control volume system (the KBA system in the German documentation).

Two out of four trains must be available to satisfy the requirements.

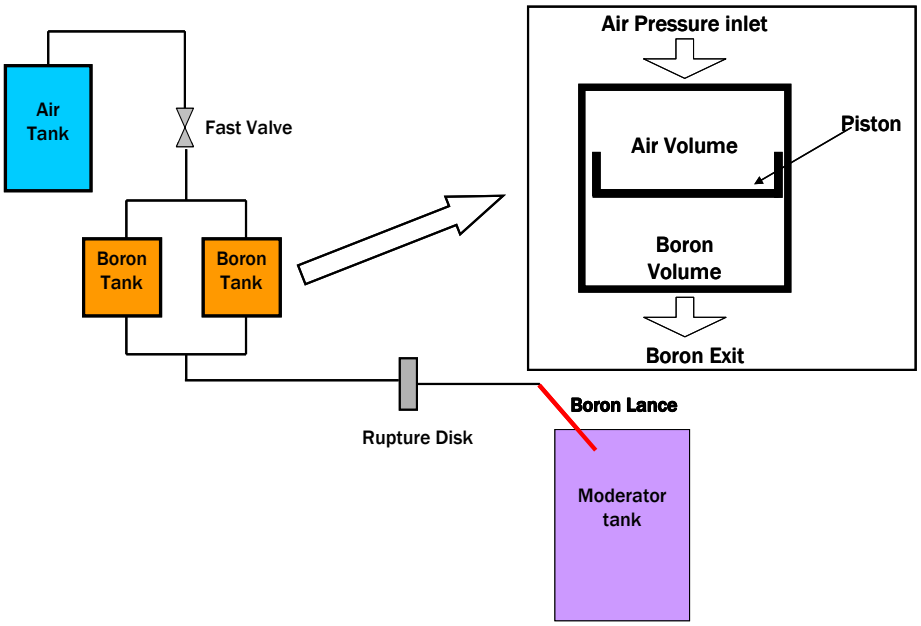

Fig. 11 – CNA-2 NPP: layout of one line of the fast boron injection system.

2.2.7 Pressurizing spray systems

Pressurizer spray systems are constituted by the pressurizer normal spray system and the auxiliary sprays. The normal sprays comprise the main spray lines that consist of two lines each splitting in two spray lines that connect each cold leg after cooling pumps to the sprays boxes. The connection is achieved by mean of four valves that are closed in normal operation and open when the pressures in the primary side increase.

The auxiliary spray of the volume control system connects via a separate spray line and separate spray box to the pressurizer. They serve to reduce the system pressure in case of loss of normal sprays function. This system differently from the previous can acts also if cooling pumps are not available.

2.2.8 Volume control system (KBA)

It is split in three subsystems capable to fulfilling individual functions:

1. Operational volume control system is connected to the reactor coolant piping via two charge lines (connected to each cold leg) and one letdown line. This system is also connected to the moderator system by mean of two charge lines and four letdown lines. In normal operation the letdown line connected to the coolant piping and the charge line connected to the moderator piping are kept open. This system fulfills:

    - Filling and pressurizing the reactor, reactor coolant and moderator systems prior to start up.
    - Compensation of volume changes in the primary side.
    - D2O chemical treatment.
    - Boron injection for reactivity control.
    - Coolant supply for the refuelling machine
    - Coolant reserve during leakage in primary circuit.
    - Injection of the secured coolant reserve during a leakage in the primary system.
    - Injection of a continuous leak-off flow to the high pressure seal of the reactor coolant pumps.

2. Leakage compensating system as to be seen as a redundancy of the normal volume control system. It can acts in case of LOCA and inject independently of the normal control volume system into the moderator system. It is constituted of two suction lines and two compensating pumps each of them branch into two other injection lines.

3. Finally the system is connected also with pressurizer via auxiliary spray line. The subsystem pressurizer relief tank cooling via the D2O circulating pumps fulfills:

    - Cooling of the fluid blow-down by the pressurizer safety valves.
    - Level regulation and purification of the liquid in the pressurizer relief tank.

2.2.9 SECONDARY SIDE

A simplified overview of the CNA-2 secondary side is presented in Fig. 12. The steam is transferred from the two SG to the turbines by mean of two main steam lines. In these lines several valves are provided to isolate secondary side to the primary and to bypass the turbines. There are three turbines: one HP and two LP turbines. Between HP-LP and LP-LP the steam passes into a moisture separator that serves to dry the steam.

Exhaust steam then is transferred to two condensers. From the condensers begin the regeneration line that is composed by a cascade of low pressure pre-heaters that preheat the water by mean of steam extracted from the turbines. The water is stored in the feedwater tank from here three high pressure suction lines provide water to the two SGs.

The peculiarity of CNA-2 is the HP feedwater pre-hating that is performed by 4 moderator coolers (heat exchangers that transfer heat from the moderator loop to the two feedwater lines). In the next discussion the attention is focused on the main steam and feedwater lines, on turbine bypass system and on condensers. General data of the secondary side are reported in Tab. 3.

2.2.10 Main steam line (LBA)

This system satisfied the following functions:

- During normal operation it transfers the steam from the SG to the HP turbine.
- During operation in partial load and in case of TUSA it transfers steam from SG to feedwater tank and to the steam auxiliary collector.
- During operation in turbines bypass it transfers the steam to the SG to the condenser by mean of the by pass valves.
- If required it isolates the reactor building by mean of main isolating valves located inside a special containment between the reactor building and the turbine building (UJE).
- It limits the steam pressure increase by mean of the relief valves.

A valves station is located inside a special valves compartment (UJE):

- MS-IV: Main steam isolation valve is the closure valve of the main steam line. During normal operation this valve is open and closes quickly in case of drop of pressure caused by a steam line break. It closes quickly also if the activity level in the SG is above the acceptance threshold.
- MS-PRIV: Main steam pressure relief isolation valve. This valve is closed in normal operation and it opens in case of pressure increases in the steam line in this case the relief valves are used to reduce steam line pressure.
- MS-IVUSV: Isolation valve upstream of main steam safety valve. This valve is open during normal operation and it closes is the safety valve fails in open position.

- MS-SV: Main steam safety valve. This valve serves to protect the SG against excessive pressure levels, it is closed in normal operation and it opens if the pressure reaches 6.8 MPa or more.

CNA-2 SECONDARY SIDE	
Generated electric power	**692 [MWe]**
Plant yield	**32%**
Steam Generator secondary Side (full load)	**Inlet feedwater temperature[°C]:** 170.7 (160.3)
	Outlet steam temperature [°C] / title [%]: 271 / 99.75
	SG total height [m]: 19.77
	SG volume [m^3]: 148.7
	Operative pressure [MPa]: 5.49
Main steam line	**MS-SV:** 1 per line
	MS-IV: 1 per line
	Steam relief control valve: 2 per line
Turbines	**HP / LP turbines number:** 1 / 2
	HP inlet / outlet steam mass flow [kg/s]: 957.13 / 956.03
	HP inlet / outlet steam pressures [MPa]: 5.362 / 0.621
	LP inlet / outlet steam mass flow [kg/s]: 824.46 / 662.133
	LP inlet / outlet steam pressures [MPa]: 0.596 / 0.0501
	Number of steam extractions: 3
Condenser	**Type / number:** KPE92x52-1TSS153 **/** 2
	Heat exchange surface per condenser [m^3]: 35690
	Operating pressure [MPa]: 0.038
Feedwater line	**N° of feedwater pumps:** 3 (2 in operation)
	FW tank volume [m^3]: 320
Moderator coolers Secondary side	**Feedwater inlet temperature [°C]:** 121
	Feedwater outlet temperature [°C]: 175.4 (237.4)
	Mass flow rate per Moderator Cooler [kg/s]: 239.3 (81.9)

Tab. 3 – CNA-2 NPP: main features of secondary side.

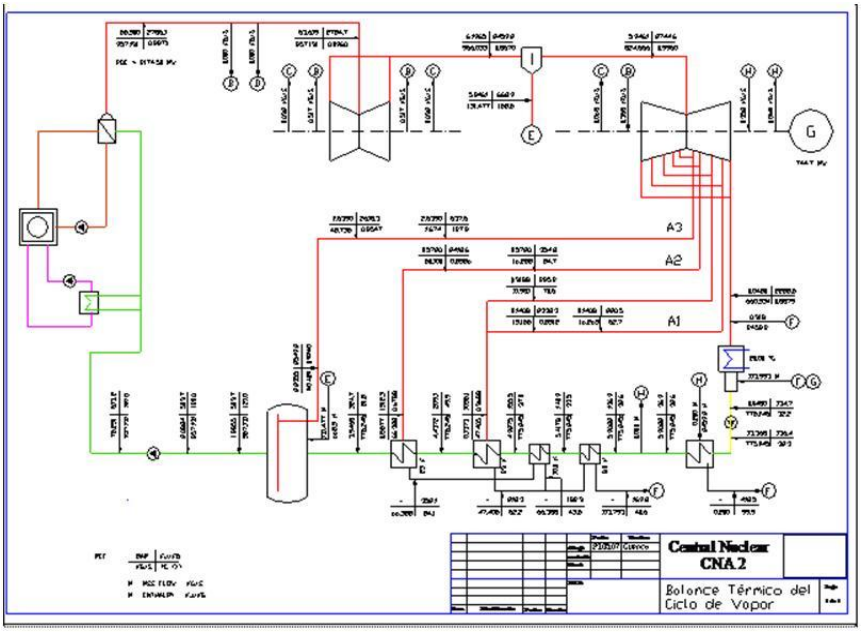

Fig. 12 – CNA-2 NPP: simplified overview of secondary side and thermal balance.

2.2.11 Condenser and condensing system (MAG)

The function of the condensing system (MAG) is to condense the steam exhausted from the two LP turbines and to produce and maintain as high a vacuum as possible (in order to increase the enthalpy drop in the turbine). The two condensers are also designed to accommodate steam from turbine bypass line.

2.2.12 By pass system (MAN)

In case of unbalance between the main steam mass flow generated in the SGs and the steam required by the turbines the bypass system is actuated and the excess of steam is discharged into the condensers in a controlled manner.

The bypass system (MAN) comprises 4 identical assemblies, each combining one stop and one control valve. An orifice is incorporated in every bypass steam inlet for a second supercritical expansion downstream of the bypass control valve. Thus, inadmissible exposure of the condenser is reduced by the staged supercritical expansion. Attemperator water from the condensate injection water system is injected into the orifices via 2 staggered attemperator water injection valves; the function of these components is to reduce the steam pressure.

The bypass system (MAN) is designed to cope 80% of the rated main steam mass flow at rated main steam pressure also if one out of four bypass assemblies fails (condition n-1). On the other hands if the pressure is not reduced the protection system of the condensers close the bypass valves if the condenser pressure increase beyond 0.06 MPa.

2.2.13 Feedwater line (LAB)

This system provides feedwater from the tank to the SG. Starting from the feedwater tank (LAA) there are three suction feedwater separated lines (2/3 used in normal operation). For each suction line there is/are: two valves (one control, one safety valve), one low velocity booster pump, one filter and one main feedwater pump (LAC). The suction lines provide water into a common line that split into two lines before the UJE compartment where. In the UJE there is one isolation valve per line. In the UJA containment each line is preheated (from 120°C to 170°C) by two moderator cooler heat exchangers.

Two moderator cooler heat exchangers bypass lines are provided in case of low temperature of the moderator. After the MO coolers the two lines are connected by a balance line that is equipped with two quick valves (they close in case of break of one of the two lines). The balance line provides equal conditions in the two lines. After this connection a control valves station is provided in each line: one block valve, one control valve. These stations can be bypassed by the low charge bypass lines (that are used if the power is under 30%, per each line there is a block valve and a control valve). Each line ends in one SG feedwater inlet. The simplified system layout is given in Fig. 13. A characterization of the Feedwater tank and associated suction pumps is reported in.

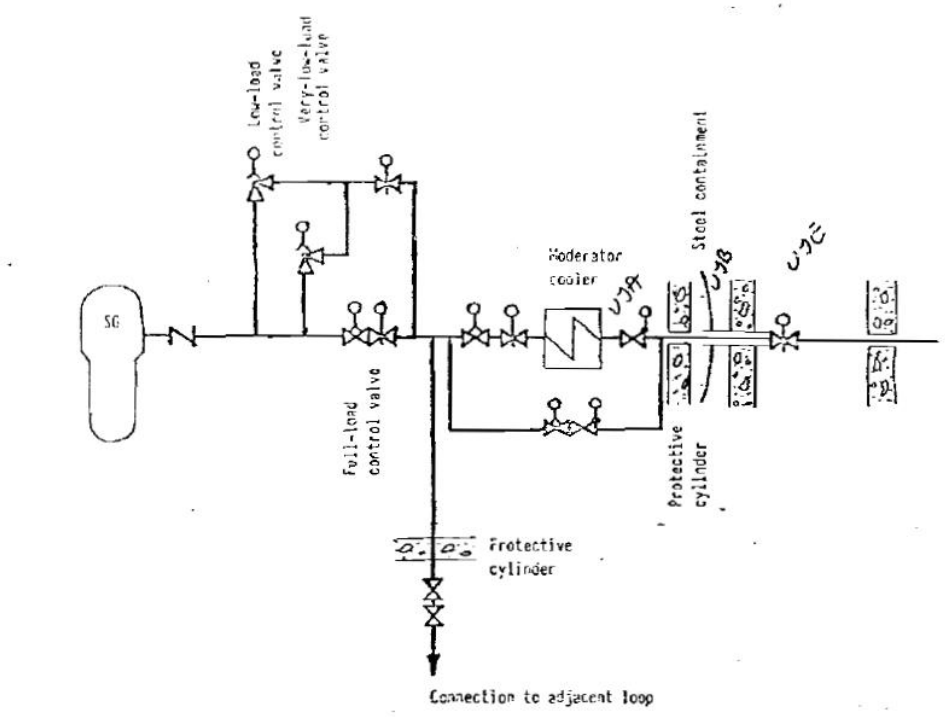

Fig. 13 – CNA-2 NPP: simplified overview of the feedwater line in UJE and UJA compartments.

2.3 Fuel management

After the equilibrium burnup is reached,. Thus, a fresh FA is introduced into the core in a position and kept there until it reaches a certain burnup (transition burnup). Then it is moved to its final location, where it is irradiated up to the discharge burnup.

Thermal power in CNA-2 is produced in 451 vertical fuel channels. The FC are sub-divided into five thermal-hydraulics zones; their correspondence is given in Fig. 14 FC are identified using an alphanumeric convention where the columns are numbered from 1 to 45 and the rows from LA to BG. The convention is using the letters as a numbering system where:

A	B	C	D	E	F	G	H	K	L
1	2	3	4	5	6	7	8	9	0

In this way, e.g. row LA corresponds to 01 and row BG to 23.

The Atucha-II plant is operated with an on-power re-fueling that is performed by a refueling machine. Fuel burnup zones are represented in Fig. 15 and they are described in this section. After the equilibrium burnup core is reached, the refueling is performed in order to move each FA just three times during its lifetime, following the rules reported below (*Parisi, 2008, Mayers, 1985*).

a) The FA stay in the core in two positions. They are introduced fresh in one FC, stay in that FC until they reach a certain burnup, then they are moved to another FC, and stay there until they reach the exit burnup.
b) With respect to fuel management, the FC are divided in three “paths”, and each “path” has two burnup zones; the FA enter the zone with lower average burnup, then is moved to the other zone (of the same “path”) until it reaches the exit burnup of the path.
c) The selection of the re-fueled FC is done by the plant physicist after he has calculated power and burnup distributions. He searches for the FA with highest average burnup, and that one is taken out from the core; then he searches for the FA of the other zone of the same path, and moves it to the other FC, putting a fresh FA in it. He should verify compliance with the FC and linear power limits and power ramp failures (Pellet Cladding Interaction, PCI) prevention criteria. He should also try to keep an approximately symmetric power distribution in each of the six azimuthal sectors of the core. In case he has problems with the compliance of the criteria, he may introduce variations in the selection of the FC, like not to choose the one with the highest burnup but the following one.
d) In practice, all FCs, and the 10 axial sectors of each FC have burnups between the value at which the FA enters the channel (which may be zero for some channels), and the value at which it leaves the channel, which may be the exit burnup for some FC.

The calculation of power and burnup distributions required for fuel management for CNA-II is done with the PUMA code (*Mayers, 1985*). There are three refueling paths, as summarized hereafter, and reported in Fig. 15 and Tab. 4:

- ***Path 1:*** Fresh fuel enters zone 6, stays until a transition burnup, moves to 5, stays until it reaches the exit burnup and leaves the core.
- ***Path 2:*** Same for zones 2 and 4.
- ***Path 3:*** Same for zones 3 and 1.

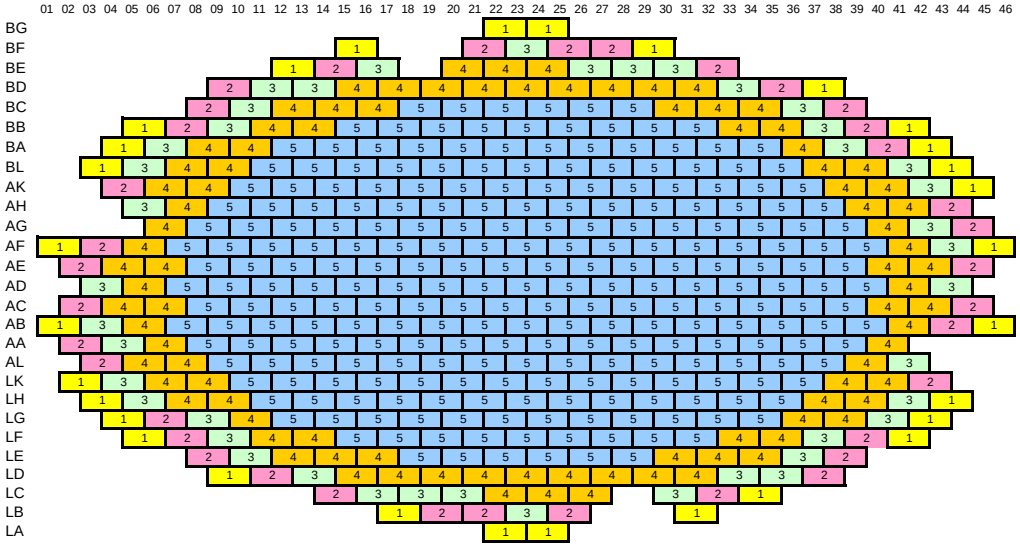

Fig. 14 – CNA-2 core: correspondence map between FC and thermal-hydraulic zones.

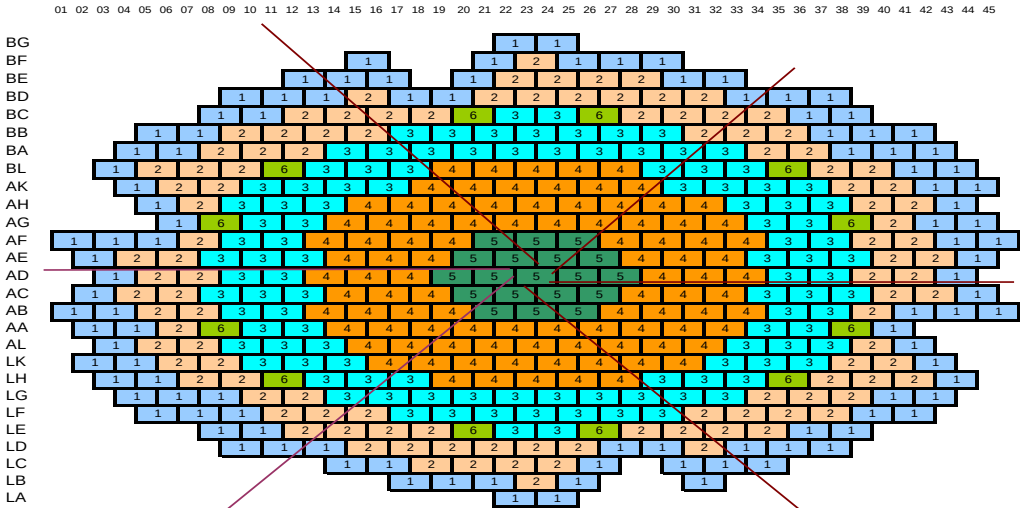

Fig. 15 – Fuel burnup zones.

Path for irradiation	Burning Zone	Channels	Transition/ Discharge Burnup (MWd/TU)
1	6 (Fuel Inlet) ↓	BC20 BC26 BL11 BL35 AG08 AG38 AA08 AA38 LH11 LH35 LE20 LE26	2886
1	5 (Inlet) ↓ Discharge	AF21 AF23 AF25 AE20 AE22 AE24 AE26 AD19 AD21 AD23 AD25 AD27 AC20 AC22 AC24 AC26 AB21 AB23 AB25	8001
2	2 (Fuel Inlet) ↓	BF23 BE22 BE24 BE26 BE28 BD15 BD21 BD23 BD25 BD27 BD29 BD31 BC12 BC14 BC16 BC18 BC28 BC30 BC32 BC34 BB09 BB11 BB13 BB15 BB31 BB33 BB35 BA08 BA10 BA12 BA34 BA36 BL05 BL07 BL09 BL37 BL39 AK06 AK08 AK38 AK40 AH07 AH39 AH41 AG40 AF07 AF39 AF41 AE04 AE06 AE40 AE42 AD05 AD07 AD39 AD41 AC04 AC06 AC40 AC42 AB05 AB07 AB39 AA06 AL05 AL07 AL39 LK06 LK08 LK38 LK40 LH07 LH09 LH37 LH39 LH41 LG10 LG12 LG34 LG36 LG38 LF11 LF13 LF15 LF31 LF33 LF35 LF37 LE12 LE14 LE16 LE18 LE28 LE30 LE32 LE34 LD15 LD17 LD19 LD21 LD23 LD25 LD31 LC18 LC20 LC22 LC24 LB23	3694
2	4 (Inlet) ↓ Discharge	BL19 BL21 BL23 BL25 BL27 AK18 AK20 AK22 AK24 AK26 AK28 AH15 AH17 AH19 AH21 AH23 AH25 AH27 AH29 AH31 AG14 AG16 AG18 AG20 AG22 AG24 AG26 AG28 AG30 AG32 AF13 AF15 AF17 AF19 AF27 AF29 AF31 AF33 AE14 AE16 AE18 AE28 AE30 AE32 AD13 AD15 AD17 AD29 AD31 AD33 AC14 AC16 AC18 AC28 AC30 AC32 AB13 AB15 AB17 AB19 AB27 AB29 AB31 AB33 AA14 AA16 AA18 AA20 AA22 AA24 AA26 AA28 AA30 AA32 AL15 AL17 AL19 AL21 AL23 AL25 AL27 AL29 AL31 LK16 LK18 LK20 LK22 LK24 LK26 LK28 LK30 LH19 LH21 LH23 LH25 LH27	8001
3	3 (Fuel Inlet) ↓	BC22 BC24 BB17 BB19 BB21 BB23 BB25 BB27 BB29 BA14 BA16 BA18 BA20 BA22 BA24 BA26 BA28 BA30 BA32 BL13 BL15 BL17 BL29 BL31 BL33 AK10 AK12 AK14 AK16 AK30 AK32 AK34 AK36 AH09 AH11 AH13 AH33 AH35 AH37 AG10 AG12 AG34 AG36 AF09 AF11 AF35 AF37 AE08 AE10 AE12 AE34 AE36 AE38 AD09 AD11 AD35 AD37 AC08 AC10 AC12 AC34 AC36 AC38 AB09 AB11 AB35 AB37 AA10 AA12 AA34 AA36 AL09 AL11 AL13 AL33 AL35 AL37 LK10 LK12 LK14 LK32 LK34 LK36 LH13 LH15 LH17 LH29 LH31 LH33 LG14 LG16 LG18 LG20 LG22 LG24 LG26 LG28 LG30 LG32 LF17 LF19 LF21 LF23 LF25 LF27 LF29 LE22 LE24	5546
3	1 (Fuel Inlet) ↓ Discharge	BG22 BG24 BF15 BF21 BF25 BF27 BF29 BE12 BE14 BE16 BE20 BE30 BE32 BD09 BD11 BD13 BD17 BD19 BD33 BD35 BD37 BC08 BC10 BC36 BC38 BB05 BB07 BB37 BB39 BB41 BA04 BA06 BA38 BA40 BA42 BL03 BL41 BL43 AK04 AK42 AK44 AH05 AH43 AG06 AG42 AG44 AF01 AF03 AF05 AF43 AF45 AE02 AE44 AD03 AD43 AC02 AC44 AB01 AB03 AB41 AB43 AB45 AA02 AA04 AA40 AL03 AL41 LK02 LK04 LK42 LH03 LH05 LH43 LG04 LG06 LG08 LG40 LG42 LF05 LF07 LF09 LF39 LF41 LE08 LE10 LE36 LE38 LD09 LD11 LD13 LD27 LD29 LD33 LD35 LD37 LC14 LC16 LC26 LC30 LC32 LC34 LB17 LB19 LB21 LB25 LB31 LA22 LA24	8001

Tab. 4 – Fuel assemblies' movements for burnup management; 6 zones for depletion and 3 paths for irradiation.

2.4 Description of the fuel

2.4.1 Fuel channel layout

Each FC contains one FA. In order to limit heat exchange between coolant and moderator, a thin stagnant D_2O film is kept around FC wall by a 0.2 mm Zry-4 sheet (see Fig. 16 and Tab. 5 for dimensions). 37 fuel rods are arranged in the FC as it is reported in Fig. 17 and Tab. 6 (*Mayers, 1985*).

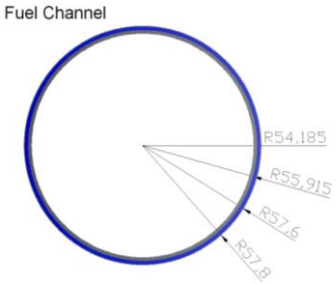

Fig. 16 – FC layout.

PARAMETER	DIMENSION	NOTES
Internal Radius of FC	54.185 mm	
External Radius of FC	55.915 mm	Zry-4 FC thickness: 1.73 mm
Stagnant D_2O External Radius	57.60 mm	
Zry-4 Sheet	57.80 mm	Zry-4 Sheet thickness: 0.2 mm

Tab. 5 – FC geometrical dimensions.

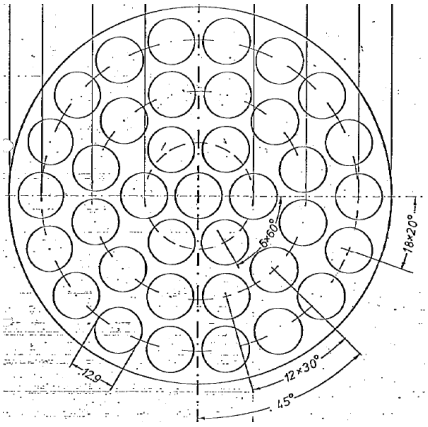

Fig. 17 – Fuel rods arrangement in a FC.

PARAMETER	DIMENSION
Radius of centers of rods in inner ring	15.475 mm
Radius of centers of rods in interm. ring	30.145 mm
Radius of centers of rods in outer ring	44.87 mm

Tab. 6 – Fuel rods arrangement in a FC.

2.4.2 Fuel assembly design

The FA are bundles of 37 closely packed fuel rods, which are arranged in 3 concentric circles with 6,12 and 18 fuel rods around a central fuel rod (see Fig. 17). A sketch of FA and of a fuel rod is shown in Fig. 18. The fuel rods are held in position with respect to each other by means of several spacer grids set along the length of the FA. To support the FA within the FC, the spacer grids carry on their outer circumference sliding shoes (*Mayers, 1985*).

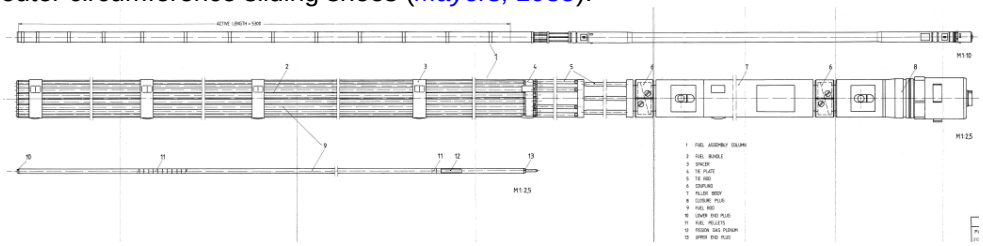

Fig. 18 – Fuel assembly and fuel rod at different scales.

2.4.3 Fuel rod design

The fuel rod consists of a stack of high density, natural enriched sintered pellets (see Fig. 19) of UO_2 ground at their surfaces, and of the Al_2O_3 compensation pellets, the supporting tube and the compression spring which are inserted into a Zircaloy-4 cladding tube. The cladding tube is backfilled with helium and welded gas-tight to the Zry-4 end plugs. The main fuel data are reported in Tab. 7.

At the upper end of the fuel rod above the fuel pellet column, there is a compression spring and a fission gas space. Although most fission products are retained within the UO_2, a fraction of the gaseous fission products is released from the pellets and accumulated in the plenum of the rod. The volume of the fission gas space is large enough to prevent inadmissible pressures which could be reached as a result of this fission gas release over the design life of the fuel. The upper part of the fuel rod has been modified according to (*Adorni, 2008, Mayers, 1985*), as shown in Fig. 20

The compression spring in the upper plenum prevents uncontrolled movement of the fuel pellets during handling and transportation and allows also accommodating the difference in axial fuel/cladding expansion during reactor operation. The fuel rod cladding thickness is adequate to be "free-standing", i.e., capable of withstanding external reactor pressure without collapsing onto the pellets. All fuel rods are internally pre-pressurized in order to reduce compressive clad stresses and creep down due to the high coolant pressure. Helium is used as pressurizing gas to get good heat transfer from fuel to cladding. The fuel pellets limit creep down of the cladding as a result of the external pressure.

The UO2 pellets (Fig. 21) are dished at both ends.

The two end faces of each pellet are shaped so as to produce a shallow concave dishing in the middle, surrounded by a narrow chamfered annular zone. In the stack, the pellets rest on each other on these edge zones. In this manner the

longitudinal thermal expansion of the pellet stack is determined only by the expansion of the outer zone of the fuel, which is at a relatively low temperature, and not by the behavior of the hot inner zone which is subject to a greater thermal expansion. The axial forces acting on the fuel pellets are transmitted from pellet to pellet via these cooler annular edge zones.

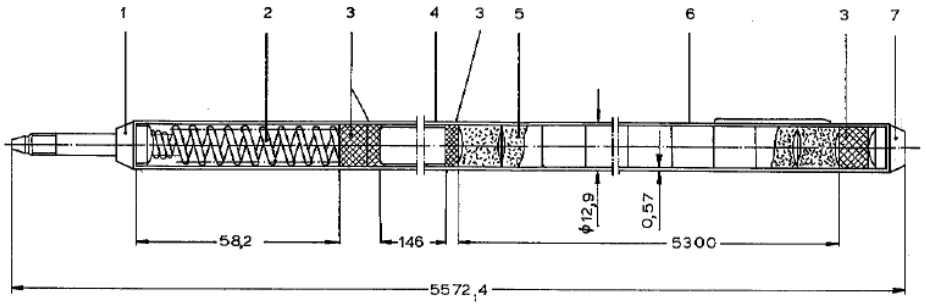

1	End Plug, Upper	Zry-4
2	Spring	1.4568
3	Pellet	Al_2O_3
4	Supporting Tube	Zry - 4
5	Pellet	UO_2
6	Cladding Tube	Zry-4
7	End Plug, Lower	Zry-4

Fig. 19 – Fuel rod.

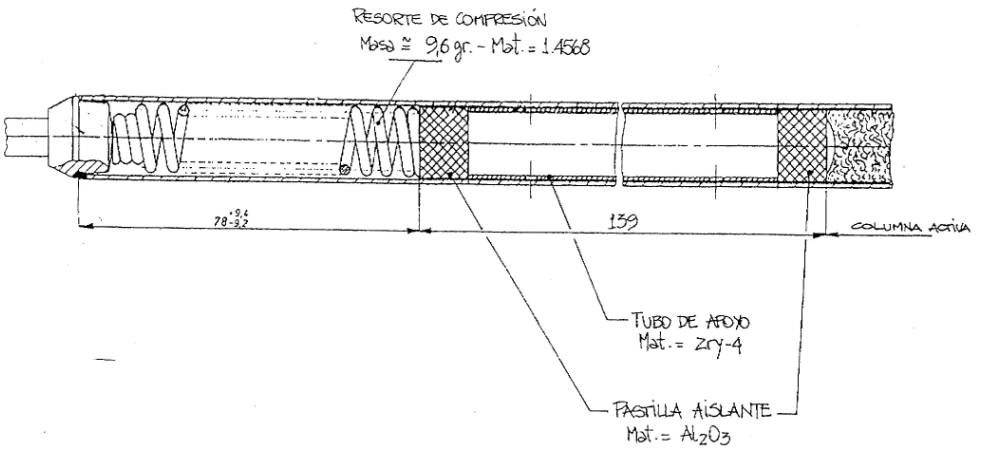

Fig. 20 – Schematic representation of the upper part of the CNA-2 fuel rod, including design modification introduced.

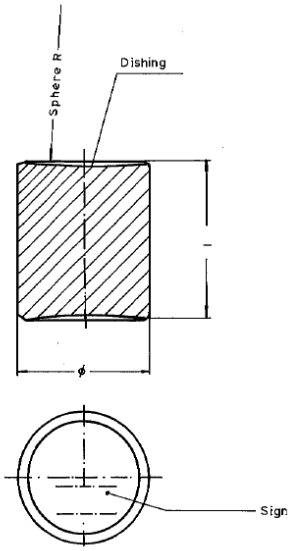

Fig. 21 – UO2 pellet.

Fuel Assembly		
Number of fuel assemblies in the reactor	451	--
Number of fuel rods	37	--
Fuel pellet		
Material	UO2	--
Density	10.55	g/cm^3
Pellet diameter	11.57	mm
Pellet length	14	mm
No of pellet	379	--
Enrichment	0.711	g/gHM
Volume of dishings/pellet	21	mm^3
Cladding		
Material	Zircaloy-4	--
Density	6.6	g/cm^3
Outside diameter	12.9	mm
Inside diameter	11.76	mm
Fuel rod		
Total length	5572	mm
Active length	5300	mm
Diam. Gap pellet/cladding	0.19	mm
Fill gas	Helium	--
Fill gas pressure (absolute)	21	bar

Tab. 7 – CNA-2 fuel data (the data shown are valid at room temperature).

3. DESCRIPTION OF LB-LOCA IN ATUCHA-II NPP

Loss of coolant accidents mean those postulated accidents that result from the loss of reactor coolant at a rate in excess of the capability of the reactor coolant makeup system from breaks in the reactor coolant pressure boundary, up to and including a break equivalent in size to the double-ended rupture of the largest pipe of the reactor coolant system.

A peculiarity of the Atucha-2 design is the positive void reactivity coefficient. This is a characteristic in common to other heavy water moderated reactors that utilize natural uranium as fuel. This implies that after a LB-LOCA event, the fission power peak at the very beginning of the transient is controlled by the void formation in the core channels, and then it is determined by the pressure wave propagation from the break. Indeed, the moderator is still liquid and flashes delayed with respect to the coolant, thus the LOCA event is also a RIA event. We will refer in the following to “Atucha-II LB-LOCA” to indicate the combined LOCA and RIA.

The Double Ended Guillotine Break LOCA (DEGB LOCA or 2A LOCA) constitutes the ‘historical’ event for the design of Emergency Core Cooling Systems (ECCS) in Water Cooled Reactors and is primarily adopted in vessel equipped Nuclear Power Plants. It is assumed that the largest pipe connected with the Reactor Pressure Vessel (RPV) can be broken: two end breaks are generated, typically at the RPV side and at the Main Coolant Pump (MCP) side.

In the case of Atucha-II the history of the construction and the agreement between the Regulatory Authority and the Utility brought to the exclusions of the 2A LOCA from the list of the Design Basis Accidents (DBA), (*UNIPI 2008, D’Auria 2008, NASA-ARN 1977*). Therefore, it is placed in an “*ah hoc*” category of events identified as Selected Beyond DBA (SBDBA).

3.1 DESCRIPTION OF THE TRANSIENT

Four phenomenological windows (Ph.W) are identified, see Fig. 22, based on the key phenomena and the relevant thermal-hydraulic aspects occurring in Atucha-2 2A LOCA. They are: I) fission power excursion; II) CHF occurrence and clad temperature excursion; III) quenching and fuel channels refill; IV) long term cooling. These phases or Ph.W are adopted instead of the classical ‘Blow-down’, ‘Refill’ and ‘Reflood’ phases adopted in systematic studies of the LBLOCA in PWR, (*D’Auria 2008*).

3.1.1 I Ph.W. – Fission Power Excursion (RIA)

From the start opening of the break till the time when total fuel energy achieves 90% of the value attained when power equals the decay value (this is to ensure that the RIA part of the transient is terminated and to include in this period possible damage mechanisms originated by energy deposition in the fuel, see Fig. 22). The duration of the first Ph.W is of the order of one second. The propagation of the depressurization wave originated at the break and the consequent occurrence of the fission power peak are the characterizing phenomenon. Start of the CHF condition occurs in this period.

3.1.2 II Ph.W. – CHF Occurrence & Clad Temperature Excursion

The second window lasts from the end of the previous window till (roughly) the time of actuation of accumulators. The duration of the second window is of the order of ten seconds. The widespread of the CHF condition and the rod surface temperature excursion including the occurrence of the peak cladding temperature and the related turnaround caused by liquid flashing and by flow reversal in the core, are the characterizing phenomena. Containment pressurization also occurs during this Ph.W.

3.1.3 III Ph.W. – Quenching & Fuel Channels Refill

The third window ends when liquid level (mixture) fills all the core channels. At the beginning of the Ph.W. early quench occurs noticeably before the actuation of emergency systems and is caused by flow reversal in the core and flashing. The ECCS intervention keeps the clad temperature down and is necessary for refilling of the fuel channels. The duration of the third phenomenological window is of the order of a few minutes. In this period equalization of pressures between containment and primary circuit occurs.

3.1.4 IV Ph.W. – Long Term Cooling (LTC)

The fourth Ph.W implies the continued containment sump recirculation operation and ensures the 'post-LOCA long term' core cooling. The behavior of the sump (liquid level and temperature, other than debris effect), the performance of the SIP and the level distribution (and stabilization) in the primary loop constitute the characterizing thermal-hydraulic phenomena.

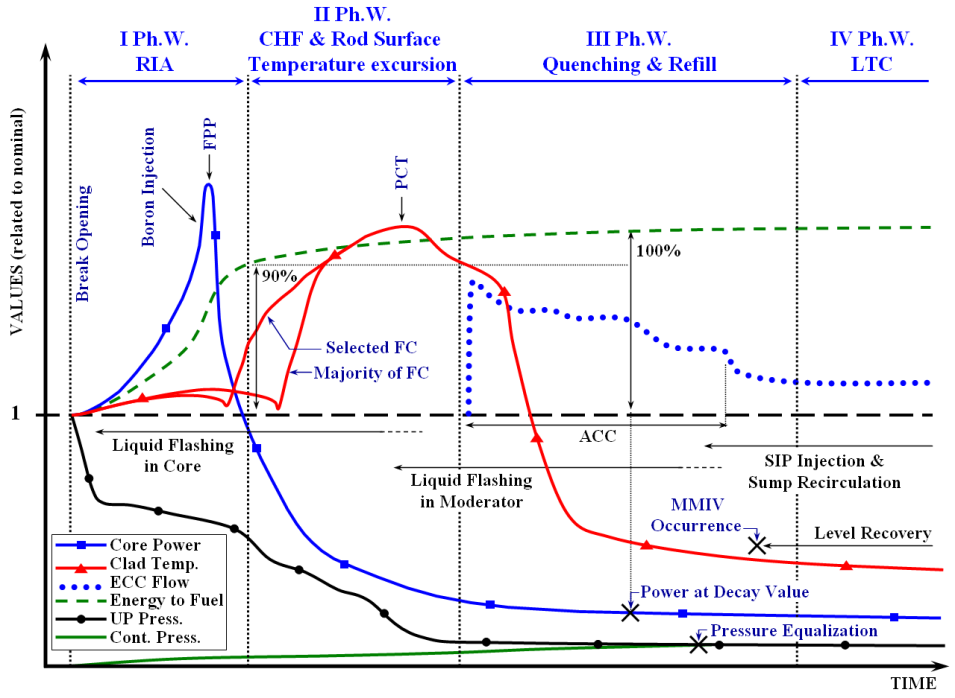

Fig. 22 – Definition of the LBLOCA phenomenological windows.

3.2 LICENSING FRAMEWORK

3.2.1 The regulatory frame work

An established regulatory framework exists in the nuclear technology in relation to the LB-LOCA analysis of vessel equipped water cooled nuclear reactors. Furthermore, an overview of the current trends on the same subject constituted a document issued within an agreement between UNIPI and NASA, i.e. (*UNIPI 2008*). The purpose of the document at (*UNIPI 2008*) has been to create the basis for the decision by NASA in relation to the structure of the FSAR of Atucha-2 and included an outline of the current international practice that is also relevant here (section 3.2.2).

It should be noted that, as for Atucha II, LB-LOCA are classified as SBDBA, the fulfillment of all DBA criteria is not mandatory but it is investigated.

A review of national acceptance criteria for LOCA and RIA accidents is beyond the scope of this section. The reader is referred to (*OECD 2009*) and (*OECD 2010-1*), in which a recent review of fuel rod failure thresholds for LOCAs and RIAs in PWRs and BWRs can be found. The review covers currently applied as well as projected failure thresholds. It should be remarked that considerable differences exist between these thresholds, in particular as to how the effects of fuel burnup and cladding waterside corrosion are accounted for.

For the sake of completeness, the report (*European Commission 1999*) describes in great detail the methodologies used by different organizations of how fuel rods are calculated to fail.

3.2.2 The international practice

The DBA, including the DEGB LBLOCA (or LOCA 2 x 100%) was intended in historical terms as a minimum set of enveloping scenarios whose positive-conservative evaluation, within the (overly)-conservative Appendix K approach could ensure that an adequate level of protection is provided by the designers.

TMI-2, Chernobyl-4 and also Fukushima unit 1 to 4, were practical demonstrations that complex accidents out of the DBA list may occur. The needs from operator training, the accident management technology and, above all, the progress in the techniques for deterministic and probabilistic accident analysis, i.e. an outcome of the research programs carried out during the last three or four decades, suggested a change in the conservative approach.

A recent issued OECD/CSNI report, (*OECD/CSNI 2007*), identifies four classes of deterministic methods that can be seen as a historical progress for the licensing approach:

1) Very Conservative (Appendix K for LOCA).
2) Best Estimate Bounding.
3) Realistic Conservative.
4) Use of Best-Estimate Plus Uncertainty (BEPU).

A similar classification was proposed earlier by IAEA, e.g. (*IAEA 2003*), in a well known table ("table of options" for deterministic analyses) where "Type of Applied Code", "Type of BIC", "Assumption on System Availability" and "Type of Approach", are distinguished.

Without entering into detail of the four classes, neither of methods nor of the IAEA table, two remarks apply:

- Drawbacks from the Applicant and from the Licensing Authority side are identified when the approaches 1) to 3), or the 'conservative' approaches of the IAEA table are pursued, see also (*IAEA 2002*).
- BEPU constitutes the current trend, as also testified by ongoing projects like OECD/CSNI BEMUSE, (*Petruzzi 2004*), or recently issued documents like US NRC RG 1.203, (*US NRC 2005*), and IAEA Safety Series Report on uncertainty methods, (*IAEA 2008*).

Thermal-hydraulic system codes, properly qualified and with techniques available for the proper application, are at the basis of the BEPU approach. The codes, noticeably, Relap5, Athlet, Cathare, Trace, Cathena, Apros and Mars, must be supplemented or connected with uncertainty methods. Two categories of uncertainty methods are distinguished, e.g. (*IAEA 2008*), with approaches based on: a) propagation of code input errors and statistical treatment of the resulting uncertainty, b) propagation of code output errors and 'deterministic' treatment of the resulting uncertainty. CSAU, GRS-method and CIAU are uncertainty methods suitable for technological applications.

The development of BEPU methods had, as specific reference framework, the deterministic accident analysis and the acceptance criteria valid within the conservative approach, i.e. items 1) to 3) above. The BEPU approach in (*OECD/CSNI 2007*) is considered as "*… the biggest effort for a proper use of best estimate models in order to minimize unnecessary conservatism while accounting for uncertainties associated to simulation results*".

The current challenge is the 'distributed' and 'comprehensive' application of the BEPU methods within the FSAR, making reference to the physical barriers, the release of fission products and to the safety functions, other than considering the existing acceptability thresholds, i.e. the heredity from the conservative approach.

The adoption of BEPU approach allows a homogeneous level of safety for all the issues that are part of the FSAR. Furthermore, the application of the BEPU methods is consistent with the best-latest available information in various technological sectors, see (*UNIPI 2008*).

3.2.3 The ARN requirements and the current status of the licensing process

The consideration of the requirements of the Regulatory Authority constitutes the most important goal for a licensing analysis. The existing "framework-of-agreement", related to the construction and licensing of the CNA-2 (or CNA-II),

between the Utility (NASA) and the Regulatory Authority (ARN) is summarized in the document at (*Argentina 2007*). The following should be noted:

1) IAEA reports at (*IAEA NS-R-1 2000, IAEA NS-R-2 2000, IAEA INSAG-19,*), are mentioned in the document at (*Argentina 2007*) as at the top of the hierarchy for the Atucha-2 licensing.
2) ARN legal requirements do not make direct reference to the detailed Appendix K type of criteria. Rather, it is requested that a Farmer type of curve (probability versus consequences) must be respected by the Licensee, (*ARN 2001*).
3) On the one hand, the ARN legal requirements (issued in (*ARN 2001*)) can be considered as a precursor to the risk-informed regulation. On the other hand, current international practice must be considered (this is consistent with ARN recommendation) although the concerned NPP design and construction start are two or three decades old, respectively.
4) ARN did not consider adequately substantiated the value of 10^{-7} event/year for the probability of the DEGB (2A or 2 x 100% LBLOCA) occurrence in Atucha-2 (this could level-down the relevance of this event).

3.3 The BEPU Approach

Based on qualified tools and analytical procedures developed or available at UNIPI, a modern and technically consistent approach has been built upon best estimate methods including an evaluation of the uncertainty in the calculated results (Best Estimate Plus Uncertainties or BEPU approach). The complete description of the approach, available in (*D'Auria 2008, UNIPI 2008*), is outside the aim of the present document. In the present section only specific notes will be provided relevant for addressing the role of the fuel pin performance tool and the analysis envisaged.

Adopting a "best estimate approach" for safety analyses means that, for each expected phenomenon, the best available tools and codes should be used. At present, no single code is capable of covering all phenomena involved in the nuclear safety field. Therefore, the best estimate analyst will meet the situation of working with two or more codes, and will have to develop an interface between those two as shown in Fig. 23 (*D'Auria 2008*).

In the overall approach, TRANSURANUS code will be used in connection with other codes, as outlined in Fig. 24 with the aim of investigating the behavior of the fuel and evaluate the performance. Fig. 25 reports the simplified flowchart of the overall approach.

In Tab. 8 acceptance criteria relevant for safety analysis are reported in a simplified form and are proposed in addition to the ARN criteria, (*D'Auria 2008*). More detailed treatment can be found in (*OECD 2010-1, OECD 2009*). For the sake of completeness, Tab. 9 reports the use of codes and nodalizations used for safety analysis.

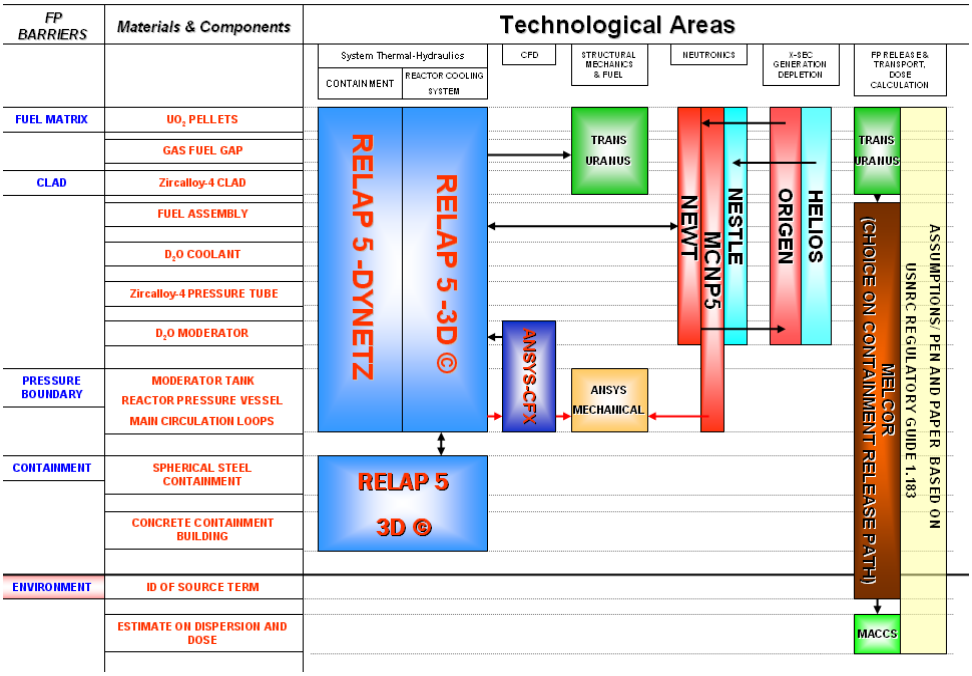

Fig. 23 – Description of the interaction between the codes.

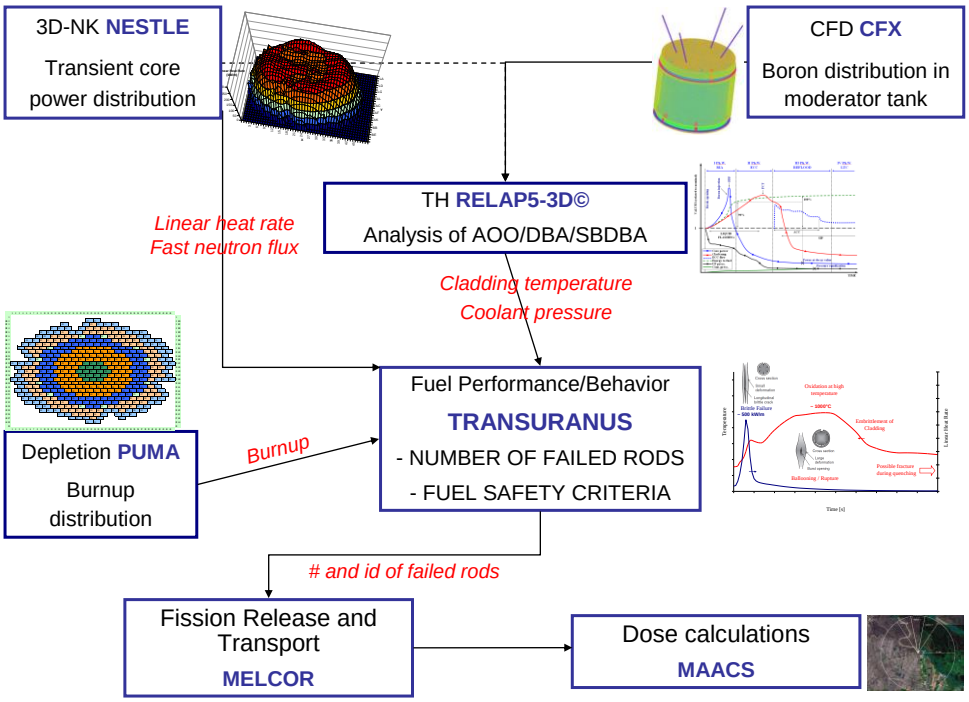

Fig. 24 – Interaction between the Codes.

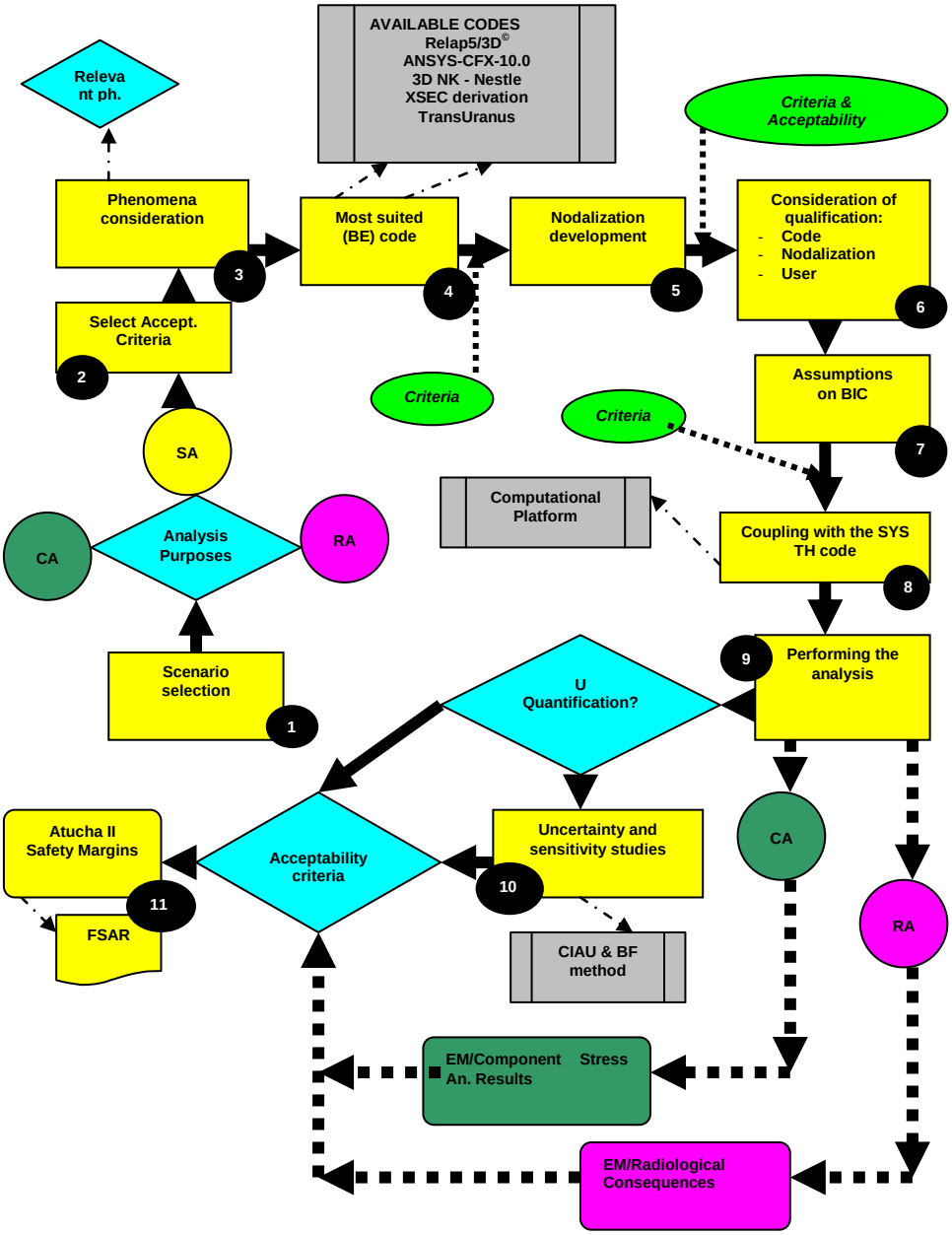

Fig. 25 – Simplified flowchart for the BEPU approach for Atucha II accident analysis from section 15.0-1 of (NASA FSAR 2011).

Parameter	Limit
Peak Cladding Temperature (PCT)	1477 K
Maximum clad oxidation	17%
Maximum amount of H2 reacting in the core	1%
Core coolability must be ensured.	--
Long term cooling must be ensured.	--
Amount of energy deposited to the fuel (MEF = Maximum Energy release to the Fuel) (this value will be eventually justify in a separate forthcoming report to be supplied to ARN).	180 cal/g
Number of failed rods	10%
Total whole body dose and thyroid dose from iodine to individuals at the exclusion area boundary,	25 rem and < 300 rem, respectively
Total whole body dose for personnel in control room	5 rem

Tab. 8 – Acceptance criteria.

No	Platform identification	Scope within the present FSAR Chapter 15
1	Relap5/3D – Dynetz	All transients (where I & C, i.e. control, limitation and protection systems, play a role).
2	Helios-Nestle	Transients analyzed by 3D coupled neutron kinetics thermal-hydraulics: spatial or local neutron flux effects are relevant – transient conditions.
3	NJOY-MCNP	3D performance of core with main reference to Keff and neutron flux – steady state conditions.
4	CFX – Relap5/3D (Nestle)	All transients where boron lances are called in operation, including or less Nestle.
5	Relap5/3D – Ansys	Focusing on PTS and structural mechanics integrity of the vessel wall.
6	Relap5/3D – CFX – Ansys	Same as above including the use of the CFD code.
7	Relap5/3D – Transuranus	All transients in relation to which the number of failed rods is calculated.

Tab. 9 – The use of codes and nodalizations.

3.4 Fuel Safety Criteria

3.4.1 Atucha-II fuel design criteria

The CNA-2 specific fuel safety criteria, available from (*NASA FSAR 2011*), are here briefly recalled. It should be noted that the verification of only 8 out of 10 criteria can be addressed by TU code. The analysis of the design of CNA-2 fuel during normal operation is propaedeutic to the subsequent transient analysis, the main objective of the work, and it is evaluated in section 5.

The criteria are here listed:

1 Temperatures.
2 Fuel rod internal pressure.
3 Cladding strain.
4 Cladding strain (limit implemented in the input).
5 Cladding corrosion.
6 Deuterium pick-up (not addressed).
7 Elastic buckling of the cladding.
8 Plastic deformation of the cladding.
9 Cladding Stresses.
10 Dynamic loads (not addressed).

3.4.1.1 Criterion 1: Temperatures

The maximum fuel centerline temperature (*NASA FSAR 2011*) must be lower than fuel melting point that is a decreasing function of burnup, according to Tab. 10.

#	Burnup [MWd/tU]	Temperature [°C]
1	0	2837.0
2	3	2827.4
3	6	2817.8
4	8	2811.4
5	10	2805.0

Tab. 10 – Fuel melting temperatures as function of burnup.

According to (*NASA FSAR 2011*), it has been demonstrated in a number of irradiation experiments that fuel rods can be operated for lengthy periods even with molten fuel without damage to the cladding tubes. The temperature limit for fuel rod design nevertheless requires that even under worst case operating conditions, the melting point of the fuel is not exceeded at the point of peak thermal power generation. This particular limit is specified to ensure that sudden relocation of molten fuel in the interior of the fuel rods can be positively ruled out. Thanks to this limitation, there is also no danger of excessive cladding tube expansion as a result of an increase in the volume of the fuel due to melting, and there is therefore no need to provide additional space (porosity, hollow pellets, etc.) in the fuel rod to accommodate such volume increase and expansion.

3.4.1.2 Criterion 2: Fuel rod internal pressure

The maximum internal gas pressure (*NASA FSAR 2011*) in the fuel rod shall not enlarge the fuel to cladding gap (i.e. the increase in the cladding tube diameter caused by the internal gas pressure is less than the increase in the pellet diameter due to fuel swelling). The maximum permissible increase in cladding tube diameter is limited by an "*ad hoc*" criterion on fuel rod internal pressure.

The fuel rod is filled with helium during manufacture. The as-filled pressure is 2.1 ± 0.1 MPa (relative) at room temperature (*Alvarez 2007*). At the beginning of the dwell period, the temperature rise during power operation and the different degrees of expansion of the cladding tube and the fuel cause this value to rise to about 40 to 50 bar. This internal pressure increases progressively during the residence time as fission gases are released. It must nevertheless be assured that the fuel to cladding gap cannot increase as a result of the internal pressure even at the end of the dwell time, i.e. that the rate of increase of the cladding tube diameter due to the maximum internal pressure must be less than the increase in pellet diameter due to fuel swelling (cladding non-lift-off design criterion (*NASA FSAR 2011*)). If this is not the case, i.e. if the gap grows wider, the reduced coefficient of heat transfer across the wider fuel to cladding gap gives rise to higher fuel temperatures and hence of increased fission gas release. This in turn causes the pressure in the fuel rod to build up still further and hence leads to continued widening of the gap. Another limit on the maximum permissible internal pressure is derived from the strain criterion explained below.

3.4.1.3 Criteria 3 and 4: Cladding strains

The equivalent plastic strain of the cladding in the tensile range (composed of axial and tangential strain) must be less than or equal to 2.5 % (*NASA FSAR 2011*). This limit is directly implemented in the input of the TU code and it is checked each time step (cladding failure criterion of plastic instability) (*Lassmann 2009*).

The total tangential strain (elastic and plastic region) of the cladding caused by fast power ramps must be less than or equal to 1 % (*NASA FSAR 2011*).

Starting from the as-fabricated clearance between fuel and cladding, an operating clearance for the warmed up condition at rated reactor power results from the elastic compressive strain in the cladding tube due to the coolant pressure and differential thermal expansion of cladding and fuel. Owing to the difference between the coolant pressure on the outside and the helium pressure on the inside the cladding tube is subject to compressive stress and contracts onto the fuel due to creepdown. Once the cladding has come into contact with the fuel, fuel swelling causes the cladding tube to expand gradually until, in the extreme case, i.e. at very high burnup, the cladding tube may expand beyond its original beginning of life dimensions. Consequently tangential deformation of the cladding is composed of creep induced compressive strain and subsequent creep under tensile stress. The tangential strain on the cladding tube is superposed with an axial strain since it is assumed that, once the cladding has come into hard contact with the pellets, it will be forced to expand axially as well due to swelling and thermal expansion of the fuel.

Furthermore, there is a possibility of pellet clad interaction (PCI) arising as a consequence of power increases. For the purpose of fuel rod design, this interaction is subdivided as follows:

- *"Fast" power increases:*
  Where power increases are concerned, the occurrence of cladding strain due to thermal expansion of the fuel is affected by factors such as the degree of burnup, the size of power change and the target power value. In this case a tangential total strain (elastic and plastic) of 1 % is taken as the design limit.

  Fast power ramps can, in principle, also lead to mechanical/ chemical pellet clad interaction (PCI/SCC). In this case the above criterion is no longer applicable. However, PCI/SCC failure can be precluded as operational regulations ensure that the reactor is not operated under conditions with the risk of PCI/SCC.

- *Long term interaction due to fuel swelling:*
  In this case the stresses in the cladding decrease as a consequence of stress relaxation. Zircaloy exhibits a very high degree of creep ductility under irradiation.

As a design criterion, a permissible equivalent plastic strain (calculated from the tangential and axial strain) less than or equal to 2.5 % is used for the cladding tube in the tensile stress range and at operating temperature. The strain limit above which damage may occur is far higher. It was not possible to observe localized deformations or even to detect defects in cladding tubes subjected to strains of up to 10 % under conditions comparable with those postulated in the present report. Also the strain limit is not exceeded if the cladding tube is caused to expand not by the fuel but by the internal gas pressure, provided that this pressure is higher than the external pressure exerted by the coolant.

3.4.1.4 Criteria 5: Cladding corrosion

The corrosion layer thickness due to uniform corrosion on the cladding tube surface must be less than or equal to 100 µm (*NASA FSAR 2011*).

Zircaloy cladding tubes undergo corrosion at slow rates in reactor operation. This causes thinning of the cladding tube walls and impairs heat transfer to the coolant. On the basis of experience to date, fuel rod failure due to corrosion may be precluded with certainty in the case of circumferentially averaged layer thicknesses of up to 100 µm. For this reason, a circumferentially averaged corrosion layer thickness of 100 µm is stipulated presently as a conservative design limit for uniform corrosion.

3.4.1.5 Criteria 7 and 8: Elastic buckling and plastic deformation of the cladding

The fuel rod design pressure must be less than the critical elastic buckling pressure of the cladding tube (*NASA FSAR 2011*). The fuel rod design pressure must be less than the critical pressure of the plastic deformation of the cladding tube (*NASA FSAR 2011*).

As a result of the difference between the external coolant pressure and the rod internal gas pressure, the fuel cladding tubes are subjected to a higher pressure on the outside. A cladding tube under such pressure may momentarily buckle elastically or, if the stresses exceed the yield point, may undergo plastic deformation. To prevent elastic buckling and plastic deformation, it has been stipulated that the maximum pressure differential is not to exceed either the pressure at which elastic buckling takes place or the pressure at which the membrane stress reaches the yield point.

Clad collapse due to creep may occur if the fuel exhibits a high degree of densification. In this case axial gaps might develop in the pellet stack. The cladding which creeps inwards onto the fuel along the active length of the stack will not be supported by the fuel at these locations. It may collapse into these gaps after a certain residence time. Siemens/KWU uses a stable fuel in which densification is partly compensated for by swelling. Thus, such axial gaps cannot occur in the pellet stack and clad collapse due to creep is ruled out. Furthermore, Siemens/KWU fuel rod cladding tubes are internally pressurized such as to reduce the possibility of the clad collapsing into any unsupported areas along the pellet stack during the residence time in the core. Siemens/KWU has never observed axial gaps in its fuel rods, except for very small gaps which are of no significance as regards clad collapse, and has never experienced a case of collapse due to creep. Analytical treatment of this clad collapse phenomenon is not necessary for Siemens/KWU fuel.

The safety margins with regard to elastic buckling and plastic deformation are calculated for the worst case conditions that are calculated through an "*ad hoc*" MATLAB program. The influence of other relevant parameters will be investigated as well.

For the calculations, the maximum possible coolant pressure (constant in the current analysis) together with the minimum fuel rod internal pressure during the overall irradiation and the most unfavorable cladding dimensions, are used, in order to get the more conservative (minimum) safety margin. These conservative values are used to calculate the buckling pressure in accordance with the following equation (*NASA FSAR 2011*):

$$P_{cr,el} = \left[\frac{E}{4(1-\mu)^2}\right]\left(\frac{h_{min}}{r_{c,o,max}}\right)^3$$

The minimum safety margin with regard to elastic buckling is:

$$S = \frac{P_{cr,el}}{P_D}$$

The pressure leading to deformation of the cladding tube up to the Rp0.2 yield point is calculated using the following formula (*NASA FSAR 2011*):

$$P_{cr,pl} = \frac{h_{min}\left(2R_{p0.2}\right)}{\left(d_{H,a} - h_{min}\right)}$$

where:

$r_{c,o,max}$	maximum value of cladding tube mean radius
$h_{min.}$	local minimum wall thickness
$R_{p0.2}$	0.2 %-yield strength *(200 MPa used as conservative value)*
$d_{H,a}$	cladding tube outside diameter
E	Young's modulus
μ	Poison's ratio
P_D	Pressure difference

The minimum safety margin with regard to plastic deformation is:

$$S = \frac{P_{cr,pl}}{P_D}$$

3.4.1.6 Criteria 9: Cladding Stresses

In addition to the stresses imposed by the difference between the coolant pressure and the rod internal pressure, a number of other stresses occur in the cladding tube, the overall effects of which must be limited. In this way the stress intensity, computed from all individual contributions of stresses according to the energy-of-distortion theory (Von Mises Yield Criterion), must be below the design limit.

The minimum specified strength values of the cladding are used to determine the allowable stresses. This is a conservative procedure as the strength of the cladding tube increases under irradiation. The design limit of the primary membrane stresses that will be used as limit value in the subsequent analysis is 135 MPa, Tab. 11.

Item	Design Limit = Minimum of the following values	400°C	Room Temperature
Primary membrane stresses	0.9 $R_{p0.2}$		
	0.5 R_m		

* Maximum value of $Rp_{0.2}$=300 MPa
$Rp_{0.2}$: 0,2 %-yield strength
R_m: tensile strength

Tab. 11 – Design limits for stress analysis.

3.4.2 Accident conditions

An overview of fuel safety criteria relevant for the fuel performance of CNA-2 NPP are briefly quoted in this section. Reference is given to the document issued by UNIPI and related to "proposal for performing the ATUCHA II accident analyses for licensing purposes (*UNIPI 2008*) according with the international practice (*OECD 2000, European Commission 1999*).

The OECD/CSNI/PWG2 Task Force on Fuel Safety Criteria (TFFSC) performed a technically review of the existing fuel safety criteria, focusing on the 'new design' elements in 1999. The table reported below (Tab. 12) is an outcome of this working group. The figure reports a list of 20 fuel safety criteria. Most of the criteria of the category "C" of the table are relevant for the current analysis, therefore related to LOCA and RIA analysis. New design criteria are not of interest of the current analysis.

In the framework of the OECD working group of fuel safety, it is under preparation a review of the (*OECD 2000*) to account for new phenomena that occurs at high burnup fuel, but it is not of interest to Atucha-II NPP.

Specific acceptance criteria for design basis accidents for CNA-2 NPP are reported in Tab. 13. Criteria that can be addressed by TU code are highlighted in red. It should be noted that, as for Atucha II, LB-LOCA are classified as SBDBA, the fulfillment of all DBA criteria is not mandatory but it is investigated.

Safety related criteria	Category	"New" elements affecting criteria	*List of "new" design elements*
(a) CPR/DNBR	A, B, C	1, 2, 5, 6, 7, 9	*1. New fuel designs*
(b) reactivity coefficient	B, C	2, 5, 6, 7, 8, 9	*2. New core designs*
(c) shutdown margin	A, B, C	1, 2, 5, 6, 7, 8, 11	*3. New cladding materials*
(d) enrichment	A, B, C	1, 2, 5	*4. New manufacturing procedures*
(e) crud deposition	A	1, 2, 3, 4, 5, 7, 10	*5. Long fuel cycle*
(f) strain level	A, B	1, 3, 4, 7, 8	*6. Uprated power*
(g) oxidation	A, B, C	3, 4, 7, 8, 10	*7. High burnup*
(h) hydride concentration	A, B, C	3, 4, 7, 8, 10	*8. MOX*
(i) internal gas pressure	A, B, C	1, 5, 6, 7, 8	*9. Mixed core*
(j) therm. - mech. loads	A, B	1, 3, 4, 7	10. *Water chemistry changes*
(k) PCI	A, B, C	1, 2, 3, 4, 6, 7, 8, 11	11. *Current / new operating practices*
(l) fuel fragmentation (RIA)	C	7, 8	
(m) fuel failure (RIA)	C	1, 3, 4, 7, 8	
(n) cladding embrittlement / PCT (non-LOCA run away oxidation)	C	3, 4, 7, 8	*Categories:*
(o) cladding embrittlement / oxidation	C	3, 4, 7, 8	*A – normal operation*
(p) blowdown / seismic loads	C	3, 7	*B – anticipated transients*
(q) assembly holddown force	A, B, C	1, 11	*C – postulated accidents*
(r) coolant activity	A, B, C	5, 6, 7, 8	
(s) gap activity	C	5, 6, 7, 8	
(t) source term	C	5, 6, 7, 8	

Tab. 12 – Fuel safety criteria from (OECD 2000).

Safety Parameter	Criterion for the DBA
Fuel temperature	$T_{max}<T_{melt}$ for 90% of pellet cross section at hot spot
Fuel enthalpy (for RIA)	Average fuel hot spot enthalpy < 230 cal/g for irradiated fuel
Heat transfer cladding/coolant	Departure from nucleate boiling (DNB) is admissible, except for the cases listed below under *
Clad temperature	T_{clad} < 1200 °C except for the cases listed below under * when T_{clad} < 650 °C
Clad integrity (for LOCA)	Limited loss of integrity admissible Maximum local oxidation < 17%
Core-wide oxidation (for LOCA)	Maximum hydrogen generation H_2 < 1% of H_{2TOTAL}
Operation of PZR safety valves	Challenge admissible
RCS pressure	ASME Code Level C Service Limit ($p < 1.2\ p_{design}$)
Secondary side pressure	ASME Code Level B Service Limit ($p < 1.2\ p_{design}$)
Containment pressure	Maximum pressure < design pressure
Permissible dose	Calculated doses below limits 10CFR50.67 0.25 Sv total effective dose equivalent 0.05 Sv total effective dose equivalent for control room

* Examples of events with potential primary medium release outside the containment are:
- SG tube or moderator cooler tube rupture (with emergency mode)
- Long term loss of main heat sink with SG or moderator cooler tube leakage (equal to operational leakages)
- Main steam line rupture outside containment with SG or moderator tube leakage
- Break of an instrument line in the annulus.

Tab. 13 – Specific Acceptance Criteria for Design Basis Accidents from (UNIPI 2008).

4. CODES AND MODELING

This section provides the description of the codes and nodalizations used for the application of the methodology developed and applied in the framework of the currnet Ph.D.

4.1 Description of the codes

4.1.1 Thermal-hydraulic code: RELAP5-3D©

The Relap5/3D© code is an outgrowth of the Relap5/Mod3 code developed at the Idaho National Engineering & Environmental Laboratory (INEEL) for the U.S. Nuclear Regulatory Commission (NRC), (*RELAP5-3D© 2005*). Development of the Relap5 code series began at the INEEL under NRC sponsorship in 1975 and continued through several released versions, ending in October 1997 with the release of the Relap5/Mod3.3. The U.S. Department of Energy (DOE) began sponsoring additional Relap5 development in the early 1980s to meet its own reactor safety assessment needs. The Relap5 code was chosen as the thermal-hydraulic analysis tool because of its widespread acceptance to perform a systematic safety analyses of all NPP installed at the United States.

The application of Relap5 to these various reactor designs created the need for new modeling capabilities (e.g. a three-dimensional flow model and heavy water properties added to the code). All together, DOE sponsored improvements and enhancements have amounted to a multimillion-dollar investment in the code.

Toward the end of 1995, it became clear that the efficiencies realized by the maintenance of a single source code for use by both NRC and DOE were being overcome by the extra effort required to accommodate sometimes conflicting requirements. The code was therefore “split” into two versions, one for NRC and the other for DOE. The DOE version maintained all of the capabilities and validation history of the predecessor code, plus the added capabilities that had been sponsored by the DOE before and after the split (*Johnsen 2008*).

The Relap5 code is highly generic and can be used for simulation of a wide variety of hydraulic and thermal transients in both nuclear and non-nuclear systems involving mixtures of steam, water, non-condensable and solute. The developers wanted to create a code version suitable for the analysis of all transient and postulated accidents in LWR systems, including small and large break Loss Of Coolant Accidents (LOCA).

Based on one-dimensional, transient, and non-homogeneous and non-equilibrium hydrodynamic model for the steam and liquid phases, Relap5 code uses a set of six partial derivative balance equations and can treat a non-condensable component in the steam phase and a non-volatile component (boron) in the liquid phase.

A partially implicit numeric scheme is used to solve the equations inside control volumes connected by junctions. The fluid scalar proprieties (pressure, energy, density and void fraction) are the average fluid condition in the volume and are

viewed located at the control volume centre. The fluid vector properties, i.e. velocities, are located at the junctions and are associated with mass and energy flows between control volumes that are connected in series, using junctions to represents flow paths. The direction associated to the control volume is positive from the inlet to the outlet.

Heat flow paths are also modelled in a one-dimensional sense, using a staggered mesh to calculate temperatures and heat flux vectors. Heat structures and hydrodynamic control volumes are connected through heat flux, calculated using a boiling heat transfer formulation. These structures are used to simulate pipe walls, heater elements, nuclear fuel pins and heat exchanger surfaces, (*RELAP5-3D© 2005*).

The most prominent attribute that distinguishes the DOE code from the NRC code is the fully integrated, multi-dimensional thermal-hydraulic and kinetic modeling capability in the DOE code. This removes any restrictions on the applicability of the code to the full range of postulated reactor accidents.

The development of the three-dimensional hydrodynamic model in Relap5 began in 1990. Since then development and testing has continued from both planned improvements and responses to user requests. The multi-dimensional component in Relap5/3D© was developed to allow the user to more accurately model the multi-dimensional flow behavior that can be exhibited in any component or region of a LWR system. Typically, this will be the lower plenum, core, upper plenum and down-comer regions. The component defines a one, two, or three-dimensional array of volumes and the internal junctions connecting them. The geometry can be either Cartesian (x, y, z) or cylindrical (r, θ, z). An orthogonal, three-dimensional grid is defined by mesh interval input data in each of the three coordinate directions.

Other enhancements include a new matrix solver, new water properties, improved time advancement for greater robustness, a Graphical User Interface, multidimensional heat conduction model for modeling graphite structures in RBMK reactors, (*Johnsen, 2008*).

Thermal-hydraulic system code
The TH SYS code is considered fully qualified for LBLOCA applications including the scenario expected in the Atucha-2 NPP, according to the requirements set in (*D'Auria 1998, D'Auria 2006*). However, specific code-nodalization validation studies focusing on phenomena expected in case of the Atucha-2 LBLOCA have been performed (*D'Auria 2008*). This also includes checks performed for evaluating differences in case of blow-down transient evolution between heavy water and light water fluid evolutions.

4.1.2 3D NK-TH coupled code: NESTLE

The Relap5-3D© code allows to calculate a 3D core power distribution thanks to multi-dimensional neutron kinetics models based on Nestle code, (*Turinsky 1994*), developed by Paul Turinsky and his co-workers at the North Carolina State

University. This feature allows computing the reactor fission power in either Cartesian or hexagonal geometry.

The Nodal Expansion Method (NEM) is used to solve the neutron diffusion equations for the neutron flux in either two or four neutron energy groups. Quartic or quadratic polynomial expansions for the transverse integrated fluxes are employed for Cartesian or hexagonal geometries, respectively. Transverse leakage terms are represented by a quadratic polynomial or constant for Cartesian or hexagonal geometry, respectively. Therefore Relap5-3D© can solve the steady state eigenvalue (criticality) and/or eigenvalue initiated transient problems.

The subroutines taken from the Nestle source code used to solve these problems were modified to be compatible with the coding standards and data storage methodology used in Relap5-3D©, and were inserted into Relap5-3D©. Relap5-3D© was modified to call the appropriate Nestle subroutines depending upon the options chosen by the user.

As said before, two or four energy groups can be utilized, with all groups being thermal groups (i.e. “up-scatter” exits) if desired. Three, two and one dimensional models can be utilized. Various core symmetry options are available, including quarter, half and full core for Cartesian geometry and one-sixth, one-third and full core for hexagonal geometry. Zero flux, non-reentrant current, reflective and cyclic boundary conditions are treated.

Discontinuity factors are utilized to correct for homogenization errors. Transient problems utilize a user specified number of delayed neutron precursor groups. Time discretization is done in a fully implicit manner utilizing a first-order difference operator for the diffusion equation. The precursor equations are analytically solved assuming the fission rate behaves linearly over a time-step. Independent of problem type, an outer-inner iterative strategy is employed to solve the resulting matrix system.

Outer iterations can employ Chebychev acceleration and the Fixed Source Scaling Technique to accelerate convergence. Inner iterations employ either color line or point SOR iteration schemes, dependent upon problem geometry.

Values of the energy group dependent optimum relaxation parameter and the number of inner iterations per outer iteration to achieve a specified L2 relative error reduction are determined a priori. The non-linear iterative strategy associated with the nodal expansion method is utilized. This has advantages in regard to reducing FLOP count and memory size requirements versus the more conventional linear iterative strategy utilized in the surface response formulation.

In addition, by selecting to not update the coupling coefficients in the non-linear iterative strategy, the finite difference method (FDM) representation, utilizing the box scheme, of the few-group neutron diffusion equation results. The implication is that the model can be utilized to solve either the nodal or FDM representation of the few-group neutron diffusion equation.

The neutron kinetics subroutines require as input the neutron cross-sections in the computational nodes of the kinetics mesh. A neutron cross-section model has been implemented that allows the neutron cross-sections to be parameterized as functions of Relap5-3D© heat structure temperatures, fluid void fraction or fluid density, poison concentration, and fluid temperatures. Thus this feature allows Relap5-3D© to be suitable for Atucha-II studies, allowing to calculate the coolant density and the fuel temperature feed-back effects.

A flexible coupling scheme between the neutron kinetics mesh and the thermal-hydraulics spatial mesh has been developed to minimize the input data needed to specify the neutron cross-sections in terms of Relap5-3D© thermal-hydraulic variables.

A control rod model has been implemented so that the effect of the initial position and subsequent movement of the control rods during transients may be taken into account in the computation of the neutron cross-sections. The control system has been modified to allow the movement of control rods by control variables.

The Helios code is used to derive macroscopic cross sections thus supporting the application of the Nestle code.

Coupled three-dimensional neutron kinetics and system thermal-hydraulics code
The requirements set in the EC funded Project CRISSUE-S and issued as OECD/NEA document, (*D'Auria 2004, Bousbia 2004*), are considered in relation to the coupled 3D NK - SYS TH code. Furthermore, the implementation of the Nestle neutron kinetics has been verified by the simulation of the NEA-CRP three dimensional benchmark problems, (*Finnemann, 1992*), involving a series of three PWR rod ejection transient scenarios at Hot Zero Power and Hot Full Power.

4.1.3 Fuel behavior code: TRANSURANUS

TRANSURANUS is a computer program for the thermal and mechanical analysis of fuel rods in nuclear reactors. The TRANSURANUS code consists of a clearly defined mechanical–mathematical framework into which physical models can easily be incorporated. The mechanical–mathematical concept consists of a superposition of a one-dimensional radial and axial description (the so called quasi two-dimensional or 1½-D model). The code was specifically designed for the analysis of a whole rod (*Lassmann 2009, Van Uffelen 2006*).

The TRANSURANUS code incorporates physical models for simulating the thermal and radiation densification of the fuel, the fuel swelling, the fuel cracking and relocation, the generation of fission gases, the redistribution of oxygen and plutonium, etc. Mainly research institutions, industries and license bodies exploit the code. Besides its flexibility for fuel rod design, the TRANSURANUS code can deal with a wide range of different situations, as given in experiments, under normal, off-normal and accident conditions. The time scale of the problems to be treated may range from milliseconds to years. The code has a comprehensive material data bank for oxide, mixed oxide, carbide and nitride fuels, Zircaloy and steel claddings and several different coolants. It can be employed in two different versions: as a deterministic and as a statistical code.

4.1.3.1 Modeling of phenomena and processes relevant to LOCA and RIA

4.1.3.1.1 Heat transfer

In general three regimes must be covered in a LWR:

1. The sub-cooled regime, where only surface boiling occurs. This regime is typical for PWR's under normal operating conditions.
2. The saturated, two phase regime. This regime is typical for BWR's under normal operating conditions.
3. The saturated or overheated regime. This regime may be reached in all off-normal situations. A typical example is a LOCA.

The fuel rod performance codes use one-dimensional (axial) fluid dynamic equations that can only cope with the first two regimes. For simulating the third type of regime, the whole reactor coolant system needs to be analyzed by means of thermo-hydraulic system codes (*Van Uffelen 2006*).

4.1.3.1.2 Burnup

The thermal and mechanical behavior of a fuel rod depends strongly on complex phenomena that vary with burnup, e.g. heat conduction, local porosity, fission gas release, as well as creep of fuel and cladding (*Lassmann 2009*). Therefore, one of the first steps in describing fuel rod behavior is to calculate at each fuel position

- the fraction of fissile material burnt (local burnup),
- the conversion of ^{238}U to ^{239}Pu and the subsequent buildup and fission of the higher Pu isotopes, and
- the buildup of fission products.

The radial distributions of the fissile material determine:

- the radial power density distribution and hence the source term for the temperature calculations;
- the radial burnup distribution from which the local concentrations of fission products such as Kr, Xe, Cs and Nd are obtained.

The equations used to describe the above phenomena constitute the so-called burnup models. Burnup is usually quoted as rod average burnup or as average burnup of a specific section of the fuel rod. Both values are not to be confused with the local value. For the current analysis, the burnup model TUBRNP is selected.

The TRANSURANUS burnup model (TUBRNP) is based on the proportionality of the local power density, $q'''(r)$, to the neutron flux, $\Phi(r)$, to the concentrations of the relevant isotopes, $N_k(r)$, and to the corresponding one-group fission cross-sections, $\sigma_{f,k}$, that are averaged over the neutron spectrum:

$$q'''(r) \propto \sum_k \sigma_{f,k} N_k(r) \Phi(r) \qquad \text{Eq. (1)}$$

The light water reactor burnup equations are extended tor heavy water reactors. Because of this, the one group, spectrum-averaged cross-sections for neutron absorption and captures used in Eq. (1). are determined.

$$p_1^{HWR} = 0.64\, p_1^{LWR}$$

Eq.(2)

The modification of the cross-sections and the modification of the constant p1 are the only differences compared with the LWR version and constitute the TRANSURANUS-HWR burnup model. The model is contained in the subroutine TUBRNP (*Lassmann 2009, Shubert 2008*).

Regards the phenomena and processes that are affecting the fuel response to the LOCA and RIA transients, as related to the safety criteria, the following considerations can be drawn.

In LOCA, with respect to PCT, the burn-up affects the fuel/cladding temperature due to heat up, in that normally the fuel operating power in normal operation decreases with burn-up due to fuel depletion, and thus also the residual heat during the transient heat up is reduced. Hence the neutron flux and fuel power distribution in the core (calculated by core physics codes) as affected by burn-up are very important. The build-up of Plutonium is also important for calculating (operating power during normal operation and) heat up in the transient. I am not convinced that the fissile radial distribution as such is so very important, but since is part of the overall fissile consumption-build up, in this sense is important.

In LOCA, with respect to ECR, if ECR is the metal wall reduction due to oxidation due to the transient only, then there is nothing to add to what said above, i.e. that burnup affect the heat-up rate and hence cladding temperature, which in turn affects ECR. However, in some countries, such as for instance USA, the ECR is considered as the sum of the metal reduction due to corrosion during base irradiation and the oxidation during the transient. In such a case, burnup has an important influence via corrosion, in that the largest is the base irradiation corrosion, the smaller will be the allowable ECR during the transient (and hence the allowable cladding temperature will also be reduced).

In RIA, with the use of a fixed limit of 230 cal/g, i.e. a value which is burn-up independent, the burn-up would play a positive role, again because the reactivity of the fuel normally decreases with burn-up, due to the decrease of fissile content. Again, core neutron calculations are important for calculating the fissile content and hence the deposited enthalpy in case of RIA. We do know however that a burnup independent criterion of 230 cal/g is totally unrealistic, although many countries still maintain it.

4.1.3.1.3 Failure

The LOCA-specific failure criteria are essential to model the behavior of the fuel rod during severe transient conditions (i.e. LOCA and RIA), which is one of the objectives of the analysis. The cladding failure is generally predicted on the basis of a stress assessment, i.e. the comparison of the calculated tangential stress with a failure threshold implemented in the code. However, due to the significant uncertainty in computing the stress when the cladding deformation is large, a strain-based failure criterion is more appropriate for LOCA conditions (*Erbacher 1982, Van Uffelen 2008, Lassmann 2009*).

The additional criteria of plastic instability and overstrain are selected for the current analysis. Plastic instability is assumed if the effective creep rate is larger than 100 1/h and the effective creep rate is larger than 2 %. Overstrain is assumed if the tangential plastic strain exceeded 50 %. These criteria can be selected by the input variable ICLFAIL.

According to the source of the TU code, the selection of ICLFAIL=1 activates the overstress criterion, ICLFAIL=2 activates the plastic instability and overstrain criteria and ICLFAIL=3 activate both failure criteria. The input parameter ICLFAIL 3 is selected for the reference calculations (*Lassmann 2009*).

Up to now, no specific failure criteria for RIA have been specifically included in the code (*Lassmann 2009*).

4.1.3.1.4 Gap pressure

The gap pressure trend is calculated by the subroutine PINPRS. As soon as a failure of the cladding is predicted the inner pressure becomes equal to the coolant one (*Lassmann 2009*).

4.1.3.1.5 Gas flow

The gas transport from the plenum to the ballooning-burst position is important for sustaining the ballooning and the fuel ejection after burst.

Axial gas flow in a fuel rod during a LOCA is a complicated function of the pre-transient state of the fuel (burnup, irradiation history) and the course of the transient itself where fuel and cladding are heated-up differently and exhibit a differential thermal expansion. The axial gas flow, even if limited by the closed gap between pellets and cladding, could obviously affect the pellet relocation process (as an additional driving force). This driving force is important and influences the timing of relocation as well as the amount of relocated fuel. Conservatively, it can be assumed that due to this force the relocation takes place right after cladding burst and that the total mass of fragments in the ballooned area is equal to the volume of the ballooned section multiplied by fuel density.

This phenomenon cannot be addressed by TU code. Indeed, it must be stressed that the influence of gas flow on fuel behaviour during LOCA is not well known. This requires the availability of specific experimental investigations (*OECD 2009, OECD 2010-5, OECD 2010-65*).

4.1.3.1.6 Anisotropy of the cladding

An important parameter to account for LOCA analysis is the anisotropy of the cladding. The zirconium alloys are very anisotropic when they are in the hexagonal α-phase condition. LOCA specific values are used for the analysis.

The anisotropy plays an important role in case of non-uniform temperature distribution along the fuel rod, since it may cause the bending of the fuel rod and impairs the coolability. The bending issue cannot be addressed by TRANSURANUS code (*OECD 2009*).

4.1.3.1.7 α-β Phase transformation

The ZRBETA subprogram gives the fraction of the β crystallographic phase in Zr-based claddings. Basically there are two approaches in TU code for defining the fraction of the β-phase in Zircaloy. The first approach is a static model in which the β-phase fraction is a simple function of the temperature assuming thermal equilibrium. The second approach is a dynamic model considering the hysteresis effect of the heating and cooling rates. Both approaches are based on Forgeron´s methodology (*Forgeron 2000, Van Uffelen 2008*). The suitable model is selected through the input variable IPHASEZR.

4.1.3.1.8 Oxidation

The effect of the outer cladding corrosion is twofold. Firstly, the corrosion layer may increase the thermal resistance of the cladding (thermal effect) and secondly, corrosion means that the cladding thickness of the original material decreases (mechanical effect). Through input options of TU, either the thermal effect alone, or both the thermal and the mechanical effect can be taken into account (subroutine OUTCOR, input parameter ICORRO).

The breakaway oxidation, which occurs at specific temperature ranges, is identified as a major problem for the cladding LOCA performance, since it is associated with a significant hydrogen pickup, which degrades post-quench properties. Therefore, careful examinations are required also for advanced high corrosion-resistance cladding alloys to examine the temperature-time range where the breakaway oxidation occurs.

The subroutine HTCLOX is incorporated in the corrosion model (OUTCOR), and it is in charge to simulate the zirconium-steam reaction during loss of coolant accident (LOCA) conditions. The routine calculates the ZrO2 layer thickness and the oxygen mass gain through a simple recursive formula, which is appropriate for transient (varying temperature) conditions, assuming an isothermal oxidation process only during one time step interval. The evolution of the oxidation in one time step is dominated by the actual value of the temperature-dependent reaction rate constant. The cumulative extent of the oxidation (oxide layer thickness or oxygen mass gain) depends also on its initial value at the beginning of the time step and on the time step length, as well.

There are five optional sets of parameters in TU code in the model to calculate the reaction rates for the mass gain and the oxide layer growth (*Lassmann 2009*).

4.1.3.1.9 Fuel fragmentation and relocation

Oxide fuel cracks into many pieces during normal operation. In a LOCA transient, temperature changes within a few seconds in parallel to radial temperature redistributions in the pellet of several hundreds of °C. This induces enough temperature stresses to promote fragmentation.

The subroutine CRCKVT of the TU code calculates the average value of the quantity "local crack volume divided by local temperature" for each axial section or slice. This is used for calculating the pin pressure.

The consequences of cracking are important in fuel performance modeling. Owing to the larger thermal expansion of the fuel fragments in comparison with that of a monolithic cylinder, and due to vibration-induced motion they move outwards. This is called pellet “relocation” and has a strong impact on the thermal behavior. It reduces the pellet-cladding gap size, thereby reducing the temperature levels in the fuel at beginning-of-life. This constitutes the largest contribution to gap closure but it is also subjected to the largest uncertainty, because of stochastic nature of the cracking process. This also raises questions about the usefulness of applying 3D stress calculations. The contribution from relocation is generally accounted for in the tangential strain.

The mechanism for relocation needs to be better characterised as related to its occurrence during the ballooning phase or after the cladding burst. The slumping of fuel fragments may involve a significant amount of fuel, with partial relocation in the ballooned region and partial dispersal outside the cladding.

The relocation of fuel fragments into the balloon and fuel dispersal have several consequences (*OECD 2009, OECD 2010-5, OECD 2010-65*).

- Change of power profile. Fuel accumulating in the balloon will create a local power peak.
- Release of fine pellet fragments through the burst opening.
- Possible accumulation of ejected fuel on grids or structures. If a significant amount of fuel is released into the assembly structure, this may impair the coolable geometry.

The relocation is calculated in the IRELOC subroutine of TU code (*Lassmann 2009*).

4.2 Description of the nodalizations

4.2.1 Description of the nodalizations: THERMAL-HYDRAULIC

Different nodalizations have been developed to run the TH - SYS and coupled 3D NK / TH - SYS codes, as summarized hereafter. The nodalizations listed in Tab. 14 have been developed and/or adopted for predicting the Atucha-2 LBLOCA performance within the current framework.

The first two nodalizations have been developed by NA-SA, the remaining 4 from UNIPI. For the nodalization identified as No 1, only the results are available at UNIPI.

A preparatory work for the analysis was performed with the aim of selected the most suitable nodalization for the subsequent fuel analysis. For this aim, two nodalizations are selected: No 5 and No 6 of Tab. 14.

The analyses performed address the short (10s), and the long (3000s) term of the transient. The former No 5, is calculated with a detailed nodalization coupled with the 3D-NK ("280ch"), the latter, No 6, is analyzed with a more simplified model ("60ch"), which uses the 0D-NK and is coupled with the protection, limitation, and control systems of the NPP (*D'Auria 2008*). Here below only a description is present, the discussion of the selection of the most suitable nodalization is performed in section 6.

#	ID	By	No of hyd. nodes / No of mesh points	Notes
1	NASA_3CH	**NASA**	Not Available	Results available at UNIPI
2	NASA_UNIPI_36CH		2527 16604	Modified at UNIPI to run with Relap5/3D©
3	UNIPI_280CH_1D-MT_0DNK	**UNIPI**	5744 66955	Consistency checks performed
4	UNIPI_280CH_1D-MT_3DNK		6342 53334	
5	UNIPI_280CH_3D-MT_3DNK		6342 53334	Sensitivity study – Reference calculation (short term)
6	UNIPI_60CH_1D-MT_0DNK		2453 21223	Full ECCS & logics – Reference calculation (long term)

Tab. 14 – Nodalizations for TH-SYS considered for the LBLOCA analysis of CNA-2.

4.2.1.1 UNIPI 280 core channels modeling

The 451 real core channels of CNA-2 are represented by 280 equivalent pipes. The criterion used to group the channels derives from the nodalization of the LP grid and the presence of the 5 throttle types. The channels that are going to be grouped belong to the same rhomboidal sub-plena (derived from the 5 radial regions and the 36 angular sectors) and have the same throttle type.

Each equivalent pipe is subdivided in 15 sub-volumes, ten of these are used to represent the active length, Fig. 26. The heat structure of the coolant channel is modeled as a cylinder including the water gap simulated as an equivalent material. Left side of such structure is connected to the hydraulic part of the channel while the right side is linked to the pipes that model the moderator tank. A second heat structure is linked to the hydraulic part of the channel to account for the active power generation (fuel), a cylindrical geometry is used too.

A global picture of the RPV nodalization is given in Fig. 27 that represents all the various parts described above and how they are interconnected. The HL and CL axis are identified together with the active length.

In order to be consistent with the 3D NK model and to simulate in a realistic manner the boron injection process into the moderator tank, the 3D capability of the RELAP5-3D© code was exploited for this component. Three 'MULTID' components have been used: one for the bottom part, one for the active zone and the last one for the upper part of the tank. The three 'MULTID' nodes have a cylindrical geometry with 6 radial rings, 16 azimuthal divisions and the active zone height divided into ten parts,
Fig. 28. More than 1000 volumes are adopted to simulate the moderator tank. The adopted code resources are reported in Tab. 15.

The tank (from the metal point of view) is simulated by a cylindrical heat structure including the water gap represented by an equivalent material. This structure is thermally connected to the DC from one side and to the radial reflector to the other.

No.	Code resource	Quantity
1	No of nodes	6342
2	No. of junctions	7155
3	No. of heat structures	8340
4	No. of mesh points	53334
5	No. of active structures	280
6	No. of trips	10
7	No. of input lines*	115918

** including the 3D NK model*

Tab. 15 – UNIPI_280CH_3D-MT nodalization: adopted code resources.

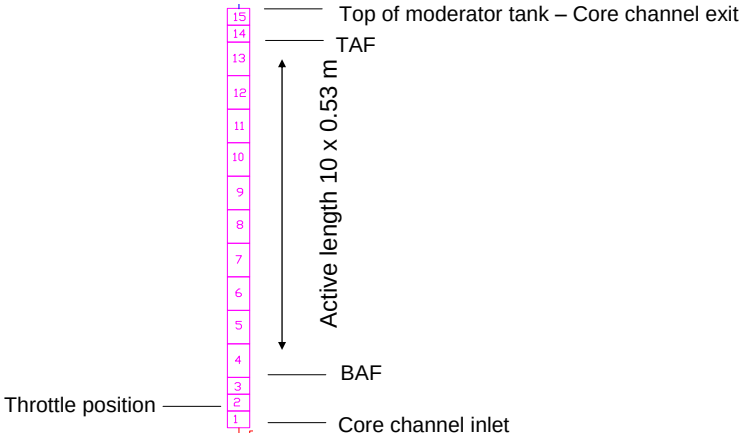

Fig. 26 – UNIPI_280CH_3D-MT nodalization: core channel and connected geometrical relevant positions.

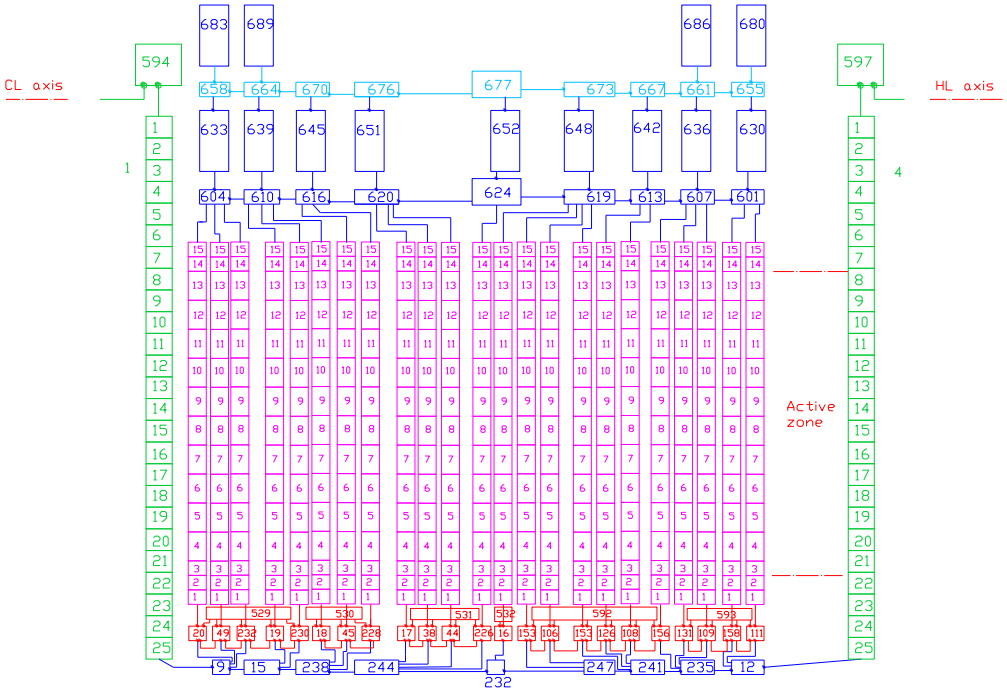

Fig. 27 – UNIPI_280CH_3D-MT nodalization: global RPV sketch including LP, DC, core channels (not all) and UP.

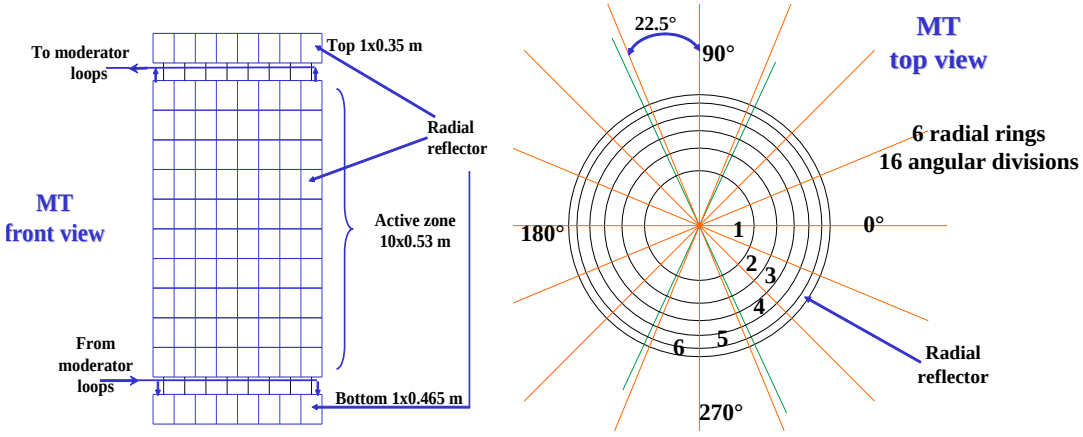

Fig. 28 – UNIPI_280CH_3D-MT nodalization: the moderator tank 3D model, front and top view.

4.2.1.2 UNIPI 60 core channels modeling

The UNIPI_60CH_1D-MT nodalization is derived from the UNIPI_280CH_1D-MT, having in mind the objective of the long term calculations. It has been set up by gathering some nodes of the RPV. The main differences between the two nodalizations are reported hereafter.

The simplifications introduced in the 60 core channels nodalization concerns the second layer of the LP and consequently the of the equivalent core channels. The 200 branches constituting the second LP have been collapsed into 25 branches replicating the same scheme adopted for the first LP layer. To reduce the core channels (from 280 to 60) the equivalent pipes are grouped belong to the same hydraulic zone, to respect the basic approach of the detailed nodalization. The core channels are connected to the first UP layer with the junctions embedded in the branch components.

The adopted code resources are given in Tab. 16.

No.	Code resource	Quantity
1	No of nodes	2453
2	No. of junctions	3073
3	No. of heat structures	2917
4	No. of mesh points	21223
5	No. of active structures	60
6	No. of trips	600
7	No. of lines of the input	20874

Tab. 16 – UNIPI_60CH_1D-MT nodalization: adopted code resources.

4.2.2 Description of the nodalizations: NEUTRON-KINETICS

In the case of 0D-NK model, the peak factors are derived from the power map supplied by NA-SA that includes 451 channels divided in 10 axial meshes. In case of lumped channels the peak factor of the corresponding pipe is evaluated normalizing the sum of each peak factors. The 0D NK model was set up for the 280 channels nodalization and then the derived for the 60 channels.

A 3D-NK model has been developed for the 280 channels nodalization, in order to maximize the number of the NK nodes coupled with a single fuel channel, thus reducing the approximation on the feedbacks. The correspondence between 451 NK nodes and 280 TH channels is reported in Fig. 29, reflector NK nodes are not reported (*Parisi 2008*).

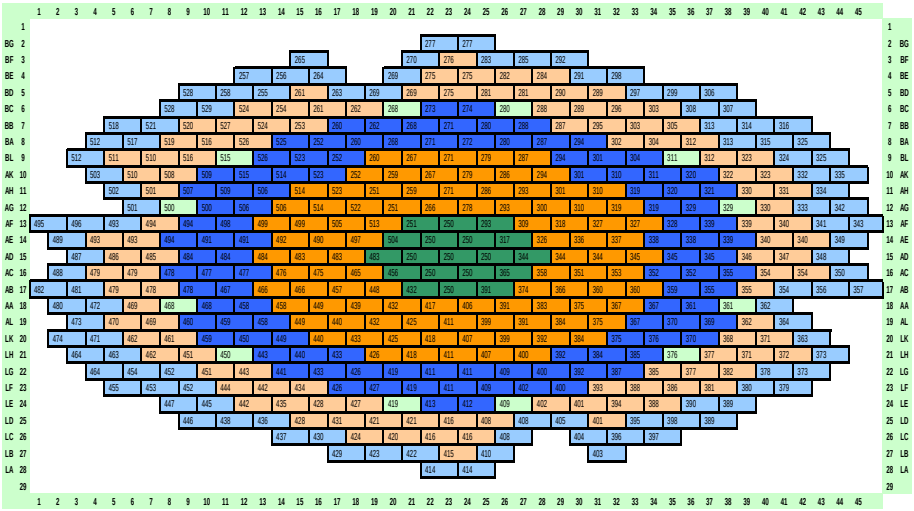

Fig. 29 – RELAP5-3D© TH-NK coupling map for the fuel channels.

4.2.3 Description of the nodalizations: TRANSURANUS

The input data is suitable to be used for the TRANSURANUS code version "*v1m1j09*". The input data of the TRANSURANUS code can be divided in two types: control options and values of various physical and numerical quantities. The setting of control options allows selecting particular submodels or bypassing a section of the code. The values of the various geometrical and physical quantities are set as input, and are specific to CNA-2.

Boundary conditions of the problem are reported in the input file in the MACRO part.

4.2.3.1 Input model: Control options

The active length of the fuel rod is divided into 10 axial segments according to the detail of the RELAP model (Fig. 30), called axial "slices". In TRANSURANUS code the analysis is performed slice per slice, starting from slice No 1 up to slice No 10. An additional slice is modeled to consider the gas plenum volume. In addition to this, because of some structures inside the plenum (e.g. the spring), the real volume is lower. This is accounted for by employing the user-supplied factor AOPL. The fuel pellet dishing is accounted for as well.

For the radial discretization, the fuel and the cladding are divided into 6 rings, 5 for the fuel and 1 for the cladding, in which the elasticity modulus E and Poisson's number v are isotropic and constant. These rings are called coarse zones. In order to perform the numerical integrations, each coarse zone is divided further into 94 finer zones (see Fig. 31).

It should be noted that at each boundary of two coarse zones in fuel and cladding two mesh points with the same radial position exist. No axial and radial variations of specific quantities are present in the model at the beginning of the calculations.

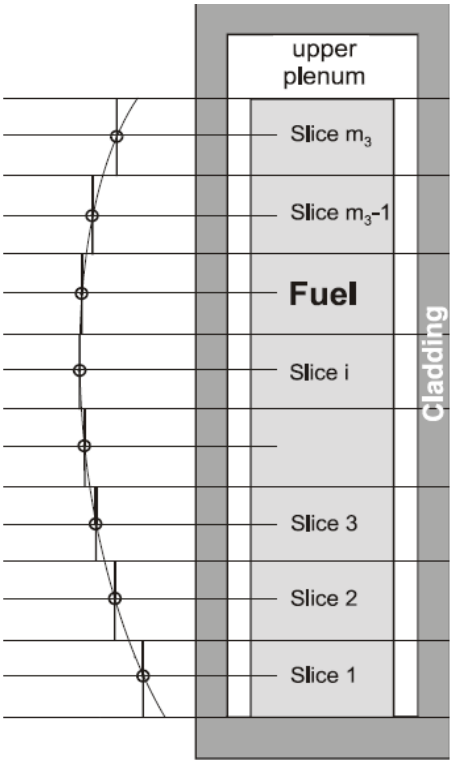

Fig. 30 – Schematic representation of the axial discretization.

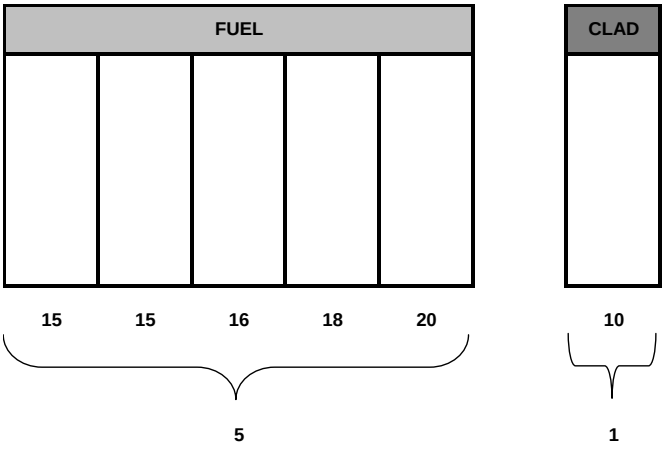

Fig. 31 – Radial discretization of a slice.

4.2.3.2 LOCA specific input

TRANSURANUS code allows the selection of material property options for the LOCA analysis in a separated block of the input. The transition from normal to LOCA-specific models occurs at a time point defined by the first input variable of the LOCA input block (TLOCA).

The boundary conditions for the accident analysis are specified in the macro input block for the time points greater that TLOCA.

On the basis of the defined boundary conditions the code calculates the temperature distribution and the fission gas release inside the fuel rod, the corresponding inner pressure, the ZrO2 thickness growth, the equivalent oxidation (ECR) and the plastic deformation (ballooning) of the cladding.

The typical stress-based failure criterion is activated in the input, together with a strain-based one that is more appropriate for LOCA because of large uncertainty in the stress computation at large cladding deformation (*Lassmann 2009, Van Uffelen 2008*) (variable ICLFAIL in the LOCA block). Strain threshold is set to 2.5% (EPSLIM) according to CNA-2 specific data, strain rate threshold is set to 100 1/h (STRLIM), default value of the code.

Cathcart-Pawel steam oxidation correlation has been selected for the calculation of the outer cladding corrosion model during LOCA analysis, in this model also the thinning of the cladding is considered.

The local creep rate and the true tangential stress at the rupture of the cladding are calculated by the correlations implemented by G. Spykman at TÜV Nord specific for Zircaloy-4 under LOCA conditions. The fraction of the β crystallographic phase in Zr-based claddings is calculated using correlation based on Forgeron´s methodology, static and dynamic models and both considered.

4.2.4 CNA-2 specifics and TU modeling

This section contains the comparisons between the specific CNA-2 properties of the fuel and the cladding and the comparison with the correlations and models implemented in the TU code. The section is divided between cladding and fuel properties. The effect of these differences on the code results is addressed in related to the sensitivity analyses.

4.2.4.1 Cladding Mechanical properties

4.2.4.2 Young's modulus

Young's modulus of elasticity of Zircaloy, as specified from (*NASA 2007*), is temperature dependent. This yields the following relation:

[redacted]

with:

E: Young's modulus (N/mm2)
(theta): Temperature (ºC)

The correlation to model the Young's modulus implemented in TU code (*NASA 2007*) produces a discrepancy of about [redacted] MPa at room temperature, the discrepancy increases up to about [redacted] MPa at 1000°C, as shown in Fig. 32.

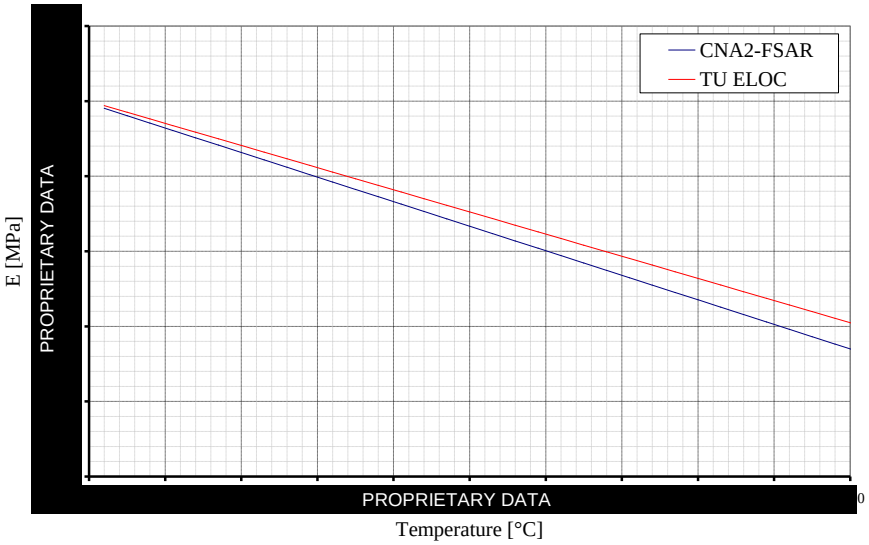

Fig. 32 – Young's modulus of elasticity of Zircaloy as available from (NASA 2007) and as implemented in TU code (Lassmann 2009).

4.2.4.3 Poisson's ratio

The Poisson's ratio available from Ref. (*NASA 2007*) is a constant value of 0.3 independent on temperature and irradiation. TU standard code version v1m1j08 uses a constant value of 0.325.

4.2.4.4 Strength

From Ref. (*NASA 2007*) the value of yield strength at room temperature and at 400°C are specified as follow:

- [redacted] N/mm^2 at room temperature;
- [redacted] N/mm^2 at 400°C.

In TU code a constant value of 350 MPa is implemented. From (*NASA 2007*) the value of tensile strength at room temperature and at 400°C are specified as follow:

- ≥ [redacted] N/mm^2 at room temperature;
- ≥ [redacted] N/mm^2 at 400°C.

The correlation to model the burst stress implemented in TU code (*Lassmann 2009*) produces a discrepancy lower than about [redacted] MPa, as shown in Fig. 33.

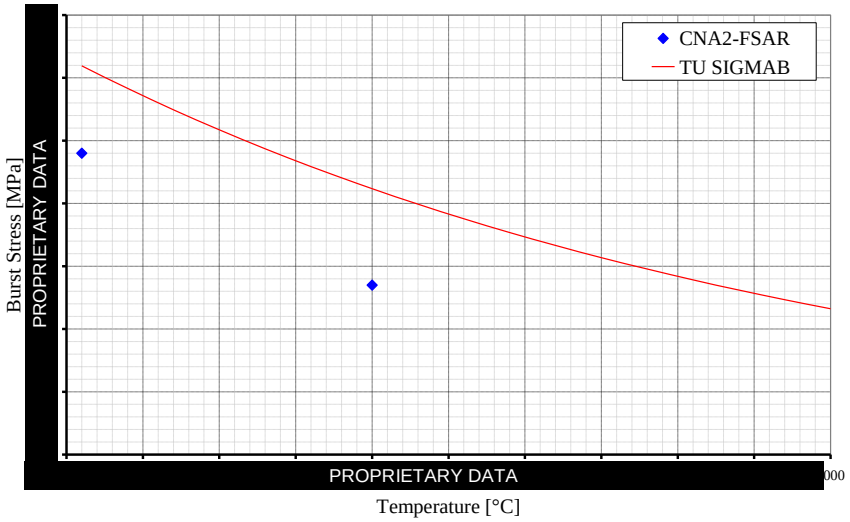

Fig. 33 – Burst stress of Zircaloy as available from (NASA 2007) and as implemented in TU code (Lassmann 2009).

4.2.4.5 Fuel thermal physical properties

4.2.4.5.1 Melting point

The melting point of pure unirradiated UO2 is 2837°C and it decrease with burnup. For design purposes, (*NASA 2007*), the following relation is used:

[redacted]

with

(theta)M: Melting point (°C)

A: Burnup (MWd/kg(U))

The correlation to model the melting temperature implemented in TU code (*Lassmann 2009*) produces a discrepancy that range from [redacted]C to about 20 °C at fresh fuel and at discharge burnup, respectively (*NASA 2007*). It should be noted that the variation of melting temperature from (*NASA 2007*) is calculated on the basis of burnup whereas the correlation to model the melting temperature implemented in TU code is based on the local plutonium concentration variation.

4.2.5 Input model: MACRO part

In general, conditions during an irradiation vary which means that time dependent quantities need to be prescribed. In order to be as flexible as possible, TRANSURANUS allows the use of any complicated time-dependency through the macro time step concept. The user prescribes varying quantities at the beginning and at the end of a macro time step which may be of any length. Within such a

macro time step all quantities are interpolated linearly. Due to the various time step control criteria, the macro time step is further divided into the so-called micro time steps (*Lassmann 2009*).

The details of the selection of the BIC for the fuel analysis, together with the description of the selected methodology for performing the analysis, are reported further in section 6.

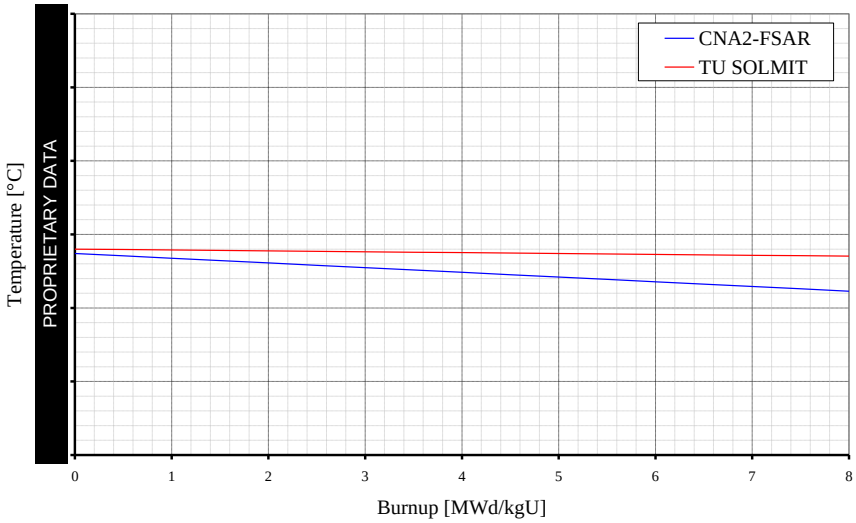

Fig. 34 – Melting temperature of UO2 as available from (NASA 2007) and as implemented in TU code (Lassmann 2009).

5. INDEPENDENT VALIDATION ACTIVITY

In the following section the results of the validation activities performed in the framework of the current PhD are discussed. The section is focused on the applicability of the TRANSURANUS code and of the methodology to CNA-2 NPP, and does not want to be related to the general applicability of TRANSURANUS code, whether it is useful for the application of the code itself. Additional details are reported in separate appendixes. The strategy adopted for the validation of the TRANSURANUS fuel performance code is described as well.

The validation activities are performed to enhance the TRANSURANUS code capabilities and to improve the reliability of the code results. Verification relies on the two main sources of data, reported in Tab. 17; namely:

- specific data on CNA-1 and/or 2, experiments or independent calculations;
- other data which are representative of the CNA-2 fuel: in particular from the International Fuel Performance Experimental database of the IAEA and the OECD/NEA.

Due to the peculiarity of Atucha-2 NPP such as the on-power refueling and the power peak expected in the case of LOCA transient, as described in section 3, the validation activities that are reported in the Tab. 17 are identified and performed to support the reliability of the analysis. The indication of the field of applicability of the analysis, such as normal operation and severe transients like LOCA and RIA are reported as well.

The table contains the general activities performed with the aim of the applicability of CNA-2 NPP. Only the specific activities performed in the framework of the current PhD are hereafter discussed. For the sake of completeness, more detailed tables, that summarizes the status of the validation, with focus on the application to CNA-2, are reported in APPENDIX F.

Tab. 18, Tab. 19 and Tab. 20 report the parameters used for the validation with the indication, for the analyzed databases, if they are or are not suitable for code assessment. The tables differ for the normal operation and severe transients, e.g. LOCA and RIA. The last column of each table reports the indication of the judgment of occurrence or not in the CNA-2 fuel.

A review of the state of the art of the fuel experiments and modeling is out of the scope of this thesis. A number of references are available on this subject (*OECD 2010-1, OECD 2009, OECD 2006-5, OECD 1995-2, OECD 1995-1*).

#	VALIDATION ACTIVITY	NORMAL OPERATION	SEVERE TRANSIENTS	
			LOCA	RIA
CNA-2 specific data				
1	Analytical investigation of power ramps	X		
2	Review of the design of CNA-2 fuel	X		
3	Investigation of data available on CNA-1 fuel and comparison with CNA-2*	X		
4	Feasibility study of combined LOCA & RIA experiment		X	X
From IFPE database				
5	BWR IR	X		
6	PWR SR	X[$]		
7	BWR SR[%]	X[$]		
8	CNEA MOX[%]	X[$]		
9	MT-4 & MT-6A		X	
10	NSRR FK-1, -2, -3			X

* Performed at the Atucha NPP site
[$] Collaboration in performing the activity
[%] Activity performed in the framework of the CNA-2 project, out of the scope of the current PhD – only the validation table is reported in appendix.

Tab. 17 – List of validation activities.

NORMAL OPERATION						
#	PARAMETERS FOR VALIDATION	BWR-IR	PWR-SR	BWR-SR[%]	CNEA-MOX[%]	CNA-2
1	Burnup	●	●	●	●	**P**
2	Cladding max creep down in BI	●	●	○	○	**E**
3	Cladding corrosion and hydrogen content prior to ramps	○	●	●	-	**E**
4	Cladding expansion during power ramp	●	●	●	○	**E**
5	Grain size after ramp (pellet centre/periphery)	○	●	●	●	**E**
6	FGR after ramp	●	●	●	-	**E**
7	Elongation after ramp	○	○	○	-	**E**
8	Ridges height (avg. and max) in BI	●	●	●	-	**E**
9	Ridges height (avg. and max) after ramp	●	●	●	●	**E**
10	Clad ovality after ramp	●	●	●	-	**E**
11	Inner cladding oxidation after ramp	○	●	●	-	**E**
12	Failure / Not Failure	●	●	●	●	**N**
13	Gap dimension	-	-	-	●	**E**
14	Active fuel weight change	●	-	-	-	**E**
15	Iodine burst test (crack dimension and stresses)	○	-	-	-	**N**

● suitable for code assessment — E Expected
○ limited suitability — P Partially expected
– not suitable — N Not expected

[%] Activity performed in the framework of the CNA-2 project, out of the scope of the current PhD, only the validation table is reported in appendix.

Tab. 18 – Normal operation: summary of relevant parameters for validation.

LOCA				
#	PARAMETERS FOR VALIDATION	MT-4	MT-6A	CNA-2
1	Burnup	--	--	P
2	Failure / Non-Failure	●	●	E
3	Pressure trend during the test	●	●	E
4	Time of failure	●	●	E
5	Ballooning	●	○	E
6	Gas flow	--	--	E
7	Cladding strain	●	○	E
8	Geometry changes	●	○	E
9	Coolability	●	○	E
10	Embrittlement	--	--	E
11	α to β-phase transformation	○	○	E
12	Oxidation	○	○	E
13	Fuel fragmentation and relocation	--	--	E
14	Fuel centerline temperature	●	--	E
15	Cladding corrosion and hydrogen content at start of transient	--	--	E
● suitable for code assessment ○ limited suitability ─ not suitable		E Expected P Partially expected N Not expected		

Tab. 19 – Accident conditions: summary of relevant parameters for validation for the LOCA analysis.

RIA					POWER PEAK DURING LOCA
#	PARAMETERS FOR VALIDATION	FK-1	FK-2	FK-3	CNA-2
1	Burnup	●	●	●	E
2	Failure / Non-Failure	--	--	--	P
3	Time of failure	--	--	--	P
4	Peak fuel enthalpy	●	●	●	E
5	Maximum enthalpy increase	●	●	●	E
6	Pulse width (FWHM)	●	●	●	E
7	Fission gas release	○	○	○	P
8	Cladding corrosion and hydrogen content at start of transient	●	●	●	P
● suitable for code assessment ○ limited suitability ─ not suitable		E Expected P Partially expected N Not expected			

Tab. 20 – Accident conditions: summary of relevant parameters for validation for the RIA analysis.

5.1 CNA-2 specific data

Validation activities are performed to enhance the TRANSURANUS code capabilities and to improve the reliability of the code results. These address the compliance with safety and operating criteria during normal operation. This is propaedeutic for the subsequent LOCA analysis. The activities are performed on the base of fuel data of CNA-1, CNA-2 and other data which are representatives of the CNA-2 fuel.

5.1.1 CNA-1&2 Investigation of normal operation

5.1.1.1 Introduction

The objective of the activity is to support the validation of TU code for analyzing the CNA-2 fuel behavior during normal operation conditions. In addition to this, the determination of the failure limits for CNA-2 (and CNA-1) fuel under power ramps is investigated as well. The comparison is performed in three steps:

- comparison with the analysis performed on CNA-1 fuel rods by TRANSURANUS code, see also Fig. 35;
- code to code comparisons with the design analyses performed by SIEMENS about the failure limits due to PCI-SCC for CNA-1 fuel under power ramps and reported in Fig. 36 (*Dusch 1980*);
- review of the design of CNA-2 fuel, according to the safety criteria set up in the FSAR Chapter 4 (*NASA 2007*), recalled in section 3.4 and reported in Tab. 21.

The detail of the modeling of the power ramps for the current report is briefly recalled in APPENDIX B (*Adorni FU-09 2009, Adorni FU-10 2009, Adorni FU-11 2009, Adorni FU-18 2010, Adorni LS_FU-02 2010*).
together with the results of the analyses.

The steps reported in Fig. 37 are performed to carry out the analytical investigation of the power ramps. This is applied to CNA-2 and also to CNA-1 analysis as well.

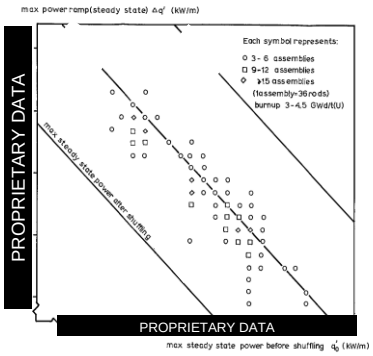

Fig. 35 – Local power ramps during on power refueling of CNA-1 (PSAR 1980).

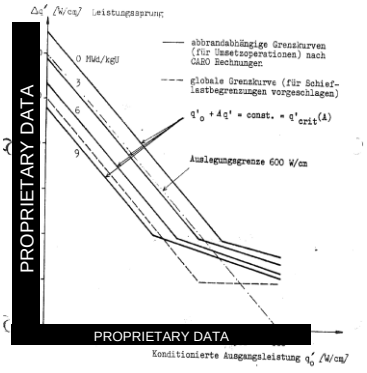

Fig. 36 – PCI limit during on power refueling of CNA-1 (Dusch 1980).

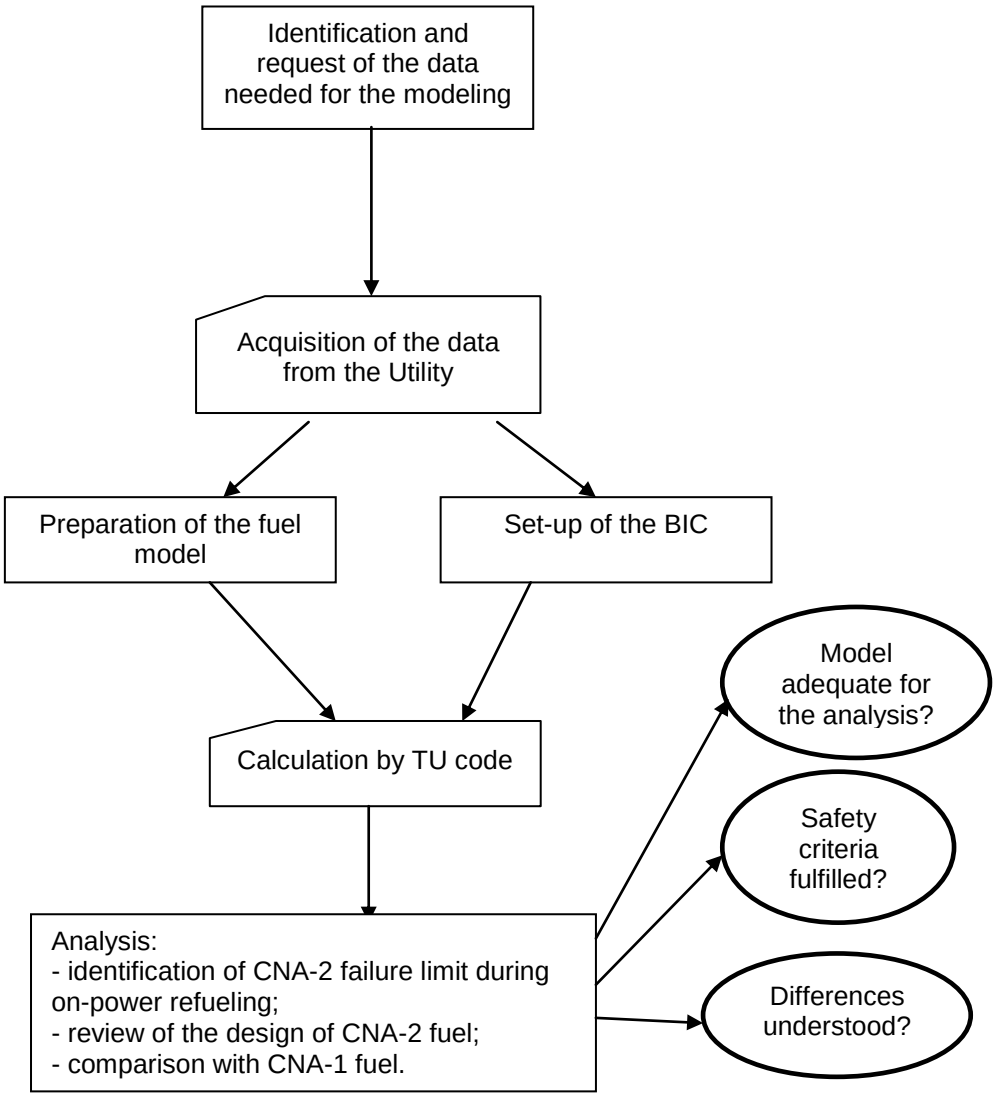

Fig. 37 – Procedure for performing the analysis.

5.1.1.2 Main achievement

The results of the analysis by TRANSURANUS are compared to those performed by (*Dusch 1980*) using SIEMENS CARO code and to the results achieved for CNA-1 fuel.

The relevant results are here briefly recalled:

- The failure maps calculated by TRANSURANUS code result equivalent to the ones obtained for CNA-1 by (*Dusch 1980*).
- The failure maps of the fuel of CNA-2 are similar to those calculated for CNA-1 in the framework of the agreement NASA-UNIPI, notwithstanding the differences between the two fuel designs. In particular, the CNA-2 fuel rods exhibit a slight higher failure limit than the CNA-1 ones, when subjected to the same boundary conditions.
- In all the cases but one (q' 20, Δq' 40) of non equal prediction of failure/non–failure, the CNA-1 fuel is predicted failed and the CNA-2 is not. This suggests that the failure limit of the CNA-2 fuel is higher than the CNA-1 one when the rods are subjected to the same boundary conditions.

Examples of results are reported in Fig. 38 and Fig. 39. The complete set of analysis is reported in (*Adorni FU-10 2009, Adorni FU-11 2009, Adorni FU-18 2010, Adorni LS_FU-02 2010*).

5.1.2 CNA-2 review of the design

The design criteria recalled in section 3.4.1 and reported in Tab. 21 are verified for the CNA-2 fuel analyzed.

The analysis shows that:

- all the rods are comprised below the power ramp failure map developed in the framework of preceding item, see Fig. 40;
- the safety margin as defined in section 3.4.1 for the CNA-2 fuel rods, have all a minimum margin of 30% for the selected quality.

To conclude, all the results are below the limit of section 3.4.1.

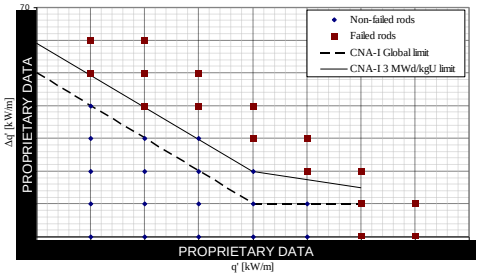

Fig. 38 – Power ramp failure map for CNA-2 fuel together with the global and burnup dependent limits of CNA-1, case of burnup = 3.

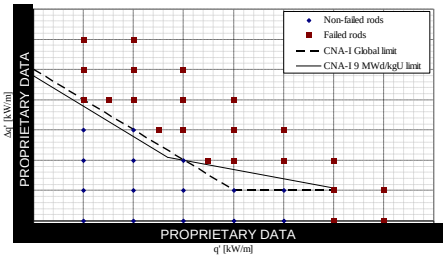

Fig. 39 – Power ramp failure map for CNA-2 fuel together with the global and burnup dependent limits of CNA-1, case of burnup = 8.

#	CNA-2 DESIGN CRITERIA	VERIFIED	NOTE
1	Temperatures	Y	
2	Fuel rod internal pressure	Y	
3	Cladding strain	Y	
4	Cladding strain	Y	Limit implemented in the model
5	Cladding corrosion	Y	
6	*Deuterium pick-up*	*N*	*Not addressed by TU code.*
7	Elastic buckling of the cladding	Y	
8	Plastic deformation of the cladding	Y	
9	Cladding stresses	Y	
10	*Dynamic loads*	*N*	*Not addressed by TU code.*

Tab. 21 – CNA-2 Fuel design criteria.

5.1.3 Feasibility study of LOCA experiment

The objectives of the experiment are to establish the fail-safe limits of the CNA-2 fuel rods during LB-LOCA scenario. Given the peculiarities of the reactor, i.e. the positive void coefficient, the CNA-2 fuel rods experience simultaneously fast energy release in the fuel matrix, such as in the reactivity accident, high temperature of cladding and fast depressurization.

The experiment should also provide relevant information on the consequences of combined power and temperature excursions to the fuel integrity, addressing:

- the failure limits;
- the failure mechanism and associated phenomena;
- the influence of the reload strategy and therefore stress corrosion cracking on failure.

The experimental data have to be useful also for code validation and therefore non-destructive and selected destructive post irradiation examinations (PIE), such as visual examination, dimensional changes, fission-gas release, fuel burn up analysis and grain size measurement, etc. are requested to be available for this purpose.

For the sake of completeness, the details of the design of the experiment are reported in APPENDIX A. The section contains the design of experiments to be performed in a research reactor (e.g. Halden reactor). The activity includes the technical specifications, the specific analyses to define the initial and boundary conditions. The economic evaluation is not reported for confidentiality reasons.

The Halden Boiling Water Reactor is chosen to perform the experiment feasibility study. The relevance of the activity is connected with the funding availability.

5.2 Normal operation: Assessment of FGR against BWR-IR and PWR-SR projects

The experiments address the behavior of standard-type BWR and PWR fuel rods, including preceding base irradiation, during the over-power ramping. The burnup values range between 10 and 45 MWd/kgU. Pre-, during-, and post- irradiation, non destructive and destructive examinations were executed, in order to determine and understand the behavior of the fuel rods, but also to provide suitable data, useful for code validation. The experimental data were used for assessing the TRANSURANUS capabilities in predicting the fission gas release.

5.2.1 Description of the BWR Inter-Ramp experiment

Between July 1, 1975 to July 1, 1979, 20 standard-type unpressurized BWR fuel rods were irradiated and power ramped in the R2 research reactor of Studsvik (Sweden). Individual fuel rod power histories were recorded in great detail, non-destructive and selectively detailed destructive examinations were also made in order to determine the fuel rod changes.

The objectives of the BWR-Inter-Ramp Project were to establish the fail-safe operating limits of 20 standard-type, unpressurized BWR fuel rods on over-power ramping at the burn-up levels of 10 and 20 MWd/kgU. This program also provided suitable data for model development and benchmarking. The over-power ramping is to be performed at a fast ramp rate of about 4 kW/m-min with the preceding base irradiation performed to represent the conditions in a typical commercial BWR power reactor. The study also investigated:

- the influence of three main design parameters on fuel rod performance under power ramping;
- cladding heat treatment (re-crystallized anneal vs cold work plus stress relief anneal);
- pellet/cladding diametral gap size;
- fuel density;
- the failure mechanism and associated phenomena.

The long term pre-ramp irradiation of the rods was performed in the Boiling Capsule (BOCA), introduced in 1973, of the Studsvik R2 research reactor. The BOCA Inter Ramp Project (BIRP) consisted of a pressurized container containing 4 fuel rods.

The power ramp irradiation was performed in the pressurized water loops of the R2 research reactor, containing one rod. The power ramp tests were performed according to the scheme shown in Fig. 41 (more details are reported in (*Mogard 1979*):

- 24 hours conditioning irradiation at the same linear heat rating of the previous cycle, in order to minimize the influence of zero-power period of several weeks;

- power ramp at a constant rate of 4 kW/m-min (~240 kW/m-h);
- ramp terminal level irradiation at ramp terminal power level held for 24 hours or until failure.
- Eleven out of twenty tested rods failed and two non failed rods have been found to contain incipient cracks.
-

Eleven out of twenty tested rods failed and two non failed rods have been found to contain incipient cracks.

Additional informations can be found in (*OECD 2010-7, Adorni 2009, Adorni 2008*).

5.2.2 Description of the PWR Super-Ramp experiment

The Studsvik Super-Ramp Project investigated the failure propensity of typical light water reactor test fuel rods when subjected to power ramps, after base irradiation to high burnup. The Project power ramped 28 individual PWR test fuel rods in a PWR subprogram, analyzed in the current paper, and 16 test fuel rods in a BWR subprogram.

The principal objective of the Super-Ramp Project was to make a substantial and valid contribution to the understanding of the pellet cladding interaction (PCI) performance under power ramp conditions for commercial type LWR reactor test fuel irradiated to high burnup. In particular, the main objectives of the PWR sub-program are here listed:

- establish through experiments the PCI failure threshold of standard design PWR test fuel rods on fast power ramping at high burnup;
- investigate whether or not a change in failure propensity or failure mode is obtained as compared to the failure behavior at lower burnup levels;
- establish the possible increase in PCI failure power levels for candidate PCI remedy design fuel rods at selected burnup levels.

Kraftwert Union AG/Combustion Engineering (KWU/CE) provided 19 fuel rods, which has been irradiated in the power reactor at Obrigheim (Germany). Westinghouse (W) provided 9 fuel rods following the base irradiation in the BR-3 reactor at Mol (Belgium). The main features of the rods are here outlined:

Kraftwert Union AG type rods, UO2 pellet column length of about 310 mm:

- PK1: 5 standard “A” rods, average axial peak position burnup between 33 and 36 MWd/kgU;
- PK2: 5 standard “A” rods, average axial peak position burnup between 41 and 45 MWd/kgU;
- PK4: 4 standard “A” rods plus Gd2O3 (4%), average axial peak position burnup between 33 and 34 MWd/kgU;
- PK6: 5 remedy “G” rods, large grain, average axial peak position burnup between 34 and 37 MWd/kgU;

Westinghouse type rods UO2 pellet column length of about 1136 mm:

- PW3: 5 standard rods rods, average axial peak position burnup between 28 and 31 MWd/kgU;

- PW5: 4 remedy rods, annular pellets, average axial peak position burnup between 32 and 33 MWd/kgU.

The KWU/CE test fuel rods were base irradiated in the commercial pressurized water reactor Obrigheim (KWO) in Germany. Obrigheim Reactor characteristics are given in (*Djurle 1984*). The test fuel rods were irradiated as the five middle members of seven rods, one on top of the other, which together formed a segmented fuel rod. In the segmented rods the axial positions for individual rods were: XXX/S, XXX/1, XXX/2, XXX/3, and XXX/4 starting from the bottom. The W test fuel rods were base irradiated in the semi-commercial pressurized water reactor BR-3 at Mol, Belgium.

The power ramping of the experimental fuel rods was performed in the R-2 reactor at Studsvik in the pressurized loop No 1 with forced circulation cooling simulating PWR conditions. The facilities used for the power ramping included the loop system, a sample exchange device, a He^3-absorber system for power control, and instruments for power measurement and fission products detection.

The power ramping of the experimental fuel rods were performed in the R2 reactor in the pressurized loop No 1 with forced circulation cooling simulating PWR coolant temperature and pressure conditions.

The power ramp tests were performed according to the following typical scheme, see Fig. 42:

- conditioning phase (from the end of the base irradiation until the power ramp phase): the objective was to adjust the rod conditions to the same conditioning level for all rods, thus equalizing the starting point of the ramp tests. This is done increasing linear heat rating with slow rates until a selected value (25kW/m) and than holding at this value for 24 h;
- ramping phase: a rapid increase of linear heat rate from the conditioning level to ramp terminal level;
- a holding phase at ramp terminal level of normally 12 hrs or until failure was evidenced by an activity increase in the fission product detection system.

Nine out of twenty-eight tested rods failed.

Additional informations can be found in (*OECD 2010-7, Adorni 2009, Adorni 2008*).

5.2.2.1 Fission Gas Release Options

The recommended URGAS algorithm with the (thermal) diffusion coefficient of Hj. Matzke and a constant athermal diffusion coefficient has been chosen for all the calculations. This option is used together with an intragranular fission gas release model.

The reference calculations are performed selecting the input parameter for the grain boundary fission gas behavior that activates the “TFGR model”, identified as option (C). The model has been newly implemented in TRANSURANUS code to consider the additional release that can be observed in the event of rapid power

variations. This model consists of two contributions: microcracking in case of power increase or reduction, and gas transport from the grain to the grain boundaries. The entire fission gas inventory stored at the grain boundaries is instantaneously released if transient conditions are met. This model should be invoked in case of power ramps. No values of the saturation limit for grain boundary gas input parameter is needed.

More details of the analysis can be found in APPENDIX C and (*OECD 2010-7, Adorni 2009, Adorni 2008*).

5.2.3 Significance for CNA-2

The only informations available for modeling the normal operation of CNA-2 are:

- the distribution of the linear heat rate for the equilibrium burnup of the reference core;
- the corresponding value of the burnup,
- the zones (but not the position) of which the fuel rods were.

Assumptions are made to perform the analysis. It should be noted that the information on the movements are needed only for the rods that are subjected to shuffling (i.e. three zones).

Fig. 40 reports the location of the CNA-2 fuel rods shuffled (corresponding to zones 1, 4 and 5) in the power ramp failure map of CNA-1 (*Adorni FU-09 2009*). The global and burnup dependent limits delimit the allowable CNA-1 operational zones.

For each refueling zone of the CNA-2 NPP, the maximum and the minimum values of the linear heat rate are considered. The rods belonging to the zones 1, 4 and 5 come from the zones 2, 3 and 6. For the latter zones, the maximum and minimum values are considered. Then the map of Fig. 40 is created subtracting the corresponding maximum and minimum value to the specific linear heat rate value. As can be noted, the values on the x axes are arranged on three values for each case.

The picture shows that the highest average power ramp heights are achieved using the minimum average conditioning linear heat rate (red squares in the figure). The blue circles represent the height of the power ramp in the case of maximum conditioning linear heat rate (and minimum power ramp height).

The maximum power ramp that is experienced by the CNA-2 fuel rods, based on the analysis (*Adorni FU-09 2009*) is 26 kW/m (not reported in the figure, local value).This would bring to a maximum local linear heat rate of 40 kW/m.

In the analysis the latter choice is used, due to the fact that these values bring to a more consistent duration of the irradiation in the core for the fuel cycle length. The influence of this different possible choice of the conditioning linear heat rate and the corresponding delta linear heat rate are addressed in the sensitivity analyses (*Adorni FU-11 2009*).

The comparison with the ramp of the BWR Inter-Ramp Project, Fig. 41, and with the PWR Super-Ramp Project, Fig. 42, show similarities in terms of maximum ramp height. Regarding the ramp rate, for the case of CNA-2 192 kW/m-h is selected for the analysis, based on (*Mazzantini 2008*). This value is lower than both databases analyzed (between 240 and 660 kW/m-h).

5.2.4 Significance for code assessment

The activity presented in this section represents an extension of the independent assessment of the FGR models carried out on the TRANSURANUS code. On the one hand the current simulations of the BWR rods in the Inter-Ramp project, indicate that the new transient fission gas release, option (C) in Fig. 43, generally overestimates the FGR measured at end-of-life, whereas a different trend is evidenced by the PWR Super-Ramp Project simulations: underestimation of FGR. This may be due to the different burnup of the fuel rods, see Fig. 44. The comparisons with the Vitanza threshold confirm the overtaken of the 1% FGR.

On the basis of these results it seems therefore necessary to refine the model for ramp release. More precisely, one might consider only a partial venting of the grain boundary inventory during rapid power variations, rather than a total release as currently implemented. Nevertheless, this will require more experimental data to be analyzed. Details of this activity can be found in APPENDIX C.

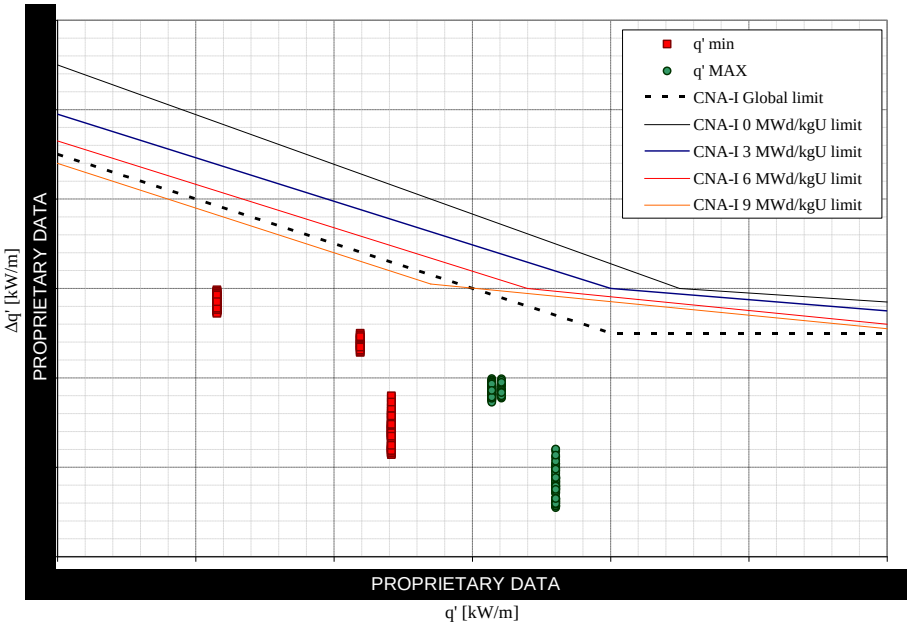

Fig. 40 – Power ramp failure map for CNA-2 fuel together with the global and burnup dependent limits of CNA-1, case of equilibrium burnup of the reference core.

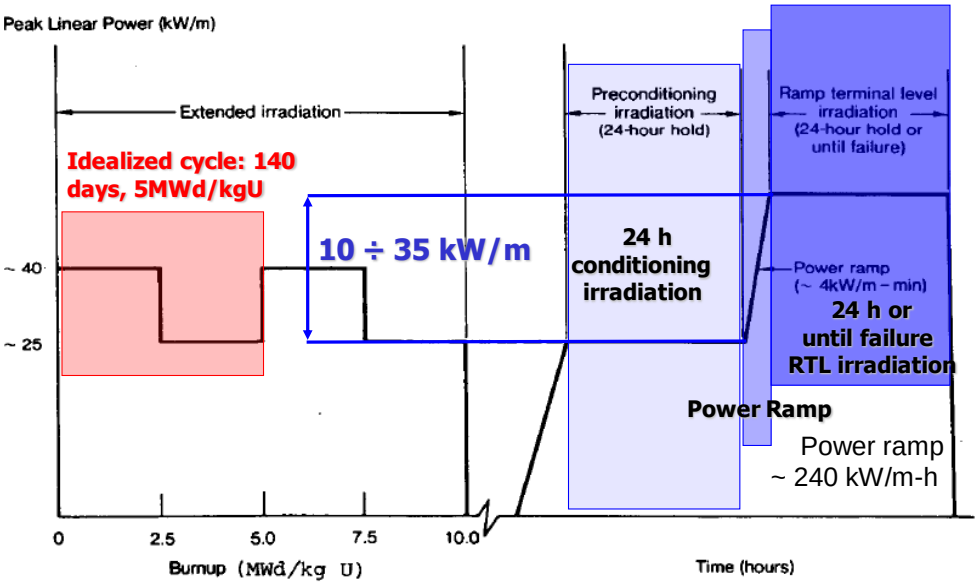

Fig. 41 – Schematic BWR Inter-Ramp irradiation history.

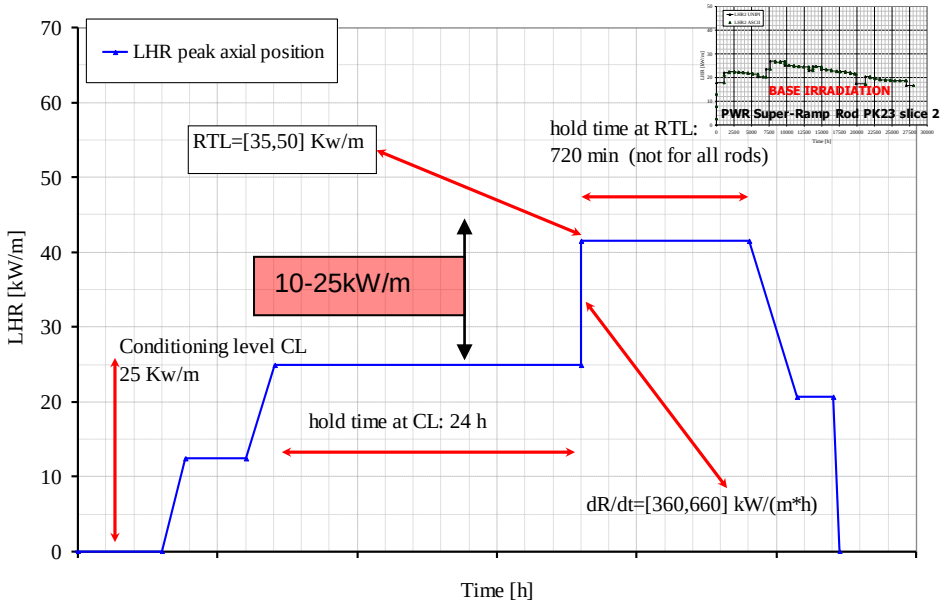

Fig. 42 – Schematic PWR Super-Ramp irradiation history.

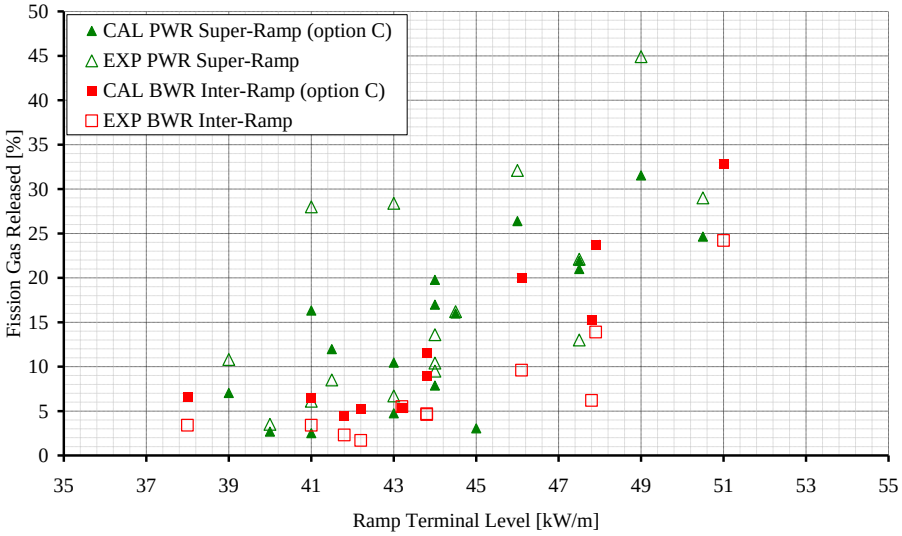

Fig. 43 – Summary of measured and calculated Fission Gas Released vs Ramp Terminal Level: BWR Inter-Ramp and PWR Super-Ramp Projects.

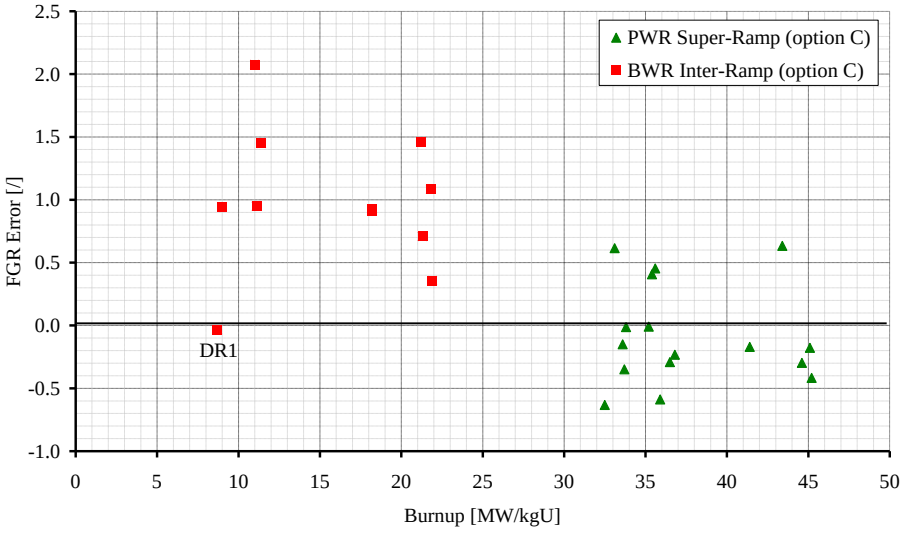

Fig. 44 – Summary Fission Gas Released errors vs Burnup: BWR Inter-Ramp and PWR Super-Ramp Projects.

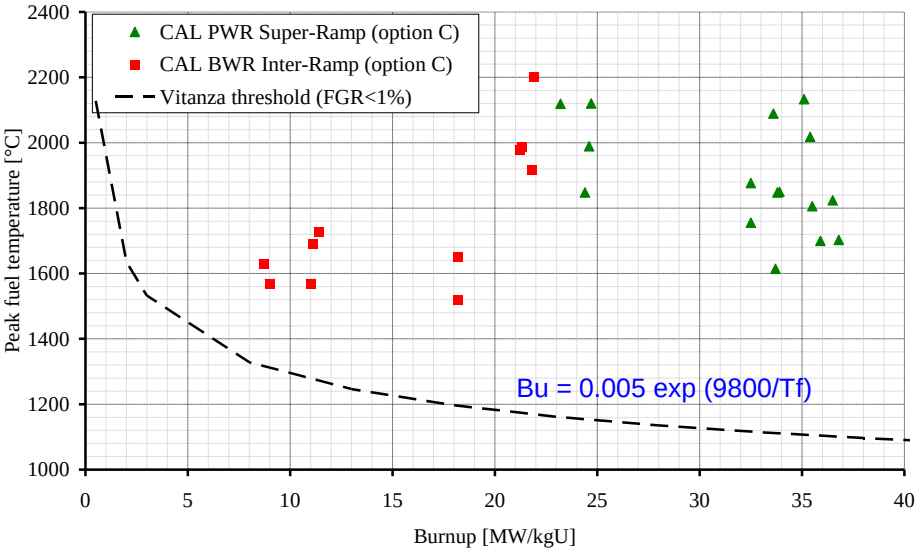

Fig. 45 – Summary Calculated peak fuel temperature vs Burnup: BWR Inter-Ramp and PWR Super-Ramp Projects and Vitanza threshold.

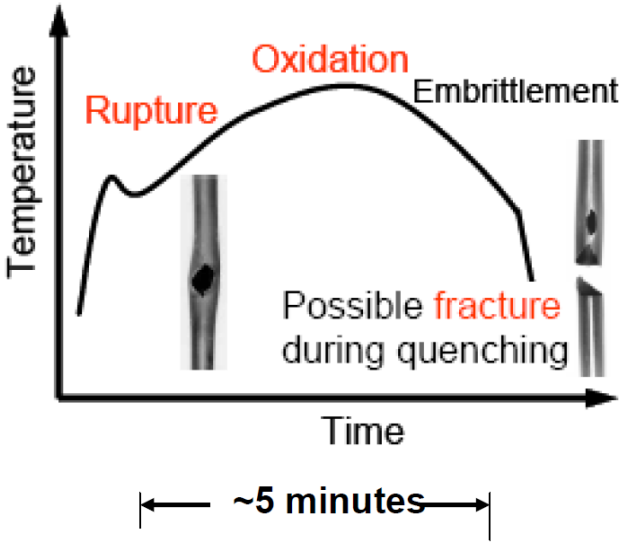

Fig. 46 – Schematic illustration of failure modes during LOCA transients (Vitanza 2008).

5.3 Severe transients: LOCA & RIA

Different phenomena involved in the heat-up, cooldown and quench may happen during a LOCA transient, due to the changes of the properties of the zirconium cladding alloys and the pellet which take place during the transient.

Typically a LOCA transient will start with the fuel under normal operating conditions. The cladding then has a temperature slightly above 300 ˚C. At the pellet cladding interface the temperature is about 400 ˚C with an approximately parabolic temperature distribution in the pellet. The centre temperature in the pellet is perhaps 1200 - 2000 ˚C depending on the local power level. At the start of the LOCA the fissions quickly cease due to the loss of moderator and insertion of control rods. With the loss of coolant the cladding will start to heat up. The stored energy in the pellet redistributes towards a more flat radial temperature profile but heatup still will occur due the decay heat of the fuel. The initial heat-up of the cladding is mainly due to the redistribution of heat, the stored energy of the pellet, but in the longer term it is the decay heat which is responsible for the heating of the cladding (*OECD 2009*). Schematic illustration of failure modes during LOCA transients is reported in Fig. 46.

A complication is present in Atucha-II NPP: the LB-LOCA is also a RIA event.

The main safety concerns in reactivity initiated accidents are loss of long-term core coolability and possible damage to the reactor pressure boundary and the core through pressure wave generation. Fuel failure, i.e. loss of clad tube integrity, is in itself generally not considered a safety concern, since fuel failures do not necessarily imply loss of coolable geometry or generation of harmful pressure waves. Fig. 47 reports a schematic illustration of two types failure modes in early and late phases of RIA transients. Nonetheless, RIA experiments and modeling have historically been focused on fuel rod failure, for several reasons:

- Fuel rod failure is a prerequisite for loss of coolable core geometry and pressure wave generation.
- The mechanisms for fuel rod failure are more easily studied, both experimentally and analytically, than those for gross core damage.
- Regulatory bodies require that the number of failed fuel rods in the core should be calculated in evaluations of radiological consequences to design basis RIA.

In an international study from 2001, a ranking of phenomena relevant during RIA was performed (*Boyak 2001*).

From RIA simulation experiments in power pulse reactors, it has been found that the fuel rod behavior under a reactivity initiated accident is affected primarily by the:

- Characteristics of the power pulse, in particular the amplitude and pulse width.
- Core coolant conditions, i.e. the coolant pressure, temperature and flow rate.

- Burnup-dependent state of the fuel rod. Among the most important properties are the pre-accident width of the pellet-clad gap, the degree of cladding waterside corrosion, the internal gas overpressure in the fuel rod, and the distribution of gaseous fission products in the fuel pellets.
- Fuel rod design. Parameters of particular importance are the internal fill gas pressure, clad tube wall thickness, fuel pellet composition (UO2/PuO2/Gd2O3, enrichment) and the fuel pellet geometrical design (solid/annular).

Fig. 48 reports the possible mechanisms for fuel and cladding damage under a RIA (*Fuketa 2005*).

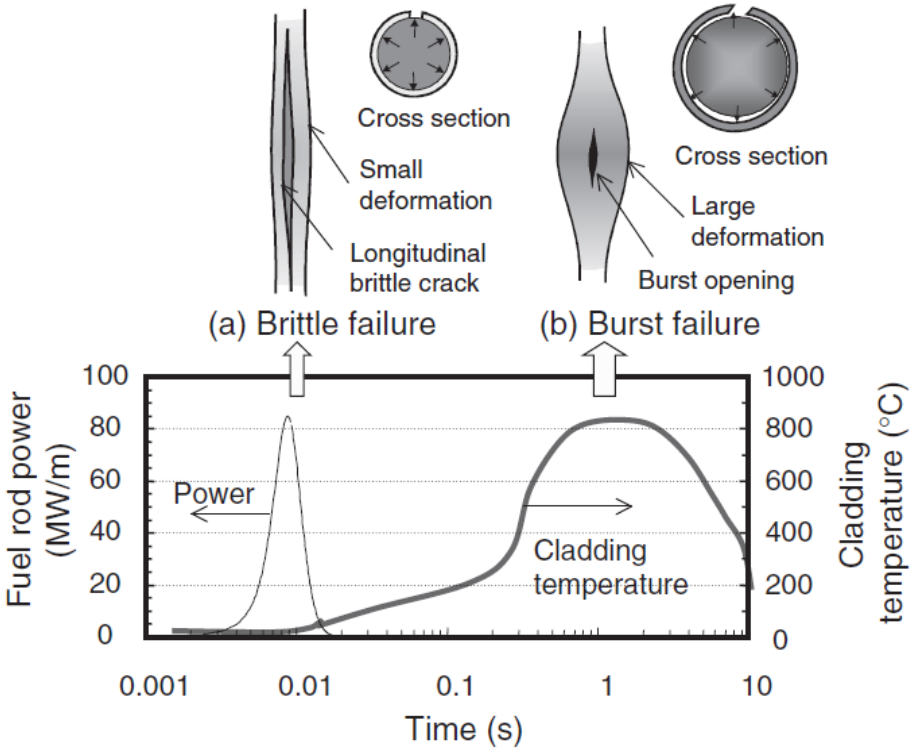

Fig. 47 – Schematic illustration of two types failure modes in early and late phases of RIA transients (Nakamura 2004).

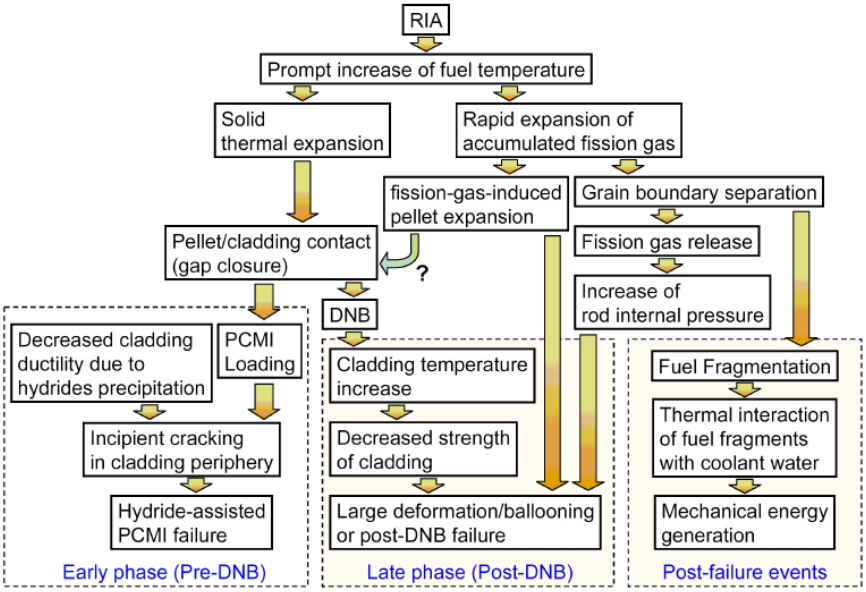

Fig. 48 – Possible mechanisms for fuel and cladding damage under a RIA (Fuketa 2005).

5.3.1 Analysis of MT-4 and MT-6A tests

The objective of the activity is the independent assessment of TRANSURANUS "v1m1j09" in predicting:

- ballooning, and
- cladding failure and related time.

5.3.1.1 Experimental database description

The U.S. NRC conducted a series of thermal-hydraulic and cladding mechanical deformation tests in the NRU reactor at the Chalk River National Laboratory in Canada. The objective of these tests was to perform loss-of-coolant-accident (LOCA) experiments using full-length light-water reactor fuel rods to study mechanical deformation, flow blockage, and coolability. Three phases of a LOCA (i.e. heat-up, reflood, and quench) were performed in situ using nuclear fissioning to simulate the low-level decay power during a LOCA after shutdown. All tests used PWR-type, non-irradiated fuel rods. 12 and 21 rods respectively were tested in the MT-4 and MT-6A experiments, providing data for one representative case for each test.

5.3.1.2 Validation domain

The validation is performed against the MT-4 and MT-6A database and its validation domain is reported in (*Adorni 2010*). It includes:

- the version code used for the independent assessment;
- the main objective of the independent assessment;

- the range of parameters for which the assessment is performed;
- the parameters, part of the experimental database, which are suitable for the comparisons.
- the parameters adopted for the comparison between the experimental data and the code results with the indication of the suitability for the code assessment.

5.3.2 Significance for CNA-2

It should be noted that the experiment analyzed is full scale and PWR type, and it can be considered representative of the Atucha-II fuel. The relevance for CNA-2 is referred to the possibility of the code to simulate the phenomena that are expected in the fuel and that are experienced in the experiments, Tab. 19.

5.3.3 Results significant for the code assessment

5.3.3.1 General conclusions

The results of the deterministic calculations demonstrate the capability of TU code in predicting the cladding failure and time of failure occurrence during LOCA scenario, before the reflood occurrence. The correct prediction of the evolution of the decreasing pressure after onset of ballooning until rupture suggests the correctness of the ballooning size prediction for both cases analyzed. In any case, this phenomenon can only be partially addressed by a 1½-D code.

The comparisons with the permanent tangential strain, measured in MT-4 test, show a under-prediction of the code in all the cases except when the failure criteria are disabled and the static model for the α to β-phase transition is used. No precise measurement of the cladding strain is available for the MT-6A. However, the information based on the visual inspection suggests TU code under-predicts the experimental trend.

The fuel centerline temperature measured in the MT-4 test is well calculated by TU code. Minor differences at the end of the transient may be explained with the minor differences in predicting the time of failure.

The sensitivity analyses evidences that the major differences from the reference case for the time of failure and the outer cladding radius at burst and are experienced by:

- mechanical analysis: IBMECH=2 instead of 0;
- creep anisotropy coefficients non-LOCA specific: ModCladJ1=0 instead of 18;
- different models for the relocation.

The results of the probabilistic analysis show a small spread of results related to the time of failure in the case of MT-4, in which the only cause of failure is plastic instability. Large spread is calculated for the MT-6A case, in which the failures are due to plastic instability and overstrain.

5.3.3.2 Author recommendations

The subroutine PINPRS that calculates the UP temperature is not enough accurate for predicting the gap pressure trend during LOCA transient: the UP temperature should be prescribed in the input deck.

The validation activity pointed out the limitations of the code in relation with the ballooning prediction during LOCA analysis. Due to intrinsic limitations of the code, the simulation of the ballooning occurring when the cladding reaches high temperature (>800 °C) should be performed by means of switching off the failure model.

5.3.3.3 Limitations of the study

The effect of burnup is not accounted in the analysis, thus the experimental database is representative of fresh fuel. Therefore, the prediction of relevant parameters should be tested at higher and more representative burnup values.

The probabilistic analysis is performed selecting the time of failure as variable of interest. However, this does not have any objective connected with the quantification of the uncertainty. Indeed, the selection of the sources of uncertainty have not been quantified rigorously.

5.3.3.4 Additional significant study findings

The use of a static α-β phase transition model, together with the hypothesis of non-failure brings to the higher prediction of the strain that in the MT4 simulation resulted representative of the experimental data.

More details are reported in APPENDIX D and (*Adorni 2010, Adorni 2011*).

5.4 Non standard application of TU code: FK-1, FK-2 and FK-3 tests

The objective of the activity is the validation of TRANSURANUS “v1m1j09” code in predicting fuel and cladding behavior under RIA conditions using the experimental databases FK-1, FK-2 and FK-3. It is pursued assessing the capabilities of the code models in simulating the phenomena and parameters involved, such as: pressure trend in the fuel rod, cladding creep, and geometry changes, (*Fuketa October 2000, Fuketa April 2000, Nakamura 2002, Nakamura 2000*). The analysis is aimed at having a comprehensive understanding of the applicability and limitations of the code in the in the conditions of the experiments.

5.4.1 Description of the experiments

Boiling water reactor (BWR) fuel rods with bumps of 41 to 45 GWd/tU were pulse-irradiated in the Nuclear Safety Research Reactor (NSRR) to investigate the fuel behavior during a reactivity initiated accident (RIA) at cold startup. BWR fuel segment rods of 8x8BJ (STEP I) type from the Fukushima Daiichi Nuclear Power Station Unit 3 were refabricated into short test rods, and they were subjected to prompt enthalpy insertion from 293 to 607 J/g (70 to 145 cal/g) within about 20 ms. The fuel cladding had enough ductility against the prompt deformation due to pellet

cladding mechanical interaction. The plastic hoop strain reached 1.5% at the peak location. The cladding surface temperature locally reached about 600 °C. Recovery of irradiation defects in the cladding due to high temperature during the pulse irradiation was indicated via X-ray diffractometry. The amount of fission gas released during the pulse irradiation was from 3.1% to 8.2% of total inventory, depending on the peak fuel enthalpy and the normal operation conditions (*Fuketa 1997, Sugiyama 2004*).

The rods FK-1, FK-2 and FK-3 were refabricated from irradiated segment fuel rods of BWR 8x8BJ (STEP I) design. The segments were irradiated to an assembly average burn-up of 30.4 MWd/kgU in Fukushima Daiichi Nuclear Power Station Unit 3 (*Sugiyama 2004*). An irradiation history is available for each rod from IFPE database.

Due to the reafbrication process that the fuel underwent, the use of the non standard restart option is envisaged.

5.4.2 Non-standard application of restart option to FK-1 test

In order to use the restart option, first of all the input should be prepared inserting the card IWERT 99 at the time at which the beginning of the restart. In addition to this, the variable INTRUP should be set to 1 and the restart file should be named “resta.old”. Than, the first case can be run.

At this stage, the models and/or parameters can be changed directly in the main file RSTRTM.FOR. In principle the following quantities can be modified:

- reactor type;
- relocation model;
- fission gas release model;
- saturation limit for grain boundary gas;
- fuel axial length;
- cladding axial length;
- upper plenum axial length;
- upper plenum free volume;
- gas content in free volume;
- gas pressure in free volume;
- gas composition in free volume.

For the analysis of the NSRR database, only the modification of the gas pressure is accounted for.

The next step is the compilation of the restart package and the creation of the new executable program-file, e.g. RSTRTM. The following subroutines should be compiled:

- RSTRTM.FOR, which is the main program for the restart file package.
- COMMON, which is the TRANSURANUS COMMON block, i.e. identical with the COMMON block used in the TRANSURANUS main program, and made available to all other files.

- RSTART.FOR (subroutine and driver), which is called from RSTRTM.FOR and manages the writing and reading of all the variables to, and from, the other files (below).
- OUTIN.FOR (subroutine), which writes and reads data to/from the restart file.
- VEKCH.FOR (subroutine), which unfolds compressed CHARACTER variables and fields.
- VEKL4.FOR (subroutine), which unfolds compressed LOGICAL variables and fields.
- VEKI4.FOR (subroutine), which unfold compressed INTEGER variables and fields.
- VEKR4.FOR (subroutine), which unfold compressed REAL variables and fields.
- VEKR8.FOR (subroutine), which unfold compressed DOUBLE PRECISION variables and fields.

The new RSTRTM program should be run and a new file with the changed data, e.g. RESTA.NEW, is created.

The last step is the run of the same input containing the modification of the variable INTRUP that should be set to 2. Note that the name of the restart-file specified on the last input command line of ITEXTK must be identical with the name of the new created restart data file, in the case analyzed RESTA.NEW (*Nordström 2003*). A scheme of this process is reports in Fig. 49.

The new fill gas pressure is defined at restart by the gas amount in the rod free volume. In order to take into account the new gas pressure and composition, the variable for *total amount of gas in the free volume* (gap, dish, upper and lower plenum, central void and fill gas), GASTOT(M,N), must be adjusted. The index M (1 to 10) defines the type of gas; 1 = He, 2 = Ar, 3 = Kr, 4 = Xe, etc and the index N (1 to 2) the value before and after an iterative time step.

The new amount of gas (GASTOT) for the restart input is derived with the use an iterative trial and error method, where test calculations are done with TRANSURANUS and the number of μmol in the RSTRTM.FOR adjusted until the initial rod pressure read from the output is correct, i.e. equal with the restart fill gas pressure. A representative case of the application of this option is reports in APPENDIX E (FK-1).

5.4.3 Significance for CNA-2

Tab. 22 reports the comparison of the range of the experiments and CNA-2 The main differences in the experiments, a part the different peak liner heat rate, is that CNA-2 fuel rods are not subjected to an adiabatic RIA due to the large duration of the pulse width. Fig. 50 repots the status of the available experiments, the red star represents the location of CNA-2 fuel. As it can be noted, the CNA-2 RIA is atypical, due to the large temperature respect to the others experiments, since the peak temperature is due to LOCA. Fig. 51 reports the fuel failure limit due to PCI.

Due to the low burnup and to the low specific enthalpy increase (45 cal/g maximum), the point of CNA-2 is well below the Japanese PCMI failure limit.

5.4.4 Results significance for the code assessment

Concerning the use of TRANSURANUS for modeling of an experimental restart case, following conclusions can be made:

- The RESTART-option is very useful by modeling the FK-1 fuel test since it account for the re-instrumentation.
- The RESTART-option works without any problem. Its construction should guarantee that any type of restart problem could be treated with TRANSURANUS.
- The RESTART-option is helpful and the standardization of this option would improve the modeling of re-instrumented rods, such as he ones tested in research reactors.

Concerning the database:

- The FGR during base irradiation is well predicted by the code, but further improvements should be needed for the transient fission gas during RIA.
- FK-1, FK-2 and FK-3 databases are suitable the validation of fuel pin mechanic codes, thus enlarging validation domain to accident conditions and improving the level of understanding of the code capabilities and limitations.

More benchmarking would be required to assure the reliability of the capability of the code in simulating RIA accidents, also analyzing databases in which the fuel rods fail. This would help the development of a failure limit for the RIA analysis.

Id	Peak enthalpy	Peak Linear Heat Rate	Pulse width	Note
FK-1	130 cal/g	95.9 MW/m	4.4 ms	--
FK-2	70 cal/g	34.2 MW/m	6.7 ms	--
FK-3	145 cal/g	114.6 MW/m	4.4 ms	--
CNA-2	170÷615 cal/g	99÷447 kW/m	500 ms	Non-adiabatic

Tab. 22 – Summary table of RIA: NSRR and CNA-2.

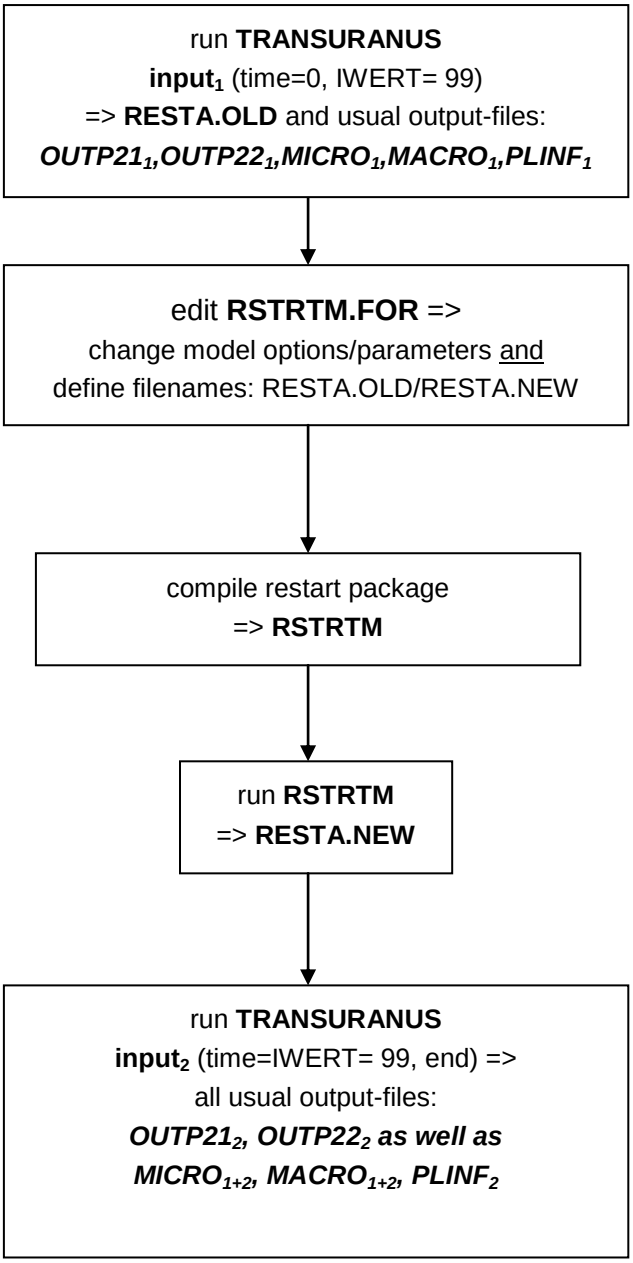

Fig. 49 – Scheme of application of restart option from (Nordström 2003).

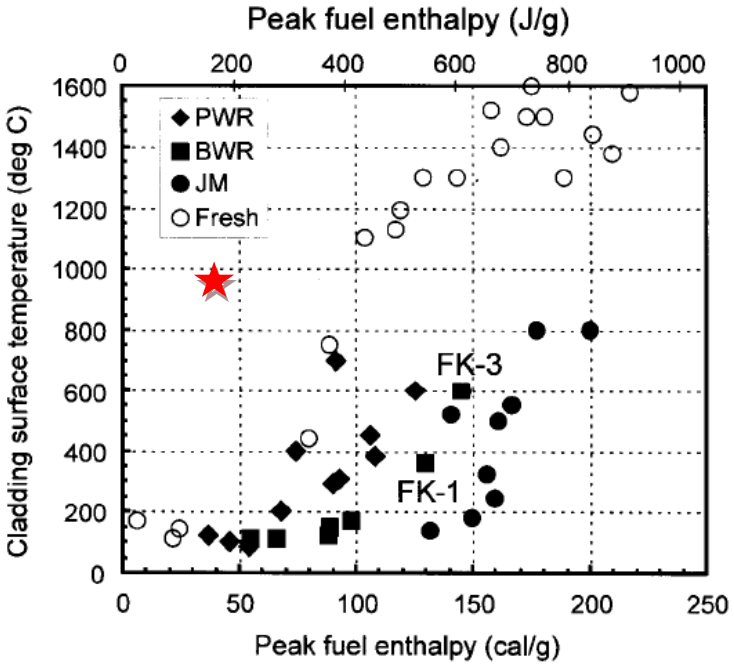

Fig. 50 – Available experiments at NSRR (Nakamura 1999).

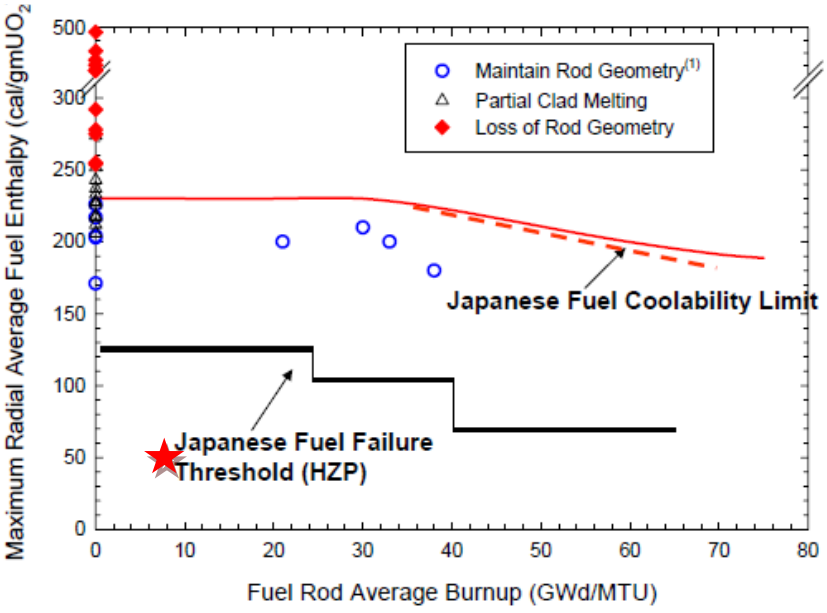

Fig. 51 – Example of Japanese fuel failure threshold for PCMI (Vitanza 2008).

6. DEVELOPMENT OF A METHODOLOGY FOR ATUCHA-II NPP

This section provides a description of the methodology for the analysis of the 2A LB-LOCA scenario in Atucha-2 NPP, focusing on the procedure adopted for the use of the fuel rod thermo-mechanical code. The methodology implies the application of best estimate thermal-hydraulic, neutron physics and fuel pin performance computer codes, with the objective to verify the compliance with the specific acceptance criteria. The fuel pin performance code is applied with the main objective to evaluate the extent of cladding failures during the transient.

The procedure consists of a deterministic calculation by the fuel performance code of each individual fuel rod during its lifetime and in the subsequent LB-LOCA transient calculations. The boundary and initial conditions (BIC) (e.g. pin power axial profiles) are provided by core physics and three dimensional neutron kinetic coupled thermal-hydraulic system codes calculations. The procedure is completed by the sensitivity calculations and the application of the probabilistic method.

6.1 Hypothesis of the TH analysis

The analyses performed in relation to the limiting break sizes (i.e. accidents classified as SBDBA) do not consider the single failure and repair assumptions. However, the loss of off-site power is assumed in all LBLOCA analyses and the corresponding (conservative) delays in the safety system actuations are considered, i.e. the Emergency Power Mode (EPM) of operation is assumed (*NASA 2011*).

Key boundary conditions are imposed as follows:

- MCP decay: the EPM assumption or LOCA signal brings to the calculation of rotor pump speed versus time.
- SG isolation (Feed-water and Steam Line): according to the EPM assumption.
- Scram by boron lances: 0.5 s after the break initiation the ‘first drop’ of highly borated liquid reaches the active core region; afterwards, calculated boron reactivity is used.
- Scram by solid control rods: according to the protection system part of the I & C of Atucha II.
- Operation of the moderator loop, intervention of accumulators and actuation of safety injection pumps (SIP): based on the LBLOCA signal.
- Decay heat: it is assumed the ANS 1999 standard decay curve.
- Containment counter-pressure according to specific calculations.

6.2 Purposes for the Analysis

The objective of the analysis is to evaluate the fuel performance, following the occurrence of a 2A Break LOCA. This includes the verification of the parameters relevant to fuel integrity and the demonstration that conditions which might involve the loss of the structural integrity of the fuel are not met during the transient.

As for Atucha II, LBLOCA are classified as SBDBA, the fulfillment of all DBA criteria is not mandatory but it is investigated.

More in detail, the specific purpose is to evaluate the extent of cladding failures performing a deterministic analysis of the fuel rods, in order to provide the source term for the radioactivity release in primary system. The assemblies corresponding to the failed rods are identified for the core configuration considered at equilibrium burn-up, according with the data provided in section 2.3.

The targets for the analysis are the evaluation of:

1. the enthalpy released to the fuel during the power excursions (see Ph.W. I described in section 3),
2. the fuel centerline temperature,
3. the amount of clad thickness reacted,
4. the total amount of hydrogen released.

The above listed quantities also constitute an output from the calculation TH-3DNK. However, the outputs of the code-nodalization adopted hereafter (i.e. TRANSURANUS), are considered as the reference results for the present study.

6.3 Acceptance Criteria

For the spectrum of selected beyond design basis accidents (SBDBA), the safety margins are estimated against the same limits or criteria as for DBA described in section 3.2, even the fulfillment is not mandatory. The most significant parameters to be considered in the fuel performance analysis are the criteria related to DBA LOCA *(UNIPI 2008, NASA 2011*):

1. Average fuel hot spot enthalpy < 230 cal/g for irradiated fuel.
2. Cross section of fuel melting at hot spot: fuel melting not admissible for 90% of pellet cross section at hot spot.
3. The oxidation of the cladding as ratio of the total cladding thickness before oxidation shall nowhere exceed 0.17.
4. The maximum calculated amount of hydrogen generated from fuel element cladding reacting chemically with water or steam shall not exceed 0.01 times of the total amount if all metal cladding were to react.

The criterion at item 1 is specific for the RIA condition. The criteria at items 2 and 3 are connected with the performance of the cladding. The criterion at item 4 is connected with hydrogen burning in the containment.

The TRANSURANUS analysis is focused on the number of failures occurring during the transient. However, no specific criteria are directly connected with the geometrical extension of cladding failures.

The following criteria are used to predict the failures of the rods, see section 4.1.3.1.3:

1. Overstress: average tangential stress overpasses the failure stress.

2. Plastic instability: specific of LOCA (*Van Uffelen 2008*), is based on the simultaneous occurrence of the effective strain rate > 100 1/hr and the effective strain is larger than 2.5%.
3. Overstrain: tangential plastic strain exceed 50%.

It shall be noted that the concerned transient is both a RIA and a LOCA, in relation to which different criteria are typically applied (e.g. LOCA or RIA in LWR). Namely, pellet/cladding mechanical interaction (PCMI) failure criterion typical of RIA is expected to be a limiting criterion when a hot (rising temperature) pellet interacts with a cold clad. In the present case, clad temperature rises before and independently of the RIA event due to lack of cooling, so the PCMI effect is negligible as a responsible of failures. Furthermore, the failures due to PCMI effect, as well as the failures originated by high clad temperature are foreseen owing to the criteria 1. to 3. above.

Specific Atucha-II core material parameters (e.g. creep parameters) relevant to fuel failure criteria are assumed to be bounded by materials considered in TRANSURANUS code (e.g. Zircaloy-4), see section 4.2.4.

6.4 Procedure for safety analysis

The results from the TH coupled 3D-NK calculations, as described in section 3.3, are used to provide the boundary and initial conditions for the analysis performed by TRANSURANUS code. A “transferring map” shown in Fig. 64 provides the correspondences among the NPP core configuration (451 fuel assemblies with 37 fuel pin each), the TH and the NK representations, 280x10 TH nodes and 451x10 NK nodes respectively.

The transient analysis requires two separate calculation steps performed by the code TRANSURANUS and the TH-3DNK coupled nodalization, see Fig. 52. The interface software utilized for actuating the sketch in this figure constitutes the “platform Relap5/3D – TRANSURANUS” adopted for the analysis of the Chapter 15 of the FSAR of Atucha-II NPP (*NASA 2011*). The first step aims at the evaluation of the initial conditions of the fuel rods at beginning of the LB-LOCA, whereas the second step calculations simulate the transient (blue and orange boxes of Fig. 52, respectively). Each step implies the execution of 451 calculations or 451 multiplied by the number of the radial power peaking factors available from the NK analysis (4 for this case).

The function of the two steps for the analysis are the following:

a) the normal operation phase: needed to achieve the initial conditions at which the LB-LOCA occurs: this is the time period from the insertion of the fresh fuel rod into the core, up to the time at which the equilibrium burn-up of the reference core is reached, as specified in Chapter 4 of (*NASA 2011*);
b) the transient phase: with conditions derived from TH and 3D-NK calculation (the details of the section of the specific calculation is reported below in this chapter).

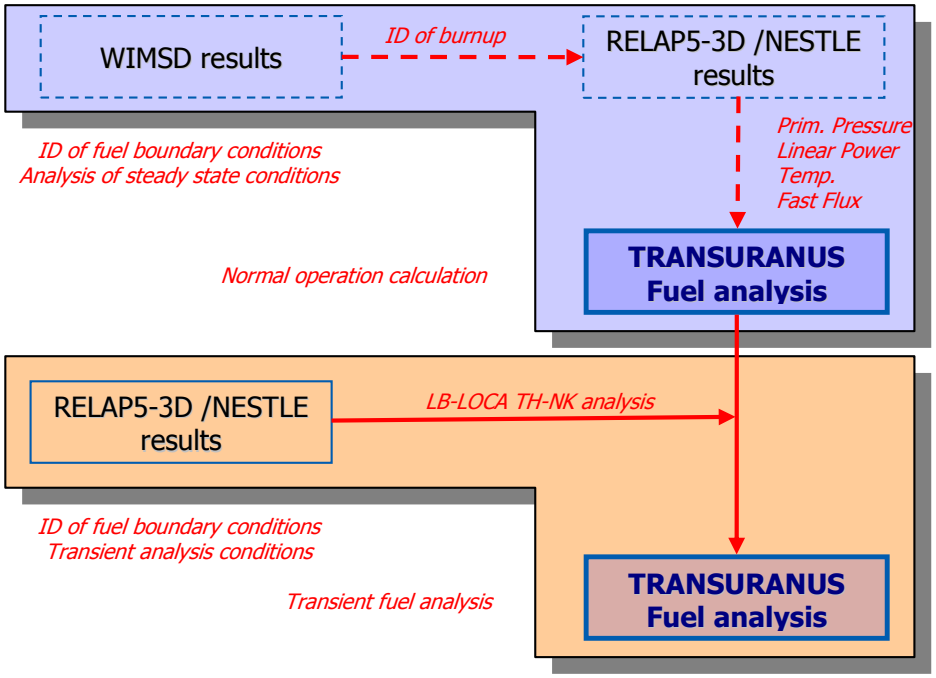

Fig. 52 – Roadmap of code connections for the application of TRANSURANUS code.

6.5 Assumed Initial and Boundary Conditions

The boundary conditions required for the fuel performance analyses are, for each individual channel:

- the channel pressure,
- the linear heat rate,
- the fast neutron flux, and
- the cladding temperature.

The values of the boundary conditions assumed in the fuel performance calculations are the results of the TH-coupled NK analysis. Several analyses were performed using the couple nodalization. In the following section a discussion of the selection of the BIC for the fuel analysis is performed.

6.5.1 Selection of the nodalizations: NK-TH

The nodalizations described in section 4.2.1 were developed and used for the analysis. There addressed short term with 3D-NK (10s), referred as '280ch', and long term with 0D-NK, referred as '60ch', (3000s) of the transient (*D'Auria 2008*).

To select the most advantageous one for performing the fuel analysis, attention is focused toward the rod surface temperature (and location where PCT is predicted) and toward the fuel power, which is proportional to the LHGR. This choice is explained with the relevance that the clad temperature and the linear heat rate have in influencing the fuel rod analysis. Those parameter trends, resulting from the system analyses preformed by RELAP5-3D© code (including the coupling with NESTLE) are also to be considered in connection with the initial condition of the fuel rod when the transient starts. Therefore the energy already released to the fuel rod (burn up), at core equilibrium, is also considered.

The importance of three-dimensional calculations is shown through Fig. 53 and Fig. 54. These figures represent the evolution of power profiles in two fuel channels. They are reported as an example of the larger changes of the shape of power profile during the transient, that is an effect that cannot be reproduced in the 60ch since a 0D-NK model is used. In the 0D-NK model the shape of the axial power distribution is constant in time during the transient. The variation of the shape of the axial power during the transient may have a very strong impact in the fuel behavior, and then the use of a 3D-NK model is envisaged.

As reported in (*D'Auria 2008*), the '60 ch' and '280 ch' nodalizations constitute the actual reference nodalizations. Based on the purpose of the analysis, i.e. best estimate evaluation of the number of possible fuel failure, the results of the '280ch' nodalization have been considered to provide the boundary conditions for the fuel analysis. The reason for this is originated by:

- The need to consider the highest detail for the individual channels: the level of detail available in the 280ch nodalization is more adequate for providing the boundary and the initial conditions needed for the analysis.

- Large changes of the axial linear power profile, caused by the local variations of the reactivity coefficients, are calculated by the 3D-NK model, but not by the 0D-NK model. Those variations implemented as boundary conditions in a fuel performance code, might have a relevant impact on the results of the analyses.

- '280 ch' predicts higher PCT than '60 ch' ones (temperature is a key parameter that strongly influences the fuel pin analysis).

- 3D NK predicts higher rate of change of the power that is a key parameter in the fuel pin analysis.

- The consideration, based on the calculated rod surface temperatures and system pressure, that possible fuel failures are expected within a time less than 10 s starting from the beginning of the transient. Anyway, the long term behavior of the fuel rods is addressed in the sensitivity analyses on the extrapolation of the results of the "60ch" nodalization (*Adorni FU-08 2009*).

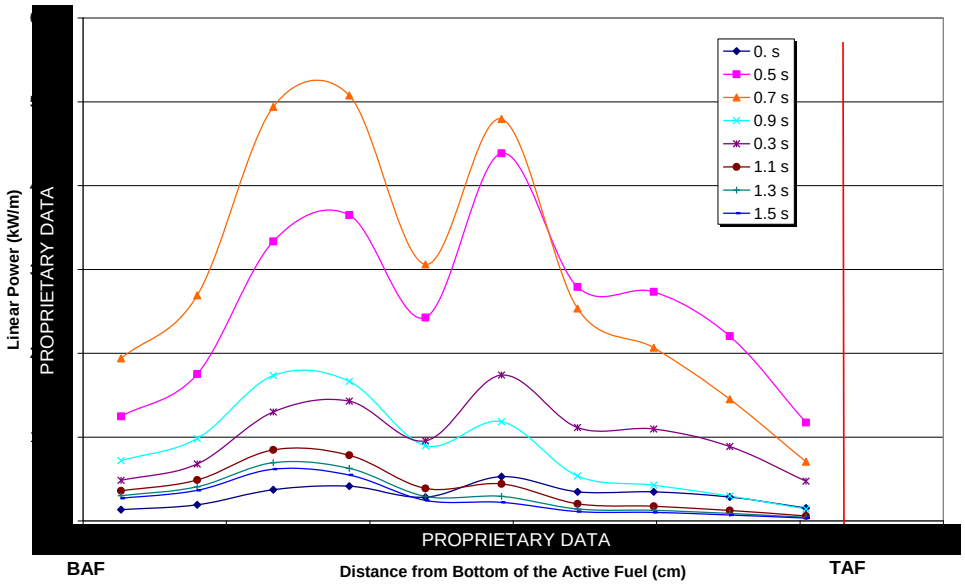

Fig. 53 – Example of evolution of power profiles in channel No 375.

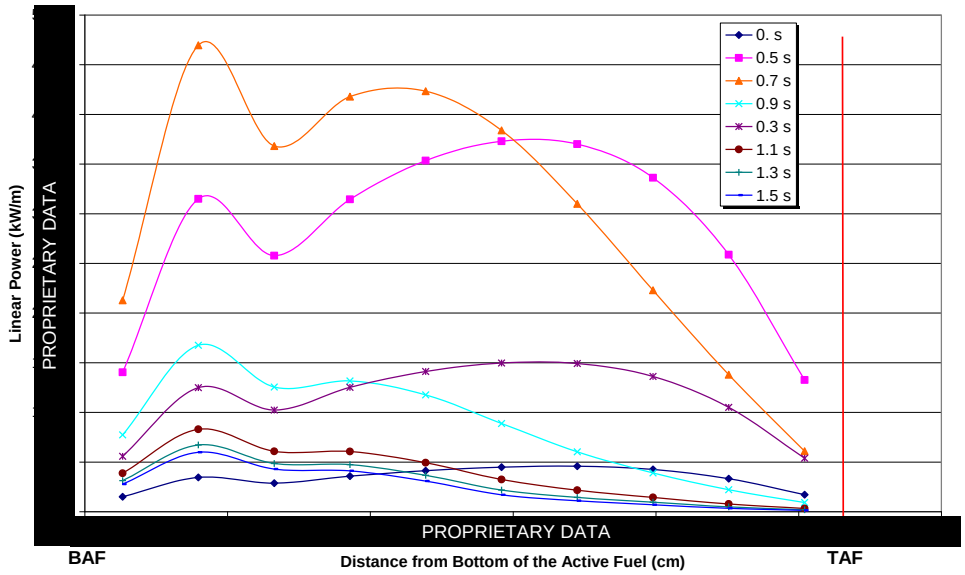

Fig. 54 – Example of evolution of power profiles in channel No 272.

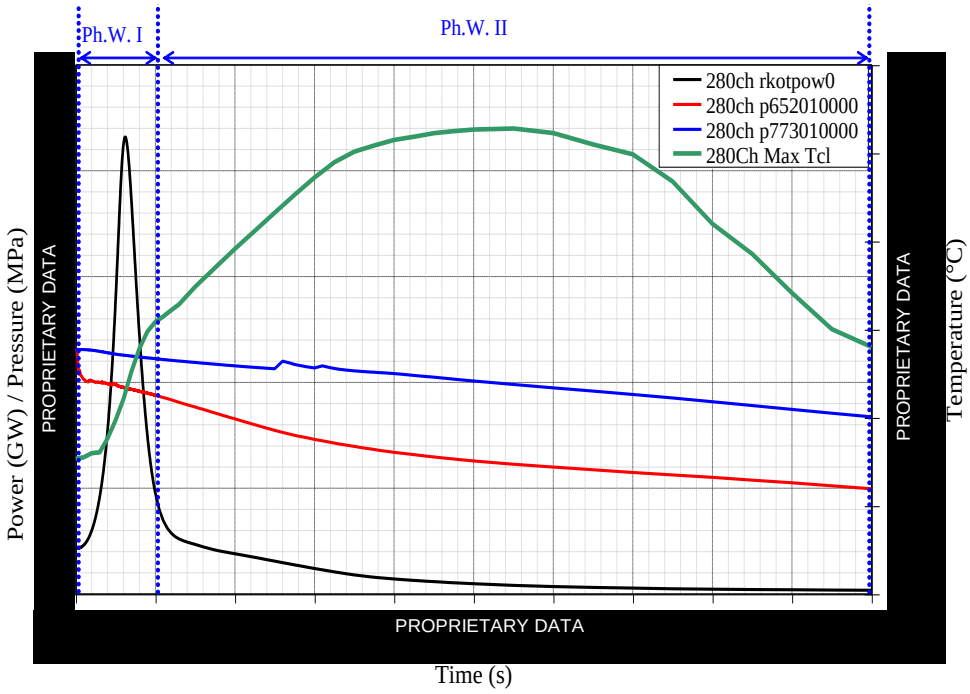

Fig. 55 – Power, pressure and maximum cladding temperature, "280ch" 3D-NK.

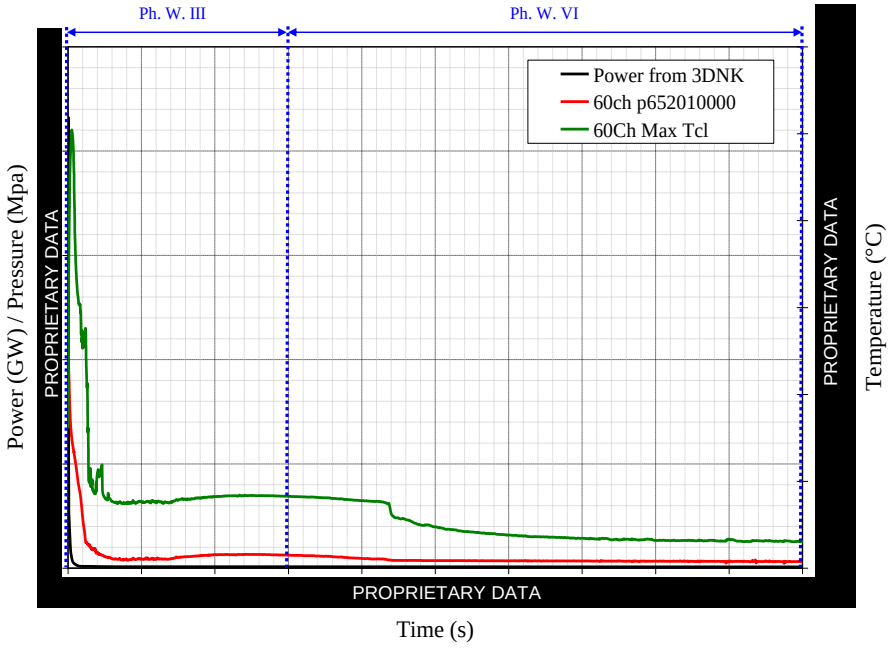

Fig. 56 – Power, pressure and maximum cladding temperature, all the transient, "60ch" 0D-NK.

6.5.2 Selected BIC for fuel analysis

6.5.2.1 Base irradiation

The LOCA transient starts at the end of the base irradiation. At the beginning of the LOCA the conditions of Tab. 23 are achieved. The average distribution of the relevant steady state conditions are reported in Fig. 57, Fig. 58 and Fig. 59.

#	Parameter	Value	Unit
1	Burn-up	PROPRIETARY DATA	MWd/kgU
2	Initial stored energy (average, one rod)		cal/g
3	Fuel rod internal pressure		MPa
4	Gas composition in the fuel rod gap		--
5	Thermal properties of fuel and cladding materials		W/mm-K
6	Pellet-to-clad gap conductance		W/mm^2-K
7	Oxide thickness		mm
8	Average linear heat rate		kW/m
9	Fast neutron flux		n/cm^{2}s
10	Average cladding temperature		°C
11	Coolant pressure		MPa
+	Filling gap pressure at 20°C		
*	Low burn-up values		
**	High burn-up values		

Tab. 23 – Selected relevant BIC related to fuel, as considered for the LBLOCA analysis.

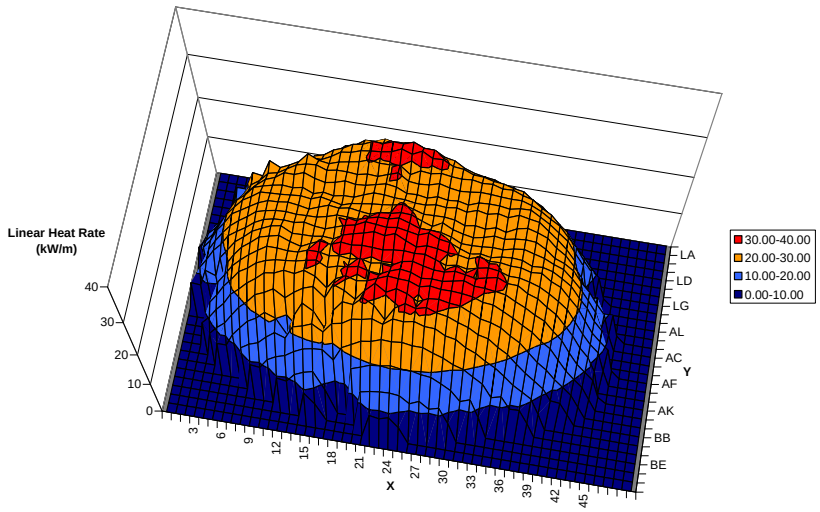

Fig. 57 – Average linear heat rate distribution, steady state conditions.

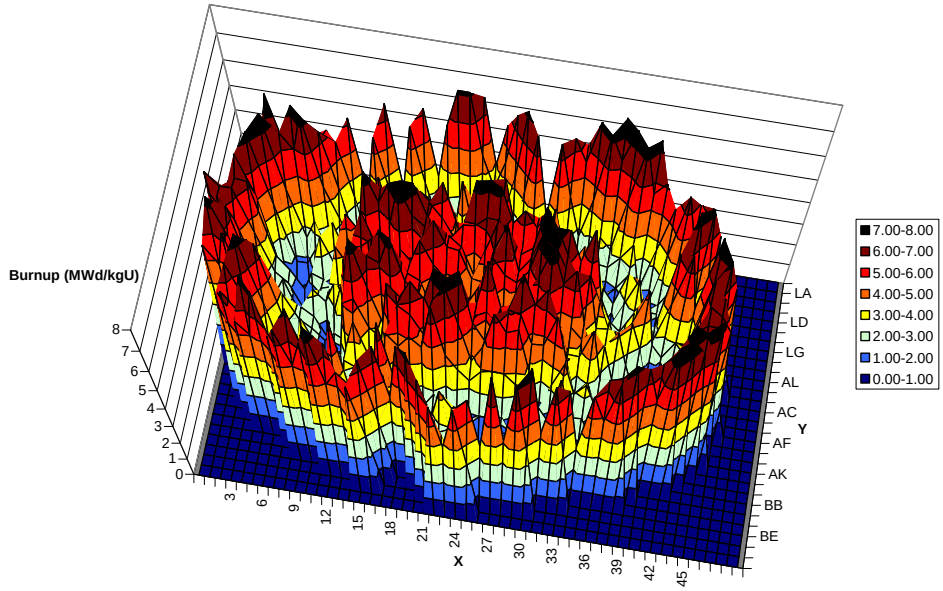

Fig. 58 – Average burnup distribution, BEQ conditions.

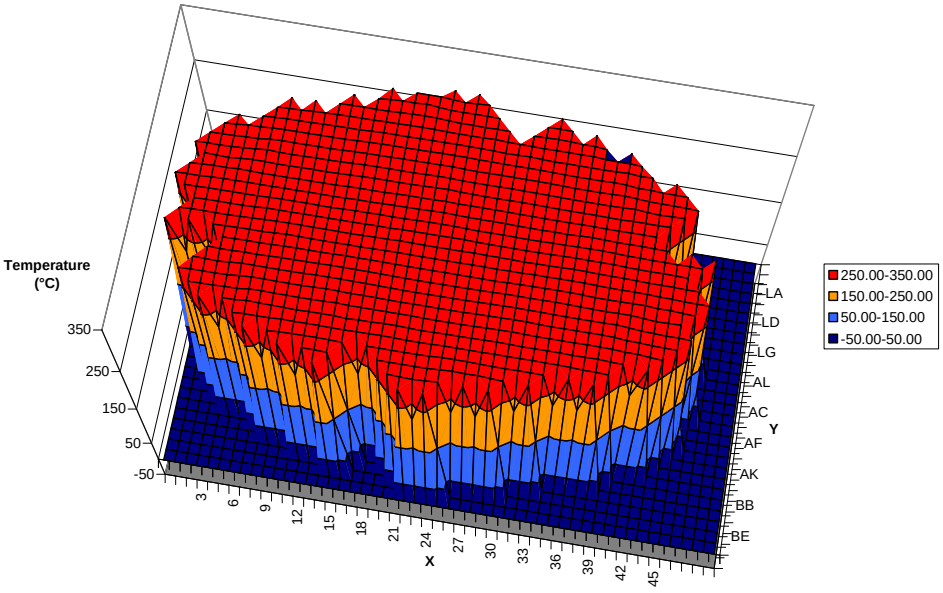

Fig. 59 – Temperature (slice 3) distribution, steady state conditions.

6.5.2.2 LB-LOCA Transient

The case analyzed is the Large Break LOCA DEGB at the nozzle connecting the cold leg and the reactor pressure vessel (SBDBA, realistic). All systems (e.g.

accumulators, safety injection pumps and moderator loop) are modeled working correctly. Four boron lances are active, the first drop of borated boron reaches the core active region at 0.5 s after the SoT. The emergency power mode is simulated. The core condition is at the equilibrium burnup of the reference core.

The coupled 280ch and the 451-10 NK nodalizations allow the calculation of linear power profile at each time in relation to each individual FC. Distribution of the average linear heat rate at the time of power peak (0.8 s, [redacted] kW/m local peak value) is reported in Fig. 66.

A key contributor to the total power is constituted by the reactivity originated by the boron injection in the moderator tank. This is calculated by "*ad hoc*" nodalizations, whose output is given to the 280ch nodalization. Details of the analysis can be found in (*D'Auria 2008*). The corresponding temperature distribution al slice 3 is reported in Fig. 61.

Peak rod surface temperature of [redacted]°C is predicted at 6s after the beginning of the LOCA. Distribution of the average linear heat rate at the time of PCT is reported in Fig. 62 and the corresponding temperature distribution at slice 3 in Fig. 63.

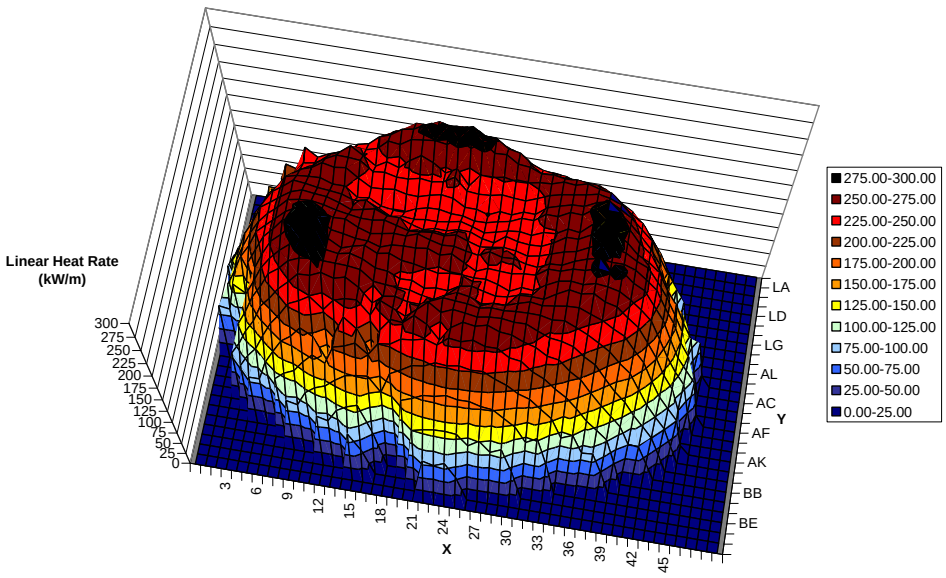

Fig. 60 – Average linear heat rate distribution at time of power peak.

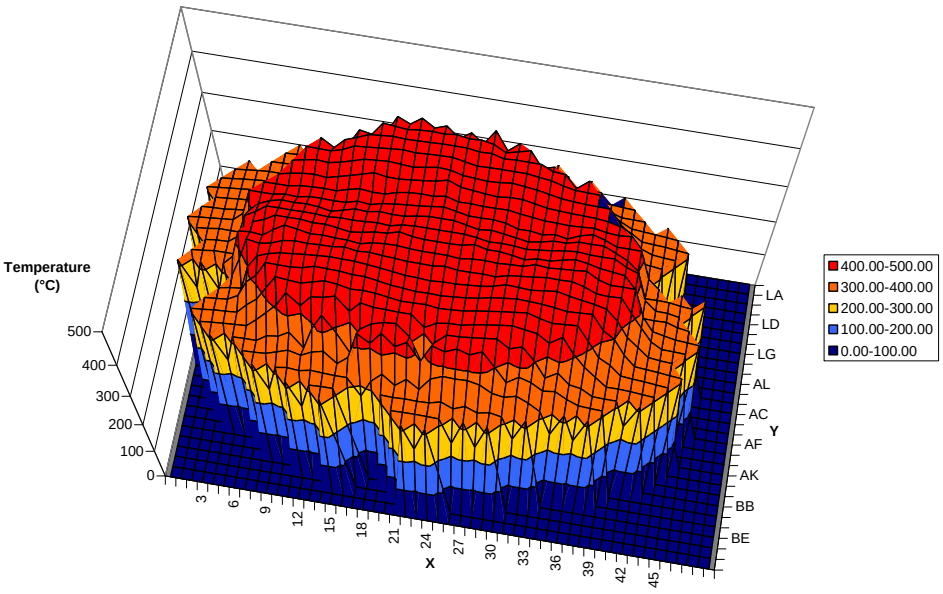

Fig. 61 – Temperature (slice 3) distribution at time of power peak.

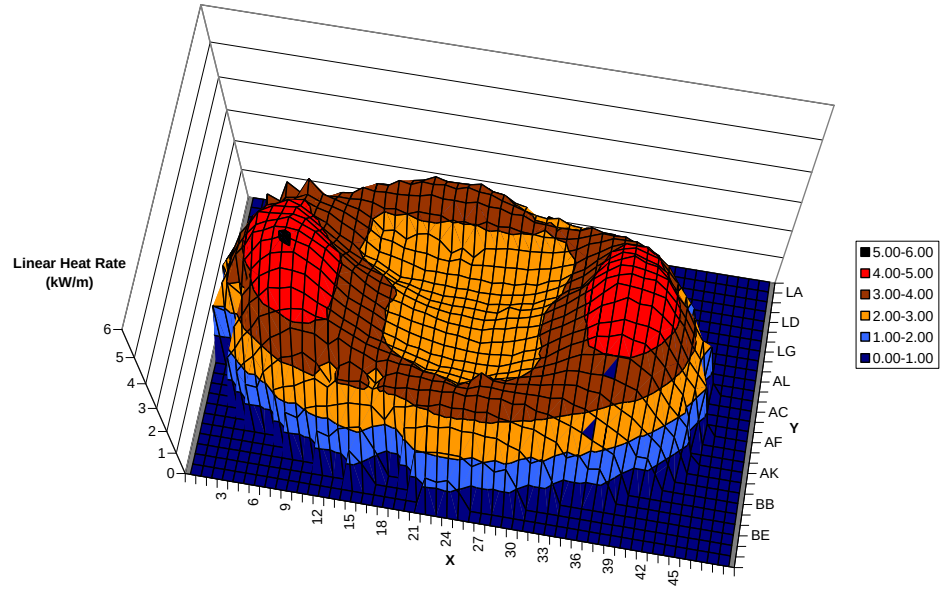

Fig. 62 – Average linear heat rate distribution at time of PCT.

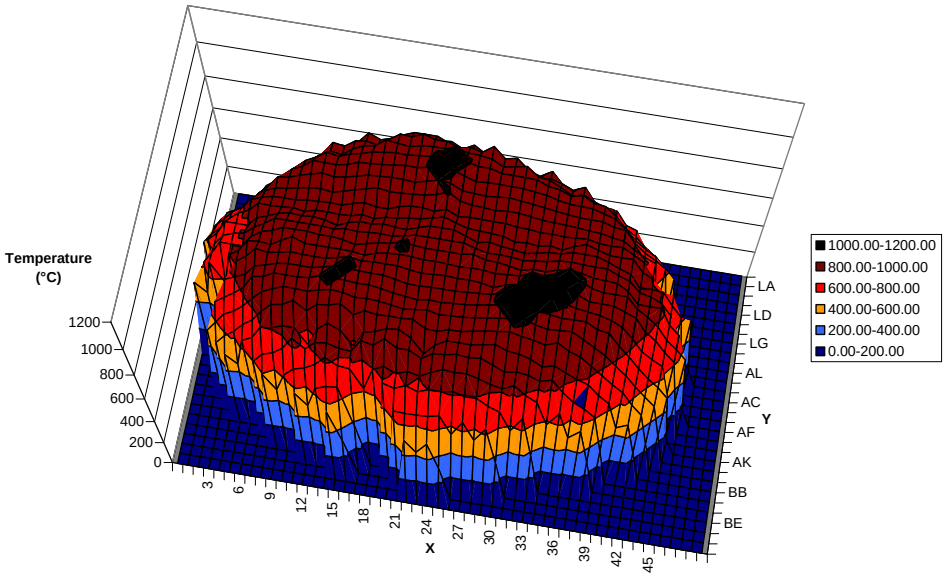

Fig. 63 – Temperature (slice 3) distribution at time of power peak.

6.5.3 Implementation of the selected boundary conditions

In the neutronic model, the 451 fuel assemblies of Atucha-II NPP have been represented one by one, whereas the thermal hydraulic model represents only 280 out of 451 channels. The association between neutronic and thermal hydraulic conditions for each fuel rod is performed according to Fig. 64 that shows the correspondence between TH and 3D-NK channels. Each number of the table correspond to a 3D-NK channel, that may correspond to more than one TH channel (TH channels are reported as consecutive numbers from 250 to 529).

Linear heat rate and the fast neutron flux are provided by the 3D-NK model (451x10 values) assuming the 37 rods of each fuel assembly contribute with the same power, whereas the temperature and the rod-external pressure (280x10) values are those corresponding to the hydraulic channel, see Fig. 64 for correspondence.

Fig. 65 reports the equilibrium burnup distribution for the reference core that are used for the calculations for each fuel assembly (*Parisi 2007*).

The time at which the equilibrium burn-up is reached, is calculated on the basis of the linear heat rate. In this way 451 different values are obtained in the calculations. The base irradiation and the refueling is modeled on the basis of the analyses of the normal operation described in section 5.1.1.

The simulation of the normal operation is performed considering the refueling strategy and the core design: six zones and three refueling paths are distinguished

to reach the initial conditions of the LOCA, according with Fig. 64 and section 2.3. Three zones include the fuel rods that do not experience the shuffling (lower burn up); the remaining zones comprise those rods that are shuffled (higher burn up). Each zone is characterized by a different transition burn-up, as reported in Tab. 24.

Path for irradiation	Burning Zone	Transition Burnup (MWd/tU)	Discharge Burnup (MWd/tU)
1	6	2886	--
1	5	--	8001
2	2	3694	--
2	4	--	8001
3	3	5546	--
3	1	--	8001

Tab. 24 – Characterization of burn-up zones for the application of Transuranus (6 zones for depletion and 3 paths for irradiation).

6.5.4 Modeling of the base irradiation

The analysis of the normal operation, described in section 5.1.1 and in APPENDIX B (*Adorni FU-09 2009*) is preparatory for the analysis of the LB-LOCA transient.

The base irradiation is the time period from the insertion of the fresh fuel rod into the core, up to the time at which the equilibrium burnup of the reference core is reached. Distinctions between rods that are/are not subject to shuffling are separately discussed in the following sections.

Base irradiation calculations are performed in order to reach the equilibrium burnup of the reference core.

6.5.4.1 No shuffling

The fuel that is not subject to shuffling (corresponding to the fuel zones 6, 2 and 3 of Fig. 64) reaches in the calculation the burnup distribution for the reference core with the axial linear heat rate, axial temperature and pressure of the steady state calculations constant in time, the resolution of the neutronic calculation is maintained (451 fuel assemblies). Each burnup equilibrium level is reached in different times, this means that for these rods, the 2A-LOCA transient starts at different times and burnup levels for each rods.

The time at which the equilibrium burnup is reached, depends on the linear heat rate. In this way the straight lines of Fig. 66 can be drawn for all the rods, and the time to reach the required burnup can be calculated, with an error less than 1%, through the use of this simplified formula:

$$TBU = BU_{AVE} * C_0 / LHR_{ave}$$

where:

TBU = time to reach the desired average burnup
BU_{AVE} = average burnup
C_0 = constant
LHR_{AVE} = average linear heat rate

Fig. 67 shows a scheme of base irradiation power history for one axial position, the relative axial heat flux is reported on the top of the picture. t_{BI} represents the time needed to reach the equilibrium burnup distribution for the reference core (Fig. 65), calculated according to Fig. 66. 2A-LOCA transient starts after the base irradiation, from the "rod specific" linear heat rate, fast neutron flux, temperature and pressure of the steady state TH-3DNK calculations.

6.5.4.2 Shuffling

For the fuel that is subjected to shuffling (corresponding to the fuel zones 1, 4 and 5 of Fig. 64), the base irradiation can be divided into three zones, Fig. 68:

a) the zone before shuffling (up to $t_{transition\ BU}$);
b) the shuffling itself (between $t_{transition\ BU}$ to t_{10}) ; and
c) the zone after the shuffling (between t_{10} to t_{LOCA}).

$t_{startup}$ identify the beginning of the base irradiation.

6.5.4.3 Zone before shuffling

Depending on the rod position, three refueling paths with a corresponding transition burnup value, as shown in Fig. 64, are envisaged (zones 1, 4 and 5). Temperature distribution and pressure of the steady state, specific for each rod, are used for the simulation of this zone.

6.5.4.4 Refueling zone

The fuel element withdrawal and insertion velocities are modeled using the value of 1m/min. The fuel residence time outside the core is set to 40 min according to (*Mazzantini 2008*). Additional assumptions are made for extraction and insertion of the fuel rod, as described in the following part.

Since the refueling strategy covers an important issue in the fuel behavior analysis, sensitivities are performed changing the extraction and insertion velocities in the framework of the normal operation activities (*Adorni FU-11 2009*).

The refueling modeling is performed in "steps". Considering that the fuel model is divided 10 axial segments and the length of each segment is 0.53m, the time elapsed for taking out of the core each segment, considering that the withdrawal and insertion velocities of 1m/min, is 0.53min. Between two values, the linear heat rate is linearly interpolated.

6.5.4.4.1 Rod extraction

The axial power history as function of time for the 10 axial positions is reported in Fig. 70. This figure represents the relative axial power as function of time; each dot represents a step of 0.53 min. During refueling, the pressure remains constant at

the steady state value. The axial cladding temperature profile changes in step from the actual value to the temperature calculated at decay power conditions with the coolant temperature of the core inlet at full power steady state.

6.5.4.4.2 Rod insertion

The axial power history as function of time for the 10 axial positions is reported in Fig. 71. This figure represents the relative axial power as function of time; each dot represents a step of 0.53 min. During refueling pressure remains constant. The axial cladding temperature profile changes in step from the actual value to the temperature calculated at decay power conditions with the coolant temperature of the core inlet at full power steady state.

6.5.4.4.3 Zone after shuffling, up to BEQ of the reference core

After the shuffling, a hold time at steady state values of the prescribed quantities is modeled, up to the time at which the rod reaches the requested burnup value. The irradiation after refueling is performed considering constant linear heat rate, clad temperature distribution and pressure up to the equilibrium burnup distribution for the reference core.

6.5.5 Modeling of the 2A-LOCA

2A-LOCA transient calculations start after base irradiation, at the time at which the equilibrium burnup of the reference core is reached for each rod.

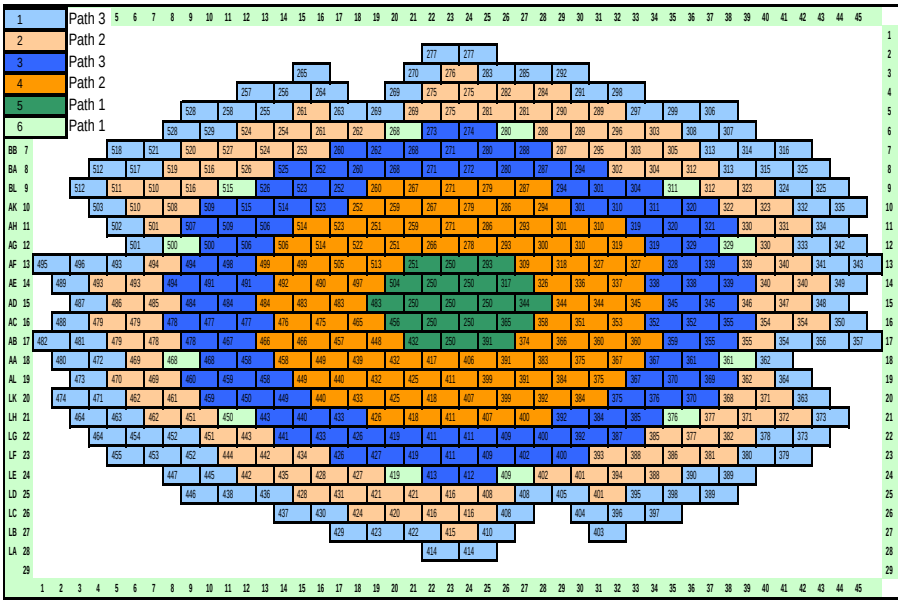

Fig. 64 – Identification of the correpondence between TH and 3D-NK core channels.

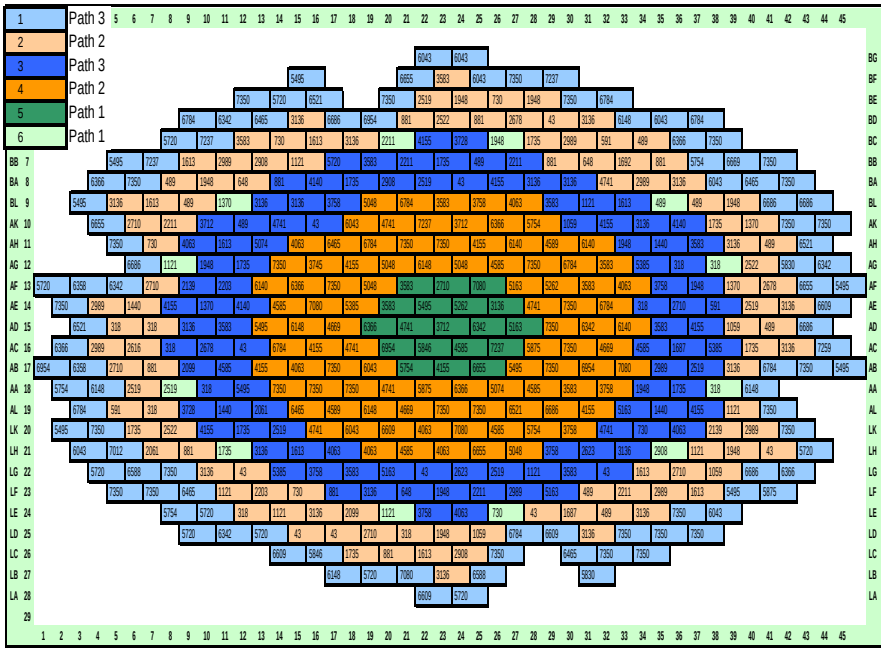

Fig. 65 – Burnup zones and values (in MWd/tU) of the equilibrium reference core.

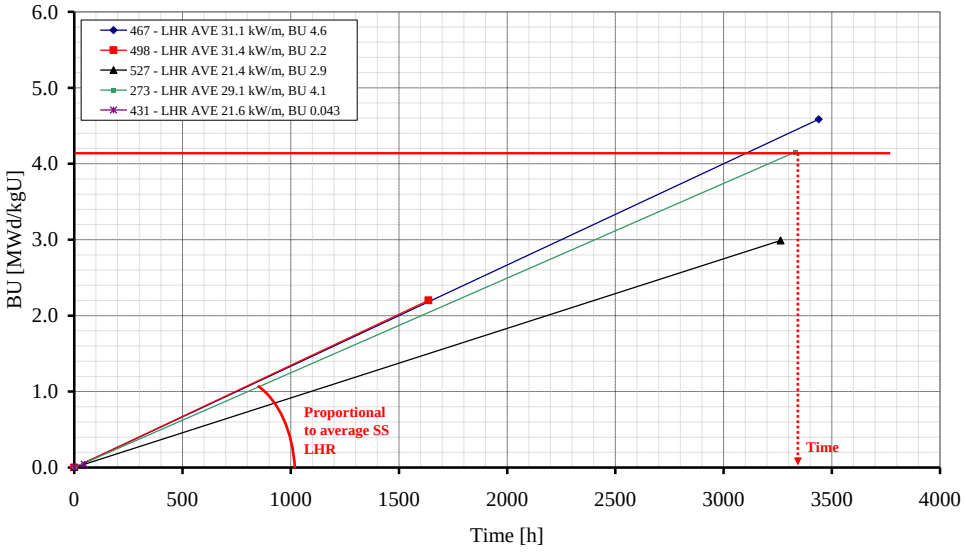

Fig. 66 - Burnup vs time at different linear heat rate, example.

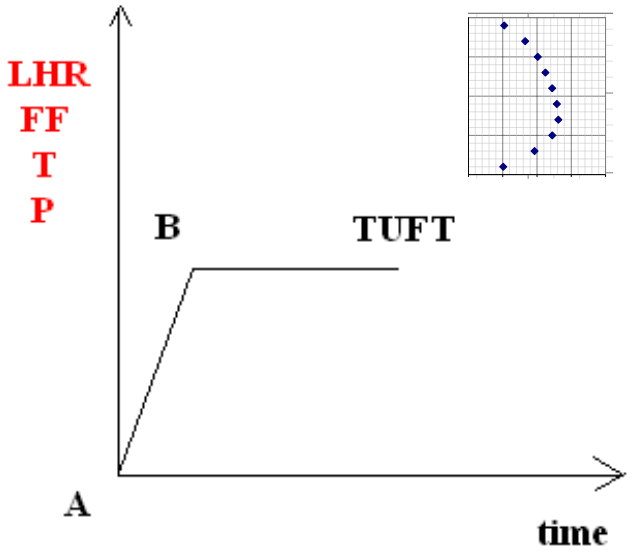

Fig. 67 - Scheme of the irradiation, burnup zones 2, 3 and 6.

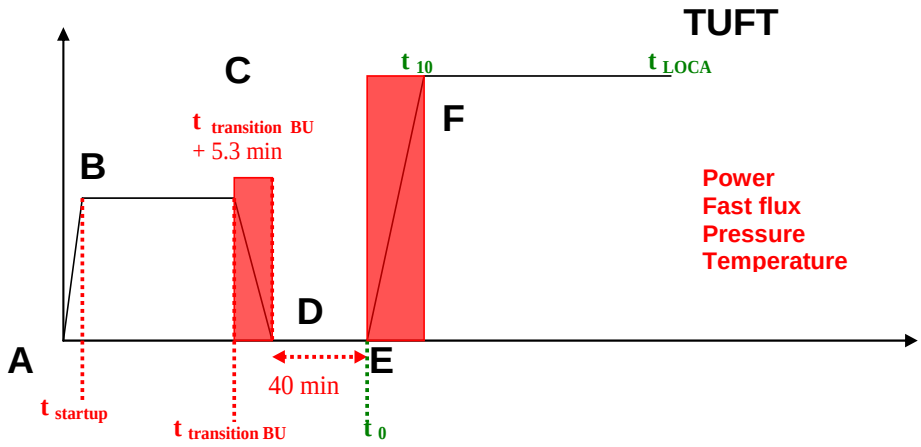

Fig. 68 – Scheme of the irradiation, burnup zone 1, 4 and 5 (refueling is simulated).

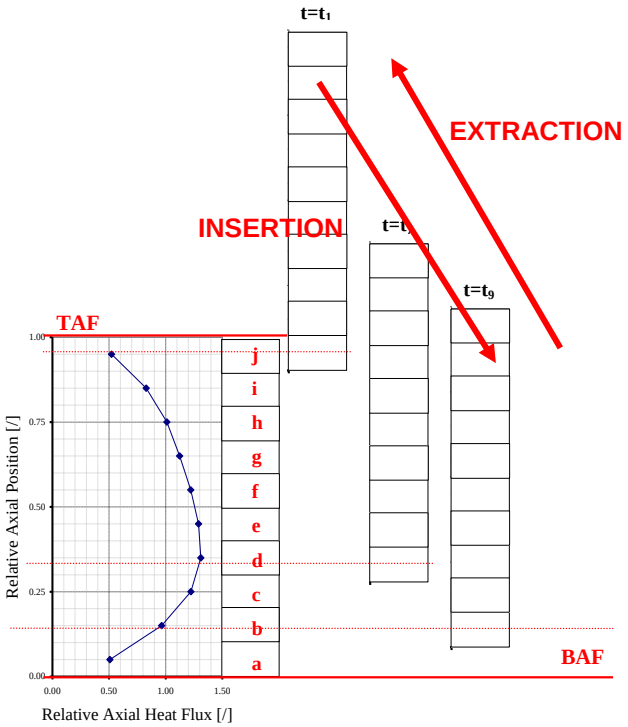

Fig. 69 - Schematic view of fuel rod extraction and insertion.

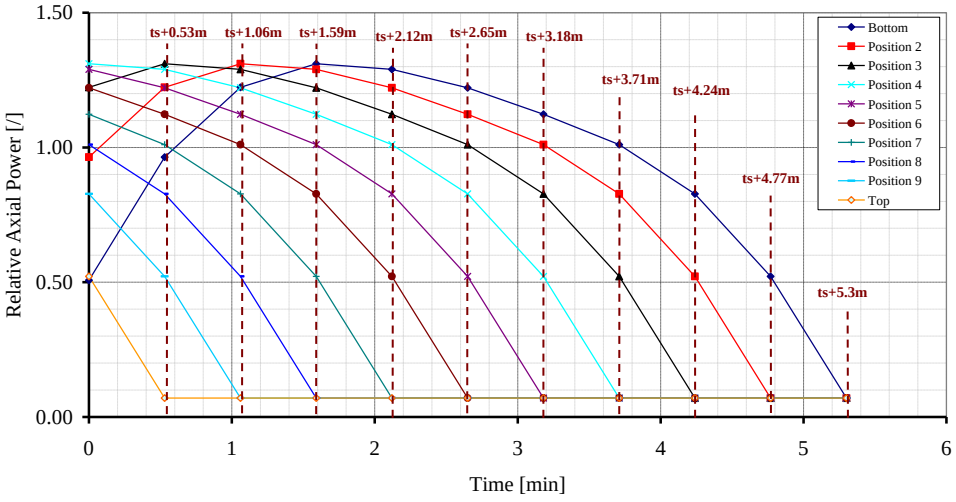

Fig. 70 - Relative axial power history during refueling as function of time for different axial position: fuel rod extraction.

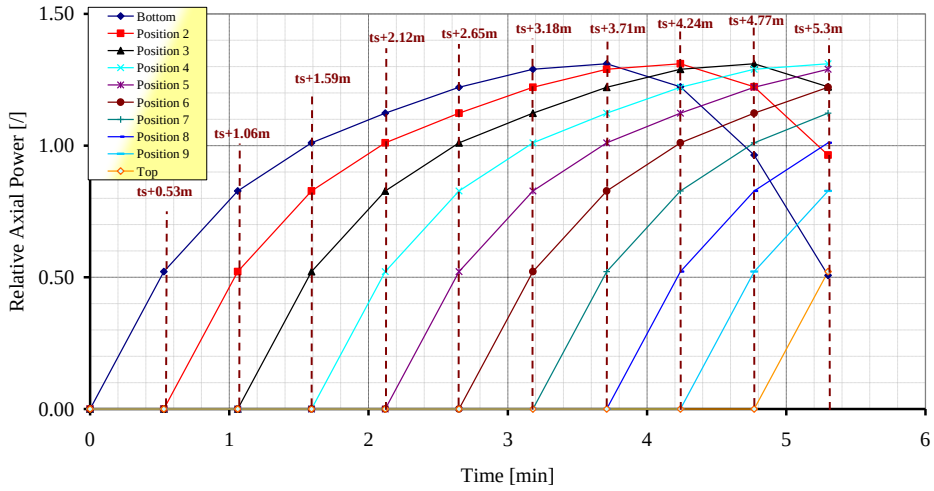

Fig. 71 - Relative axial power history during refueling as function of time for different axial position: fuel rod insertion.

6.6 Description of the procedure

The overall procedure for determining the number of failed fuel rods for the CNA-2 FSAR has been repeated three times within the framework of the safety analysis of Atucha-II (LBLOCA studies 2A-DEGB of Atucha-II), in all cases utilizing the 280ch nodalization results (reported below in the order of increasing value of calculated PCT), keeping as reference calculation:

1. 280ch_BP1, row 0 of Table 15.6.5.1.3.1.4-1 [redacted]
2. 3DNK-ref, row 2 in Table 20 of ref. [11] in section 15.0 [redacted]
3. 280ch_BP1bis, row 22 of Table 15.6.5.1.3.1.4-1 [redacted]

The relevant outcome from the above analyses is that no fuel failures are calculated in the case 1), [redacted] (roughly, see below) fuel failures are calculated in the cases 2) and 3), respectively. This shows the expected relevance of the clad temperatures (somewhat connected with the PCT) upon the failure occurrence and, at the same time, that current results are close to a phenomenological edge separating no failure from 100% fuel failures.

Reference to the 3rd one is reported in the subsequent sections, no differences are evidenced for the application to the other cases.

In addition to the calculation of the BEQ core case, two series of runs are performed at burnup levels for all the rods of 0 MWd/kgU (fresh fuel) and 8 MWd/kgU (maximum burnup allowed), considering the following assumption for the base irradiation of the latter case, see Fig. 73:

- axial distribution of linear heat rate, constant in time at the value of the steady state neutron kinetic calculations (specific for each rod);
- axial distribution of the fast neutron flux, constant in time at the value of the steady state neutron kinetic calculations (specific for each rod);
- axial distribution of temperature, constant in time at the value of the steady state thermal hydraulic calculations (specific for each rod); and
- channel pressure value of the steady state thermal hydraulic calculations (specific for each rod).

The radial peaking factors per each fuel channel are considered in the sensitivity analyses (*Adorni FU-08 2009*) and differentiate the predicted behavior of the rods belonging to the same assembly, see Fig. 74. The applied radial peaking factors, Fig. 72 , for the linear heat rate are reported below (*Mazzantini 2008*):

- 3rd ring containing 18 rods, linear heat rate multiplication factor: 1.1065;
- 2nd ring containing 12 rods, linear heat rate multiplication factor: 0.9296;
- 1st ring containing 6 rods, linear heat rate multiplication factor: 0.8508;
- central rod, linear heat rate multiplication factor: 0.8222.

Finally, probabilistic analysis is performed with the aim to cope with the unavoidable uncertainties present in the analysis (*Adorni FU-17 2010*).

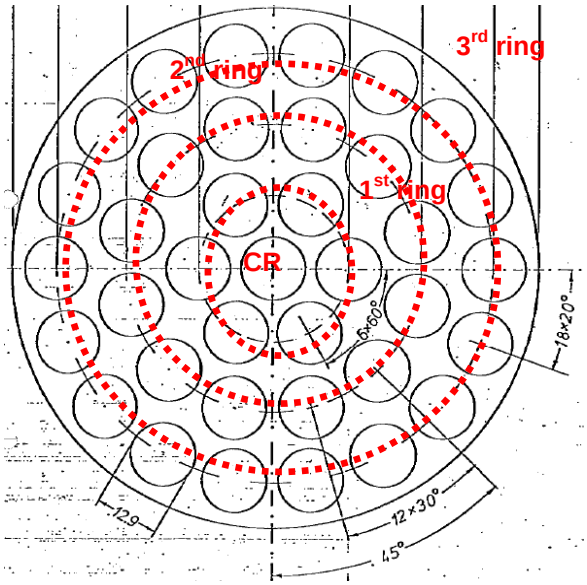

Fig. 72 – Fuel channel radial peaking factors considered for the application of Transuranus.

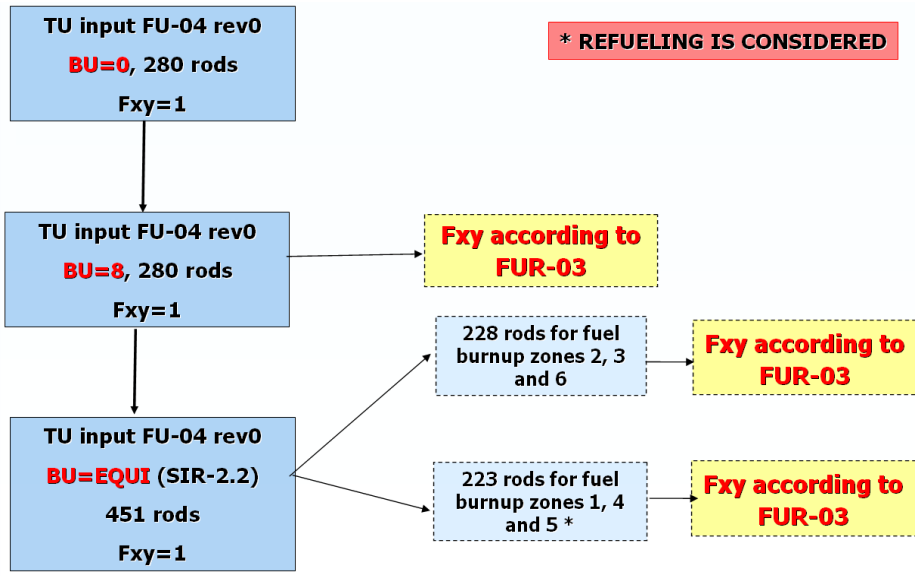

Fig. 73 – Simplified scheme of the calculation procedure for the reference case.

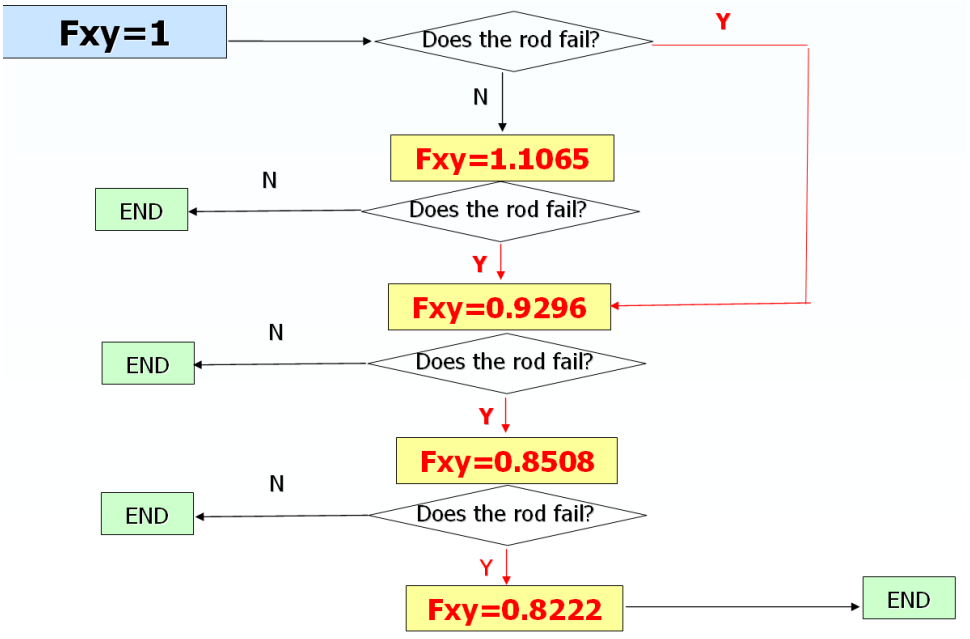

Fig. 74 – Simplified scheme of the calculation procedure for the case of use of radial peaking factors.

6.6.1 MATLAB transfer program

The number of cases to be analyzed, and the variety of the boundary conditions needed for the analysis calls for the use of programs to perform the analysis and post-processing the results, see section 4.2.3.

The boundary conditions for the fuel analysis are extracted from the TH-3DNK analysis and implemented in the TRANSURANUS MACRO part for the subsequent run with the aid of “ad hoc” written MATLAB scripts. The boundary conditions selected for the fuel analysis to be implemented in the MACRO part of the input are:

- linear heat rate;
- fast neutron flux;
- rod surface temperature;
- pressure.

6.6.2 Code interactions

Fig. 76 illustrates codes interactions.

RELAP5-3D© provides:

- power in [W], for 451 hydraulic channels, 10 axial positions;
- fast neutron flux [n/m^{2}s], for 451 hydraulic channels, 10 axial positions;
- cladding temperature in [K], for 280 hydraulic channels, 10 axial positions;
- pressure in [Pa]; for 280 hydraulic channels, 1 axial positions.

The information needed as input in the TRANSURANUS MACRO part are:

- linear heat rate [kW/m];
- fast neutron flux [n/cm^{2}s];
- cladding temperature [°C];
- pressure [MPa].

The MATLAB transfer program can cope with the different format and units of the data from RELAP5-3D© output to TRANSURANUS input ad the number of core channels.

6.6.3 Implementation of BIC

Boundary conditions and code runs are performed thought an automatic program to be run with MATLAB. The general description of program is documented in (*Adorni 2008, Adorni 2011*). The main MATLAB programs used for the preparation of the BIC are listed in Tab. 25.The main MATLAB programs used for the deterministic analysis of the CNA-2 fuel rods are listed in Tab. 26. The table reports the identification of the program, the burnup (in MWd/kgU) used for the analysis, if the shuffling is modeled or not, how many values of temperature, pressure, linear heat rate and fast flux are used as boundary conditions, for which burnup zone the program is made for, the TU input used for the analysis and

notes. The supporting programs are listed in Tab. 27, which contains also a brief description of them. In the framework of UNIPI-NASA agreement, the documentation of all the subroutines is performed.

The program is written to run with MATLAB 7 Release 14, and is prepared in order to perform automatically the analysis of all the fuel rods at the selected burnup and considering the refueling strategy. An outline of the program block is reported in Fig. 77

The program needs as input:

- the output of the RELAP5-3D© code;
- the control option part of the TU input;
- the TRANSURANUS code and annexes files;
- some "*additional files*" in order allow the program to perform automatically the runs.

Moreover it is written in blocks in order to be easily reviewed.

First of all the program opens the RELAP5-3D© code output and starts to read it line by line writing in a separate working file the selected variables, for each rod, that are:

- time [s];
- rod internal heat source [W], 10 axial position;
- fast neutron flux in [n/m^{2}s];
- cladding temperature [K], 10 axial position;
- pressure [Pa], 1 axial position.

The channel scale is the calculated based on channel number through a program block that uses an "*additional files*" containing the transferring map from 250 to 451 channels.

The above mentioned value is used in the block written to change the units from RELAP5-3D© values to TRANSURANUS suitable ones that are:

- Time [h];
- Linear heat rate [kW/m];
- Fast neutron flux [n/cm^{2}s];
- Cladding temperature [°C];
- Pressure [MPa].

At this stage the data are rearranged in TRANSURANUS format, and implemented in the reference input model (*Adorni FU-04 2008*).

Finally the program automatically runs TRANSURANUS code and stores the results, for all the rods. The program is able to cope with different radial peaking factor, different burnup and refueling strategy. A sample scheme of one of these programs is reported in Fig. 78.

6.7 Engineering handbook

The creation of a fuel model for computer codes is an interactive procedure that includes the selection of specific models, material properties, appropriate BIC and eventually the modification of the source code e.g. for implementing specific models, preparation of the code input deck, and documentation of these activities. A key role is played by the possible interaction with other codes for providing the BIC (*IAEA 2002*).

Depending on the objectives of the analysis e.g. run of chain of calculations or modeling of an experiment, the code input deck and the BIC, could be accident dependent. The documentation of all these steps, that can be called "engineering handbook", is developed in parallel with the development of the code input deck, the BIC preparation and the eventual source code modification. This handbook for the Atucha-II analysis consists in a series of documents containing a full description and records of how the database has been converted into an input deck for the particular computer code, Fig. 75 and the implementation of the BIC. The documents contain detail of:

a) Methods, simplifying assumptions and calculations made to convert the technical fuel data to the necessary format for the input deck (*Adorni FU-04 2008*).
b) References to documents used for the preparation of the input (*Adorni FU-04 2008*).
c) All modeling assumptions made, adequately described and explained (*Adorni FU-04 2008*).
d) Assumptions made for BIC preparation (e.g. chain of codes or extrapolation of data from experimental database) and eventually description of code interactions (*Adorni FU-06 2008*).
e) Detailed description of code modifications and compilation (*Adorni FU-09 2009*).

IP	Description of the IP	Value	Meaning of the value	Ref	Note
kanf	Identification of the beginning of data set/ Restart option	**IDEN**			
intrup	Control variable for the restart option	**0**	Standard calculation without restart		
nkomm	Number of text lines at the beginning of the data set	**9**			
pincha (1)	Pin characterisation: Reactor Type	**HWR**	Heavy Water Reactor	[6],[7]	
pincha (2)	Pin characterisation: Flux	**THE**	Thermal, epithermal and fast neutron spectrum (thermal reactor)	[6],[7]	
pincha (3)	Pin characterisation: Fuel Material	**OXI**	Oxide fuel	[6],[7]	
pincha (4)	Pin characterisation: Clad material	**ZIR**	Zircaloy cladding	[6],[7]	
ITEXTK(J)		*Input test records*			
ITEXTK(J)		*Input test records*			
ITEXTK(J)		*Input test records*			
ITEXTK(J)		*Input test records*			
ITEXTK (NKOMM-4)	Statistic file	**cna2r1.sta**			
ITEXTK (NKOMM-3)	Plot information file	**cna2r1.pli**			
ITEXTK (NKOMM-2)	Micro step file	**cna2r1.mic**			
ITEXTK (NKOMM-1)	Macro step file	**cna2r1.mac**			
ITEXTK	Restart file	**cna2r1.rst**			

Part of the table used to document the input deck

Fig. 75 – Sample of the table used to document the input deck (Adorni FU-04 2008).

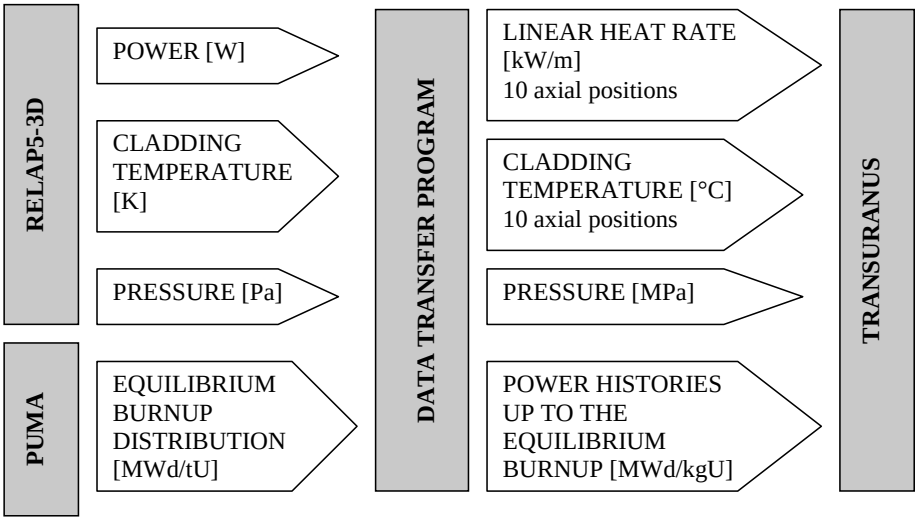

Fig. 76 – Outline of code interactions.

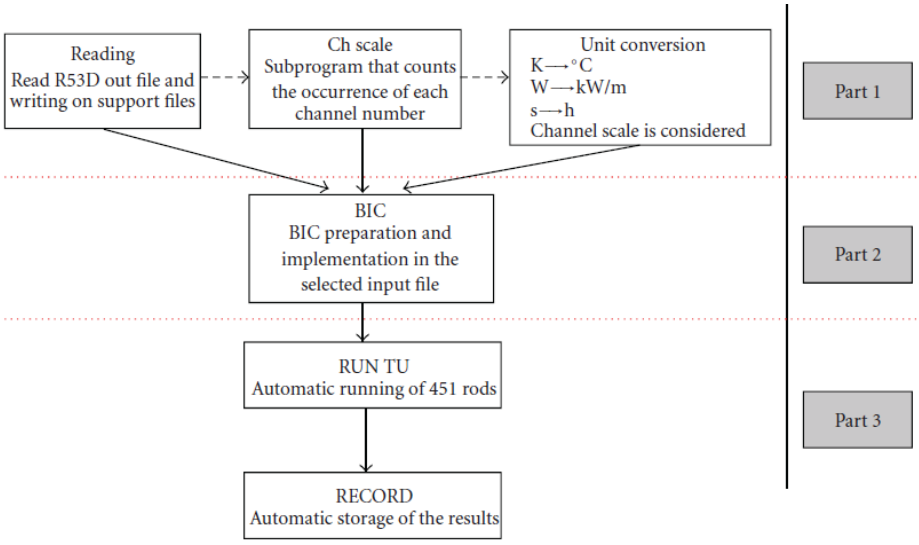

Fig. 77 – Outline of program blocks.

#	ID	BU zone	#P	#T	#LHR	#FF	NOTE
1.1	cna2_loca2_r2b.m	2, 3 and 6	228	228	228	-	
1.2	cna2_loca2_r2c.m	2, 3 and 6	228	228	228	-	As Above, without time section
2	cna2_loca2_R1_r2b.m	1	108	108	108	-	
3	cna2_loca2_R4_r2b.m	4	96	96	96	-	
4	cna2_loca2_R5_r2b.m	5	19	19	19	-	
5.1	Power_r0b.m	All	-	-	-	-	
5.2	BALL_LHR_r0.m	All	-	-	-	-	
5.2	cna2_loca_LHR_rev5.m	All	-	-	451	-	
6.1	FF_r0i.m	All	-	-	-	-	
6.2	FF_E_ALL_r2.m	All	-	-	-	451	

Tab. 25 – M- programs for BIC preparation.

#	ID	BU	SHUF	# T, P, LHR	# FF	# BU	BU zone	INPUT	NOTE
1	cna2_loca_ALL_0_r2.m	0	N	280	451	1	All	FU04rev0*	--
2	cna2_loca_ALL_BUEQ_r2.m	8	N	280	451	1	All	FU04rev0*	--
2a	cna2_loca_BUEQ_r2.m cna2_locaR1_8_BUEQ_r2.m cna2_locaR4_8_BUEQ_r2.m cna2_locaR5_8_BUEQ_r2.m	BEQ	N Y Y Y	280	451	451	2, 3 and 6	FU04rev0*	--
3	cna2_loca_BUEQ_r2.m	BEQ	N	139	108	108	2, 3 and 6	FU04rev0*	**
4.1	cna2_R1_loca_BUEQ_r2.m	BEQ	Y	96	96	96	1	FU04rev0*	
4.4	cna2_R4_loca_BUEQ_r2.m	BEQ	Y	70	19	19	4	FU04rev0*	
4.5	cna2_R5_loca_BUEQ_r2.m	BEQ	Y	11	19	19	5	FU04rev0*	

*FU04rev0a as FU04rev0 except for:
- **INSTA**=1 (transient thermal analysis (mixed implicit–explicit) with automatic switch-over to a steady-state (implicit) analysis if the time step is larger then 0.01 h);
- **TLOCA**=time of LOCA initiation

**** The sum of T, P and LHR BIC is greater that 280 because the same rod may belong to different BU zones

Tab. 26 – Main M-programs for RUN the calculations.

#	ID	DESCRIPTION	NOTE
A	lit_count_r0.m	Channel scale calculation	In the main program
B	CNA2_SS_Fy.m CNA2_SS_Fy_451.m	Axial peaking factors calculation	
C	cna2_loca_PCT_r1.m	Peak cladding temperature identification	
D	cna2_loca_LHR_r1.m	Linear heat rate identification	
E	cna2_loca_236_FAILURE_r6.m cna2_loca_1_FAILURE_r6.m cna2_loca_4_FAILURE_r6.m cna2_loca_5_FAILURE_r6.m	Id of failed rods	
F	cna2_loca_ALL_FAILURE_r6.m	Id of failed rods	
G	cna2_loca_ BU_EI_r0b.m	Determination of burnup	
H	cna2_loca_ECR_r0b.m cna2_loca_ECR_r0d_SOLOLOCA_r2.m cna2_loca_ECR_r0d_ENDBI_r2.m	Equivalent cladding reacted and maximum value during LOCA evaluation	
I	cna2_loca_ENTHALPHY_MAXLOCA_r0b.m cna2_loca_ENTHALPHY_MAXLOCA_r0b2solodat.m	Enthalpy and maximum value during LOCA evaluation	
J	cna2_loca_FGR_MAXLOCA_r0b.m	Fission gas release and maximum value during LOCA evaluation	
K	cna2_loca_GapWidth_MAXLOCA_r0b.m cna2_loca_GapWidthmin_r0d_SOLOLOCA_r2.m	Gap width and maximum value during LOCA evaluation	
L	cna2_loca_P_MAXLOCA_r0b.m	Gap pressure and maximum value during LOCA evaluation	
M	cna2_loca_RHA_r0b.m cna2_loca_RHA_r0d_SOLOLOCA_r2.m	Cladding outer radius and maximum value during LOCA evaluation	
N	cna2_loca_SOXIDE_MAXLOCA_r0b.m	Oxide thickness and maximum value during LOCA evaluation	
O	cna2_loca_Tcl_r0b.m cna2_loca_Tcl_r0d_SOLOLOCA_r2.m	Fuel centerline temperature and maximum value during LOCA evaluation	

Tab. 27 – Main support M-programs.

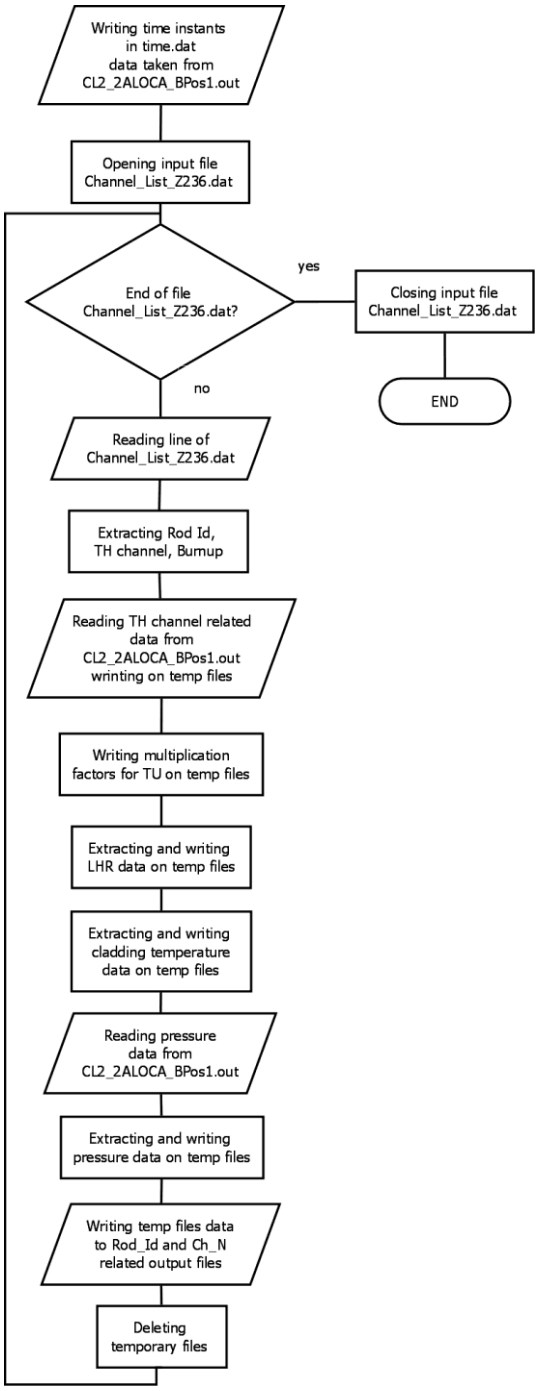

Input files:

CL_2ALOCA_BPos1.out
Channel_List_Z236.dat
NUMBERING.i

Output files:

Time.dat
BIC-LHRTcl_'Ch_N'.dat
BIC-P08_'Ch_N'.dat
A_'Rod_Id'.txt
B_'Rod_Id'.txt
C_'Rod_Id'.txt
D_'Rod_Id'.txt

Fig. 78 – Sample scheme of M-Programs.

7. APPLICATION OF THE METHODOLOGY TO ATUCHA-II NPP

7.1 Calculated Results

The LB-LOCA transient starts at the time when the equilibrium burn-up conditions are reached for each rod. Base irradiation is modeled in the calculations according to section 6.4. The fuel analysis consists in the simulation of the 451 rods, each one representing one fuel assembly. The application of assembly radial peaking factors allows the prediction of different performances for the rods belonging to the same assembly.

The discussion of the results addresses the investigation of the fuel performance with main reference to the parameters discussed in the section 6.2.

The energy released to the fuel during the power peak is calculated as the difference between the value of the enthalpy of each fuel pin (representing the average pin of each fuel assembly) at the end of power excursion and the value at the beginning of the transient. The maximum is selected for each fuel pin as the calculated radial average energy density at any axial location. Fig. 79 reports the 451 values of the enthalpy released to the fuel calculated for each fuel pin, grouped according with the different zones. The maximum value is calculated in zone 3 and is slightly below [redacted] This ensures that the core damage and core cooling capability is not impaired due to the thermal expansion of the fuel (the assumed DBA acceptance criteria for RIA is 230 cal/g).

Fig. 80 shows the trend of the maximum fuel temperature of the fuel pellet at hot spot during the transient. According to the FSAR Chapter 4 (*NASA 2007*), the fuel melting temperature is a function of burn-up that ranges between [redacted] or fresh fuel and [redacted] at the discharge burn-up. The results of the calculation demonstrate that the melting temperature is not met at any point of the fuel pellet during the LB-LOCA transient. In the same figure the Vitanza threshold provides an idea of the 1% limit for fission gas release.

The oxidation of the cladding, calculated as the ratio of the total cladding thickness before oxidation, is reported in Fig. 81. The predicted values are always below [redacted] of the cladding thickness. The maximum predicted value for cladding oxidation is far from the DBA acceptance criteria for LOCA transient (17%).

The H2 production calculated is [redacted] of the total H2 which might be generated in the core ([redacted] considering only the metal of the fuel pins. As this value ([redacted] kg) considers only the H2 produced by the reaction of the metal of the fuel pins, the actual percentage of the hydrogen produced during the transient including all zircaloy mass that may react inside the active core region (e.g. spacer grids and channel tubes) is much lower than [redacted]. Indeed, the fuel pins are the components more stressed from the thermal and mechanical point of view and therefore more prone to the metal-water reaction. The maximum predicted value for H2 production is far from the DBA acceptance criteria for LOCA transient (1%).

The calculated overall number of fuel failures is about [redacted] of the total number of fuel assemblies in the core. The spatial distribution of failures is provided in Fig. 82. This value is calculated assuming flat radial power distribution inside each assembly and includes the cases of code failures due to convergence problem (around [redacted] of the total number of fuel assemblies in the core). In the case when the radial power distribution is considered, see previous section, the overall number of fuel assembly failures is less than [redacted]. In the first case the total number of damaged fuel pins is calculated as [redacted] x 451 x 37 and equal to [redacted] failures. Starting from the latter, the consideration of inside-assembly power distribution brings to a more precise number of pin failures that remains below [redacted] failures (excluding code failures). Therefore, the result of [redacted] i.e. [redacted] fuel assembly failed) pin failures is taken as the final result from the analysis and used for the prediction of radiological releases.

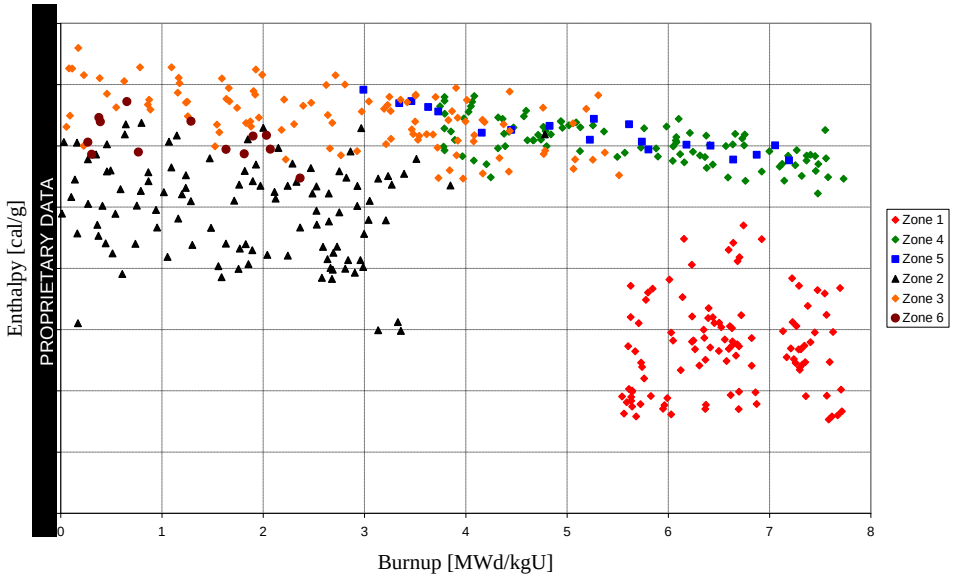

Fig. 79 – Enthalpy released to the fuel.

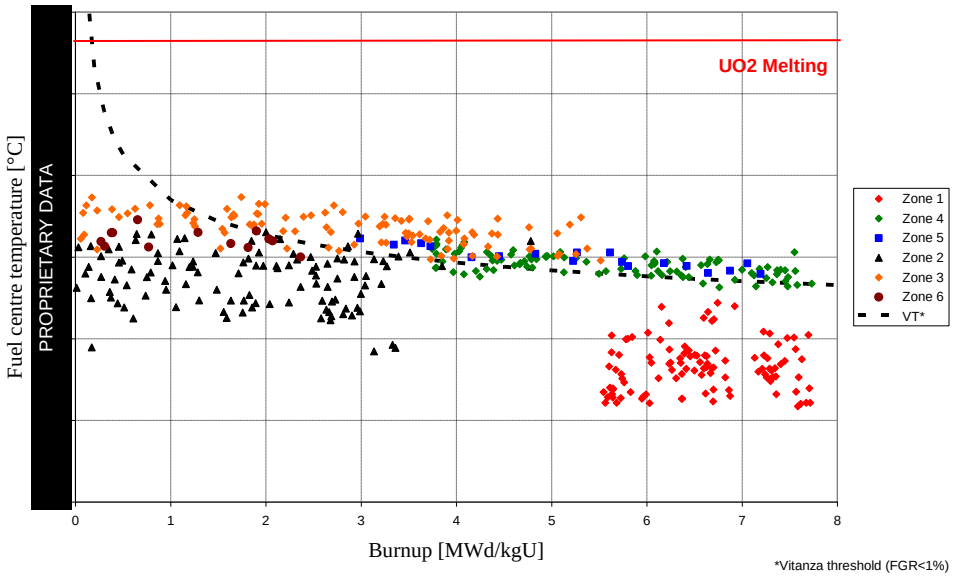

Fig. 80 – Fuel pellet temperature at hot spot.

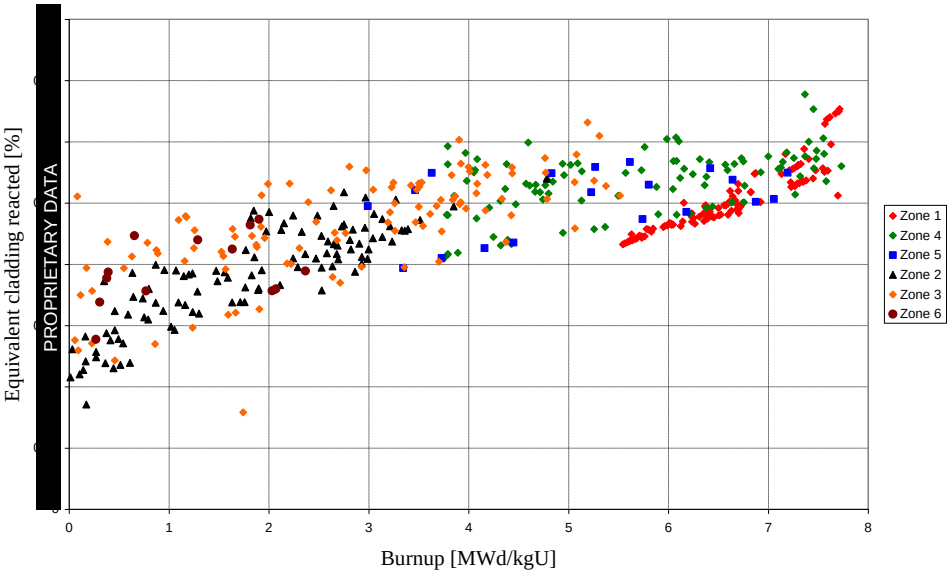

Fig. 81 – Equivalent cladding thickness reacted.

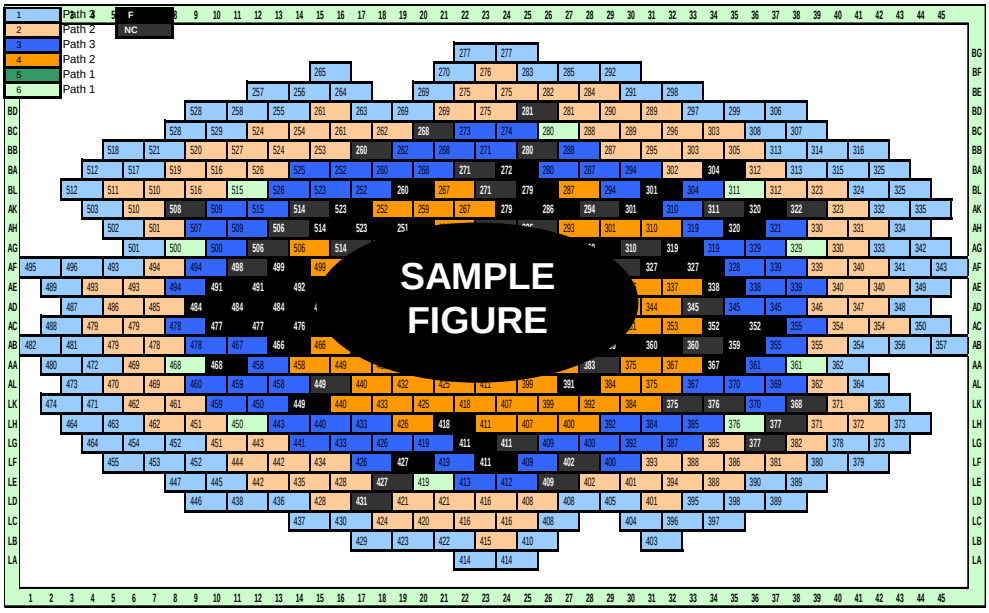

Fig. 82 – Map of failed fuel channels.

The key mechanism of fuel failure is the plastic instability involving the phenomenon of ballooning. The maximum average equivalent stress versus the maximum cladding temperature for the 451 fuel pins representing the average conditions of the each fuel assembly is reported in Fig. 83. All fuel failures are concentrated in the region where the clad surface temperature overpasses 900 °C. Numerical convergence problems are connected with a high value of rod surface temperature (typically > 915 °C).

The equivalent stress versus maximum cladding temperature as function of the time at the elevation where the rupture occurs is reported for three rods in the same Fig. 83. The rod 268_BA20 fails because the overstress criterion is met; the rod 505_AF17 overpasses the plastic instability criterion; and the third rod, i.e. 367_AA32, is calculated to overpass both criteria simultaneously.

Few rods fail due to overstress criterion caused by the phenomenon of the PCMI (i.e. rod 268_BA20 in the figure below). These rods have the gap closed at the beginning of the transient due to the “creep-down”. The other failures are caused by high strain rate (plastic instability) and by ballooning of the cladding.

The pin failure is also observed when clad temperature overpasses 1200 K = 927 °C.

Fig. 84 summarize the time of failures discriminating between failure and non convergence. In the same figures the identification of the range of times at which the PCT happens is identified as well. Finally, Fig. 85 highlight possible failure modes during combined LOCA and RIA.

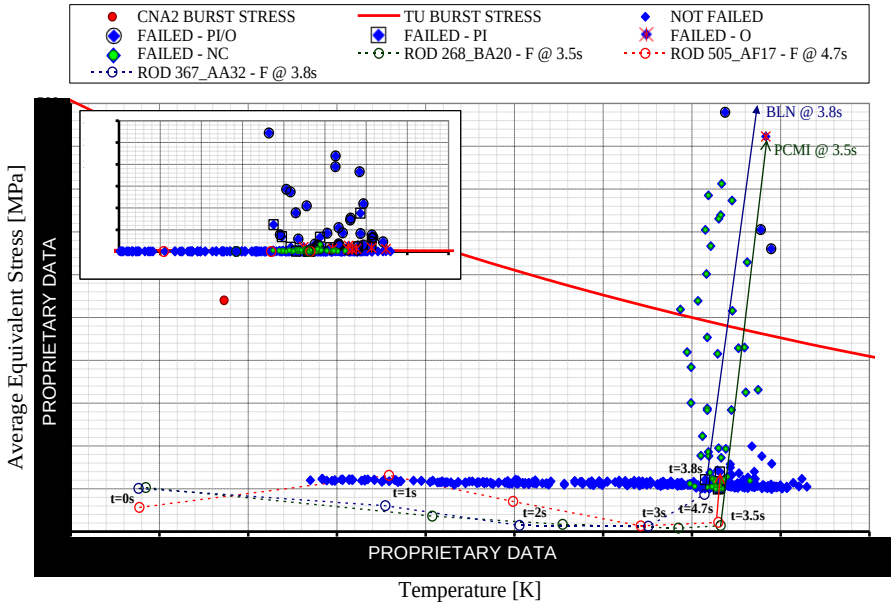

Fig. 83 – Characterization of the rod failure mechanism: Maximum average equivalent stress versus the maximum cladding temperature for the 451 fuel pins representing the average conditions of the Atucha II FC.

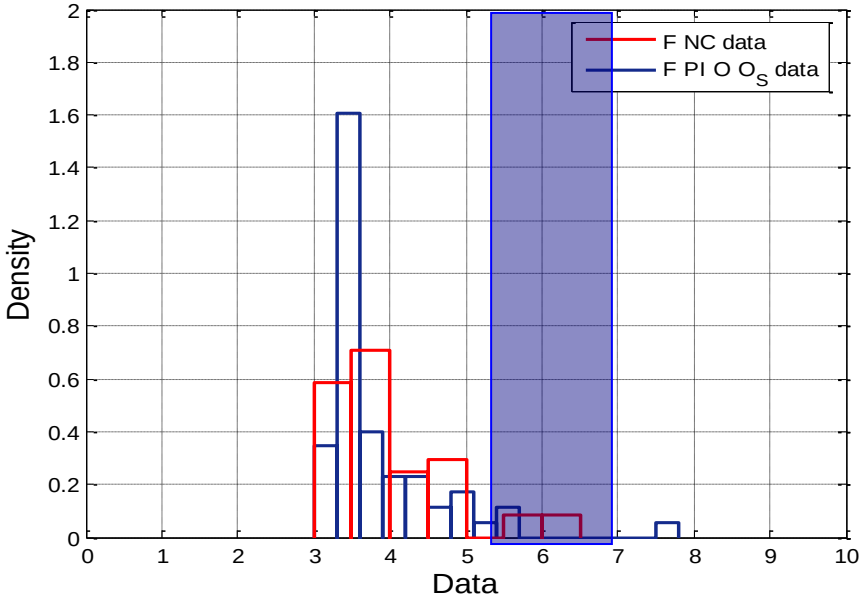

Fig. 84 – Distribution of the failure times.

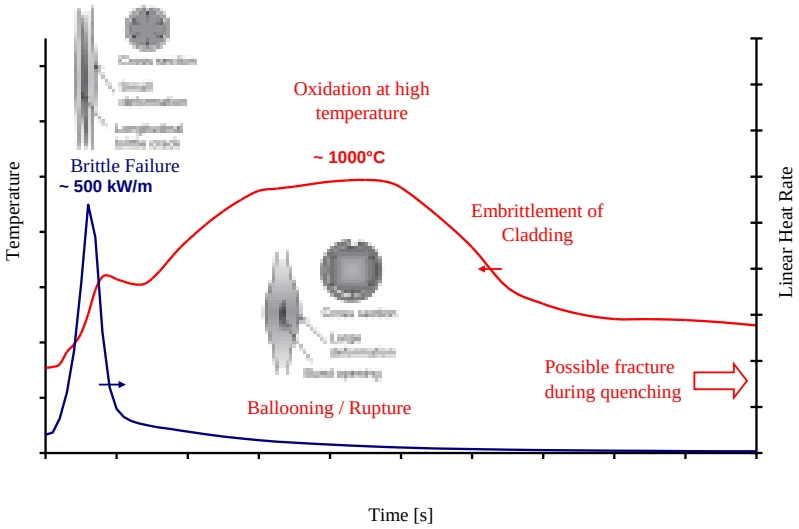

Fig. 85 – Scheme of failure modes during combined LOCA and RIA.

7.2 Radiological consequences: failure of fuel rods and release of fission products into the primary system coolant

The evaluation of radiological consequences includes several steps. Each step has its own initial and boundary conditions, only the role of TRANSURANUS results are highlighted in this section.

The results of the analysis documented in previous sections provides the number and the identification of the failed rods. The source term therefore derives from the failed rods and from the fission products released to primary system coolant, to the containment and, possibly, to the environment. The number of failed rods has been calculated by the code TRANSURANUS. In addition to the total number of failed rods TRANSURANUS provides also the information which channels contain failed rods.

In order to calculate the total amount of fission products released from the failed fuel rods to the primary system coolant three sets of information have been considered:

- The affected channels have been singled out by the TRANSURANUS calculation.
- The inventory of the assembly of the affected channel has been taken from the MCNP5-Origen calculation.
- The release fractions from the assembly to the coolant have been based on the recommendations in RG 1.183, making reference to release fractions for LOCA analysis in PWR.

Mode detail can be found in (*NASA 2011*).

7.3 Conclusive remarks

The LB-LOCA constitutes the 'historical' event for the design of Emergency Core Cooling Systems (ECCS) in Water Cooled Reactors and is primarily adopted in vessel equipped Nuclear Power Plants. In the case of Atucha-II the history of the construction and the agreement between the Regulatory Authority and the Utility brought to the exclusions of the 2A-LOCA from the list of the DBA, and the adoption of the break size of ten percent on reactor coolant pipe (0.1 A) as the basis for fulfilling traditional regulatory requirements.

Therefore, Atucha-II LB-LOCA is classified as selected beyond design basis accidents (SBDBA). For the spectrum of the SBDBA, the safety margins are estimated against the same limits or criteria as for DBA, and the fulfillment of all DBA criteria is not mandatory.

As the aim for the analyses within the SBDBA spectrum is to demonstrate the existence of extended design provisions, a best estimate approach was applied with calculation uncertainties quantified determining the still available safety margins in the case of DEGB (2 x100% in CL) LBLOCA-RIA.

The analysis performed in relation to the DEGB (2 x100% in CL) LBLOCA-RIA in Atucha-II confirms the BDBA nature of the transient. Namely, the results of the event analysis demonstrate that not all the DBA acceptance criteria for the performance of the engineered safety features were met. In addition to this, related to the traditional DBA requirements for the event analysis, the assumptions regarding the availability of the engineered safety systems were not consistent with the n+2 approach.

8. CONCLUSIONS

Licensing requirements vary by country in terms of their scope, range of applicability and numerical values and in general imply the use of complex system thermal hydraulic computer.

Depending on the specific event scenario and on the purpose of the analysis, it might be required the availability of calculation methods that are not implemented in the standard system thermal hydraulic codes, as for burst temperature, burst strain and flow blockage calculations. This may imply the use of a dedicated fuel rod thermo-mechanical computer code such as TRANSURANUS.

This thesis consists in the development and application of a methodology for the analysis of the 2A LB-LOCA scenario in Atucha-2 nuclear power plant (NPP), focusing on the procedure adopted for the use of the fuel rod thermo-mechanical code and its application for the safety analysis of Atucha-II NPP (Chapter 15 FSAR). The methodology implies the application of best estimate thermal-hydraulic, neutron physics and fuel pin performance computer codes, with the objective to verify the compliance with the specific acceptance criteria. The fuel pin performance code is applied with the main objective to evaluate the extent of cladding failures during the transient.

The steps below were performed to fulfill the objectives:

- acquisition of expertise in the nuclear fuel field, taking advantage from the participation in international activities;
- investigation of issues related to the use of the fuel pin mechanics codes;
- development of a methodology/procedure for predicting the fuel performance in safety analysis (including the connection with the FSAR) by means of fuel pin mechanics code;
- application of the methodology/procedure in case of combined LOCA and RIA transient (selected BDBA in the Chapter 15 of the FSAR of Atucha-2 NPP) for evaluating the number of failed rods and the release of the fission products;
- validation activities to support the reliability of the analyses.
- completion of the activity considering the environmental release.

8.1 Innovations

The application of the methodology helps to assess the number of the fuel element that can fail in case of the selected accident, identification of the failed fuel rods for the subsequent evaluation of the radiological release. Analysis were performed to support the study of normal operation for the simulation of irradiation fuel rods during normal operation as it defines the status of fuel at the beginning of transient; In addition to this, the activities performed to support the reliability of the code results and constitute an enlargement of the TU validation domain (an example of non standard application is analyzed as well).

Within the overall objective of the research, the following relevant results may be highlighted:

1. Application of the methodology developed, to the FSAR Chapter 15 of Atucha-II NPP in construction in Argentina.
2. Demonstration that the application of the proposed methodology allows evaluating the performance of the fuel and to the required level of safety (including the review and selection of these criteria, for normal operation (design review) and for the selected accident conditions (LOCA and RIA combined)).
3. Identification and extension of the "validation domain" of the TRANSURANUS code. to enhance the code capabilities and to improve the reliability of the code results.
4. Feasibility study of an experiment to be conducted in a research reactor, including the preparation of the technical specifications and cost analysis, extremely challenging from the scientific point of view.

8.2 Future development

For the safety analysis of the CNA-2 NPP the activity can be considered concluded and no further development are envisaged.

For the code development, the following considerations can be useful to point out possible future development of the activity:

1. Internal coupling of the TRANSURANUS code (or a generic fuel pin mechanics code) with a thermal-hydraulic system code, with the aim of produce a more user friendly tool, for standard applications. This specific point will be performed in the framework of current agreements.
2. Possibility to introduce a multi-pin analysis, see (*Ammirabile 2003*), to better account for possible loss of coolability due to ballooning.
3. Improvement of the transient option of TRANSURANSU code, that is not yet a standard option, due its possible use to better amount for the refabrication process at which undergoes the rodlets that are commonly used for experiments.
4. Further LOCA and RIA experiments should be analyzed, from both experimental and modeling point of view, due the need to improve the understanding of the complex phenomena that happen during irradiation of fuel rods. This will be the subject of future activities e.g. IAEA CRP FUMEX-III CRP, Sandia Fuel Project, Halden Reactor Group experimental programs.
5. Three-dimensional stress calculations.

REFERENCES

Adorni M., A. Del Nevo, F. D'Auria, O. Mazzantini
Modeling LB-LOCA: in Reactor Fuel Bundle Materials Test MT-4 and MT-6A
ICONE-19, Makuhari, Japan, 16-19 May 2011.

Adorni M., A. Del Nevo, F. D'Auria, O. Mazzantini
A procedure to address the fuel rod failures during LB-LOCA transient in Atucha-2 NPP
Science and Technology of Nuclear Installations, Article ID 929358, doi:10.1155/2011/929358, 2011.

Adorni M,, D'Auria F.
Behavior of irradiated fuel under RIA conditions: tests FK-1, -2 and 3
Contract NA-SA UNIPI 03 - Atucha II, Pisa, Project task report 305/2010.

Adorni M, D. Rozzia, Del Nevo A., D'Auria F.
Modeling LB-LOCA: in Reactor Fuel Bundle Materials Test MT-4 and MT-6A
Software Licensing Agreement Ref. No. 30645, ITU and UNIPI – University of Pisa Report, FUEL/ITU31263/01(10) Rev. 1, December 2010.

Adorni M., A. Del Nevo, F. D'Auria
A procedure to address the fuel rod failures during LB-LOCA transient in Atucha-2 NPP
ICONE18, Xi'an, China, 17-21 May 2010.

Adorni M., A. Bonelli, Del Nevo A., D'Auria F.
Investigation of PCI failure thresholds of CNA-1 fuel: Deterministic calculations
Contract NA-SA UNIPI 03 - Atucha II, Atucha-II, Project task report LS_FU-02 2010.

Adorni M., Del Nevo A., D'Auria F.
Probabilistic fuel rod analysis during Normal Operation
Contract NA-SA UNIPI 02 - Atucha II, Pisa, Project task report FU-18 2010.

Adorni M., Del Nevo A., D'Auria F.
Probabilistic fuel rod analysis during LB-LOCA accident
Contract NA-SA UNIPI 02 - Atucha II, Pisa, Project task report FU-17 2010.

Adorni M., Rozzia D., Del Nevo A., D'Auria F.
Investigation of PCI phenomenon in PWR fuel with TRANSURANUS code
IAEA Technical Meeting on Safety Issues related to the Use of High-burnup Fuel and to the Long Residence Time of Fuel in the Reactor, Vienna, Austria, 1-4 December 2009.

Adorni M., A. Del Nevo, P. Van Uffelen, F. Oriolo, F. D'Auria
Assessment of TRANSURANUS fuel performance code against Studsvik Inter-Ramp BWR database
ICONE17, Brussels, Belgium, 12-16 July 2009.

Adorni M., A. Del Nevo, F. D'Auria
Sensitivity analysis during normal operation
Contract NA-SA UNIPI 02 - Atucha II, Pisa, Project task report FU-11 2009.

Adorni M., A. Del Nevo, F. D'Auria
Deterministic analysis of the fuel during power ramp
Contract NA-SA UNIPI 02 - Atucha II, Pisa, Project task report FU-10 2009.

Adorni M., A. Del Nevo, F. D'Auria
Definition and implementation of the boundary and initial conditions for fuel pin analysis, Normal Operation
Contract NA-SA UNIPI 02 - Atucha II, Pisa, Project task report FU-09 2009.

Adorni M., A. Del Nevo, F. D'Auria
Sensitivity fuel rod analysis during LB-LOCA by TU code
Contract NA-SA UNIPI 02 - Atucha II, Pisa, Project task report FU-08 2009.

Adorni M., A. Del Nevo, F. D'Auria
Deterministic fuel rod analysis during LB-LOCA by TU code
Contract NA-SA UNIPI 02 - Atucha II, Pisa, Project task report FU-07 2009.

Adorni M., A. Del Nevo, F. D'Auria
Design of Experiments to be Performed in Halden Research Reactor
Contract NA-SA UNIPI 02 - Atucha II, Pisa, Project task report FU-01 2009.

Adorni M., A. Del Nevo, F. D'Auria
Design of Experiments to be Performed in Halden Research Reactor
Contract NA-SA UNIPI 02 - Atucha II, Pisa, Project task report FU-01 2009.

Adorni M., Del Nevo A., D'Auria F., Luzzi L.
Verification of TRANSURANUS code versions "v1m1j07" and "v1m1j08" against BWR-Inter-Ramp experiments
Software Licensing Agreement Ref. No. 30645, ITU and UNIPI – University of Pisa Report, DIMNP NT631(08)Rev.2, December 2008.

Adorni M., A. Del Nevo, F. D'Auria
Definition and implementation of the boundary and initial conditions for fuel pin analysis, LB-LOCA
Contract NA-SA UNIPI 02 - Atucha II, Pisa, Project task report FU-06 2008.

Adorni M., A. Del Nevo, F. D'Auria
Review LB-LOCA analysis
Contract NA-SA UNIPI 02 - Atucha II, Pisa, Project task report FU-05 2008.

Adorni M., A. Del Nevo, F. D'Auria
Development and set up of fuel pin model by TU code
Contract NA-SA UNIPI 02 - Atucha II, Pisa, Project task report FU-04 2008.

Ammirabile L.
Coupled Mechanical Thermohydraulic Multi-pin Deformation Analysis of a PWR Poss of Coolant Accident
PhD Thesis. Imperial College London, 2003.

Bousbia Salah A.
Overview of coupled system thermal-hydraulic 3D Neutron Kinetic code applications
PhD Thesis, University of Pisa, June 2004.

Alvarez
Barra combustibile EC CNA-2 plano No 1.0.16.505
Contract NA-SA UNIPI 02 - Atucha II, FUR-05, 17 September 2007.

ARN
Norma básica de seguridad radiological
AR 10.1.1. Revisiòn 3, Aprobada por Resolución del Directorio de la Autoridad Regulatoria Nuclear Nº 22/01 (Boletín Oficial Nº 20/11/01), 2001.

Argentina
Argentinean National Report for the Convention on Nuclear Safety
Buenos Aires, 2007.

Boyack, B. E., et al.
Phenomenon Identification and Ranking Tables (PIRTs) for Loss-of-Coolant Accidents in Pressurized and Boiling Water Reactors Containing High Burnup Fuel
Los Alamos National Laboratory, U.S. Nuclear Regulatory Commission, NUREG/CR-6744, LA-UR-00-5079, December 2001.

Chantoin P., E. Sartori, J.A. Turnbull
The Public Domain Database on Nuclear Fuel Performance Experiments (IFPE) for the Purpose of Code Development and Validation
ANS, Topical Meeting on Light Water Reactor Fuel Performance, Portland, Oregon, 2-6 March 1997.

Cunningham, M.E. et al.
FRAPTRAN: Integral Assessment
NUREG/CR-6739, Vol. 2 (PNNL-13576), Pacific Northwest National Laboratory, Richland, WA, 2001.

Cunningam, M.E. et al.
FRAPTRAN: A Computer Code for the Transient Analysis of Oxide Fuel Rods
NUREG/CR-6739, Vol. 1 (PNNL-13576), Pacific Northwest National Laboratory, Richland, WA.

D'Auria F., Mazzantini O., Cherubini M., Giannotti W., Parisi C., Moretti F., Melideo D., Del Nevo A., Galassi G.M., Araneo D., Terzuoli F., Adorni M., Muellner N., Petruzzi A., Lazzerini D., Santoro R., Bousbia-Salah A.
DEGB LBLOCA (2 X 100% Break in CL) in Atucha-2 NPP.
Contract NA-SA UNIPI 01 - Atucha II, University of Pisa Report, DIMNP NT 628(08) - rev. 1, Pisa, March 2008.

D'Auria F., A. Bousbia-Salah., A. Petruzzi, A. Del Nevo
State of the Art in Using Best Estimate Calculation Tools in Nuclear Technology
J. Nuclear Engineering and Technology, Vol. 38, No. 1, pages 11-32, February 2006.

D'Auria F., Reventos F., Sjoberg A., Sandervag O., Anhert C., Verdù G., Macek J., Ivanov K., Rizwan-Uddin, Sartori E., Frid V., Panayotov D.
Revisiting Critical Issues in Nuclear Reactor Design / Safety by Using 3D Neutronics / Thermal-hydraulics models: State-of-the-art (CRISSUE-S)
Invited at FISA-2003 Conf. on EU Research in Reactor Safety - Luxembourg (L), EUR 20281, ISBN 92 894-3455-4, 10-13 November 2003.

D'Auria F., G.M. Galassi
Code Validation and Uncertainties in System Thermal-hydraulics
J. Progress in Nuclear Energy, Vol. 33 No 1/2, pp 175-216, 1998.

Dusch J, Hosl
Atucha-1: Betriebsempfehlungen zur Verringerung des Risikos von PCI-Schaden in den Brennelementen
KWU, B 11/R 122/86/80, Erlangen, 29.05.1980.

Djurle S., et al
The Super-Ramp Project, Final report of the Super-Ramp project
STIR-32, Studsvik AB Atomenergi, Studsvik, Sweden, 1984.

Erbacher F. J. et al.
Burst Criterion of Zircaloy Fuel Claddings in a Loss-of-Coolant Accident, Zirconium in the Nuclear Industry
5th Symposium, ASTM STP 754, p. 271-283 (1982).

European Commission
Fuel cladding failure criteria
European Commission, EUR 19256EN, September 1999.

Finnemann H. and Galati A.
NEACRP 3-D LWR Core Transient Benchmark – Final Specifications
NEACRP-L-335 (Revision 1), January, 1992

Forgeron T. et al.
Experiment and Modeling of Advanced Fuel Rod Cladding Behavior Under LOCA Conditions: Aplha-Beta Phase Transformation Kinetics an EDGAR Methodology
Zirconium in the Nuclear Industry, 12th Symposium, ASTM STP 1354 (2000).

Fuketa, T., F. Nagase, and T. Sugiyama
RIA- and LOCA-simulating experiments on high burnup LWR fuels
IAEA technical meeting on fuel behaviour modelling under normal, transient and accident conditions and high burnups, Kendal, United Kingdom, September 5-8, 2005.

Fuketa, T., H. Sasajima, and T. Sugiyama
Behavior of high-burnup PWR fuels with low-tin Zircaloy-4 cladding under reactivity-initiated-accident conditions
Nuclear Technology, 01. 133: pp. 50-62, 2001.

Fuketa et al.
High Burnup BWR Fuel Response to Reactivity Transients and a Comparison with PWR Fuel Response
Proceedings of the Twenty-Eighth Water Reactor Safety Information Meeting, NUREG/CP-0172, pp. 191-203, October 23-25, 2000.

Fuketa et al.
Behavior of PWR and BWR Fuels During Reactivity-Initiated Accident Conditions
Proceedings of the ANS International Topical Meeting on Light Water Reactor Fuel Performance, Park City, pp. 359-374, April 10-13, 2000,.

Fuketa T., T. Nakamura and K. Ishijima
The Status of the RIA Test Program in the NSRR
Proceedings of the 25th Water Reactor Safety Information Meeting, NUREG/CP-0162 Vol.2 pp.179-198 High Burnup Fuel Research, October 20-22, 1997.

Gyory C., A. Schubert, J. van de Laar,P. Van Uffelen .
Recent LOCA-specific developments of the TRANSURANUS fuel performance code
Enlarged Halden Programme Group Meeting, Norway,19-22 May 2008.

Hart, R. S.
CANDU Technical Summary
Atomic Energy of Canada Limited, October 1997.

Halden Reactor Project
Halden Boiling Water Reactor
www.ife.no, IFE, Halden, January 2003.

Horn G.R., Babcock and Wilkox Company, Linchburg, VA (1973) quoted by C.E. Beyer, C.R. Hann, D.D. Lanning, F.E. Panisko, L. J. Parchen
GAPCON-THERMAL-2: A computer program for calculating the thermal behaviour o fan oxide fuel rod
BNWL-1898, NRC 1 and 3, 1975.

IAEA
Best Estimate Safety Analysis for Nuclear Power Plants: Uncertainty Evaluation
IAEA Safety Reports Series No 52, pp 1-162 Vienna (A), 2008.

IAEA
Safety margins of Operating Reactors, Analysis of Uncertainties and Implications for Decisions Making
IAEA Tecdoc 1332, Vienna (A) 2003.

IAEA
Maintaining the Design Integrity of Nuclear Installations throughout their Operating Life
IAEA INSAG-19, pp 1-20 Vienna (A), 2003.

IAEA
Accident Analysis for Nuclear Power Plants
IAEA Safety Reports Series No 23, pp 1-121 Vienna (A), 2002.

IAEA
Safety of Nuclear Power Plants: Operation
IAEA Safety Standard Series No. NS-R-2, pp 1-40 Vienna (A), 2000.

IAEA
Safety of Nuclear Power Plants: Design
IAEA Safety Standard Series No. NS-R-1, pp 1-73 Vienna (A), 2000.

Johnsen G.
Key features of the RELAP5-3D© code
Idaho National Laboratory, 02/08/2008.

Kollmar
KWU/ENACE Collaboration and Transfer of Tasks in the Nuclear Design Area
FUR-02, June 29th, 1983.

Lanning D. D., C. E. Beyer, G. A. Berna
FRAPCON-3: Integral Assessment
NUREG/CR-6534 Volume 3 PNNL-11513, December 1997.

Lassmann K., A. Schubert, P. Van Uffelen, Cs. Gyory, J. van de Laar
Transuranus Handbook Version "v1m1j09
EC, JRC, ITU, January 2009.

Lassmann K.
TRANSURANUS: a fuel rod analysis code ready for use
Journal of Nuclear Material 188 295-302, 1992.

Lassmann K.,
TRANSURANUS: a fuel rod analysis code ready for use
Journal of Nuclear Material 188 295-302, 1992.

Lassmann K.
The statistical version of the URANUS programme
Nuclear Engineering and Design, 56 pags. 35-40, 1980.

Nordström L. Å.
TRANSURANUS Restart Option applied to a Fuel Rod Test (IFA-550.11)
TRANSURANUS user meeting, ITU, Karlsruhe, 22 - 23 September, 2003.

Mayers, Steinbeck
Reactor, Reactor Coolant and Moderator System JA, JE, JF
ARG010/010/XS/JA/JE/JF,11 November 1985.

Matzke H.
Gas release mechanisms in UO2-a critical overview
Radiation Effects, Vol. 53, pp. 219-242, 1980.

Mogard H., et al.
The Studsvik Inter-Ramp Project
Final Report of the Inter-Ramp Project, STIR-53, Studsvik AB Atomenergi, Studsvik, Sweden ,1979.

Mazzantini O.
INFORMATION REQUESTED THROUGH DIT (dated 20MAR2008)
Contract NA-SA UNIPI 02 - Atucha II, NASA-UNIPI 06, August 28 2008.

Nakamura, T, et al.
High-Burnup BWR Fuel Behavior Under Simulated Reactivity-Initiated Accident Conditions
Nuclear Technology, Volume 138, No. 3, pp. 246-259, June 2002.

Nakamura, T, et al.
Boiling Water Reactor Fuel Behavior Under Reactivity-Initiated-Accident Conditions at Burnup of 41 to 45 GWd/tonne U
Nuclear Technology, Volume 129, pp. 141-151, February 2000.

NASA
Final Safety Analysis Report – Chapter 15 "Accident Analysis"
20011

NASA
Final Safety Analysis Report – Chapter 4
2007

NASA
Preliminary Safety Analysis Report
1980

NASA-ARN
Protocol of Common Understanding on the Basic Licensing Concept and some safety subjects
Prepared 8./9.11.1977

OECD
Benchmark calculations on HALDEN IFA-650 LOCA test results
Nuclear Safety, NEA/CSNI/R(2010)65, 2010-65.

OECD
Nuclear Fuel Behavior During Reactivity Initiated Accidents
Nuclear Safety, NEA/CSNI/R(2010)7, 2010-7.

OECD
Safety significance of the Halden IFA-650 LOCA test results
Nuclear Safety, NEA/CSNI/R(2010)5, 2010-5.

OECD
Nuclear Fuel Behavior under Reactivity-Initiated Accident (RIA), State-of-the-art Report
NEA No. 6847, NEA/CSNI/R(2010)1, 2010-1.

OECD
Nuclear Fuel Behavior in Loss-of-coolant Accident (LOCA) Conditions, State-of-the-art Report
NEA No. 6846, 2009.

OECD
Task Group on Safety Margins Action Plan (SMAP), Final Report
NEA/CSNI/R(2007)9, Paris (F), 2007-9.

OECD
Review of high burn-up RIA and LOCA database and criteria
NEA/CSNI/R(2006)5, 2006-5

OECD
Fuel Safety Criteria Technical Review
Task Force on Fuel Safety Criteria, NEA/CSNI/R(99)25, 2000-25.

OECD
Review of Nuclear Fuel Experimental Data
Fuel Behavior Data Available from IFE-OECD Haldekn Project, January 1995-2.

OECD
Scientific Issues in Fuel Behavior
NEA/Nuclear Science Committee Task Force, January 1995-1.

Parisi C.
Identification and characterization of a relevant core status
Contract NA-SA UNIPI 01 - Atucha II, SIR-2.1 – rev0, Pisa, January 2008.

Parisi C., K. Ivanov
Derivation of one database of macroscopic cross sections suitable for a neutron kinetics nodalization
Contract NA-SA UNIPI 01 - Atucha II, SIR-2.2 – Rev0, Pisa 28 July 2008.

Petruzzi A., D'Auria F., Micaelli J-C., De Crecy A., Royen J.
The BEMUSE programme (Best-Estimate Methods – Uncertainty and Sensitivity Evaluation)
Int. Meet. on Best-Estimate Methods in Nuclear Installation Safety Analysis (BE-2004) IX, Washington D.C. (US), Nov. 14-18, 2004, ANS copyright © 2004.

RELAP5-3D© Code Development Team
RELAP5-3D© Code Manual Volume I: Code Structure, System Models, and Solution Methods
INEEL-EXT-98-00834, Volume I Revision 2.4, Idaho National Laboratory, June 2005.

Reventos F., et al.
BEMUSE Phase V DRAFT Report Uncertainty and Sensitivity Analysis of a LB-LOCA in ZION Nuclear Power Plant
OECD/NEA BEMUSE PROGRAMME, NEA/CSNI/R(2008)6/Vol.1, Vol.2 and Vol.3, 26 Nov 2008.

Rininsland, H., et al.
Stand der Reaktorsicherheitsforschung in Projekt Nukleare Sicherheit
KfK Jahrescolloquium, 1982.

Rozzia D., M. Adorni, A. Del Nevo, F. D'Auria
Capabilities of TRANSURANUS code in simulating power ramp tests from the IFPE database
Nuclear Engineering and Design Volume 241, Issue 4, Pages 1078-1086, April 2011.

Rozzia D., M. Adorni, Del Nevo A., D'Auria F.
Capabilities of TRANSURANUS code in simulating power ramp tests from the IFPE database (BWR-Inter-Ramp experiment)
Software Licensing Agreement Ref. No. 30645, ITU and UNIPI – University of Pisa Report, DIMNP NT647(10)Rev.0, March 2010.

Rozzia D., M. Adorni, Del Nevo A., D'Auria F.
Capabilities of TRANSURANUS code in simulating power ramp tests from the IFPE database (PWR-Super-Ramp experiment)
Software Licensing Agreement Ref. No. 30645, ITU and UNIPI – University of Pisa Report, DIMNP NT647(10)Rev.0, March 2010.

Schubert, A., P. Van Uffelen, J. van de Laar, C.T. Walker, W. Haeck
Extension of the TRANSURANUS burn-up model
Journal of Nuclear Materials, 2008.

Schubert A. et al.
Analysis of fuel centre temperature with the TRANSURANUS code
International Conference on Nuclear Fuel for Today and Tomorrow - Experiences and Outlook (TopFuel-2003), Würzburg (Germany), 16-19 March 2003.

Sugiyama T., T. Nakamura, K. Kusagaya, H. Sasajima, F. Nagase and T. Fuketa
Behavior of Irradiated BWR Fuel under Reactivity-Initiated-Accident Results of Tests FK-1, -2, and -3
JAERI-Research 2003-033, January 2004.

Turinsky P. J. et al.
Nestle: Few-Group Neutron Diffusion Equation Solver Utilizing the Nodal Expansion Method for Eigenvalue, Adjoint, Fixed-Source Steady State and Transient Problems
Electric Power Research Center, North Carolina State University, Raleigh, NC 27695-7909, June 1994

UNIPI-GRNSPG
A proposal forperforming the ATUCHA II accident analyses for licensing purposes
Contract NA-SA UNIPI 01 - Atucha II, University of Pisa Report, DIMNP NT (08) – rev3, Pisa, August 2008.

US NRC
Regulatory Guide 1.203: Transient and Accident Analysis Methods
US NRC RG, December 2005.

Van Uffelen P., C. Gyori, A. Schubert, J. van de Laar, Z. Hózer, G. Spykman
Extending the application range of a fuel performance code from normal operating to design basis conditions
Journal of Nuclear Material, 383 137-14, 2008.

Van Uffelen P.
Modeling of Nuclear Fuel Behavior
Publications Office JRC Publications, Report EUR 22321 EN, European Commission, 2006.

Van Uffelen P., A. Schubert, J. van de Laar, C. Győri
Development of a transient fission gas release model for TRANSURANUS
Water Reactor Fuel Performance Meeting, Seoul, Korea, October 19-23, 2008.

Vitanza C.
A review and interpretation of RIA experiments
Korea, 2008

Vitanza C.
Fuel safety limits, with particular reference to high burnu-up
Thicket 2008.

Vitanza C.
Overview of the OECD–Halden reactor project
Nuclear Engineering and Design, Volume 207, Issue 2, Pages 207-221, July 2001.

Wiesenak W.
Proposal for a Pulse Test to be performed in the Halden Boiling Water Reactor
Halden Reactor Project, September 2008.

Wiesenack W., Tverberg T.
The OECD Halden reactor project fuels testing programme: methods, selected results and plans
Nuclear Engineering and Design, Volume 207, Issue 2, July 2001, Pages 189-197.

Wilson C. L., et al.
Large-Break LOCA, In-Reactor Fuel Bundle Materials Test MT-6A.
PNL 8829 UC 520, Battelle, U.S. NRC, 1993.

Wilson C. L., et al.
LOCA Simulation in NRU Program
NUREG/CR-3272 PNL-4669 R3, U.S. NRC, Washington D.C., 1983.

APPENDIX A. DESIGN OF LOCA EXPERIMENT

The starting point is the analysis of the existing research reactors, with suitable characteristics for the execution of an experiment involving a combined power and temperature excursions. The selected research reactor is the Halden Boiling Water Reactor (HBWR) located in Norway. For this reason a more detailed description of the HBWR is reported.

This contains the technical specification to the Halden Staff to investigate the feasibility of the experiment and the feedback received by the Halden Staff (*Wiesenak 2008*).

A.1 Introduction

A small percentage of the research reactors in operation are suitable to perform experiments beyond cladding failure. Moreover, the specific features of the experiment require the capability to measure the fuel rods parameters in both failed and not failed conditions and appropriate facilities to treat irradiated material.

Phenomena involved during heat-up, cooldown and quench during a LOCA scenario are very complex and comes from the changes of properties of the zirconium cladding alloys which take place during the transient. In addition, main safety concerns in RIA scenario, such as loss of long-term core coolability and possible damage to the reactor pressure boundary and the core through pressure wave generation should be accounted for as well. In CNA-2 the two transients occur simultaneously, since the LOCA, characterized by loss of coolant inventory and high fuel temperature, imply a simultaneous RIA, characterized by high power excursion.

To date, more than a thousand pulse irradiation tests have been carried out on fresh fuel rods, and about 140 tests have been done on pre-irradiated samples. Experimental database currently developed address LOCA or RIA separately (*OECD 2010-1, OECD 2009*). No experiments of combined LOCA and RIA has been addressed experimentally yet.

A.2 Objectives of the experiment

The objectives of the experiment are to establish the fail-safe limits of the CNA-2 fuel rods during LB-LOCA scenario. Given the peculiarities of the reactor, i.e. the positive void coefficient, the CNA-2 fuel rods experience simultaneously fast energy release in the fuel matrix, such as in the reactivity accident, high temperature of clad and fast depressurization.

The experiment has to provide relevant information on the consequences of combined power and temperature excursions to the fuel integrity, addressing:

- the failure limits;
- the failure mechanism and associated phenomena,

- the influence of the reload strategy and therefore of stress corrosion cracking on the failures.

The experimental data have to be useful also for code validation and therefore non-destructive and selected destructive post irradiation examinations (PIE), such as visual examination, dimensional changes, fission-gas release, fuel burn up analysis and grain size measurement, etc. are requested to be available for this purpose.

A.3 Outline of the research reactors suitable for combined LOCA and RIA experiment

This section contains a brief description of the existing research reactors that should be suitable to execute the experiment. Focus is given to the Halden Boiling Water Reactor that is the selected to perform the experiment feasibility study.

A.3.1 IGR, Republic of Kazakhstan

A.3.1.1 General information

IGR (Impulse Graphite Reactor) research reactor is a pulse reactor on thermal neutrons with homogeneous uranium-graphite core of thermal capacity type. Graphite high thermal capacity enabled to do without the system of forced removal of heat released in the core during the reactor operation. Absence of standard coolant circuit considerably reduces the risk of radiation accident at the reactor.

IGR reactor nuclear safety is specified by a considerable level of negative reactivity coefficient that provides guaranteed shutdown of any physically possible power impulse, initiated by positive reactivity insertion through control and protection system (CPS) rods removal. Among pulse reactors, IGR reactor has the highest fluency of thermal neutrons and integral gamma radiation dose in the experimental cavity of 228 mm in diameter and 3825 mm high. Main characteristics are outlined in Tab. A. 1.

A.3.1.2 Relevant test performed

In 1995 all 13 VVER-1000 high burnup fuel tests were conducted in the IGR reactor and analyzed. Energy depositions, cladding condition and failure mechanism were determined. Post irradiation examination was also conducted on the test rods. The results were presented at an OECD/NEA specialist meeting in France in September 1995 and also at US NRC's Water Reactor Safety Meeting in October 1995. Key results obtained so far include:

- fuel cladding rupture occurred by a different mechanism (ductile failure) than in some French, Japanese and US tests (brittle failure).
- VVER cladding (Zr,Nb) oxidizes less than standard LWR cladding (Zr, Sn) and oxidation affects the failure mechanisms.
- cladding failures occur at about the same energy level in VVER fuel as in lightly oxidized LWR fuel.

Technical Data	
Neutron flux maximum density	7×10^{16} n/cm^2·s
Thermal neutron maximum fluence	$3{,}7\times10^{16}$ n/cm^2
Minimum half-width of impulse	120 ms
Reactor Type	Tank WWR
Thermal Power, Steady (kW)	10,000.00
Max Flux SS, Thermal (n/cm2-s)	2.00E+14
Max Flux SS, Fast (n/cm2-s)	8.00E+13
Thermal Power, Pulsed (MW)	0
Moderator	Light Water
Coolant	Light Water
Forced Cooling	1500 m3/h
Coolant Velocity in Core	2.8 m/s
Reflector	H2O
Control Rods Material	B4C
Control Rods number	8
Experimental Facilities	
Horizontal Channels	6
Horizontal Max Flux (n/cm2-s)	2.00E+08
Horizontal Use	Nuclear Physics
Vertical Channels	35
Vertical Max Flux (n/cm2-s)	2.00E+14
Vertical Use	Material Science
Core Irradiation Facilities	3
Core Max Flux (n/cm2-s)	2.00E+14
Reflector Irradiation Facilities	6
Fuel data	
Equilibrium Core Size	76
Rods per Element	1
Dimensions of Rods, mm	24X600 H
Tubes per Element	6
Dimensions of Tubes, mm	65.4;54.8;44.2;33.6;24.0; Hexahedral
Cladding Material	Al Alloy
Cladding Thickness, mm	1
Fuel Thickness, mm	0.5
Uranium Density, g/cm3	0.045
Burnup on Discharge, max %	40
Burnup Average, %	35

Tab. A. 1 – IGR reactor characteristics.

A.3.2 NSRR, Japan

A.3.2.1 General information

The Nuclear Safety Research Reactor (NSRR) is a TRIGA design nuclear research reactor operated by the Japan Atomic Energy Agency in operation since 1975. As of 2006, the reactor has preformed 3033 pulses and 1280 nuclear fuel experiments. In 1989 the reactor underwent a power uprate. Main characteristics are outlined in Tab. A. 2.

A.3.3 Relevant test performed

Large amount of RIA fuel test at cold coolant conditions has been performed. Tests have been made with both PWR and BWR fuel.

Technical Data	
Reactor Type	TRIGA ACPR
Thermal Power, Steady (kW)	300
Max Flux SS, Thermal (n/cm2-s)	1.9 E12
Max Flux SS, Fast (n/cm2-s)	6.30E+12
Thermal Power, Pulsed (MW)	23,000.00
Max Flux Pulsed, Thermal (n/cm2-s)	1.5 E17
Max Flux Pulsed, Fast (n/cm2-s)	3.00E+17
Moderator	H2O,ZrH
Coolant	Light Water
Natural Convection Cooling	YES
Coolant Velocity in Core	15 CM/S
Reflector	Graphite,H2O
Control Rods Material	B4C
Control Rods number	6
Vertical Channels	1
Vertical Max Flux (n/cm2-s)	1.00E+17
Vertical Use	Fuel Behavior Experiments under RIA
Fuel data	
Equilibrium Core Size	157
Rods per Element	1
Dimensions of Rods, mm	37.5
Dimensions of Tubes, mm	587
Cladding Material	SS
Cladding Thickness, mm	0.5
Fuel Material	UZrH
Uranium Density, g/cm3	7.1

Tab. A. 2 – NSRR reactor characteristics.

A.3.4 CABRI, France

A.3.4.1 General information

The CABRI reactor (power of 25 MW) is a pool type research reactor devoted to study the behavior of irradiated fuel pins during fast power transients, in particular for reactivity insertion accident (RIA). The test may lead to cladding failure or melting, which may lead to thermo-mechanical interaction between fuel and the coolant.

A test loop is installed at the centre of the “driver” core. It receives an experimental device containing the irradiated fuel pin and the instrumentation and has its own cooling system. Reactivity insertions are provided by the depressurization of tubes filled with He-3. Starting from an initial value of about 100 kW, the core power can reach about 10 GW in few milliseconds. The pulse width is typically range of 9-75 ms. Main characteristics are outlined in Tab. A. 3.

A.3.4.2 Relevant test performed

Large amount of RIA fuel test at hot coolant conditions has been performed. Tests have been focused on PWR fuel.

Technical Data	
Reactor Type	Pool
Thermal Power, Steady (kW)	25,000.00
Max Flux SS, Thermal (n/cm2-s)	1.90E+14
Max Flux SS, Fast (n/cm2-s)	1.50E+17
Thermal Power, Pulsed (MW)	20,000.00
Max Flux Pulsed, Thermal (n/cm2-s)	1.50E+17
Max Flux Pulsed, Fast (n/cm2-s)	1.20E+20
Moderator	Light Water
Coolant	Light Water
Forced Cooling	3200 m3/h
Coolant Velocity in Core	5 m/s
Reflector	Graphite
Reflector Number of Sides	4
Control Rods Material	HF
Control Rods number	6
Experimental Facilities	
Horizontal Channels	1
Horizontal Use	Hodoscope measurement of test fuel motion
Loops Number	1
Loops Max Flux	4.70E+14
Loops use	Experimental sodium loop

Tab. A. 3 – CABRI reactor characteristics.Part 1 of 2.

Fuel data	
Origin of Fissile Material	France (CEA)
Enrichment Supplier	France
Equilibrium Core Size	40
Rods per Element	77
Dimensions of Rods, mm	800
Cladding Material	SS
Cladding Thickness, mm	0.4
Fuel Thickness, mm	8.85 Pellet diameter
Uranium Density, g/cm3	10.3
Fuel Fabricator	SICN, France

Tab. A.3 – CABRI reactor characteristics. Part 2 of 2.

A.3.5 BIGR, Russian Federation

A.3.5.1 General information

The BIGR research reactor is located at the Institute of Experimental Physics (VNIIEF) in Sarov, Russia, it is a uranium-graphite impulse type, air cooled with a power of 2,500 MJ per impulse. The fuel can use up to 7kg of 90% HEU, the core contains about 833 kg of 90% enriched uranium.

The fast pulse reactor BIGR possesses the record values of fast neutron fluences in large volumes accessible for irradiation, namely, about 1 10^{15}n/cm2 at the external surface of the core of about 800mm in diameter. One of BIGR reactor distinctions is the possibility of generating two types of pulses: with half-width of about 2^{-10}ms and greater that 0,4s. This makes it possible:

- to compare the behavior of VVER fuel with PWR and BWR fuels (in the most complete program on fuel testing that have been being realized in Japan on NSRR reactor for more than 20 years with PWR and BWR fuels there can be used as a rule “short” pulses of about 3^{-15}ms;
- to analyze abnormal situations with duration (half-width) of pulse energy release of about 1^{-3}s.

The main goals of the works were as follows:

- development and creation of irradiating device ensuring the levels of pulse energy input to the models of NPP fuel elements (including those with the burnt out fuel) achieving the thresholds of their destruction;
- definition of fuel element operability boundaries and getting of experimental results to provide for fuel testing and licensing;
- creation of database for codes verification through the calculation of fuel elements behavior under abnormal situations.

A.3.6 HBWR, Norway

A.3.6.1 General information

The Halden Boiling Heavy Water Reactor (HBWR) is in operation since 1959 in Halden, a coastal town in south-east Norway near to the border to Sweden. The reactor vessel primary circuit system is inside a rock cavern. Heat removal circuits are either placed inside the reactor hall or in the reactor entrance tunnel. Control room and service facilities are placed outside the excavation. The utilization of the reactor is 24 hours per day, 7 days per week, 28 weeks per year producing 4000 MWdays/year.

A.3.6.2 Reactor System

The Halden Boiling Heavy Water Reactor (HBWR) is a natural circulation boiling heavy water reactor, Fig. A. 1. The maximum power is 25 MW (thermal), and the water temperature is 240°C, corresponding to an operating pressure of 33.3 bar. Pressurization tests are performed at regular intervals using a pressure of 40 bars. Fig. A. 2 shows a simplified flow sheet of the reactor system.

The reactor pressure vessel is cylindrical with a rounded bottom. It is made of carbon steel and the bottom and the cylindrical portion are clad with stainless steel. The flat reactor lid has individual penetrations for fuel assemblies, control stations and experimental equipment. 14 tons of heavy water act as coolant and moderator. A mixture of steam and water flows upwards by natural circulation inside the shroud tubes which surround the fuel rods. Steam is collected in the space above the water while water flows downwards through the moderator and enters the fuel assemblies through the holes in the lower ends of the shroud.

The steam flows to two steam transformers where heat is transferred to the light water secondary circuit. Condensate from the steam transformers returns to the reactor by gravity. An external subcooler loop is installed to provide experimental variation of void fraction in the fuel assemblies and the moderator, and is also used for heating and cooling purposes. In the secondary circuit, two circulation pumps pass the water through the steam transformers, a steam drum and a steam generator where steam is produced in the tertiary circuit. The tertiary steam is normally delivered as process steam to the nearby paper mill, but may also be dumped to the river. There is generally no access to the reactor hall when the reactor is operational, and therefore all control and supervision is carried out from the control room.

Light water, high pressure loops provide facilities for testing under prototypic BWR and PWR conditions. Nominal power operating data are outlined in Tab. A. 4.

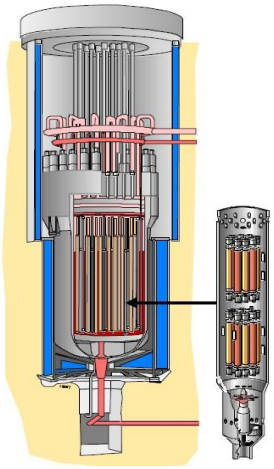

Fig. A. 1 – *Simplified sketch of the reactor.*

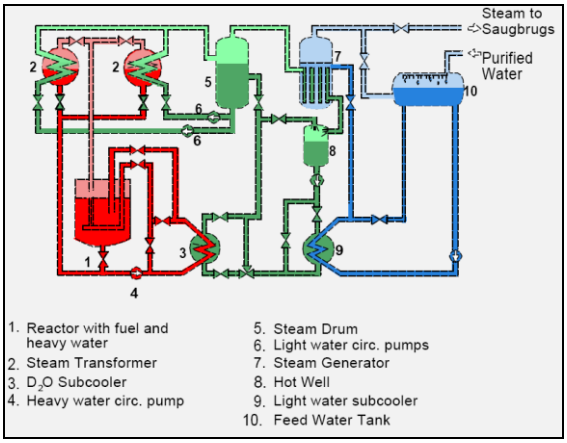

Fig. A. 2 – *Simplified flow sheet of the reactor system.*

Nominal Reactor Operating Data	
Power Level	up to 20 MW (th)
Reactor Pressure	33.3 bar
Heavy Water Saturation Temperature	240°C
Maximum Subcooling	3.0 MW
Primary Steam Flow (both circuits)	160 ton/h
Return Condensate Temperature	238°C
Subcooler Flow	160 ton/h
Plenum Inlet Temperature	237°C

Tab. A. 4 – Nominal reactor operating data.

A.3.6.3 Core Configuration

The core consists of about 110 - 120 fuel assemblies, including the test fuel, in an open hexagonal lattice with a lattice pitch of 130 mm. 30 lattice positions are occupied by control stations. The maximum height of the fuel section is 1710 mm, and the core is reflected by heavy water. Selected core data are given in Tab. A. 5 and Fig. A. 3 shows a typical core map. The central position in the core is occupied by an emergency core cooling tube with nozzles, and between eight and fourteen core positions contains pressure flasks for light water, high pressure test loops.

Test rig for determining the consequence of short-term dryout is reported in Fig. A. 4. The tests can be performed as follow. Three pre-irradiated, commercial fuel rodlets, after service in a reactor, are re-fabricated, instrumented and loaded into this rig. Each subchannel which contained one fuel rod, can be individually operated at reduced coolant flow conditions, producing dryout in the upper portion of the fuel rod.

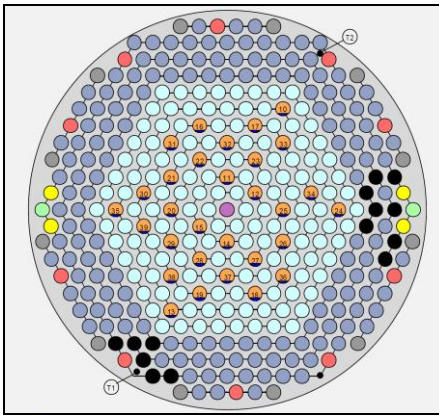

Fig. A. 3 – Typical core map.

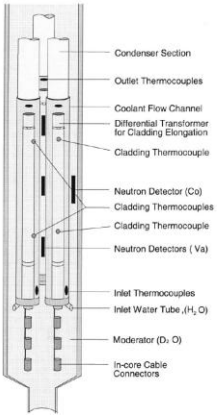

Fig. A. 4 – Typical test rig.

Technical Data	
Reactor Type	Heavy Water
Thermal Power, Steady (kW)	20,000.00
Max Flux SS, Thermal (n/cm2-s)	1.00E+14
Max Flux SS, Fast (n/cm2-s)	1.00E+14
Moderator	Heavy water
Coolant	Heavy water
Natural Convection Cooling	YES
Forced Cooling	YES
Coolant Velocity in Core	1-3 m/s
Reflector	D2O
Reflector Number of Sides	4
Control Rods Material	Ag,Cd,Al
Control Rods number	30
Experimental Facilities	
Vertical Channels	300
Vertical Max Flux (n/cm2-s)	1.00E+14
Vertical Use	Fuel & core material performance studies
Core Irradiation Facilities	40
Core Max Flux (n/cm2-s)	1.00E+14
Reflector Irradiation Facilities	5
Loops Number	04-ago
Loops Max Flux	1.00E+14
Loops use	Fuel & core material studies: BWR, PWR condit.

Tab. A. 5 – HBWR reactor characteristics. Part 1 of 2.

Fuel data	
Equilibrium Core Size	100-110
Rods per Element	8
Dimensions of Rods, mm	9-14 DX800
Tubes per Element	1
Dimensions of Tubes, mm	Shroud 71 OD.
Cladding Material	ZR
Cladding Thickness, mm	0.6-0.8 PWR,BWR
Fuel Thickness, mm	8-12 diameter
Uranium Density, g/cm3	10.5
Burnup on Discharge, max %	VAR
Burnup Average, %	40 MWd/kg (Driver El
Fuel Fabricator	Institutt for Energiteknikk, Norway
Utilization	
Hours per Day	24
Days per Week	7
Weeks per Year	28
MW Days per Year	4000
Materials/fuel test experiments	Number of runs: 35

Tab. A.5 – HBWR reactor characteristics. Part 2 of 2.

A.3.6.4 Plant Status

The design working pressure of the HBWR pressure vessel is 40 bar with a saturation temperature of 250°C. The hydraulic acceptance pressure test was carried out at 54 bar, 35 % above the design pressure. The normal operating pressure is 33.3 bar, with corresponding saturation temperature of 240°C. The stresses in the vessel are low compared with the code requirements. Thermal stresses are also normally low. There are normally 2-3 main shutdowns per year, dictated primarily by the experimental programs and a few additional cooling downs for special tests. The normal heating and cooling rates are 10°C/h. Inspection and recertification pressure tests are performed every 3rd year at 10 % overpressure. These pressure tests are performed with water/steam at saturation temperature. According to the requirements set by Norwegian Boiler Authority, the inspection and test programs include ultrasonic examination of vessel welds, lid, bolts, bottom nozzle and primary system piping, and evaluation of radiation induced material changes.

The outcome of the material testing, fluence evaluations, inspections, and pressure testing, form the basis for the assessments of vessel integrity. Internationally accepted codes, rules and recommendations are used in a consultative manner. The material tests and the analysis performed indicate that the reactor can be operated safely well beyond year 2020.

A.3.6.5 Fuel Test Program

The fuels testing program conducted in the Halden reactor (heavy boiling water reactor (HBWR)) is aimed at providing data for a mechanistic understanding of phenomena, which may affect fuel performance and safety parameters.

The investigations address:
- thermal property changes;
- fission gas release as influenced by power level and operation mode,
- fuel swelling, and
- pellet–clad interaction.

Relevant burnup levels (>50 MWd/kgU) are provided through long-term irradiation in the HBWR and through utilization of re-instrumented fuel segments from commercial light water reactors (LWR).

Both uranium and MOX fuels are being studied regarding thermal behavior, conductivity degradation, and aspects of fission gas release. Experiments are also conducted to assess the cladding creep behavior at different stress levels and to establish the overpressure below which the combination of fuel swelling and cladding creep does not cause increasing fuel temperatures. Clad elongation measurements provide information on the strain during a power increase, the relaxation behavior and the extent of a possible ratcheting effect during consecutive start-ups. Investigations include also the behavior of MOX and Gd-bearing fuel and other variants developed in conjunction with burnup extension programs. Some LWR-irradiated fuel segments will undergo a burnup increase in the HBWR to exposures not yet achieved in LWRs, while others will be re-instrumented and tested for shorter durations.

Investigations of fuel performance in steady state and transient operation conditions have constituted a major part of the experimental work carried out in the heavy boiling water reactor (HBWR) at Halden since its start-up in 1959.

The in-core studies were supported by the development and perfection of instrumentation and experimental rig and loop systems where reactor fuels and materials can be tested under PWR and BWR conditions.
Fuels testing at the Halden Reactor Project (HRP) have for a number of years focused on implications of extended burnup operation schemes aimed at an improved fuel cycle economy. The experimental programs are, therefore, set up to identify long-term property changes with an impact on performance and safety. While PIE ascertains the state existing at the end of irradiation, in-core instrumentation provides a full description of performance history, cross-correlation between performance parameters, on-line monitoring of the status of the test, and a direct comparison of different fuels and materials. Trends developing over several years, slow changes occurring on a scale of days or weeks, and transients from seconds to some hours can be monitored. The data generated in the fuels testing programs originate from in-pile sensors, which allow assessing:

- fuel centre temperature and thus thermal property changes as function of burnup;
- fission gas release as function of power, operational mode and burnup;
- fuel swelling as affected by solid and gaseous fission products;
- pellet–cladding interaction manifested by axial and diametral deformations.

The irradiation of instrumented fuel rods is carried out in specialized rigs according to test objectives, e.g. long-term base irradiation, diameter measurements or ramps and overpower testing.

When specific coolant conditions are required, such as for cladding and structural materials studies, water loops are available. The loops can be operated in different thermal-hydraulic and water chemistry conditions, covering a range of BWR and PWR requirements. Totally, 7 loops are currently in operation at the Halden reactor, serving 12 in-pile experiments. The distinctive specialty of the HBWR fuel and material experiments resides in the ability to perform high quality in-reactor measurements, which provide unique and well characterized data during operation; that is, while mechanisms are acting.

Fuel rods extracted from commercial reactors can be segmented and re-fabricated into rodlets suitable to further specialized testing at Halden. In addition to fuel instrumentation, some rods in experimental rigs have gas lines attached to their end plugs. This allows the exchange of fuel rod fill gas during operation and makes it possible to determine gas transport properties as well as the gap thermal resistance and its influence on fuel temperatures. It is also possible to analyze *sw*ept out fission products for assessment of structural changes and fission gas release. Other instruments required for the tests are also available. These operations and post irradiation examinations (PIE) can be carried out in the hot cells located at the Kjeller establishment. Other operations including non-destructive examinations can be performed in shielded compartments situated near the Halden reactor.

Similarly, structural materials extracted from LWR cores can be machined, fatigue pre-cracked if necessary and suitably instrumented for the Irradiation Assisted Stress Corrosion Cracking (IASCC). This technique is important in that it provides very representative materials already irradiated to doses typical of ‘aged’ plants. The experimental work is supported by the hot cells for re-fabrication and post-irradiation examinations, by workshops, electronics and chemistry laboratories and by a computerized data bank.

A.3.6.6 Rod design and specifications

The DEGB LB-LOCA transient, as expected in CNA-2, is featured by a power excursion that reaches the peak of 10 times the LHR during the normal operation in 0.5 sec (*D’Auria 2008*). Only a peak up to 5 times the desired one can be simulated in HBWR reactor, therefore the test will be scaled preserving the total amount of the energy to be released to the fuel as well as the maximum pellet and cladding temperature. The estimation of the Halden Staff is that the reactor should

be able to reach 260kW/m plus a further margin of 10-15% with the optimization of the reactor core and test assembly configuration.

It should be noted that such power may be achieved only using enriched fuel in the experiment: the value of the estimated enrichment is in the range of 6-15% per power pulse ranging between 160 and 260kW/m.

Six instrumented fuel rods will be fabricated to reproduce as far as possible the CNA-2 fuel rods: three will be base irradiated and then power ramped, and three will be only power ramped, Tab. A. 6. Three levels of energy depositions are planned to be investigated (see Tab. A. 6) ranging from below and above fuel melting for each set of rods. The maximum length allowed for the rods is 50 cm according to the features of Halden reactor and of the test rigs that will be used.

Two types of test rigs will be specifically designed and fabricated for the irradiation of CNA-2 fuel rods: one for base irradiation and one for power pulse. The experiment to be performed will be divided into two phases accordingly: the base irradiation and the power pulse phases.

The base irradiation of three CNA-2 fuel rods will be carried out simultaneously, due to the features of the CNA-2 burnup accumulation test rig, Fig. A. 5. Once these fuel rods will reach the desired burnup, the power pulse testing will start in the CNA-2 power pulse rig represented in Fig. A. 6, where only one rod can be placed per each test. Finally, the remaining three un-irradiated fuel rods will be tested in the power pulse test rig, one per test. A pressure flask will constitute the pressure boundary between the HBWR and the moderator in both cases. The loop system might be probably operated with light water.

The LHR for base irradiation and conditioning before power pulse will be about 40-60kW/m.

The required burnup for the pre-irradiated fuel rods will be between 5 and 8 MWd/kgU, achievable in two reactor irradiation cycles which length is approximately 90 full power days (FPD) each one. Since the typical availability of the HBWR is about 45-50%, this could be reached in about 1 year.

The test parameters will be monitored online using the instrumentation available in the research reactor as hereafter summarized:

- fuel centerline thermocouples;
- cladding thermocouples (4 to 6 per each rod);
- cladding/fuel rod elongation and internal pressure detectors;
- self-powered neutron detectors;
- coolant thermocouples (inlet, two intermediate levels and outlet).

The experimental data will be constituted by the above mentioned online measurement, and by the data from the post irradiation examination. These will be executed at Kjeller hot-laboratory (Norway), see section 5.5.

Id	Rod No	Burnup [MWd/kgU]	Energy deposition levels	Base Irradiation	Power pulse	Base irradiation duration
1st set of rods	1	Between 5 and 8	Below fuel melting	X	X	90 FPD
	2	Between 5 and 8	At fuel melting	X	X	90 FPD
	3	Between 5 and 8	Above fuel melting	X	X	90 FPD
2nd set of rods	4	0 (fresh fuel)	Below fuel melting	--	X	--
	5	0 (fresh fuel)	At fuel melting	--	X	--
	6	0 (fresh fuel)	Above fuel melting	--	X	--

Tab. A. 6 – Proposed test matrix.

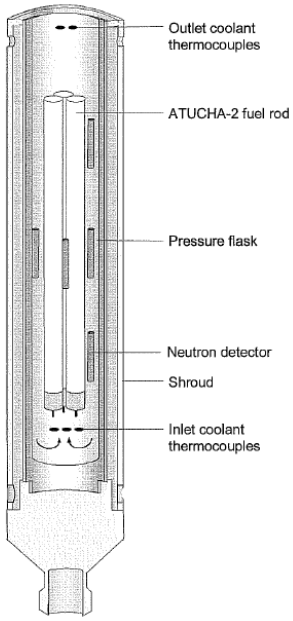

Fig. A. 5 – Test rig for burnup accumulation layout.

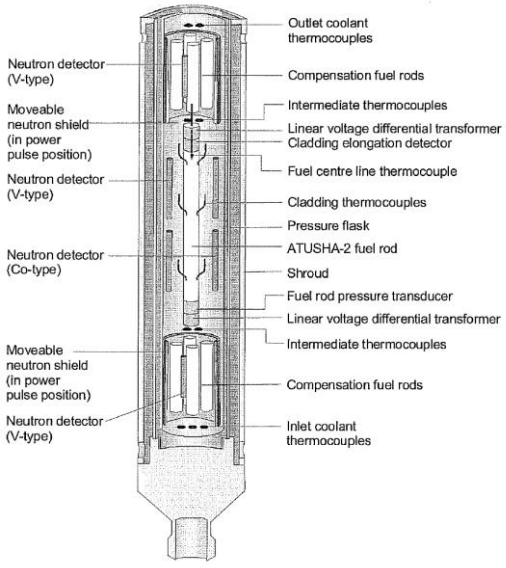

Fig. A. 6 – Test rig for power pulse testing layout.

A.3.6.7 Base irradiation experimental setup

The layout of the test rig for the base irradiation is reported in Fig. A. 5 and can accommodate simultaneously a cluster of 3 instrumented fuel rods, having the thermal mechanical characteristics similar of those used in the CNA-2 nuclear power plant.

The main operating parameters will be directly monitored. All the rods will be instrumented with thermocouples to measure fuel centerline, cladding and coolant temperatures at different positions. In addition, all the rods will be instrumented with fuel and cladding rod elongation and internal pressure detectors. An online gamma-detector will also be installed, to monitor activity release.

The test rig will be put into a pressure flask, that constitutes the physical separation from the region where the experiment is performed and the HBWR moderator. The function of the pressure flask is to reproduce the thermal hydraulic conditions occurring in the CNA-2 reactor during the DEGB LB-LOCA scenario.

A.3.6.8 Base irradiation boundary conditions

Three out of six rods will be pre-irradiated in the burnup accumulation rig in order to reach the selected burnup of 5 to 8 MWd/kgU, that can be achieved with a LHR of about 40-60kW/m in about one year in the HBWR.

This burnup will be reached in 2 reactor irradiation cycles which length is approximately 90 full power days (FPD). When the burnup target is reached, the fuel rods will be transferred to the power pulse test rig. During the base irradiation it will be possible to reproduce the phenomena that can occur in the fuel due to the shuffling (e.g. PCI).

A.3.6.9 Power pulse irradiation experimental setup

Power pulse test of three un-irradiated and three pre-irradiated fuel rods will be performed in a test rig specifically designed for CNA-2 NPP, Fig. A. 6. The test rig allows the power pulse irradiation of one rod per test.

Special features of the CNA-2 power pulse test rig are the compensation fuel rods that will be inserted in the rig, in order to avoid the excess of reactivity changes in the HBWR core when performing the power pulse testing. These rods will be covered by the neutron shield when the fuel is uncovered.

Analogously for the base irradiation, the main operating parameters are directly monitored. All the rods will be instrumented with thermocouples to measure fuel centerline, cladding and coolant temperatures at different positions. Anyway, the fuel centerline thermocouples are expected to fail towards the end of the power pulse due to the very high temperatures encountered. In addition, all the rods will be instrumented with fuel and cladding rod elongation and internal pressure detectors. An online gamma-detector will also be installed, in order to monitor possible activity release.

The test rig will be connected with a pressure flask, representing the pressure boundary between the HBWR moderator and the rig in order to reproduce the designed transient LB-LOCA conditions of CNA-2 reactor. A simplified layout of the loop is presented in Fig. A. 7, which was used for the LOCA test IFA-650.6 already performed. During normal operation prior to the test, the rig will be connected to the loop.

A.3.6.10 Transient irradiation boundary conditions

Six CNA-2 fuel rods will be power pulsed, among them three will be pre-irradiated and three will be fresh fuel, both at three different energy deposition levels, see Tab. A. 6. A "conditioning" period before power pulse will be operated in the power pulse test rig, for a predetermined period of time, with an average LHR of 40 to 50 kW/m. An increase of LHR of 4 to 5 times is feasible in the HBWR with an enrichment of 12 to 15%.

Two movable neutron shields, to be moved rapidly away from the CNA-2 fuel rods, will be designed to simulate the power pulse testing. One half will be moved downward, the other upward in order to uncover the full length of the CNA-2 fuel rods and cover the compensation fuel rods. The power pulse will be terminated by reactor scram.

The boundary conditions necessary to simulate the transient, as calculated are summarized in Fig. A. 7, Fig. A. 8 and Fig. A. 9. They represent the linear heat rate, cladding temperature and pressure as function of time at 10 axial positions of the active part of the fuel. Linear heat rate increases of a factor about 10 from the steady state power in 0.5 s according to Fig. A. 7. Each subchannel which contained one fuel rod, should be individually operated at reduced coolant flow conditions, producing dryout according to Fig. A. 8. The pressure history foreseen is reported in Fig. A. 9. The target peak cladding temperature (PCT) is 1000 °C.

According with the specific characteristics of the HBWR, the duration of the power pulse will be increased in order to preserve the total amount of energy deposition, that the fuel rod would experience in the 2A LOCA scenario of Atucha2 NPP.

Tab. A. 7 represents the evaluation of the required linear heat rate (ΔLHR) in order to achieve fuel centerline melting (enthalpy deposition of 650 kJ/kg), in case of different pulse time. Adiabatic conditions and an initial linear heat rate of 60 kW/m are considered. Maximum linear heat rate is reported as well. For example, for a pulse time of 3 s, a peak rating in excess of 260 kW/m conditions is required in order to achieve fuel central melting.

Tab. A. 8 provides the estimations of the required fuel enrichments for reaching different linear heat rates.

A.3.6.11 Post Irradiation Examinations

Before irradiation and after burnup accumulation phase, in addition the online measurement, the dimensional measurements and visual inspections will be executed.

After completing the power ramp pulse testing, CNA-2 fuel rods will be shipped to Kjeller hot-laboratory for post irradiation examinations (PIE). The PIE will include:

- visual inspection (with photographs);
- dimensional measurements (diameter and length profiles);

- gamma scanning (for determining power profiles and/or dislocation of fuel), Fig. A. 11;
- leak-testing;
- characterization of fuel failures (if any); and
- metallography/ceramography (three cross sections for each rod).

A.3.6.12 Possible outcomes

A general overview of the issues that cold be addressed during the experiment is listed below:

- failure mechanism and associated phenomena,
- thermal mechanical behavior changes:
    - pellet cracking,
    - fuel densification,
    - fuel swelling,
    - cladding creepdown,
    - cladding growth,
    - FGR,
- fission gas release as influenced by power level and operation mode,
- geometry changes in order to address the coolability issue (i.e. ballooning),
- pellet–clad interaction,
- fuel performance anomalies such as:
    - crude deposition as affected by water chemistry and heat rating,
    - axial offset anomalies caused by local boron accumulation on the surface of the fuel rods,
    - degradation of failed fuel resulting in large exposure of the fuel to the coolant and consequent increase of radiation level in the coolant,
    - control rod sticking as the result of axial growth of guide tubes during service,
- oxidation and hydrogen pick-up,
- maximum rod overpressure,
- start of ballooning (cladding deformation detected by rod pressure measurement),
- cladding failure,
- gap closure,
- fuel centre temperature and thus thermal property changes as function of burnup,
- fission gas release as function of power, operational mode and burnup,
- fuel swelling as affected by solid and gaseous fission products,
- pellet–cladding interaction manifested by axial and diametral deformations,
- rod pressure,
- corrosion of hydriding,
- stress corrosion cracking.

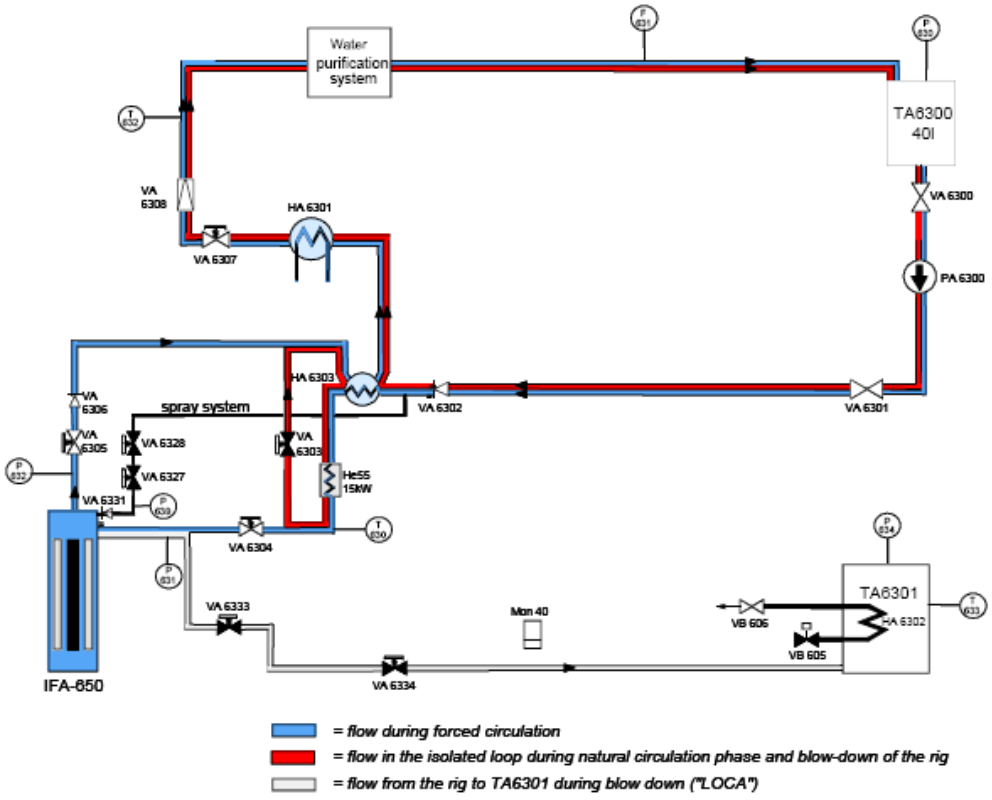

Fig. A. 7 – Simplified drawing of the loop, IFA-650.6 test.

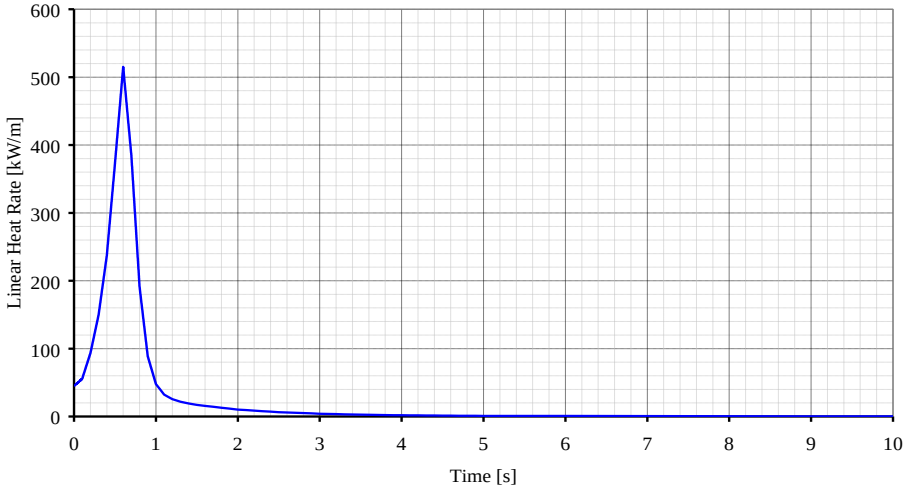

Fig. A. 8 – Linear heat rate.

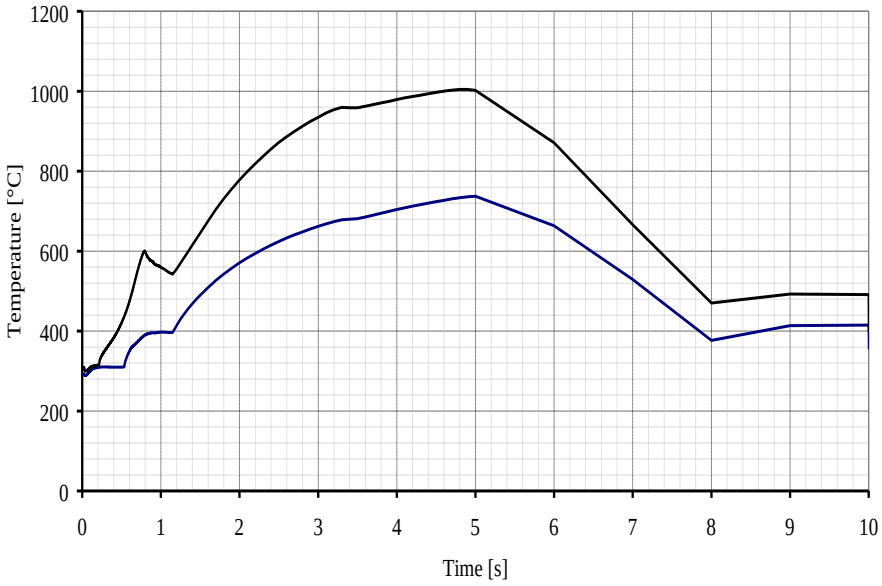

Fig. A. 9 – Range of temperatures.

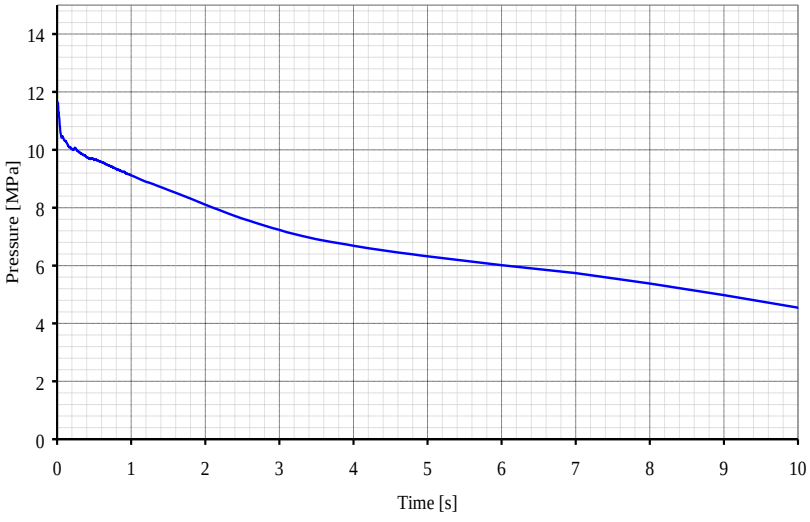

Fig. A. 10 – Pressure.

Pulse time [sec.]	*ΔHR* [W/cm]	LHR_{Max}
1.0	8000	8600
1.5	5300	4700
20	4000	4600
2.5	3200	3800
3.0	2600	3200
3.5	2300	2900
4.0	2000	2600
4.5	1800	2400

Tab. A. 7 – Required ΔLHR for fuel centerline melting (650 kJ/kg).

Enrichment [wt.%]	*ALHR* [kW/m]
6.0	1600
8.0	1900
10.0	2125
13.0	2375
15.0	2525

Tab. A. 8 – Heat rates for different fuel enrichments.

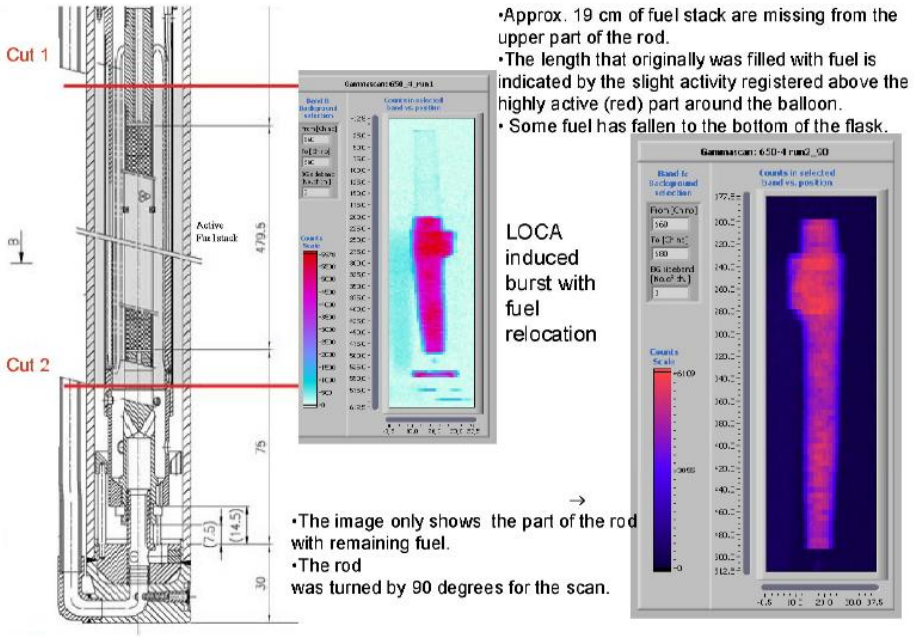

Fig. A. 11 – Example of gamma scanning during LOCA test (Vitanza 2008).

A.4 Time schedule

The Tab. A. 9 below summarizes the proposed time schedule for the project, distinguishing from different phases. The scheduled overall project duration is 36 months.

From the starting of the project, 3 moths are needed to design the instrumented CNA-2 fuel rods, the burnup-accumulation and the power pulse test rig and the corresponding pressure flask. The mock-up and prototype for power pulse test rig will be performed in parallel.

After 14 months, the burnup accumulation test rig and the corresponding pressure flask together with the 3 instrumented fuel rods will be ready for irradiation.

The remaining 3 rods, the power pulse test rig and pressure flask will be ready for irradiation 18 months after the starting of the project. The power pulse test of the three un-irradiated fuel rods (one reactor cycle needed, about 3 months) could start together with the base irradiation of the other three rods (two reactor cycles needed, about one year).

The fist set of fuel rods will be shipped to Kjeller for PIE, that will be completed after 30 months from the starting of the project. Finally, also the three remaining rods will be shipped to Kjeller, in order to have the complete set of PIE ready 36 months after the starting of the project.

A.5 Conclusions

This document contains the design of experiments to be performed in a research reactor (e.g. Halden reactor). The activity includes the technical specifications, the specific analyses to define the initial and boundary conditions and the economic evaluation of the activity. The Halden Boiling Water Reactor is chosen to perform the experiment feasibility study.

The reasons to perform an experiment are to establish the fail-safe limits of the CNA-2 fuel rods during LB-LOCA scenario. The experiment has to provide relevant information on the consequences of combined power and temperature excursions to the fuel integrity, addressing:

- the failure limits;
- the failure mechanism and associated phenomena;
- the influence of the reload strategy stress corrosion cracking.

The experiment should provide also suitable data for modeling.

The relevance of the activity is connected with the funding availability.

No	Id	Estimated months after the starting of the project				
1	**Design Phase**	**0 - 3**				
1.1	Design of the instrumented CNA-2 fuel rods	0 - 3				
1.2	Design of the burnup accumulation rig	0 - 3				
1.3	Design of the power pulse rig	0 - 3				
1.4	Design of the pressure flask	0 - 3				
2	**Fabrication Phase**	**3 - 18**				
2.1	Mock-up and prototype testing for power pulse rig	0 - 3				
2.2	Fabrication of burnup accumulation rig with pressure flask – Completed and ready for irradiation		3 – 14			
2.3	Fabrication of 3 instrumented fuel rods– Completed and ready for irradiation		3 – 14			
2.4	Fabrication of power pulse test rig with pressure flask – Completed and ready for irradiation			14 – 18		
2.5	Fabrication of 3 instrumented fuel rods– Completed and ready for irradiation			14 – 18		
3	**Test Phase**				**18 – 33**	
3.1	Power pulse testing of the 3 un-irradiated fuel rods (one reactor cycle needed to complete these tests) - 3 months needed				18 - 21	
3.2	Irradiation of 3 rods in the burnup accumulation rig (two reactor cycle needed) - Two period of irradiation of 3 months needed (1 year)				18 – 30	
3.3	Power pulse testing of the 3 irradiated fuel rods (one reactor cycle needed to complete these tests) - 3 months needed				30 – 33	
4	**PIE**				**21 - 36**	
4.1	PIE of the power pulse testing of the 3 un-irradiated fuel rods (starting 3 months after irradiation, estimated duration: 3-5 months)				21 – 30	
4.2	PIE of the power pulse testing of the 3 irradiated fuel rods (estimated duration: 3-5 months)				33 – 36	

Tab. A. 9 – Time schedule of the project.

APPENDIX B. NORMAL OPERATION OF CNA-2 NPP

B.1 Code version

The current activity is performed through TRANSURANUS code, version "v1m1j09", using the deterministic option, steady state thermal and mechanical analysis. The version of the manual (*Lassmann 2009*) is "v1m1j09". Calculations are run on Windows XP environment using a computer Intel Core2 Duo CPU 2.20 GHz.

The source code has been modified in order to account for the stress corrosion cracking specifics of CNA-2 (see following sections).

B.2 Input model

Starting from the reference input used to perform LOCA analysis described in section 5, the following modifications are implemented in the input:

- complete removal of the "LOCA block" and LOCA specific models;
- replacement of HWR with PWR reactor type.

B.3 TRANSURANUS PCI-SCC specific features

The stress-corrosion cracking (SCC) model SPAKOR implemented in TU code is based on the observation that iodine SCC failures usually begin as an intergranular fracture, which becomes a "cleavage and fluting" fracture at some point in crack growth. It is assumed in the model that the intergranular portion of the failure is due to chemical attack, which is independent of applied stress, while the cleavage and fluting portion of the failure can be described by linear elastic fracture mechanics.

Chemical crack growth is assumed to continue until critical stress intensity for cleavage and fluting, KISCC, is reached. At this point, cleavage and fluting fracture initiates and continues up to failure.

Chemical crack growth is assumed to initiate if the following conditions are satisfied:

- The cladding temperature must exceed a critical value (270 °C).
- The strain rate in the cladding must exceed a critical value, which is temperature dependent.
- The hoop stress must be positive.

The burn-up limit of 5000 MWd/tU has been deactivated in the source code for the current analysis. Once a crack has been initiated, a new formation of a protective layer is not considered.

B.4 Implementation of BIC

In all the cases analyzed, the boundary conditions implemented for the analyses are:

- linear heat rate at 10 axial position;
- fast neutron flux at 10 axial position;
- cladding temperature at 10 axial position; and
- pressure.

B.5 Case of analytical investigation of power ramps

13 MATLAB programs were prepared to investigate the behavior of the CNA-2 fuel during power ramps and perform the post-processing of the parameters. The list of the programs is reported in Tab. B. 1. The conditioning linear heat rate (q') and the height of the power ramp (Δq') used as boundary conditions for the analysis are reported in (*Adorni FU-09 2008*).

A sample scheme of a power ramp is reported in Fig. B. 1. Fuel irradiation starts at ambient conditions, considering 12 hours time to get the nominal conditions (points A-B of Fig. B. 1).

The base irradiation (points B-C of Fig. B. 1) is performed at different conditioning linear heat rate (q') that is selected according to the x axis of Fig. B. 2. During this conditioning, the fast neutron flux distribution has been selected as the maximum value of the steady state calculated by RELAP5-3D©. Cladding temperature and pressure are selected as average values deriving from RELAP5-3D© steady state calculations as well (*D'Auria 2008*).

The difference between ramp terminal level linear heat rate and the conditioning linear heat rate (points C-D of Fig. B. 1) has been selected according to the y axis (*Adorni FU-09 2008*). For the aim of the current analysis, a constant ramp rate of 192 kW/m-h is selected. The investigation of the influence of different ramp rate on the behavior of the CNA-2 fuel rods will be addressed in the sensitivity analyses.

Finally, an end of irradiation at a ramp terminal level of 48 hours has been modeled (points D-TUFT of Fig. B. 1).

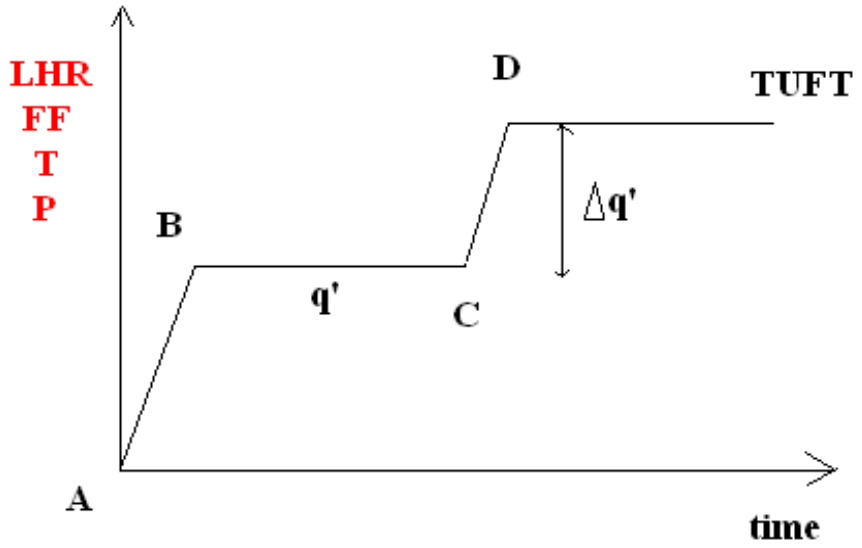

Fig. B. 1 – Power ramp shape scheme.

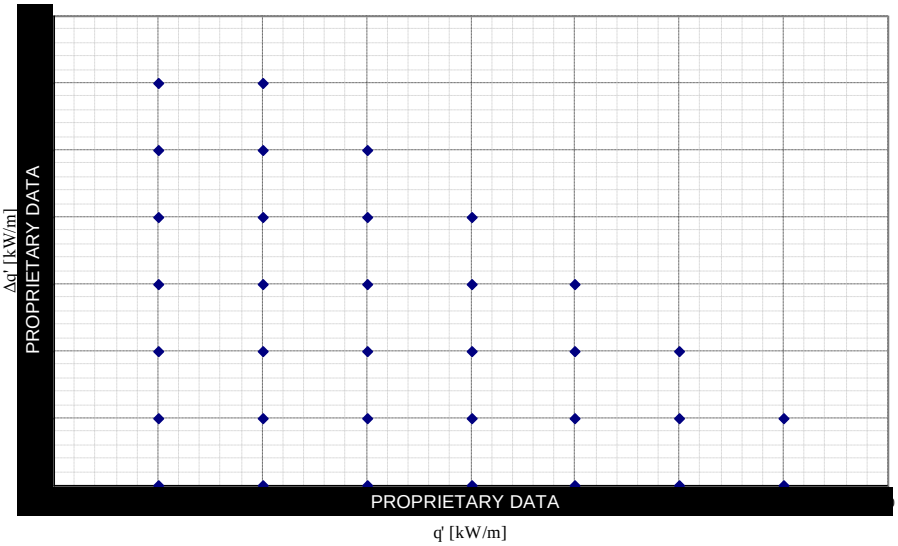

Fig. B. 2 – BIC of the analytical analysis of the power ramps.

#	ID	DESCRIPTION
A	**PCI_map_r3b.m**	Run of the code with the possibility to select different burnups.
B	cna2_loca_DAT_r0.m cna2_loca_MAXTcl_r1.m	Create data files of the fuel pellet centerline temperature and prepare a data file containing the maximum value per rod.
C	cna2_loca_DAT_r2.m cna2_loca_MAXP_12s_r2.m cna2_loca_minP_12s_r2.m	Create data files of the fuel pin internal pressure and prepare a data file containing the maximum and minimum values per rod.
D	cna2_loca_DAT_r3.m cna2_loca_MAXStress_r3.m	Create data files of the stresses and prepare a data file containing the maximum value per rod.
E	cna2_loca_DAT_r4.m cna2_loca_MAXStrain_r4.m	Create data files of the strains and prepare a data file containing the maximum value per rod.
F	cna2_loca_DAT_r5.m cna2_loca_MAXCORR_r5.m	Create data files of the corrosions and prepare a data file containing the maximum value per rod.
G	cna2_loca_DAT_r6.m cna2_loca_MAXGW_r6.m	Create data files of the fuel gap width temperature and prepare a data file containing the maximum value per rod.
H	cna2_loca_DAT_r7.m	Create data files of the outer cladding radius (RHA)
I	cna2_loca_DAT_r8.m	Create data files of the inner cladding radius (RHI)
J	cna2_loca_DAT_r9.m	Create data files of the outer fuel radius (RBA)
K	cna2_loca_param_variation_r3.m cna2_loca_criteria78_r3.m cna2_loca_criteria78plus_r3.m	Create data files and supporting files containing the necessary information to calculate the safety margins related to elastic buckling and plastic instability.
L	cna2_loca_FAILURE_r8.m	Identification of the failed rods.
M	cna2_loca_MELTING_r8c	Identification of the melted rods.

Tab. B. 1 – Main MATLAB programs for the analytical investigations of the power ramps.

B.6 Case of analyses of normal operation

18 MATLAB programs were prepared to investigate the behavior of the CNA-2 fuel during normal operation and perform the post-processing of the parameters for all the 451 fuel assembly, each one represented by one fuel rod. The list of the programs is reported (*Adorni FU-09 2008*).

Due to differences in irradiation history, fuel rod models can be grouped as follow:

- the rods that crossed the transition burnup; for these, shuffling is simulated in the current analysis; and
- the rods that have not yet exceeded it.

In both cases, the irradiation starts at ambient conditions, considering 12 hours time to get the nominal conditions.

Rods that have been subjected to shuffling (zone 1,4 and 5).
Since detailed data of the movement of the fuel rods are not available, the hypotheses of conditioning linear heat of the pre-shuffling zone, investigated in (*Adorni FU-06 2008*), are recalled. Calculations are performed according to (*Adorni FU-06 2008*), considering the minimum conditioning linear heat rate per burnup zone, in order to maximize the power ramps and the residence time in the reactor.

(*Adorni FU-09 2008*) reports a scheme of the irradiation for the rods that are subjected to shuffling. After a base irradiation (up to point C), shuffling timing is modeled according to (*Mazzantini 2008*). The duration of the fuel element withdrawal and insertion are selected considering a velocity of the refueling machine of 1 m/min. The time elapsed from the beginning of the withdrawal until the complete insertion of the fuel in its new channel is approximately 1 hour (points CDEF).

A simple formula to calculate the time to reach the desired final burnup (point TUFT of (*Adorni FU-09 2008*), on the basis of the linear heat rate (different for each rod), is implemented in the MATLAB programs used for the analysis. The after shuffling linear heat rate, fast flux, temperature and pressure distribution have been selected correspondent to the steady state values of the RELAP53D© calculations (*D'Auria 2008*) (different for each rod).

Fig. B. 5 reports the location of the CNA-2 fuel rods in the power ramp failure map of CNA-1 (*Dusch 2008*). The global and burnup dependent limits delimit the allowable CNA-1 operational zones[1]. The picture reports the highest local power ramp heights that are achieved using the minimum conditioning linear heat rate of (*Adorni FU-09 2008*) (blue rhombus in the figure). The corresponding average values are reported by the red squares. For the sake of completeness, the green circles represent the height of the power ramp in the case of maximum conditioning linear heat rate of (*Adorni FU-09 2008*).

It should be noted that, as expected, all the values are below all the limit curves (of CNA-1).

Rods that have not been subjected to shuffling (zone 2, 3 and 6).
The fuel that is not subjected to shuffling (corresponding to the fuel zones 6, 2 and 3 of (*Adorni FU-09 2008*)) reaches in the calculation the burnup distribution of the reference core with the axial linear heat rate, axial temperature, axial fast flux and pressure of the steady state calculations, constant in time. The resolution of the neutronic calculation is maintained.

(*Adorni FU-09 2008*) shows a scheme of the irradiation for the rods that are not subjected to shuffling. In this case only a value constant in time of the boundary conditions (i.e. fast flux, linear heat rate, temperature and pressure) is modeled (different for each rod).

[1] Exceptions can be found in Ref. 0 (not reported here).

A simple formula to calculate the time to reach the desired final burnup (point TUFT of (*Adorni FU-09 2008*)), on the basis of the linear heat rate (different for each rod), is implemented in the MATLAB programs used for the analysis. The linear heat rate, fast flux, temperature and pressure distribution have been selected correspondent to the steady state values of the RELAP53D© calculations (*D'Auria 2008*) (different for each rod).

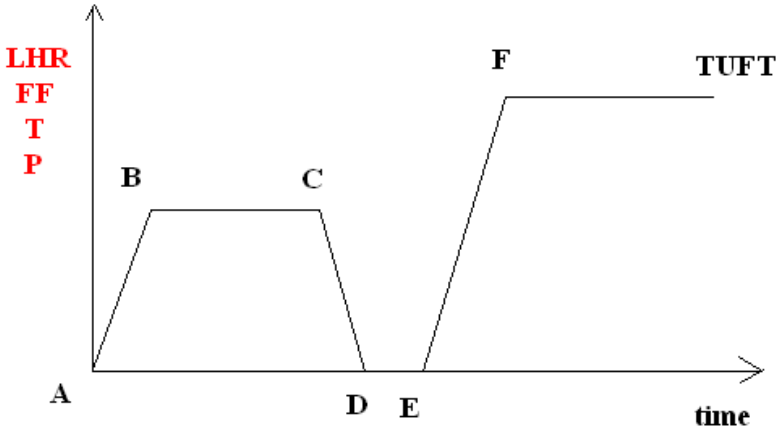

Fig. B. 3 – *Scheme of the irradiation, burnup zone 1, 4 and 5 (refueling is simulated).*

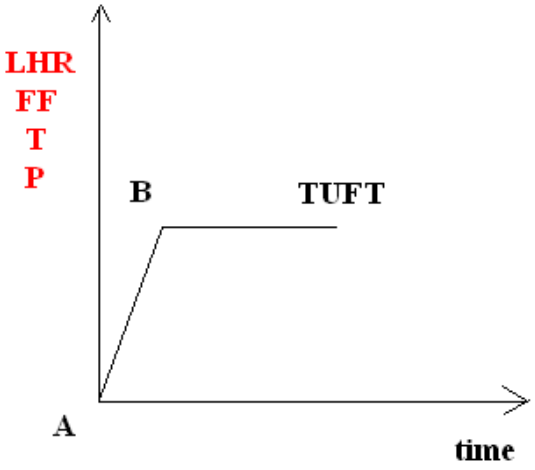

Fig. B. 4 – Scheme of the irradiation, burnup zones 2, 3 and 6.

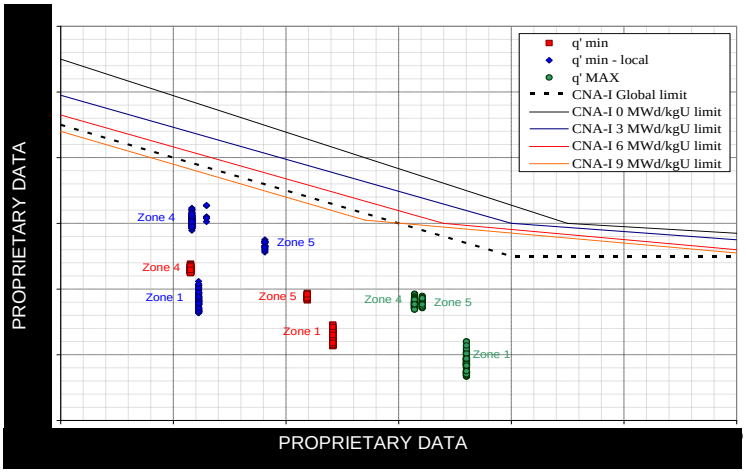

Fig. B. 5 – Power ramp failure map for CNA-2 fuel together with the global and burnup dependent limits of CNA-1, equilibrium burnup of the reference core.

#	ID	DESCRIPTION
A	BIC_C53.m	Preparation of the BIC (i.e. LHR, FF, T anc P) for the subsequent analysis.
B	**PCI_236_r1.m**	Run of the fuel assembly representing the fuel rods belonging to burnup zones No 2, 3 and 6.
C	**PCI_1_r1.m**	Run of the fuel assembly representing the fuel rods belonging to burnup zone No 1.
D	**PCI_4_r1.m**	Run of the fuel assembly representing the fuel rods belonging to burnup zone No 4.
E	**PCI_5_r1.m**	Run of the fuel assembly representing the fuel rods belonging to burnup zone No 5.
F	cna2_loca_BU_EOI_r0.m	Create data files of the average fuel rod burnup and prepare a data file containing the end of irradiation value per rod.
G	cna2_loca_DAT_r0.m cna2_loca_MAXTcl_r1.m	Create data files of the fuel pellet centerline temperature and prepare a data file containing the maximum value per rod.
H	cna2_loca_DAT_r2.m cna2_loca_MAXP_12s_r2.m cna2_loca_minP_12s_r2.m	Create data files of the fuel pin internal pressure and prepare a data file containing the maximum and minimum values per rod.
I	cna2_loca_DAT_r3.m cna2_loca_MAXStress_r3.m	Create data files of the stresses and prepare a data file containing the maximum value per rod.
J	cna2_loca_DAT_r4.m cna2_loca_MAXStrain_r4.m	Create data files of the strains and prepare a data file containing the maximum value per rod.
K	cna2_loca_DAT_r5.m cna2_loca_MAXCORR_r5.m	Create data files of the corrosions and prepare a data file containing the maximum value per rod.
L	cna2_loca_DAT_r6.m cna2_loca_MAXGW_r6.m	Create data files of the fuel gap width temperature and prepare a data file containing the maximum value per rod.
M	cna2_loca_DAT_r7.m	Create data files of the outer cladding radius (RHA)
N	cna2_loca_DAT_r8.m	Create data files of the inner cladding radius (RHI)
O	cna2_loca_DAT_r9.m	Create data files of the outer fuel radius (RBA)
P	cna2_loca_param_variation_r3.m cna2_loca_criteria78_r3.m cna2_loca_criteria78plus_r3.m	Create data files and supporting files containing the necessary information to calculate the safety margins related to elastic buckling and plastic instability.
Q	cna2_loca_FAILURE_r8.m	Identification of the failed rods.
R	cna2_loca_MELTING_r8c	Identification of the melted rods.

Tab. B. 2 – Main MATLAB programs for the analyses of the normal operation.

B.7 Deterministic fuel rod analysis

This section presents the results of the deterministic fuel rod analysis calculated using the version "v1m1j09" of TRANSURANUS code. The analysis is divided in two sections:

- analytical investigation of power ramps, Fig. B. 1, and
- analysis of normal operation, (*Adorni FU-09 2008*).

B.7.1 Investigation of the power ramps and failure maps

The aim of the current analysis is the determination of the failure limits for CNA-2 fuel under power ramps. The modeling of the power ramps for the current report is based on the report of (*Adorni FU-09 2008*) that was developed for CNA-1. The boundary conditions used for the analysis are described in (*Adorni FU-09 2008*). The fuel safety criteria of (*Adorni FU-09 2008*) will be checked in the following sections.

Relevant figures are reported in appendix 1. The figures report the fuel rod failure as function of conditioning linear heat rate (q') and the difference between the ramp terminal level and the conditioning linear heat rate (Δq') for different burnup levels. The CNA-1 global and burnup-dependent limits are reported in the same figures as well. It should be noted that the results of the calculations of CNA-2 fuel rods are very similar to CNA-1 limits.

B.7.1.1 Verification of the normal operation

In the following sections the results of the verification of the fulfillment of the limits during normal operation are reported. The boundary conditions used for the analysis are described in (*Adorni FU-09 2009*).

The fuel design criteria of section 3.4.1 are checked in the following sections for a selected core status. Fig. 40 reports the location of the CNA-2 fuel rods shuffled (corresponding to zones 1, 4 and 5) in the power ramp failure map of CNA-1. The global and burnup dependent limits delimit the allowable CNA-1 operational zones[2]. The picture reports the highest local power ramp heights that are achieved using the minimum conditioning linear heat rate of Fig. B. 5 (blue rhombus in the figure). The corresponding average values are reported by the red squares (used in the current analysis). For the sake of completeness, the green circles represent the height of the power ramp in the case of maximum conditioning linear heat rate of Fig. B. 5. The influence of this different possible choice of the conditioning linear heat rate and the corresponding delta linear heat rate will be addressed in the sensitivity analyses.

Tab. 28 summarizes the safety margins related to the CNA-2 specific fuel safety criteria for the case of normal operation of 451 fuel assemblies each one

[2] Exceptions can be found in (*Dush 1980*) (not reported here).

represented by one rod. The minimum safety margin per each rod is calculated according to the following formula:

$$s_x = (\text{CNA-2 min specific limit})/(\text{max calculated value})$$

The indication MAX and min of Tab. 28, represents the maximum and minimum values over all the 451 rods. The same values are also represented in Fig. B. 5.

Appendix 8 contains all the results concerning the verification of the fuel safety criteria during normal operation. Each figure contains 451 dots representing a different fuel rods, each one representative of one CNA-2 fuel assembly, as function of burnup. Furthermore, different zones are reported in different colors. The CNA-2 specific design limits from section 3.4.1 are reported in the same figure.

B.7.1.1.1 Criterion 1: Temperatures

Fig. B. 11reports the maximum fuel centerline temperature as function of burnup, different colors represent different burnup zones. The burnup-dependent UO2 melting limit is reported on the top of the figure as well. Zone 3 exhibits the minimum safety margin of 1.844.

B.7.1.1.2 Criterion 2: Fuel rod internal pressure

The maximum internal gas pressure in the fuel rod may not enlarge the fuel to cladding gap (i. e. the increase in the cladding tube diameter caused by the internal gas pressure is less than the increase in the pellet diameter due to fuel swelling). The maximum permissible increase in cladding tube diameter is limited by an "*ad hoc"* criterion on fuel rod internal pressure.

Fig. B. 12 reports the maximum fuel rod internal pressure as function of burnup, different colors represent different burnup zones. The coolant pressure is reported on the top of the figure as well. The safety margin is calculated considering the ratio between the maximum cladding gap width (from the reaching of the reactor operating conditions, 12h from the SoT) and the nominal gap width. The safety margin is constant and equal to 1.391 for all the zones, since the maximum value is calculated about at the beginning of the dwell time and it is the same for all the cases analyzed.

B.7.1.1.3 Criteria 3 and 4: Cladding strains

The equivalent plastic strain of the cladding in the tensile range (composed of axial and tangential strain) must be less than or equal to 2.5 %. This limit is directly implemented in the input of the TU code and it is checked each time step (cladding failure criterion of plastic instability).

The total tangential strain (elastic and plastic region) of the cladding caused by fast power ramps must be less than or equal to 1 %. For the sake of clarity, in this case

the limit of 1% is checked for all the irradiation instead of just the power ramps (conservative case).

Fig. B. 13 reports the maximum cladding strain as function of burnup, different colors represent different burnup zones. The 1% limit is reported on the top of the figure as well. The calculations exhibit increasing values with burnup. Zone 4 exhibits higher strain values. It should be noted that zone 4 is characterized by the lower conditioning linear heat rate values. This burnup zone exhibits the minimum safety margin of 1.320.

B.7.1.1.4 Criterion 5: Cladding corrosion

Fig. B. 14 reports the maximum oxide thickness as function of burnup, different colors represent different burnup zones. The limit of 100μm is not reported on the figure.

The calculations exhibit an increasing of the corrosion thickness with burnup. Zone 4 exhibits higher oxide thickness values, this is due to the higher residence time of the fuel in the reactor, since the fuel belonging to this zone is conditioned at the lower linear heat rate values. Anyway the values are well below the limits, and the related safety margins are in all the cases above 100.

B.7.1.1.5 Criteria 7 and 8: Elastic buckling and plastic deformation of the cladding

Fig. B. 15 reports the maximum pressure difference between the rod internal gas pressure and the external coolant pressure, calculated data and critical elastic buckling pressure limit on the bottom, different colors represent different burnup zones. Zone 1 exhibits the minimum safety margin of 2.227.

Fig. B. 16 reports the maximum pressure difference between the rod internal gas pressure and the external coolant pressure, calculated data and plastic instability limit on the bottom, different colors represent different burnup zones. Zone 1 exhibits the minimum safety margin of 2.417.

It should be noted that in all that in all the cases, the critical elastic buckling limit is restrictive respect to the plastic instability one.

B.7.1.1.6 Criteria 9: Cladding Stresses

Fig. B. 17 reports the maximum average equivalent stress as function of burnup, different colors represent different burnup zones. The minimum design limit between 0.9 $R_{p0.2}$ and 0.5 R_m limit that is 135 MPa is reported on the top of the figure as well. The rods that are subjected to shuffling (zone 1, 4 and 5) exhibit higher value than the non shuffled rods (zones 1, 4 and 5).

Zone 1 exhibits the minimum safety margin of 1.886.

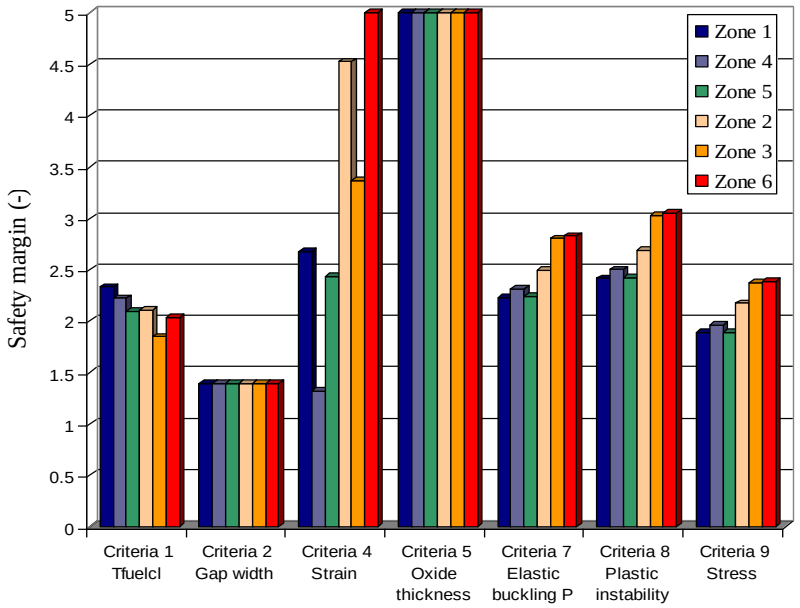

Fig. 86 – Summary of the minimum safety margins per burnup zone.

Fuel safety criteria		Zone 1	Zone 4	Zone 5	Zone 2	Zone 3	Zone 6
Criteria 1 MAX Tfuelcl	MAX	2.335	2.713	2.404	3.894	2.438	2.397
	min	2.329	2.220	2.092	2.102	1.844	2.037
Criteria 2 Gap width	MAX	1.391	1.391	1.391	1.391	1.391	1.391
	min	1.391	1.391	1.391	1.391	1.391	1.391
Criteria 4 MAX Strain	MAX	4.114	1.734	4.777	>100	>100	91.996
	min	2.674	1.320	2.437	4.522	3.366	8.761
Criteria 5 MAX Oxide	MAX	>100	>100	>100	>100	>100	>100
	min	>100	>100	>100	>100	>100	>100
Criteria 7 Elastic buckling P	MAX	2.242	2.317	2.239	3.020	3.427	3.079
	min	2.227	2.311	2.239	2.492	2.803	2.825
Criteria 8 Plastic instability	MAX	2.422	2.502	2.419	3.259	3.701	3.326
	min	2.417	2.499	2.419	2.691	3.028	3.051
Criteria 9 MAX Stress	MAX	1.886	1.960	1.885	2.540	2.714	2.593
	min	1.886	1.960	1.885	2.172	2.369	2.386

Tab. 28 – Summary of the maximum and minimum safety margins per burnup zone.

B.8 Conclusions

This appendix contains the description of the boundary conditions that are used for the analysis of the fuel behavior during normal operation as well as how they are

implemented in the documented input deck (*Adorni FU-04 2008*) of TRANSURANUS code.

Two cases are investigated in the current report:
- the analytical investigation of the power ramps, and
- the analysis of the normal operation.

The set up of the model for the analytical investigation of the power ramps is performed in order to study the influence of conditioning linear heat rate and ramp height of CNA-2 failure propensity.

The set up of the boundary conditions for the analysis of the normal operation are set up in order to verify that the CNA-2 specific safety criteria are fulfilled, and to calculate the values of the safety margins.

All the process is automated thought he use of "*ad hoc*" programs written to run with MALTAB.

The analyses bring to the following relevant results.

The analytical investigation of the power ramps shows that:
- the failure maps result very similar of the ones obtained for CNA-1;
- the verification of the CNA-2 specific fuel safety criteria shows that they are fulfilled in all the cases for the non failed rods.

The analysis of the normal operation shows that:
- all the rods are comprised below the power ramp failure map developed in the framework of preceding item;
- the safety margin for the CNA-2 specific fuel safety criteria for all the rods are all above 1.3.

In conclusion, the analyses of the fuel behavior by TU code during normal operation shows that in all the cases the results are below the limit of section 3.4.1.

Additional information, including sensitivity and uncertainty analyses can be found in (*Adorni FU-11 2009, Adorni FU-18 2009*).

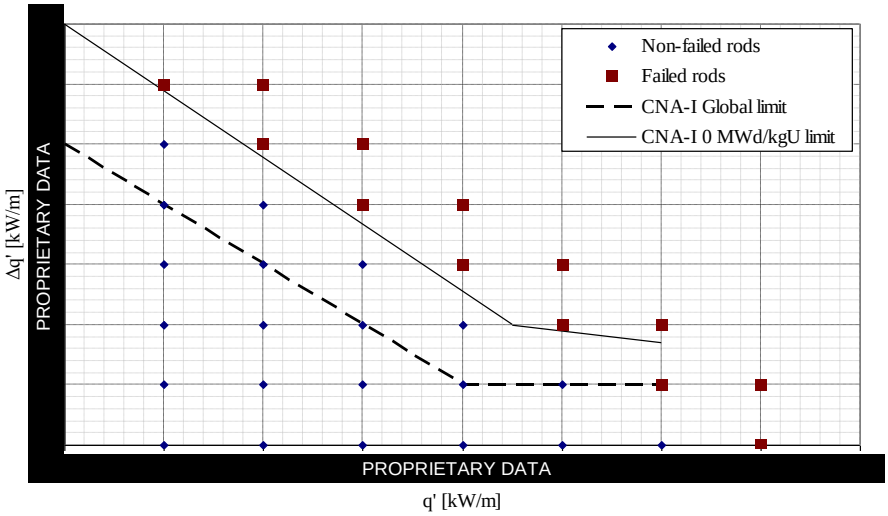

Fig. B. 6 – Power ramp failure map for CNA-2 fuel together with the global and burnup dependent limits of CNA-1, case of burnup = 0.

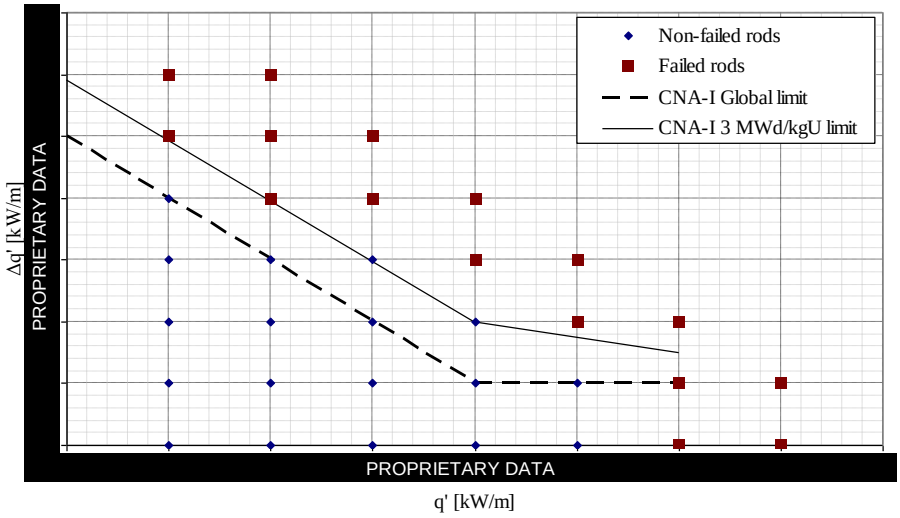

Fig. B. 7 – Power ramp failure map for CNA-2 fuel together with the global and burnup dependent limits of CNA-1, case of burnup = 3.

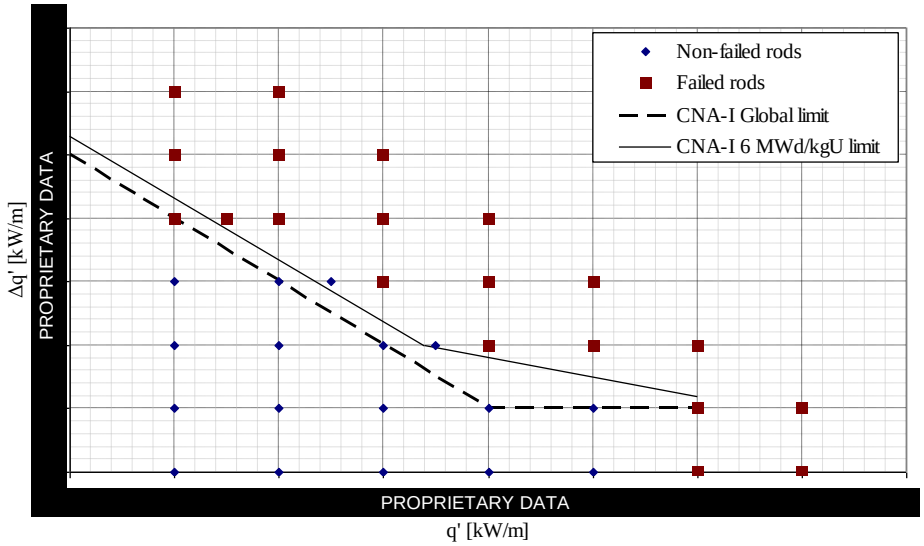

Fig. B. 8 – Power ramp failure map for CNA-2 fuel together with the global and burnup dependent limits of CNA-1, case of burnup = 6.

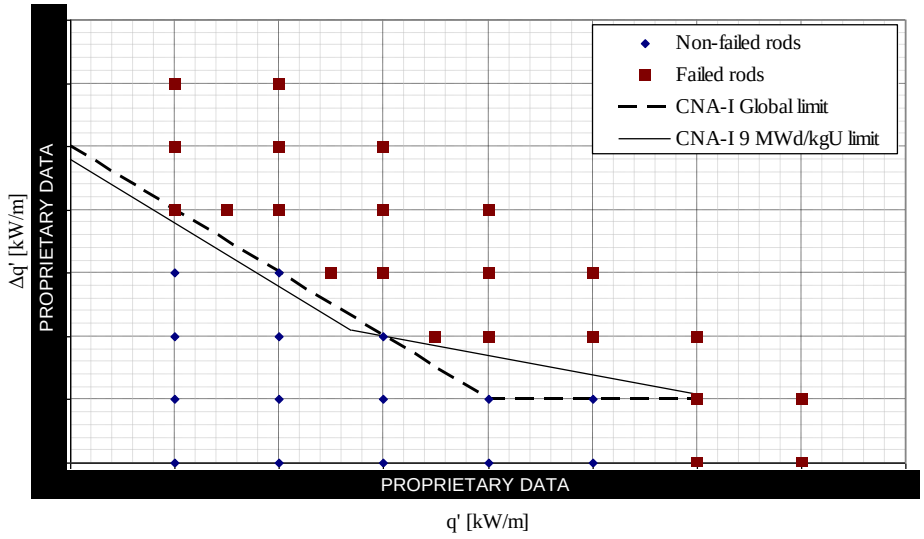

Fig. B. 9 – Power ramp failure map for CNA-2 fuel together with the global and burnup dependent limits of CNA-1, case of burnup = 8.

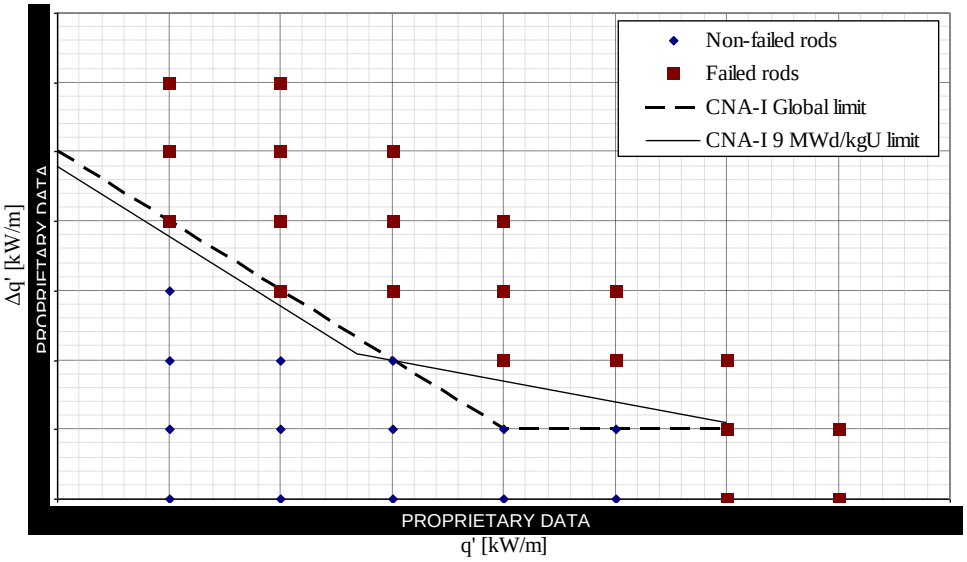

Fig. B. 10 – Power ramp failure map for CNA-2 fuel together with the global and burnup dependent limits of CNA-1, case of burnup = 10.

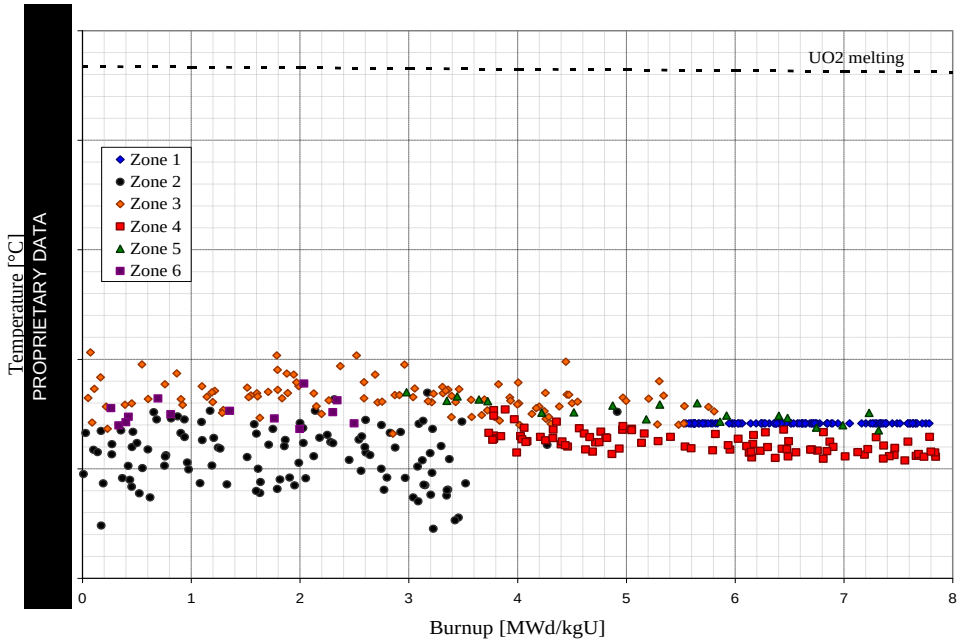

Fig. B. 11 – Fuel safety criteria 1: Maximum fuel centerline temperature, calculated data and limit.

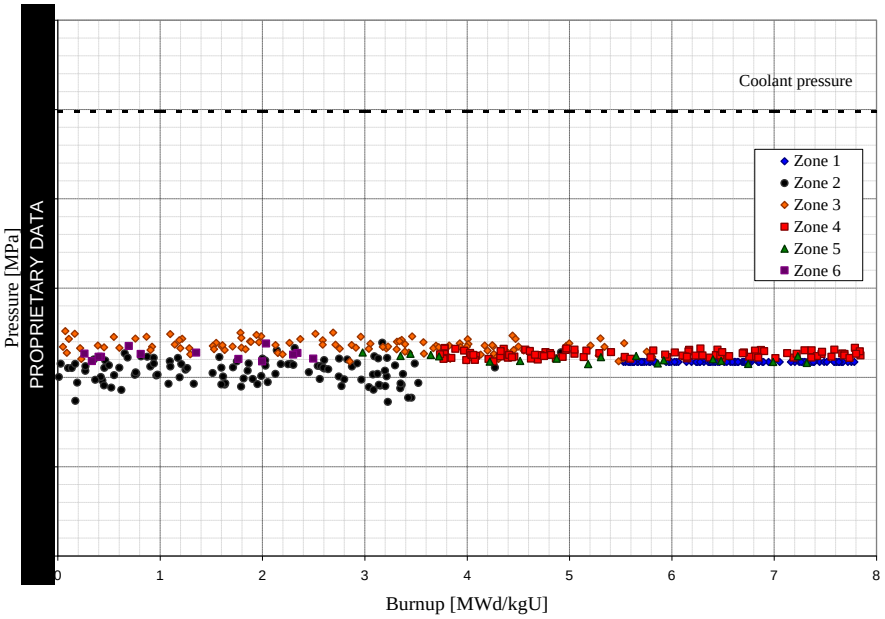

Fig. B. 12 – Fuel safety criteria 2: Maximum fuel rod internal pressure, calculated data and limit.

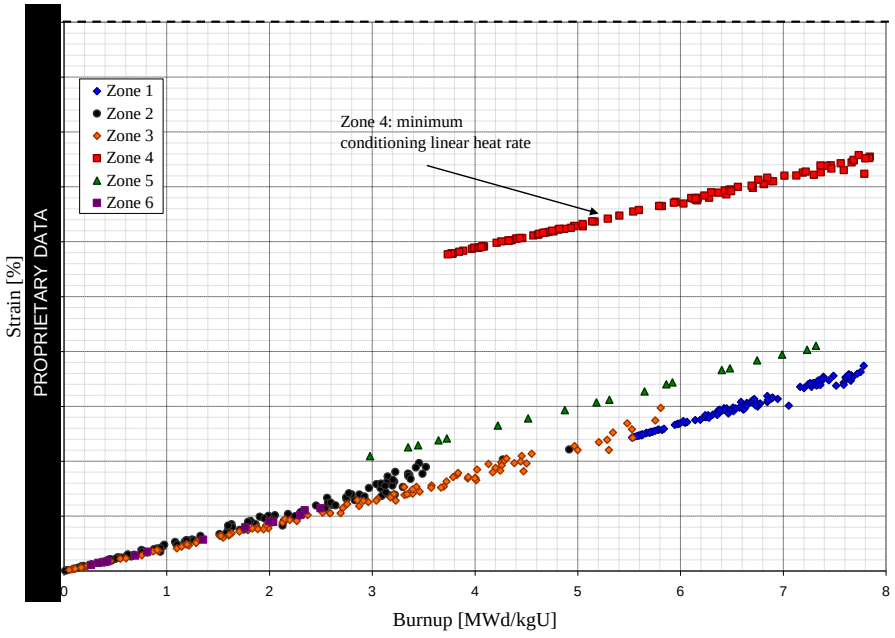

Fig. B. 13 – Fuel safety criteria 4: Maximum cladding strain, calculated data and limit.

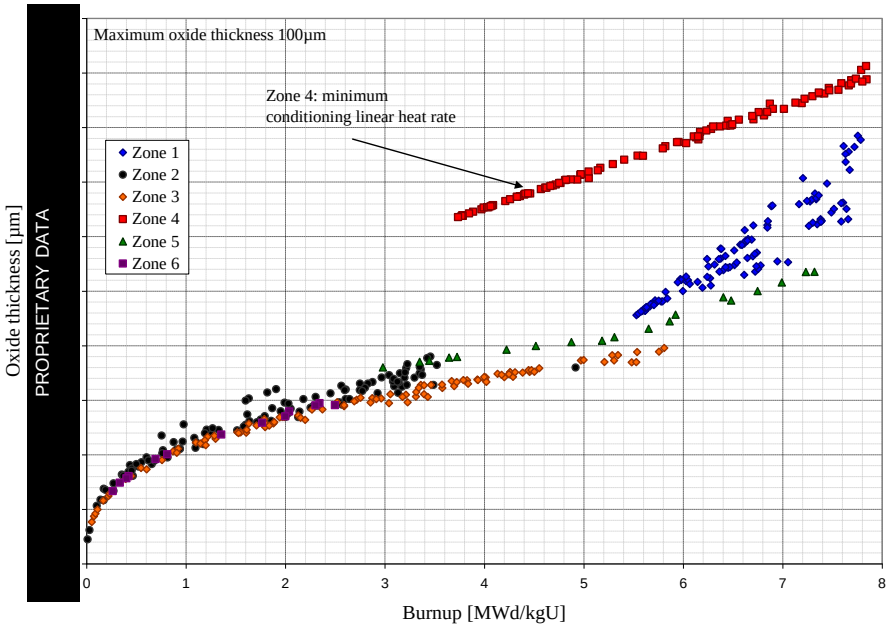

Fig. B. 14 – Fuel safety criteria 5: Maximum oxide thickness, calculated data and limit.

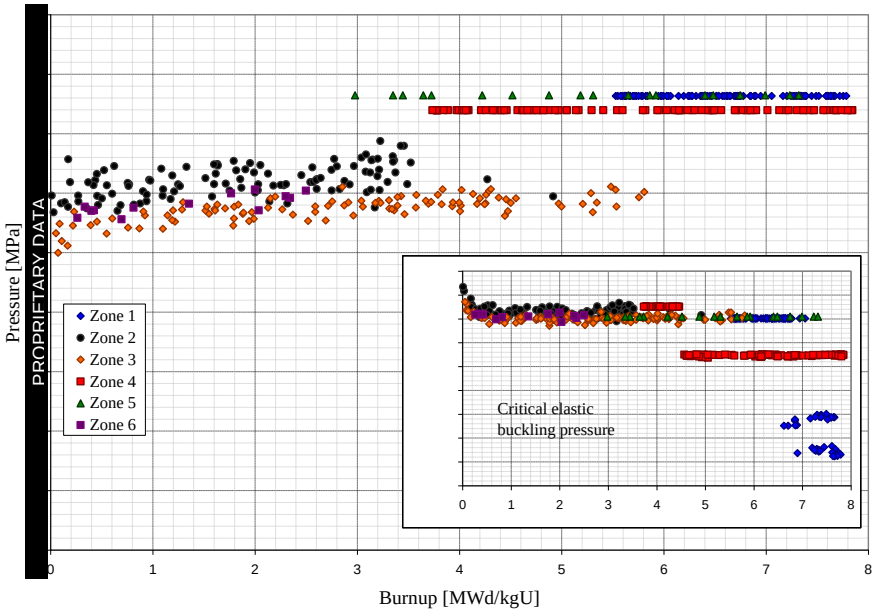

Fig. B. 15 – Fuel safety criteria 7: Maximum pressure difference between the rod internal gas pressure and the external coolant pressure, calculated data and critical elastic buckling pressure limit.

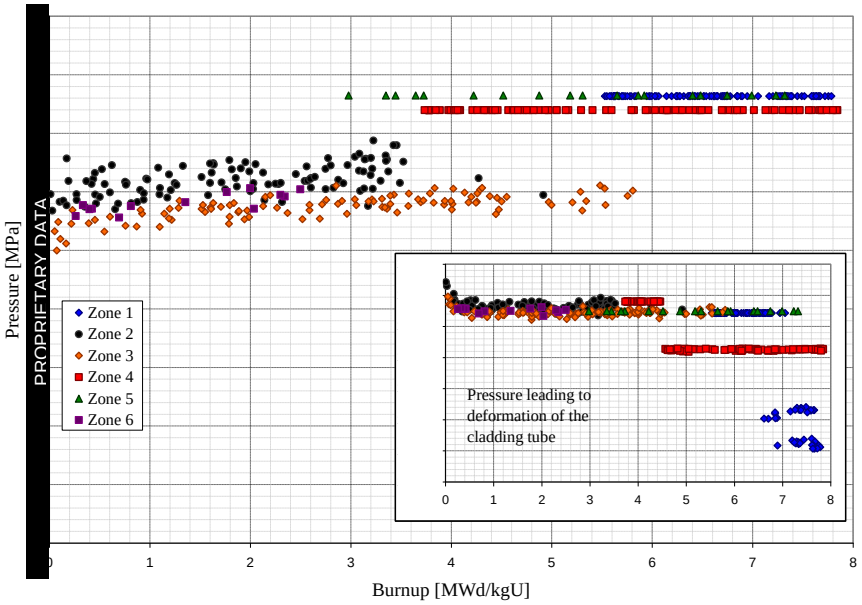

Fig. B. 16 – Fuel safety criteria 8: Maximum pressure difference between the rod internal gas pressure and the external coolant pressure, calculated data and plastic instability limit.

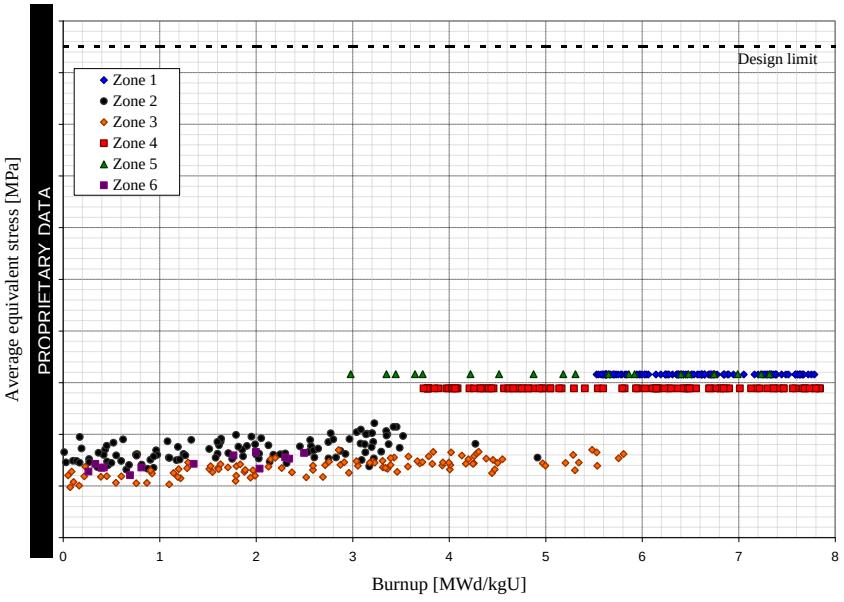

Fig. B. 17 – Fuel safety criteria 9: Maximum average equivalent stress, calculated data and design limit.

APPENDIX C. INVESTIGATION OF FGR DURING POWER RAMPS: BWR INTER-RAMP AND PWR SUPER-RAMP

The fuel matrix and the cladding constitute the first barrier against radioactive fission product release. Therefore a defense in depth concept requires also the comprehensive understanding of fuel rod behavior and accurate prediction of the lifetime in normal operation and in accident condition as well.

Investigations of fuel behavior are carried out in close connection with experimental research operation feedback and computational analyses. In this connection, OECD NEA sets up the “public domain database on nuclear fuel performance experiments for the purpose of code development and validation – International Fuel Performance Experiments (IFPE) database”, with the aim of providing a comprehensive and well-qualified database on UO2 fuel with Zircaloy cladding for model development and code validation.

This paper describes the application of the TRANSURANUS code against power ramp tests executed in the research reactor R2 at Studsvik, Sweden. The datasets are part of the International Fuel Performance Experiments (IFPE) database.

The experiments address the behavior of standard-type BWR and PWR fuel rods, including preceding base irradiation, during the over-power ramping. The burnup values range between 10 and 45 MWd/kgU. Pre-, during-, and post- irradiation, non destructive and destructive examinations were executed, in order to determine and understand the behavior of the fuel rods, but also to provide suitable data, useful for code validation.

The experimental data were used for assessing the TRANSURANUS capabilities in predicting the fission gas release (FGR). Focus is given on the prediction of the different FGR model options available in the code.

The objective of the activity has been fulfilled developing input decks suitable for the assessment of TRANSURANUS code version “v1m1j08”. The assessment is focused on fission gas release models available in TRANSURANUS code, with particular emphasis to the new “Transient Fission Gas Release Model (TFGR)” which is implemented for taking into account the events of rapid power variations.

C.1 Introduction

TRANSURANUS is a computer program for the thermal and mechanical analysis of fuel rods in nuclear reactors (*Lassmann 2009, Van Uffelen 2006, Lassmann 1992*). The TRANSURANUS code consists of a clearly defined mechanical–mathematical framework into which physical models can easily be incorporated. The mechanical–mathematical concept consists of a superposition of a one-dimensional radial and axial description (the so called quasi two-dimensional or 1½-D model). The code was specifically designed for the analysis of a single cylindrical rod.

In the current paper, the application of the TRANSURANUS code to the Studsvik BWR Inter-Ramp (*Mogard 1979*) and PWR Super-Ramp (*Djurle 1984*) Projects are presented. The activity has been performed in the framework of an agreement between JRC-ITU and the University of Pisa and also of the IAEA FUMEX III project.

The objective of the activity is the assessment of the fission gas release model of TRANSURANUS code verison“v1m1j08”, against the above mentioned databases. It constitutes an independent verification of a new model that was implemented at ITU for dealing with release during rapid power changes (*Van Uffelen 2008*).

The dataset of the BWR Inter-Ramp and PWR Super-Ramp Projects are part of the International Fuel Performance Experiments (IFPE) database (*Chantoin 1997*). The first addresses the behavior of twenty standard-type unpressurised BWR fuel rods, including preceding base irradiation, during the over-power ramping. Two different values of base irradiations burnup were adopted for the experimental database: about 10 and 20 MWd/kgU. The latter addresses the behavior of twenty-eight light water reactor fuel rods when subject to power ramps (twenty-six are modeled for the current activity), after base irradiation to high burnup (28 to 45 MWd/kgU).

Pre-, during-, and post- irradiation, non destructive and destructive examinations were executed, in order to determine and understand the behavior of the fuel rods, but also to provide suitable data, useful for code validation.

The experimental data were used for assessing the TRANSURANUS capabilities in predicting the fission gas release. Focus is given on the prediction of the different FGR model options available in the code. The objective of the activity has been fulfilled developing forty-six input decks suitable for the assessment of TRANSURANUS code version “v1m1j08” (*Adorni 2008, Adorni 2009*). The assessment is focused on fission gas release models available in TRANSURANUS code version “v1m1j08”, with particular emphasis to the new “TFGR model” which is implemented for taking into account the events of rapid power variations. The current paper reports the main outcome of the assessment of the calculations. Conclusive remarks of the activity are provided in the last section.

C.2 Description of the BWR Inter-Ramp Experiment

Between July 1, 1975 to July 1, 1979, 20 standard-type unpressurized BWR fuel rods were irradiated and power ramped in the R2 research reactor of Studsvik (Sweden). Individual fuel rod power histories were recorded in great detail, non-destructive and selectively detailed destructive examinations were also made in order to determine the fuel rod changes.

The objectives of the BWR-Inter-Ramp Project were to establish the fail-safe operating limits of 20 standard-type, unpressurized BWR fuel rods on over-power ramping at the burn-up levels of 10 and 20 MWd/kgU. This program also provided suitable data for model development and benchmarking. The over-power ramping is to be performed at a fast ramp rate of about 4 kW/m-min with the preceding base

irradiation performed to represent the conditions in a typical commercial BWR power reactor. The study also investigated:

- the influence of three main design parameters on fuel rod performance under power ramping;
- cladding heat treatment (re-crystallized anneal vs cold work plus stress relief anneal);
- pellet/cladding diametral gap size;
- fuel density;
- the failure mechanism and associated phenomena.

The long term pre-ramp irradiation of the rods was performed in the Boiling Capsule (BOCA), introduced in 1973, of the Studsvik R2 research reactor. The BOCA Inter Ramp Project (BIRP) consisted of a pressurized container containing 4 fuel rods.

The power ramp irradiation was performed in the pressurized water loops of the R2 research reactor, containing one rod. The power ramp tests were performed as follow:

- 24 hours conditioning irradiation at the same linear heat rating of the previous cycle, in order to minimize the influence of zero-power period of several weeks;
- power ramp at a constant rate of 4 kW/m-min (~65 W/m-s);
- ramp terminal level irradiation at ramp terminal power level held for 24 hours or until failure.

Eleven out of twenty tested rods failed and two non failed rods have been found to contain incipient cracks.

C.3 Description of the PWR Super-Ramp Experiment

The Studsvik Super-Ramp Project investigated the failure propensity of typical light water reactor test fuel rods when subjected to power ramps, after base irradiation to high burnup. The Project power ramped 28 individual PWR test fuel rods in a PWR subprogram, analyzed in the current paper, and 16 test fuel rods in a BWR subprogram.

The principal objective of the Super-Ramp Project was to make a substantial and valid contribution to the understanding of the pellet cladding interaction (PCI) performance under power ramp conditions for commercial type LWR reactor test fuel irradiated to high burnup. In particular, the main objectives of the PWR sub-program are here listed:

- establish through experiments the PCI failure threshold of standard design PWR test fuel rods on fast power ramping at high burnup;
- investigate whether or not a change in failure propensity or failure mode is obtained as compared to the failure behavior at lower burnup levels;
- establish the possible increase in PCI failure power levels for candidate PCI remedy design fuel rods at selected burnup levels.

Kraftwert Union AG/Combustion Engineering (KWU/CE) provided 19 fuel rods, which has been irradiated in the power reactor at Obrigheim (Germany). Westinghouse (W) provided 9 fuel rods following the base irradiation in the BR-3 reactor at Mol (Belgium).

The main features of the rods are here outlined:

Kraftwert Union AG type rods, UO2 pellet column length of about 310 mm:

- PK1: 5 standard "A" rods, average axial peak position burnup between 33 and 36 MWd/kgU;
- PK2: 5 standard "A" rods, average axial peak position burnup between 41 and 45 MWd/kgU;
- PK4: 4 standard "A" rods plus Gd2O3 (4%), average axial peak position burnup between 33 and 34 MWd/kgU;
- PK6: 5 remedy "G" rods, large grain, average axial peak position burnup between 34 and 37 MWd/kgU;

Westinghouse type rods UO2 pellet column length of about 1136 mm:

- PW3: 5 standard rods rods, average axial peak position burnup between 28 and 31 MWd/kgU;
- PW5: 4 remedy rods, annular pellets, average axial peak position burnup between 32 and 33 MWd/kgU.

The power ramping of the experimental fuel rods were performed in the R2 reactor in the pressurized loop No 1 with forced circulation cooling simulating PWR coolant temperature and pressure conditions.

The power ramp tests were performed as follow5:

- conditioning phase, with a rather slow increase of linear heat rating from an initial value to 25 kW/m (conditioning level) and 24 hours holding time at this value;
- power ramp at a constant rate of 10 kW/m-min (~165 W/m-s) to a pre-selected ramp terminal level;
- holding phase at ramp terminal level held for about 12 hours or until failure.

Nine out of twenty-eight tested rods failed.

C.4 Fission Gas Release Options

The recommended URGAS algorithm with the (thermal) diffusion coefficient of Hj. Matzke (*Matzke 1980*) and a constant athermal diffusion coefficient has been chosen for all the calculations. This option is used together with an intragranular fission gas release model.

The reference calculations are performed selecting the input parameter for the grain boundary fission gas behavior that activates the "TFGR model", identified as option (C), Tab. C. 1. The model has been newly implemented in TRANSURANUS code to consider the additional release that can be observed in the event of rapid

power variations. This model consists of two contributions: microcracking in case of power increase or reduction, and gas transport from the grain to the grain boundaries. The entire fission gas inventory stored at the grain boundaries is instantaneously released if transient conditions are met. This model should be invoked in case of power ramps. No values of the saturation limit for grain boundary gas input parameter is needed.

The “TRANSURANUS standard” option for code version “v1m1j07”, and available also in code version “v1m1j08”, is identified in the current report as option (A). This option refers to a model in which the grain boundary saturation concentration is a constant which can be set by an input variable.

The model referred to as option (B) in this report is a grain boundary fission gas behavior model similar to the previous one, in which the grain boundary saturation concentration depends on the temperature. Also in this case the grain boundary saturation concentration should be set as an input.

In the last case, option (D), the fission gas behavior at grain boundaries is not treated (i.e. the grain boundary saturation concentration is equal to zero) that should be considered as an “upper release limit”.

ID	MODEL	NOTE
(A)	TU standard	Standard option for code version “v1m1j07”. The grain boundary saturation concentration is a constant.
(B)	Simple grain boundary fission gas behavior model	The grain boundary saturation concentration depends on the temperature.
(C)	TFGR model	Model option to be invoked during power ramps
(D)	FGR at grain boundary is not treated	“Upper release limit”

Tab. C. 1 – FGR at grain boundary options.

C.5 Boundary Conditions

The boundary conditions implemented for the analysis are listed below:

- linear heat rate at four axial positions;
- cladding temperature histories at 4 axial positions;
- fast flux;
- pressure.

Outline of the maximum ramp rate, linear heat rate at ramp terminal level (RTL) and hold time at RTL are summarized in Tab. C. 2and Tab. C. 3 for the BWR Inter-Ramp and PWR Super-Ramp respectively.

Linear heat rate and temperatures are those at the given time which have been constant over the interval time step, ie. the data are in histogram format. The rate

of increase/decrease between different constant linear heat rate spans has been selected as 6 kW/m-h (Fig. C. 1 (a) and (b) for the BWR Inter-Ramp and PWR Super-Ramp respectively). Inclination between two values of constant linear heat rate is calculated on the basis only of the peak linear heat rate position. In case of a time step that is too small to apply the above mentioned method, the measured slope of the database is maintained.

The power ramp has been "constructed" according to original ASCII files together with data available from tables, i.e. considering the original files using the selected "6 kW/m-h" except for the ramp in which the rate has been taken directly from the tables.

Hold time at ramp terminal level is modeled according to the LHR histories from ASCII files, see Fig. C. 2 (a) and (b) for the BWR Inter-Ramp and PWR Super-Ramp respectively. The coolant is not considered in the calculations since cladding temperature histories were provided from ASCII files.

BIRP No	Rod No	Rod Label	F/NF	Max Ramp Rate [kW/m-h]	LHR at RTL [kW/m]	Hold time at RTL [min]
1	1	LR1		288*	43.80	1440
	2	LR2		252	45.7	1440^{12} (84^{4})
	3	LR3		234	50.1	103
	4	LR4		234	65.4	5
3	5	LR5		306	42.7	1440
	6	LS1		324	48.2	1440^{12} (35^{4})
	7	LS2		234	43.8	1440
	8	TR1		252	42.2	1440
5	9	LS3		234	41.8	1440
	10	LS4		252**	50.7	92
	11	TS1		252	47.3	319
	12	DR1		270	43.2	1440
2	13	HR2		270	38.0	1440
	14	HR3		234	43.2	316
	15	HR4		252	46.1	1440
	16	HR5		252	47.9	1440
4	17	HS1		234	47.8	26
	18	HS2		234	41.0	59^{12} (1440^{4})
	19	HS3		252	44.9	59
	20	BR1		234	51.0	1440

* Pause of 2 minutes at 32 kW/m

** From 29.6 kW/m with a rate of 0.28 kW/m-s to 40.8 kW/m

Tab. C. 2 – BWR-Inter-Ramp experiments, maximum ramp rate and linear heat rate.

BIRP No	Rod No	F/NF	Max Ramp Rate [kW/m-h]	LHR at RTL [kW/m]	Hold time at RTL [min]
PK1	1	NF	540	41.5	720
	2	NF	480	44.0	720
	3	NF	510	47.5	720
	4	NF	570	47.5	720
	S	NF	360	42.0	720
PK2	1	NF	510	41.0	720
	2	NF	570	46.0	720
	3	NF	510	49.0	720
	4	NF	510	44.0	1[$]
	S	NF	510	44.0	720
PK4	1	NF	480	39.0	720
	2	NF	510	44.5	720
	3	NF	660	50.5	720
	S	NF	510	43.0	720
PK6	1	F	540	45.0	55
	2	NF	540	40.0	720
	3	NF	540	43.0	720
	4	F	600	44.0	60
	S	NF	600	41.0	720
PW3	1	F	600	40.0	22
	2	NF	600	35.3	720
	3	NF	600	37.2	720
	4	F	570	37.7	12
	S	F	600	40.5	17
PW5	1	F	540	42.7	118
	2	F	540	40.3	26
	3	F	540	38.2	38
	4	F	510	38.0	72

[$] Intentionally interrupted

Tab. C. 3 – PWR-Super-Ramp experiments, maximum ramp rate and linear heat rate.

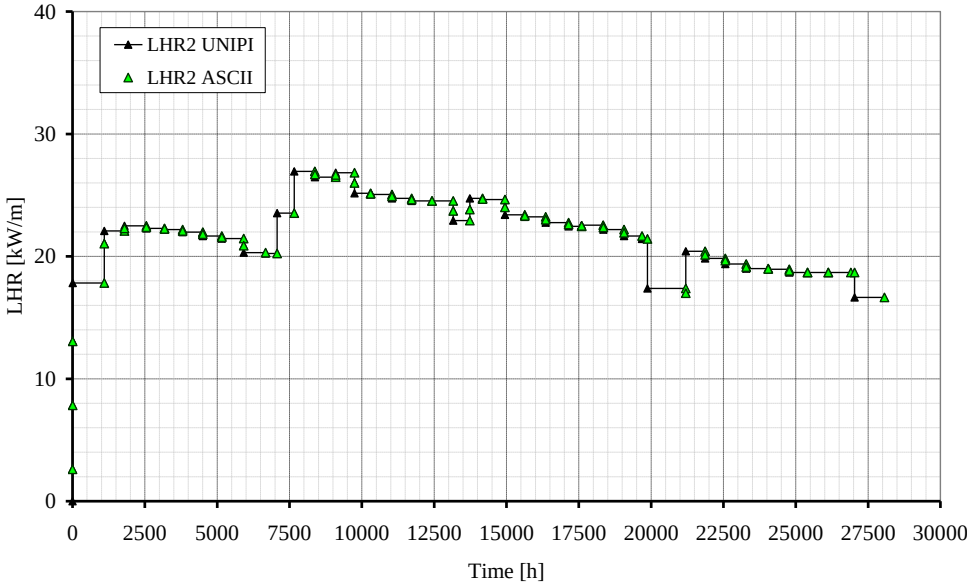

(a) BWR Inter-Ramp Rod LR1 slice 2

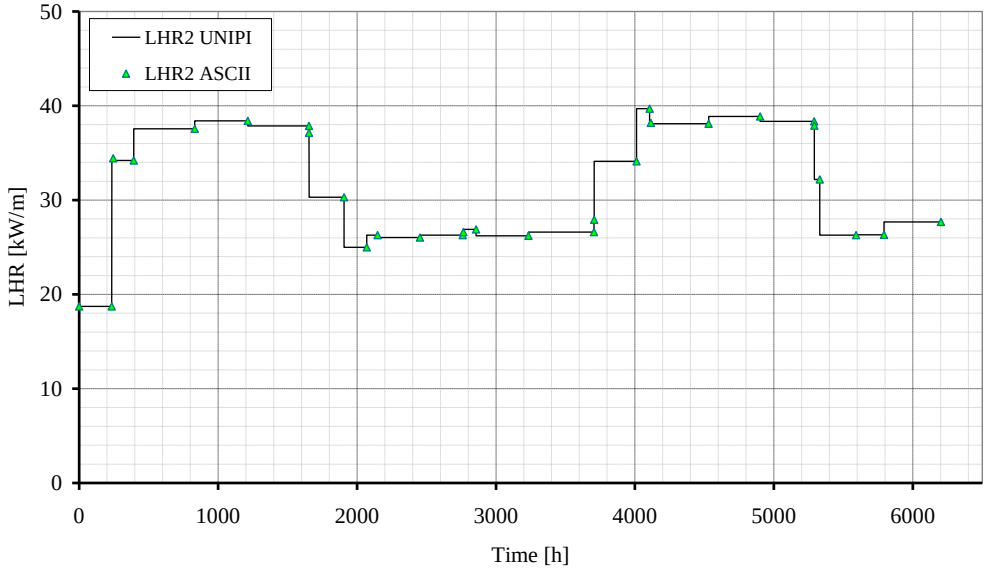

(b) PWR Super-Ramp Rod PK23 slice 2

Fig. C. 1 – Base irradiation: implemented TU LHR history.

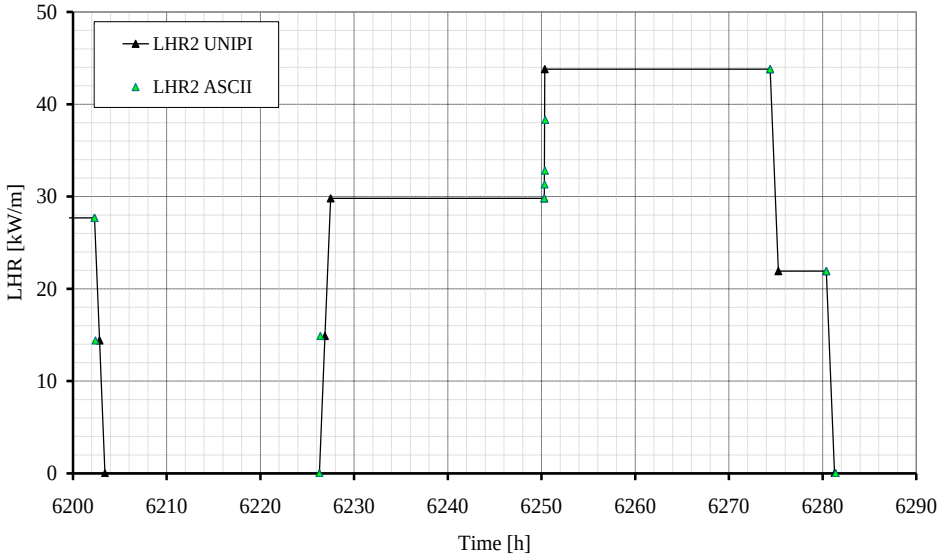

(a) BWR Inter-Ramp Rod LR1 slice 2

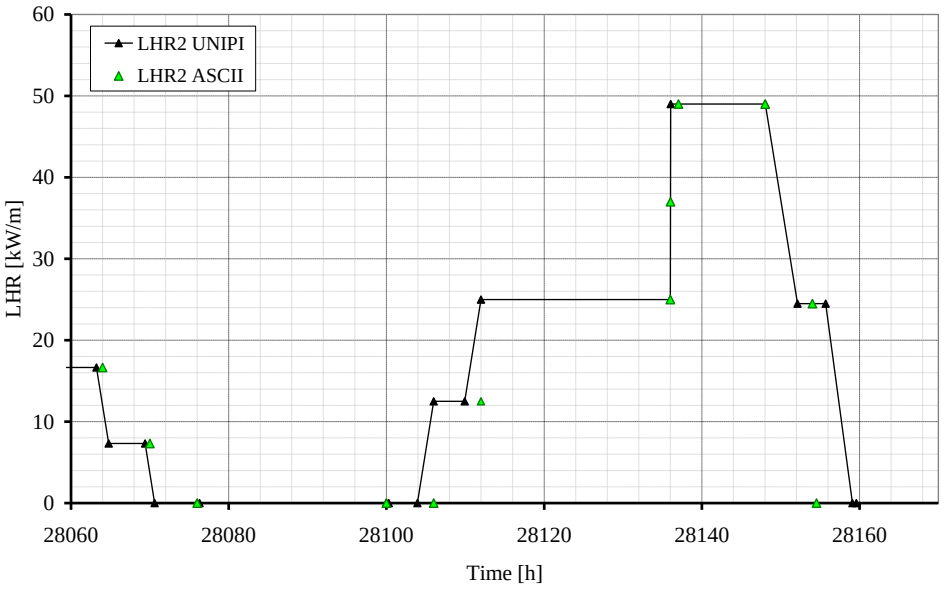

(b) PWR Super-Ramp Rod PK23 slice

Fig. C. 2 – Power ramp: Implemented TU LHR history.

C.6 Assessment of the TU Code

In the following sections, results from analysis with the TRANSURANUS code version “v1m1j08” are presented. Then the FGR results of the two code versions are compared for base irradiation and power ramps.

C.7 Reference Case Results

With reference to Tab. C. 1, the option (C) (“TFGR model” for fission gas release at grain boundary) has been assumed as reference case for the current paper. However, the results of the post test calculations are reported together (and compared) with the analysis performed using the other three options available in TRANSURANUS code of fission gas release at grain boundary, option A, B and D of the same table.

In the following the results of FGR are discussed separately for the BWR Inter-Ramp and PWR Super-Ramp Projects.

Two figures are reported in order to summarize the outcomes of both experiments:

- Fig. C. 3 reports the comparison between experimental measures and calculated results for both cases. This figure highlights the accuracy of the code results, evidencing the -50%+100% error.
- Fig. C. 4 shows fission gas released (FGR) calculated with TRANSURANUS code options (C) and measured for both the databases, as a function of the ramp terminal level.

C.8 BWR Inter-Ramp: Fission Gas Released

The experimental data of the FGR are measured during the PIE for 11 rods. Among them, nine were found non-failed and two (labeled HS1 and BR1 belonging to BIRP4) failed during the PIE. The evaluation of the FGR has been executed using two different methods based on the percentage of Kr and Xe, respectively.

The comparison between experimental measures and calculated results is summarized in Fig. C. 3 (a) for PIE using Kr%. This figure highlights the accuracy of the code results, evidencing the -50%+100% error. Rod labels are reported with different colors, that represents different BIRP numbers.

Fig. C. 4 (a) shows FGR calculated with TRANSURANUS code options (A) and (C) and measured with Kr%, as a function of the ramp terminal level. Higher values of FGR correspond to higher values of linear heat rate.

Calculations performed using option A and option B show very similar predictions in all the simulations, values above about 5.5% using these two options seem to be better predicted than lower ones. The “TFGR model” (option C, reference case) overestimates systematically the fission gas release for all cases except for rod No 12 DR1.

Evolution of linear heat rate for the hottest axial fuel slice and calculated fission gas release time trend for different TRANSURANUS model options is reported for the case of rod 16 in Fig. C. 5 (a), focusing on power ramp. For the sake of clarity, in the same figure the linear heat rate history is reported as well. In the figure the calculated data for the end of the base irradiation and the power ramp from FRAPCON-3 are also reported, taken from. The complete set of FGR time trends is reported in (*Lanning 1997*). FGR time trend figures show that, considering the reference case (option C), a noticeable increment of fission gas release during the ramp and hold time at ramp terminal level is observed in all the cases. Moreover, the comparison with the experimental data shows a systematic overestimation of FGR (all cases except rod No 12 DR1).

The different behavior of rod DR1 may stem from a low density of the fuel compared to the other rods, leading to a large open porosity fraction. It should be mentioned that the open porosity is not directly taken into account in the fission gas release model of TRANSURANUS code. Finally, in all the cases, as expected, the upper release limit overestimates the release of fission gas.

In summary:

- The two options A and B, which differ for the grain boundary saturation concentration modeling, constant in the first case and a function of the temperature the latter, exhibit negligible differences in the FGR predictions.
- Comparisons (on two rods) between TRANSURANUS and FRAPCON-3 codes reveal analogous results during base irradiation, as well as during power ramp. Considering the different FGR models applied in the TRANSURANUS simulations, the better results were obtained with the options A and B (only one result is reported in the current paper).
- The “TFGR model” (option C, reference case) overestimates systematically, the fission gas release due to the complete and immediate release of the FGR at the grain boundary at the power ramps occurrence.
- The upper release limit model (option D), overestimates systematically the final fission gas released - the grain boundary saturation concentration is set to 0.

C.9 PWR Super-Ramp: FGR

Fission gas analysis was performed on all non-failed rods except PK1/S. The fission gas release values are based on the fraction released of the total fission gas present into the fuel rods. The two non-failed Westinghouse rods are not modeled for the current analysis.

The comparison between experimental measures and calculated results is summarized in Fig. C. 3 (b). This figure highlights the accuracy of the code results, evidencing the -50%+100% error.

Fig. C. 4 (b) shows FGR calculated with TRANSURANUS code options (A) and (C) and measured, as a function of the ramp terminal level. Calculations performed using option A and option B show very similar predictions in all the simulations. These options underestimate systematically the FGR in all cases but rods PK1/4

and PK2/S. The “TFGR model” (option C, reference case) improve the prediction providing higher values of FGR.

Evolution of linear heat rate for the hottest axial fuel slice and calculated fission gas release time trend for different TRANSURANUS model options is reported for the case of rod PK2/3 in Fig. C. 5 (b), focusing on power ramp. For the sake of clarity, in the same figure the linear heat rate history is reported as well.

Finally, the upper release limit case, option D, exhibits a very similar behavior of the option C, reference case. In summary:

- The two options A and B, which differ for the grain boundary saturation concentration modeling, constant in the first case and a function of the temperature the latter, exhibit negligible differences in the FGR predictions. The results with both options underestimate systematically the FGR (all cases but two).
- The TFGR fission gas release model (option C, reference case):
  - overestimates the FGR in 4 out of 16 cases;
  - good agreement for 2 out of 16 rods;
  - underestimates the FGR all the remaining 10 out of 16 rods.
- The upper release limit model (option D) exhibits a very similar behavior compared to the reference case.

C.10 Conclusions

The experimental data of twenty fuel rods irradiated in the BWR Inter-Ramp and twenty-six out of twenty-eight rods irradiated in the PWR Super-Ramp Projects have been compared with the simulations performed by TRANSURANUS code version “v1m1j08”. The activity is carried out in order to assess the performance of the new fission gas release model, “TFGR model”, implemented in the last version of the code, in predicting the fission gas release during power ramps. The reference calculations have been executed using this “TFGR model” (IGRBDM 3) of fission gas release at grain boundary.

The analyses performed allow stating the following conclusions.

- BWR Inter-Ramp (option A) exhibits the best prediction at high FGR values (above about 5.5%).
- BWR Inter-Ramp (option A):
  - underestimates FGR for low values of ramp terminal level;
  - overestimates higher FGR at higher values of ramp terminal level.
- BWR Inter-Ramp FGR calculated by (option C) overestimates systematically the FGR.

- PWR Super-Ramp (option A) underestimates systematically the experimental data in all cases but two (rods PK1/4 and PK2/S).
- PWR Super-Ramp (option C) underestimates the FGR for 10 out of 16 rods.

The activity presented in this paper represents an extension of the independent assessment of the FGR models carried out on the TRANSURANUS code. On the

one hand the current simulations of the BWR rods in the Inter-Ramp project, indicate that the new "TFGR model" generally overestimates the FGR measured at end-of-life, whereas a different trend is evidenced by the PWR Super-Ramp Project simulations: underestimation of FGR. On the basis of these results it seems therefore necessary to refine the model for ramp release. More precisely, one might consider only a partial venting of the grain boundary inventory during rapid power variations, rather than a total release as currently implemented. Nevertheless, this will require more experimental data to be analyzed.

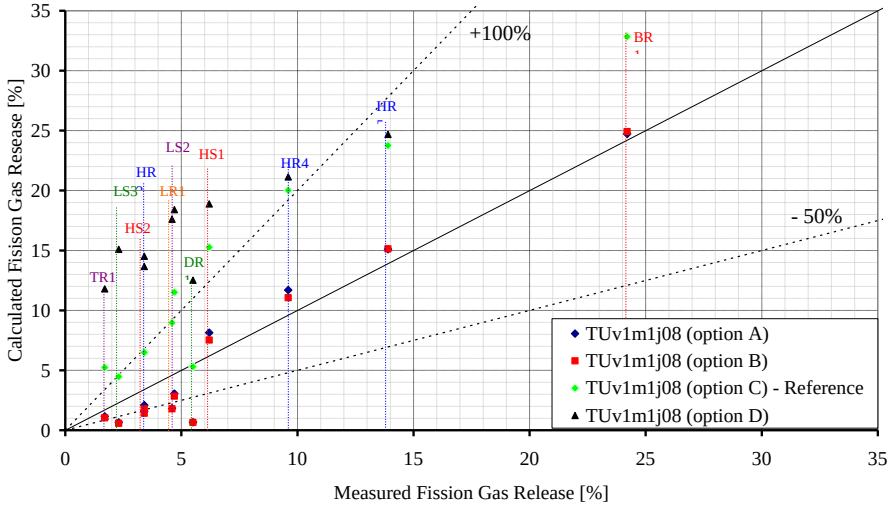

(a) BWR Inter-Ramp (Kr%)

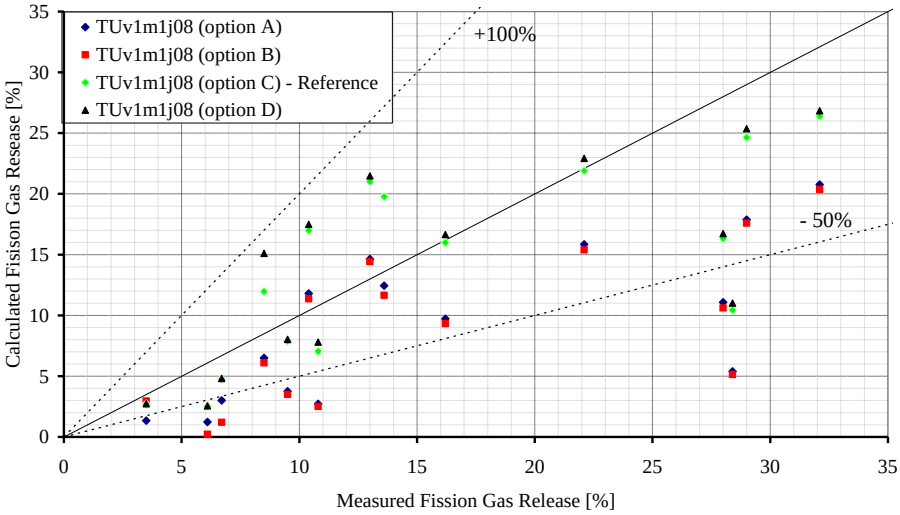

(b) PWR Super-Ramp Rod (Kr+Xe%)

Fig. C. 3 – Summary of PIE and calculated values (options A, B, C and D) at the end of the experiments: Fission Gas Released.

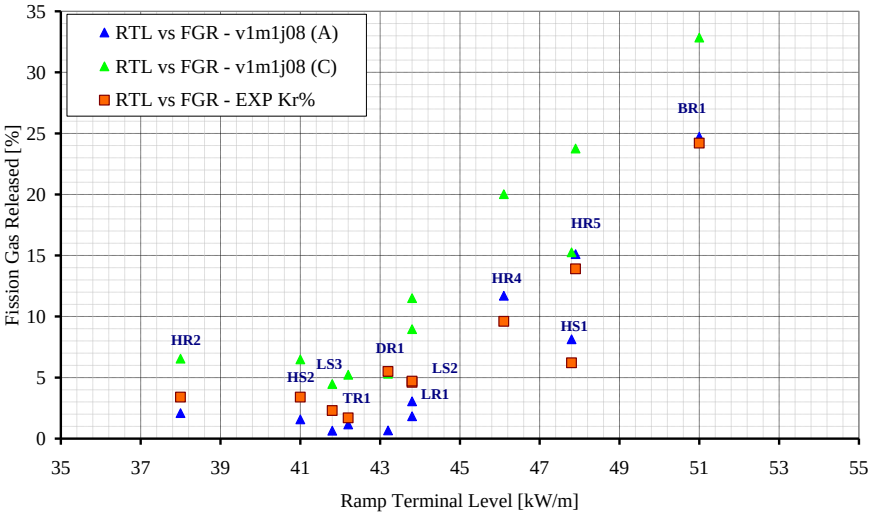

(a) BWR Inter-Ramp (Kr%)

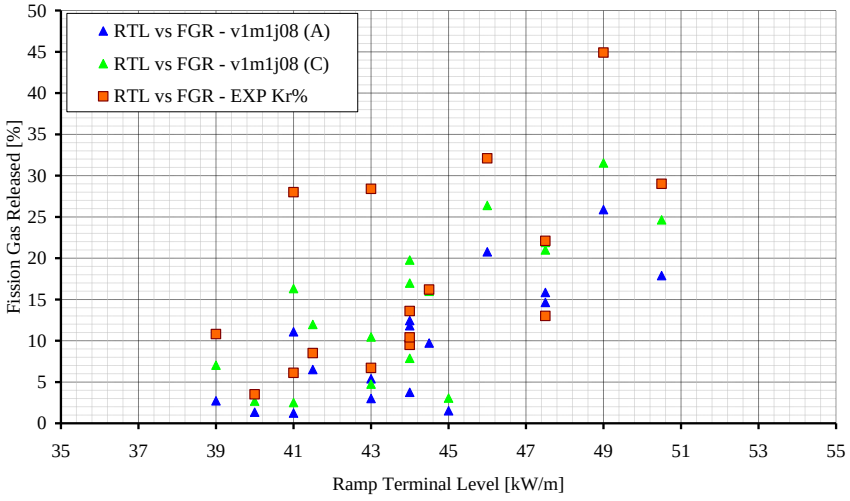

(b) PWR Super-Ramp Rod (Kr+Xe%)

Fig. C. 4 – Calculated reference case: Ramp Terminal Level vs Fission Gas Released measured Kr% and calculated.

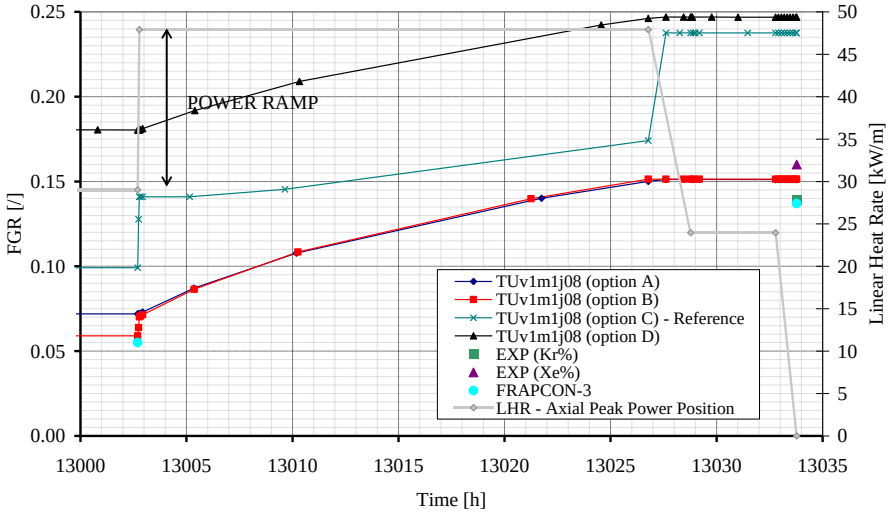

(a) BWR Inter-Ramp Rod #16 BIRP2 HR5

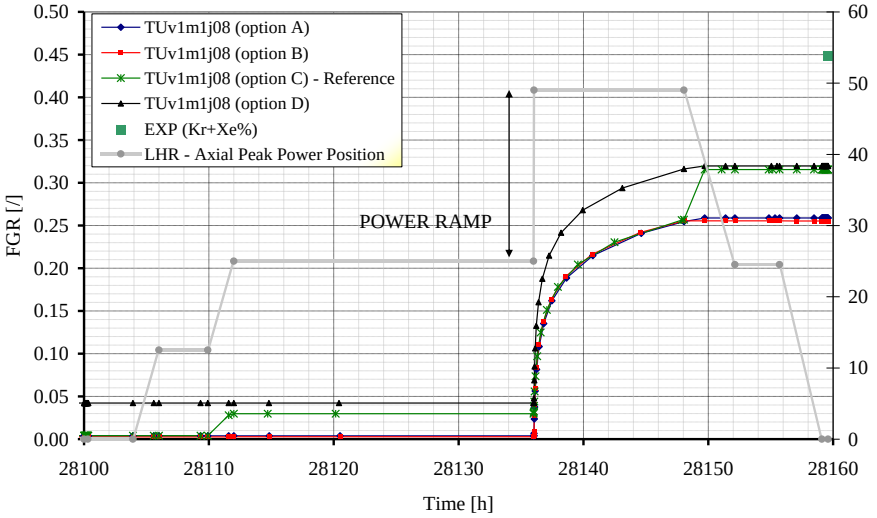

(b) PWR Super-Ramp Rod PK2/3

Fig. C. 5 – Calculated time trends of Fission Gas Released (options A, B, C and D), experimental data, Linear Heat Rate: zoom on ramp.

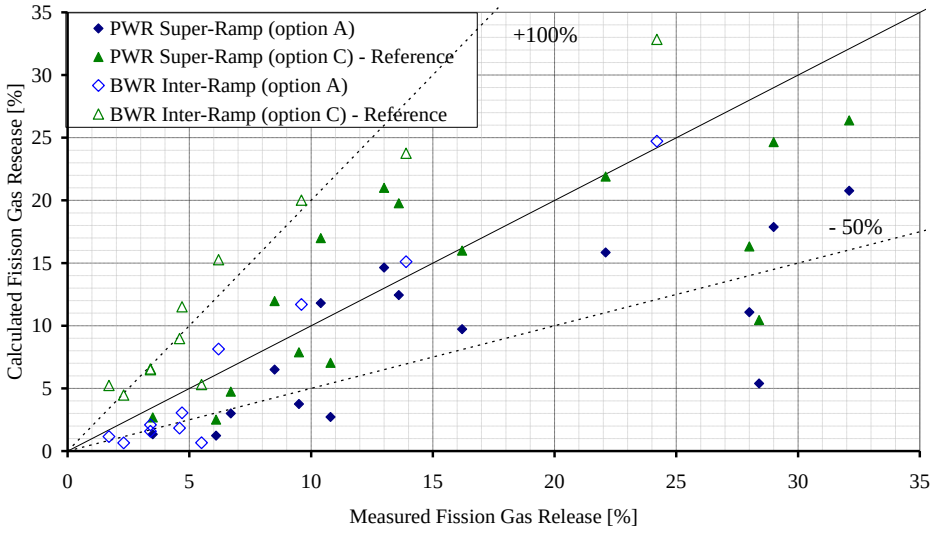

Fig. C. 6 – Summary of measured and calculated Fission Gas Released: BWR Inter-Ramp and PWR Super-Ramp Project.

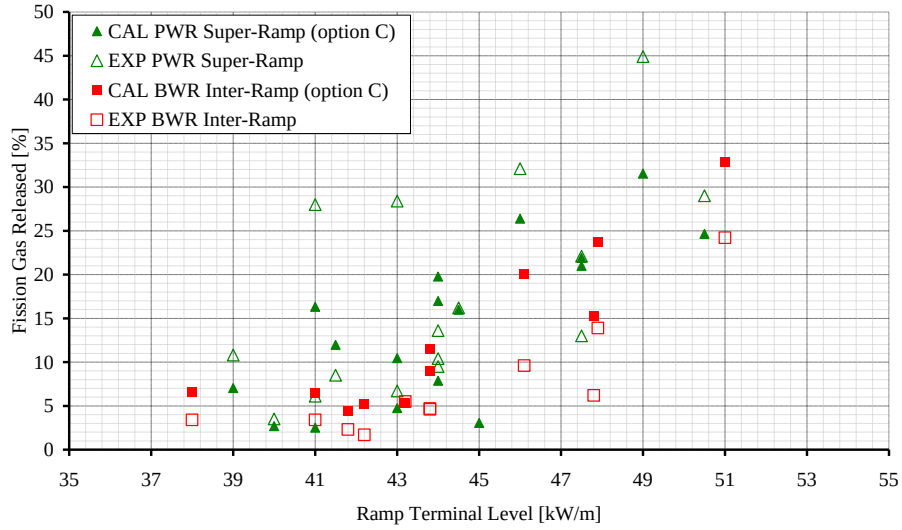

Fig. C. 7 – Summary of measured and calculated Fission Gas Released vs Ramp Terminal Level: BWR Inter-Ramp and PWR Super-Ramp Project

APPENDIX D. MODELING OF LB-LOCA: MT-4 MT-6A TESTS

The fuel matrix and the cladding constitute the first barrier against radioactive fission product release. Therefore a defense in depth concept requires also the comprehensive understanding of fuel rod behavior and accurate prediction of the lifetime in normal operation and in accident condition as well.

Investigations of fuel behavior are carried out in close connection with experimental research, operation feedback and computational analyses. In this connection, OECD/NEA sets up the “public domain database on nuclear fuel performance experiments for the purpose of code development and validation – International Fuel Performance Experiments (IFPE) database”. This database includes the data set of the projects MT-4 and MT-6A analyzed in the current paper. The objectives of these projects included: 1) providing sufficient time in the α-Zircaloy ballooning window to allow the pressurized test rods to rupture before reflood cooling was introduced, 2) obtaining data to determine heat transfer coefficients for ballooned and ruptured rods, and 3) measuring rod internal gas pressure during rod deformation. Other outcomes of the experiments are: a) evaluating expansion characteristics of a bundle in which all fuel rods expand and rod-to-rod interaction can occur; and b) provide data on the rate of cooling for a bundle where all rods have expanded and ruptured.

The MT-4 test bundle simulated a 6x6 section of a 17x17 3% enriched, full-length non-irradiated PWR fuel assembly. There were 20 non-pressurized guard fuel rods to isolate the 12 central, pressurized tests rods; the four corner rods were deleted. In the MT-6A test, the 20 guard rods used in the previous tests were replaced with 9 pressurized thus, a total of 21 test rods were in MT-6A. Only limited destructive post irradiation examination was performed on these two tests.

The analyses performed address the behavior of two equivalent full lengths fuel rods, one for each test. The experimental data are used for assessing the TU capabilities in predicting phenomena related to LOCA and the fuel failure. The activity has been performed in the framework of an agreement between JRC-ITU and the University of Pisa.

The objective of the activity is the validation of TRANSURANUS “v1m1j09” code in predicting fuel and cladding behavior under LOCA conditions using the experimental databases MT-4 and MT-6A. It is pursued assessing the capabilities of the code models in simulating the phenomena and parameters involved, such as: pressure trend in the fuel rod, cladding creep, α to β-phase phase transformation, oxidation, geometry changes and finally failure prediction. The analysis is aimed at having a comprehensive understanding of the applicability and limitations of the code in the conditions of the experiments. Finally, probabilistic calculations are performed to compete the analysis.

D.1 Introduction

When a LB-LOCA occurs, the fissions quickly cease due to loss of moderator and insertion of control rods. The radial temperature profile changes from a typical

parabolic shape (normal operating conditions) towards a roughly flat profile after SCRAM. The flashing of the coolant in the core, due to system depressurization, causes critical heat flux condition on the cladding and the cladding starts to heat up. During the cladding heat-up, the pressure in the gap increases. The gap contains a mixture of fill gas and fission gases. In these conditions, the strength of the cladding is reduced and the cladding may undergo plastic deformations and creep *(OECD 2009).*

Analytical modeling and interpretations of experiments is complex. First of all, the zirconium alloys generally are very anisotropic when they are in the hexagonal alpha phase condition. In addition to this, the phase transformation takes place at temperatures around 800 ˚C and above. At this temperature range, when zirconium alloy starts to transform to the beta phase, the oxidation rate increases and becomes relevant. However, the main source of embrittlement is not the oxidation, but the absorption of oxygen. Another important effect of oxidation is that it strengthens the cladding so that the creep rate slows down in cases where the cladding tubes have not yet ruptured.

About the fuel, during normal operation, it cracks so that a pellet is actually a conglomerate of several mm-sized fragments. If the cladding balloons, there is a possibility that these fragments move and fill the additional space in a balloon. Changes of temperature and geometry may impair the core coolability.

A LB-LOCA is characterized by a global temperature increase in the core of the reactor, which is later terminated by a cool down phase. In literature, three phases are identified from the initiating event up to the complete cooldown of the core: blowdown refill and reflood. During these phases, temperature gradients may imply the bending of fuel bundles and thermal stresses due to differences in thermal expansion (e.g. control rod guide tubes and fuel rods). Impaired coolability could result from plastic deformation of the cladding, leading to constriction of the sub-channels between rods, or from fragmentation of the cladding through oxidation and embrittlement.

D.2 TRANSURANUS overview

TRANSURANUS is a computer program for the thermal and mechanical analysis of fuel rods in nuclear reactors *(Lassmann 1992, Lassmann 2009, Van Uffelen 2006, Van Uffelen 2008)*. The TRANSURANUS code consists of a clearly defined mechanical–mathematical framework into which physical models can easily be incorporated. The mechanical–mathematical concept consists of a superposition of a one-dimensional radial and axial description (the so called quasi two-dimensional or 1½-D model). The code was specifically designed for the analysis of a single cylindrical rod.

On the basis of the defined boundary conditions the code calculates the temperature distribution and the fission gas release inside the fuel rod, the corresponding inner pressure, the ZrO2 thickness growth, the equivalent oxidation and the plastic deformation of the cladding. Fuel rod burst is checked through appropriate failure criteria.

TRANSURANUS code can also be applied in design basis accident (DBA) analyses, including LOCA and RIA, to complement system level simulations and to verify the fuel-specific safety acceptance criteria on the basis of detailed thermo-mechanical computations.

The LOCA-specific models available in the code are validated up to value of cladding temperature equal to 1200 °C.

D.3 TU LOCA specific failure criteria

Three different failure criteria are available in TRANSURANUS code, specific for LOCA conditions *(Lassmann 1992, Lassmann 2009, Van Uffelen 2008, Erbacher 1982, Gyory 2008, OECD 2000).*

The first cladding failure criterion is based on stress assessment, i.e. the comparison of the calculated tangential stress with a distinct failure threshold ("overstress criterion"). The failure threshold of the cladding alloy is defined as a function of the actual temperature and oxidation level in the material property function.

The second failure principle is a simple "plastic instability criterion" based on the simultaneous assessment of the effective true strain and the strain rate. When both the strain and the strain rate exceed the threshold values of 0.02 and 100 1/h, respectively, the cladding is assumed to be ruptured. This criterion is applied concurrently to an "overstrain criterion" (third out of three criteria) i.e. if plastic instability is not indicated then the overstrain criterion is checked automatically. This criterion limits the true tangential plastic strain to the maximum of 50%. These criteria were introduced particularly for LOCA analyses, due to the significant uncertainty of the stress computation at large cladding deformation.

D.4 Description of the experiments

The U.S. Nuclear Regulatory Commission (NRC) conducted a series of thermal-hydraulic and cladding mechanical deformation tests in the National Research Universal (NRU) reactor at the Chalk River National Laboratory in Canada. The objective of these tests was to perform loss-of-coolant-accident (LOCA) experiments using full-length light-water reactor fuel rods to study mechanical deformation, flow blockage, and coolability. Three phases of a LOCA (i.e. heat-up, reflood, and quench) were invstigateed in situ using nuclear fissioning to simulate the low-level decay power during a LOCA after shutdown. All tests used PWR-type, nonirradiated fuel rods.

The test rods for the LOCA cases in NRU reactor were irradiated in flowing steam prior to the transient, stagnant steam during the transient and prior to reflood, and then reflood conditions to complete the transient. Both cladding inner surface and outer surface temperatures were measured, in addition to coolant temperatures. However, only cladding inner surface temperatures were generally presented in the reports of the tests *(Cunningam 2001, Wilson 1983, Wilson 1993).*

After the experiments, the test train was dismantled and cladding rupture sites were determined and fuel rod profilometry was performed in the spent fuel pool. Only limited destructive post-irradiation examinations were carried out on these two tests.

D.4.1 Design and objectives: MT-4 test

The MT-4 test bundle simulated a 6x6 section of a 17x17 PWR fuel assembly. There were 20 non-pressurized guard fuel rods to isolate the 12 central, pressurized tests rods; the four corner rods were deleted. The 12 test rods were fresh rods while the 20 guard rods had been used in previous tests. The analysis addresses the behavior of only one equivalent fuel rod.

The primary objectives of the MT-4 test, *(Cunningam 2001, Wilson 1983)* included:

- providing sufficient time in the α-Zircaloy ballooning window of 760 to 927 °C to allow the 12 pressurized test rods to rupture before reflood cooling was introduced,
- obtaining data to determine heat transfer coefficients for ballooned and ruptured rods, and
- measuring rod internal gas pressure during rod deformation.

D.4.2 Design and objectives: MT-6A test

A principal difference between the MT-6A and the MT-4 tests was a redesign of the test train to reduce cladding circumferential temperature gradients and thus induce greater amounts of cladding ballooning and flow blockage *(Cunningam 2001, Wilson 1993)*. In addition, the 20 guard rods used in the previous tests were replaced with nine pressurized rods that had been used in a previous test. Thus, a total of 21 test rods were in MT-6A. Also in this case a only fuel rod is modeled.

A malfunction of the computer controlling the test occurred during the test. As a result of this malfunction, system pressure during the transient heat-up was not at 0.28 MPa but was at 1.72 MPa. In addition, the desired temperature control was not achieved.

This test was intended to provide the fuel cladding sufficient time in the α -Zircaloy temperature region (777-867°C to maximize expansion and to cause the fuel rods to rupture before they were cooled by reflooding. Other objectives included:

- evaluating expansion characteristics of a bundle in which all fuel rods expand and rod-to-rod interaction can occur; and
- provide data on the rate of cooling for a bundle where all rods have expanded and ruptured.

The MT-4 and MT-6A rods were tested at zero burnup, therefore, as-built dimensions are assumed to apply (i.e. no fuel densification/swelling, no cladding creepdown).

D.4.3 Experimental/Operating Conditions

For both MT-4 and MT-6A, the initial condition was flowing steam with the transient beginning when the steam was shutoff and a stagnant condition introduced.

A preconditioning phase for the non-irradiated test rods was conducted for MT-4 with water cooling at a pressure of 8.27 MPa and a flow rate of 16.3 kg/s. Two short runs at full power were made under these conditions for permitting the crack and relocation of the fuel pellets. Three transients were run prior to the actual test for MT-4 (designated MT-4.04). These transients were for reflood calibration and assuring that the correct powers were used to obtain the desired cladding heat-up rate of approximately 8.3 °C/s.

In the desired MT-4 transient (MT-4.04), there was a short heat-up phase of approximately 1.5 min and a longer phase at temperature that lasted approximately 20 min before shutting off the steam flow. Reflood was initiated 57 s after steam flow was shutoff. The rod failures occurred from 52 to 58 s, all but one failed during the adiabatic heat-up before reflood occurred.

The MT-6A test consisted of a pre-conditioning phase, preliminary calibration tests, water and steam calorimetry tests, and then the actual transient phase.

For tests MT-4 and MT-6A, the test rods were pressurized prior the final transient. The gas pressure was measured at a manifold in the reactor hall at room temperature. This manifold was connected via a capillary line to the test rods in the reactor core. Therefore, though the pressure in the rods was as-measured, the rods were at higher temperatures in the core than the manifold in the reactor hall. Thus, the quantity of gas actually in the test rods was less than would be calculated from the design parameters and measured pressure at room temperature.

D.5 Results

In the case of the MT-4 experiment, cladding temperatures at time of failure ranged from 804 to 841 °C. Peak internal gas pressures were approximately 8.9 to 9.3 MPa (initial value of 4.62 MPa), with gas pressures at failure of approximately 5.6 to 6 5 MPa.

In the case of MT-6A experiment, gas pressures at failure of approximately 6.07 to 7.93 MPa. No post-irradiation examination data were carried out for this test.

D.5.1 TU models and cases analyzed

The activity is performed using TRANSURANUS code, version “v1m1j09”, with the deterministic and probabilistic options, thermal and mechanical analysis. The version of the manual is “v1m1j09”.

LOCA-specific models are directly selected in the base input file.

The reference input deck for MT-4 test is prepared complying with the information available in the code manual *(Lassmann 2009)*. The models selected are generally the standard ones. Only the active part of the fuel is accounted for the simulation. It is divided into 8 axial sections of different length. The UP temperature is prescribed, according to the experimental data available. For all the calculations, the nominal geometrical values are used when available, since tolerances are not specified.

The input deck of MT-6A rod differs from the MT-4 one for the:

- subdivision in 9 axial slices instead of 8 and related elevations of the slices;
- filling gas pressure and temperature; and
- boundary conditions of cladding temperatures and coolant pressure.

All runs are performed automatically though the preparation of ad-hoc programs.

D.5.2 Results of the analysis MT-4

The LOCA transient (test MT-4) starts with the fuel at steady state conditions, and at decay heat. The rods are tested at zero burnup therefore, as-built dimensions are assumed to apply (i.e. no fuel densification/swelling, no cladding creep-down), Fig. D. 1, Fig. D. 2 and Fig. D. 3.

When LOCA occurs, the initial heat-up of the cladding is mainly due to the redistribution of the heat and the stored energy of the pellet; in the long term, the decay heat is responsible for the heating of the cladding.

The initial condition of the MT-4 transient is flowing steam with the transient beginning when the steam is shut-off and a stagnant condition introduced. Reflood is initiated 67 s (57 s after steam-off). The cladding temperature is prescribed in the calculations. The steam shut-off occurs at 10s from the beginning of the transient and causes the cladding heat-up. The PCT of 875.6 °C is observed at 74 s after the BOT at 243 cm from the bottom. The corresponding axial position in the TU model is the slice number 5. The transient is terminated at 90s.

The external coolant pressure falls to a 0.28 MPa at the beginning of the transient and then remains constant. The tensile stress, which is produced in the cladding by the internal gas pressure, is sufficient to cause plastic distension. The creep strength of zirconium alloys falls rapidly with temperature so that strain rates can reach the value of 1% s-1. Furthermore, the ductility of the alloys is so high that strains of 50% or more are possible. The spacing of the test fuel rods is such that adjacent rods straining by about 33% will touch. The key question is thus whether strains of this magnitude or greater can occur in practice, in adjacent rods at the same level in the assembly *(OECD 2009)*. This issue is not addressed in the current analysis.

Sensitivity analyses were performed addressing the boundary and initial conditions.

- Initial free volume in the fuel UP. The gap pressure trend highlighted negligible differences, on the contrary the timing of cladding failure was affected: as low is the initial free volume, as bigger is the time of failure, up to the non-failure (Fig. D. 4).
- Filling gas pressure. The gap pressure at time of failure increases with its initial value. On the contrary, the time of failure decreases (Fig. D. 5).
- Cladding temperature. Higher cladding temperature corresponds to higher initial gas pressure and then to lower time to failure. Lower temperature exhibits non-failure. The predicted gap pressure at time of cladding failure seems not be influenced changing the cladding temperature.
- Model options. The model options that highlighted the larger influences on the time of failure and the outer cladding radius at burst are (Fig. D. 6):
    - option for mechanical analysis;
    - creep anisotropy coefficients non-LOCA specific;
    - different models for the relocation;
    - static model instead of dynamic for the α to β-phase transition. In the hypothetical case of the disabling of the failure model, the use of the static approach brings to the highest value of the calculated strain.

Finally, the following considerations are derived from the probabilistic analysis.

- The failures are predicted by plastic instability, only. The ranges of time of failures are between 62 and 68 s in the experiments, and between 50 and 75 in TU probabilistic analysis (Fig. D. 7).
- Representing the results as a normal distribution, the spread of the data related to the time of failure is not very large, and the mean may be considered as representative of the values experimental value.

D.5.3 Results of the analysis MT-6A

The LOCA transient for the test MT-6A starts with the fuel at steady state conditions, and at decay heat. The rods were tested at zero burnup, therefore as-built dimensions are assumed to apply (i.e. no fuel densification/swelling, no cladding creep-down), Fig. D. 8, Fig. D. 9 and Fig. D. 10.

The average cladding temperature is about 408 °C, ΔT in the cladding is about 40 °C. The initial condition of the MT-6A transient is flowing steam with the transient beginning when the steam is shut-off and a stagnant condition introduced. Reflood is initiated 70 seconds (60 s after steam-off). The cladding temperature is prescribed in the calculations. The steam shut-off occurs at 10 s from the beginning of the transient and causes the cladding heat-up. The PCT of 952.8 °C is exhibited between 100 and 110 s after the BOT at 276.86 cm from the bottom. The corresponding axial position in TU model is the slice number 6. The transient is terminated at 160s. The system coolant pressure falls at 1.72 MPa instead of 0.28 MPa as foreseen.

Sensitivity analyses were performed, addressing the boundary and initial conditions and the model options.

- Initial free volume in the UP. The gap pressure trend highlighted negligible differences, on the contrary the timing of cladding failure was affected: as low is the initial free volume, as bigger is the time of failure, up to the non-failure. Due to different failure modes, the MT-6A case exhibits high-pressure failures caused by plastic instability and low-pressure failures due to overstrain (Fig. D. 11).
- Filling gas pressure. The gap pressure at time of failure increases with its initial value. On the contrary, the time of failure decreases. At low initial gap pressure the overstrain is the dominant failure mechanism (plastic instability in all the other cases),Fig. D. 12.
- Cladding temperature. Higher temperature corresponds to higher initial gas pressure and then to lower time to failure. Lower temperature exhibits non-failure. The predicted pressure at failure seems not be influenced by the variation of the BIC on cladding temperature.
- Model options. The model options that highlighted the larger influences on the time of failure and the outer cladding radius at burst are (Fig. D. 13):
    - option for mechanical analysis;
    - creep anisotropy coefficients non-LOCA specific;
    - different models for the relocation.

The following considerations are derived from the probabilistic analysis (Fig. D. 14) *(Lassmann 1980, Reventos 2008)*.

- The failures are caused by plastic instability and overstrain. The ranges of time of failures are between 68 and 74 s for the experimental case, and between 40 and 80 in the case of failure for plastic instability and between 80 and 100 for failures due to overstrain.
- The spread of the data in this case is very large, considering both cause of failure. The data together (i.e. plastic instability and overstrain failures) cannot be represented by a normal distribution.
- The mean can be considered representative only for the cases in which the failures are caused by overstrain. On the contrary, the times of failures due to overstrain are out of the range of the failures experiences in the test.

D.6 Conclusions

The capability of TRANSURANUS code version “v1m1j09” in predicting the fuel and cladding behavior under LOCA conditions is assessed using the experimental database based of MT-4 and MT-6A rods. The MT-4 and MT-6A tests address the behavior of two equivalent full lengths, 3% enriched 17X17 PWR fuel rods with the aim of studying the cladding ballooning and rupture during heat-up of LOCA. All tests used PWR-type, non-irradiated fuel rods.

MT-4 and MT-6A databases are suitable for validating fuel pin mechanic codes, thus enlarging validation domain to DBA conditions and improving the level of understanding of the code capabilities and limitations.

The following approach is pursued for the analysis:

1. set-up, run and analysis of the reference input deck;
2. execution of sensitivity analyses on the basis of the reference results;
3. execution of the probabilistic analyses;
4. comparison of the results of the reference calculation to the experimental data when available.

The results of the deterministic calculations demonstrate the capability of TU code in predicting the cladding failure and time of failure occurrence during LOCA scenario, before the reflood occurrence, as highlighted in Tab. D. 1. The correct prediction of the evolution of the decreasing pressure after onset of ballooning until rupture suggests the correctness of the ballooning size prediction for both cases analyzed. In any case, this phenomenon can only be partially addressed by a 1½-D code..

The comparisons with the permanent tangential strain, measured in MT-4 test, show an under-prediction of the code in all cases except when the failure criteria are disabled and the static model for the α to β-phase transition is used No precise measurement of the cladding strain is available for the MT-6A. However, the information based on the visual inspection suggests TU code under-predicts the experimental trend.

The fuel centerline temperature measured in the MT-4 test is well calculated by TU code. Minor differences at the end of the transient may be explained with the minor differences in predicting the time of failure.

The sensitivity analyses evidences that the major differences from the reference case for the time of failure and the outer cladding radius at burst, notwithstanding the variations of the results with the variations of the BIC, are experienced by:

- option for the mechanical analysis;
- creep anisotropy coefficients non-LOCA specific;
- different models for the relocation.

The results of the probabilistic analysis show a small spread of results related to the time of failure in the case of MT-4, in which the only cause of failure is plastic instability. Larger spread is calculated for the MT-6A case, in which the failures are due to plastic instability and overstrain.

Finally, we should conclude also that, the effect of burnup is not accounted in the analysis, thus the experimental database is representative of fresh fuel. Therefore, the prediction of relevant parameters should be tested at higher and more representative burnup values.

The probabilistic analysis is performed selecting the time of failure as variable of interest. However, this does not have any objective connected with the quantification of the uncertainty. Indeed, the selection of the sources of uncertainty has not been quantified rigorously.

D.6.1 Results significant for the code assessment

The results of the deterministic calculations demonstrate the capability of TU code in predicting the cladding failure and time of failure occurrence during LOCA scenario, before the reflood occurrence. The correct prediction of the evolution of the decreasing pressure after onset of ballooning until rupture suggests the correctness of the ballooning size prediction for both cases analyzed. In any case, this phenomenon can only be partially addressed by a 1½-D code.

The comparisons with the permanent tangential strain, measured in MT-4 test, show a under-prediction of the code in all the cases except when the failure criteria are disabled and the static model for the α to β-phase transition is used. No precise measurement of the cladding strain is available for the MT-6A. However, the information based on the visual inspection suggests TU code under-predicts the experimental trend.

The fuel centerline temperature measured in the MT-4 test is well calculated by TU code. Minor differences at the end of the transient may be explained with the minor differences in predicting the time of failure.

The sensitivity analyses evidences that the major differences from the reference case for the time of failure and the outer cladding radius at burst and are experienced by:

- mechanical analysis: IBMECH=2 instead of 0;
- creep anisotropy coefficients non-LOCA specific: ModCladJ1=0 instead of 18;
- different models for the relocation.

The results of the probabilistic analysis show a small spread of results related to the time of failure in the case of MT-4, in which the only cause of failure is plastic instability. Large spread is calculated for the MT-6A case, in which the failures are due to plastic instability and overstrain.

D.6.1.1 Author recommendations

The subroutine PINPRS that calculates the UP temperature is not suitable for predicting the gap pressure trend during LOCA transient: the UP temperature should be prescribed in the input deck.

The validation activity pointed out the limitations of the code in relation with the ballooning perdition during LOCA analysis. Due to intrinsic limitations of the code, the simulation of the ballooning occurring when the cladding reaches high temperature (>800 °C) should be performed by means of switching off the failure model.

D.6.1.2 Limitations of the study

The effect of burnup is not accounted in the analysis, thus the experimental database is representative of fresh fuel. Therefore, the prediction of relevant parameters should be tested at higher and more representative burnup values.

The probabilistic analysis is performed selecting the time of failure as variable of interest. However, this does not have any objective connected with the quantification of the uncertainty. Indeed, the selections of the sources of uncertainty have not been quantified rigorously.

D.6.1.3 Additional significant study findings

The use of a static α-β phase transition model, together with the hypothesis of non-failure brings to the higher prediction of the strain that in the MT4 simulation resulted representative of the experimental data.

Additional information can be found in (*Adorni 2010, Adorni 2011*).

Parameters for validation		
Item	**Experiment MT-4/MT-6A**	**TU simulation MT-4/MT-6A**
Burnup	**--/--**	**--/--**
Failure / Non-Failure	**●/●**	**P/P**
Pressure trend during the test	**●/●**	**Q/P**
Time of failure	**●/●**	**Q/P**
Ballooning	**●/○**	**Q/Q%**
Gas flow	**--/--**	**N/N**
Cladding strain	**●/○**	**Q/Q%**
Geometry changes	**●/○**	**Q/Q%**
Coolability	**●/○**	**N/N**
Embrittlement	**--/--**	**--/--**
α to β-phase transformation	**○/○**	**Q/Q**
Oxidation	**○/○**	**Q/Q**
Fuel fragmentation and relocation	**--/--**	**--/--**
Fuel centerline temperature	**●/--**	**P/--**
● Suitable for code assessment ○ Limited suitability -- Not suitable	**P** Predictable by the code **Q** Qualitatively predictable **N** Not predictable -- Not addressed	
* One average fuel rod for each test % Partially predictable by 1½-D code X Addressed in the validation process		

Tab. D. 1 – Validation domain.

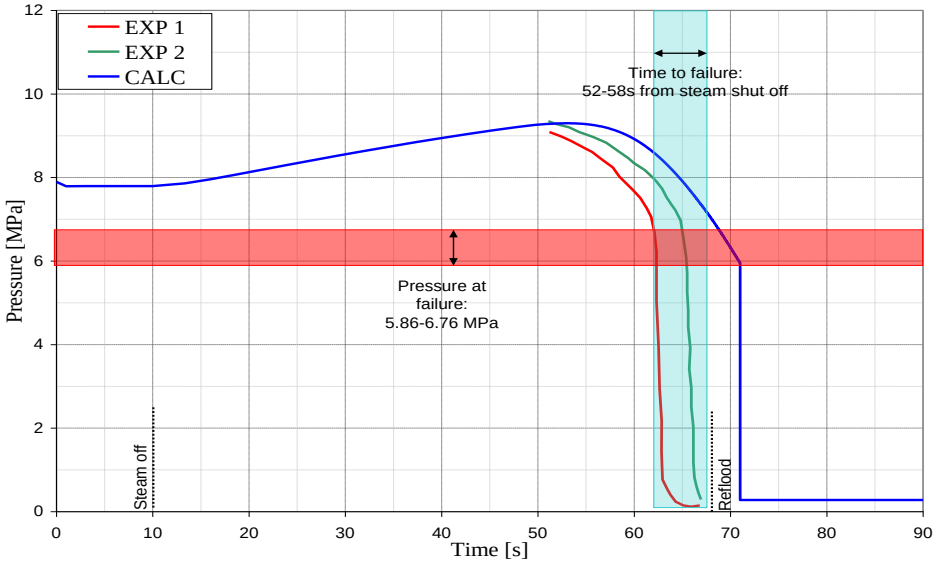

Fig. D. 1 – MT-4: Fuel internal pressure as function of time: measured and calculated.

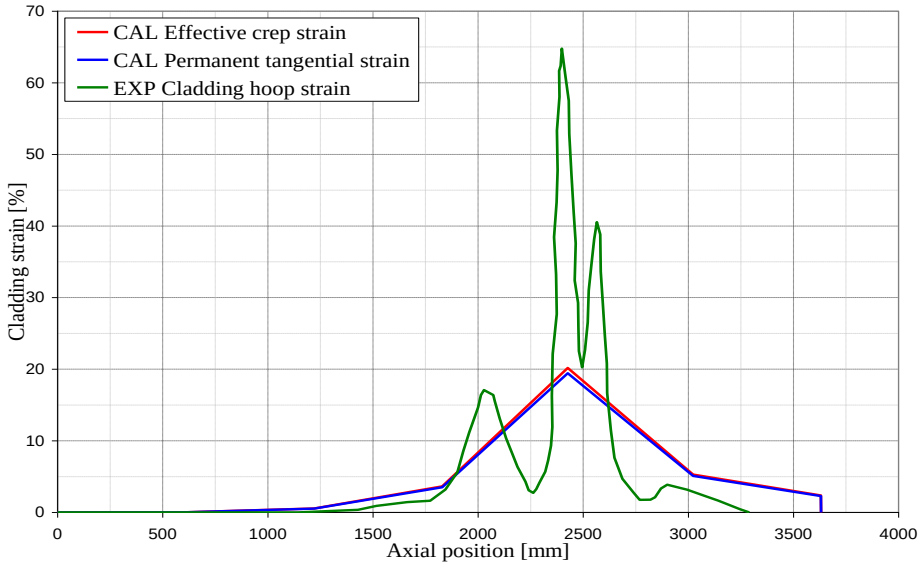

Fig. D. 2 – MT-4: Effective creep and permanent tangential strains calculated at end of irradiation.

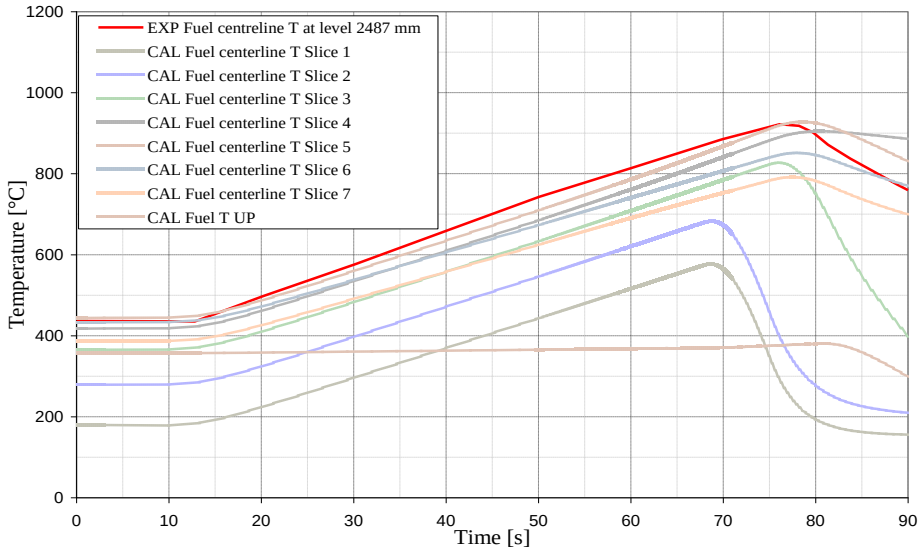

Fig. D. 3 – MT-4: Fuel central temperature as function of time, different axial positions.

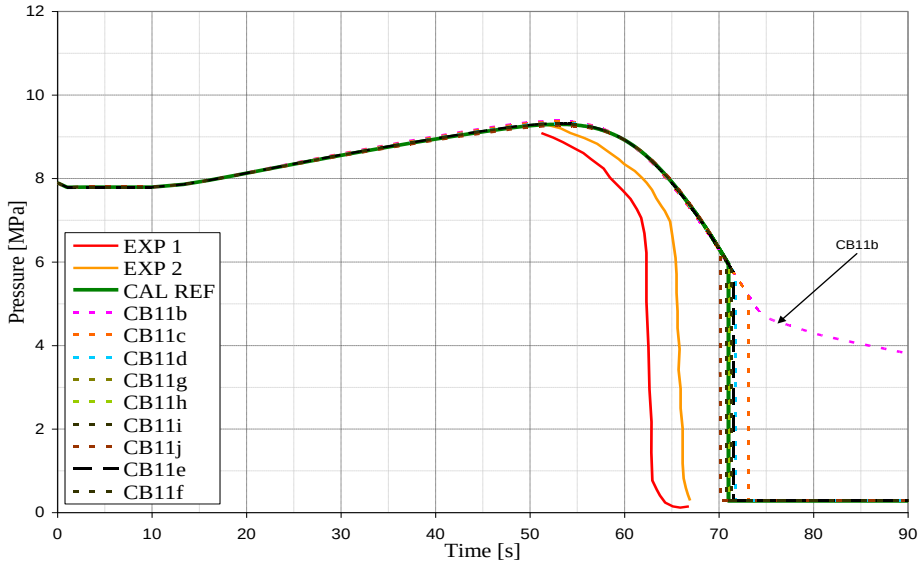

Fig. D. 4 – MT-4: Initial free volume in the fuel UP sensitivities: fuel internal pressure as function of time, measured and calculated.

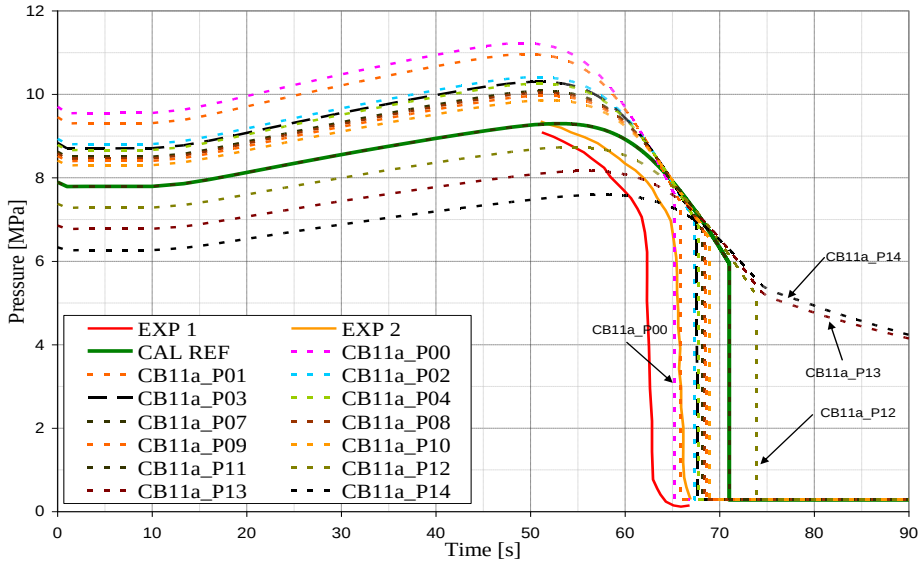

Fig. D. 5 – MT-4: Fill gas pressure sensitivities: fuel internal pressure as function of time, measured and calculated.

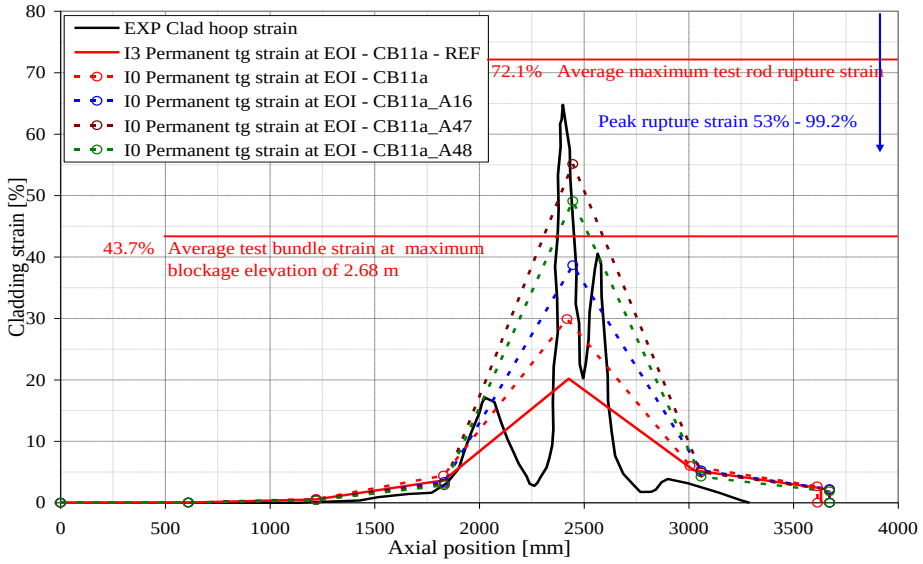

Fig. D. 6 – MT-4: Model option sensitivities: summary of measured and calculated permanent tangential strains at time of burst.

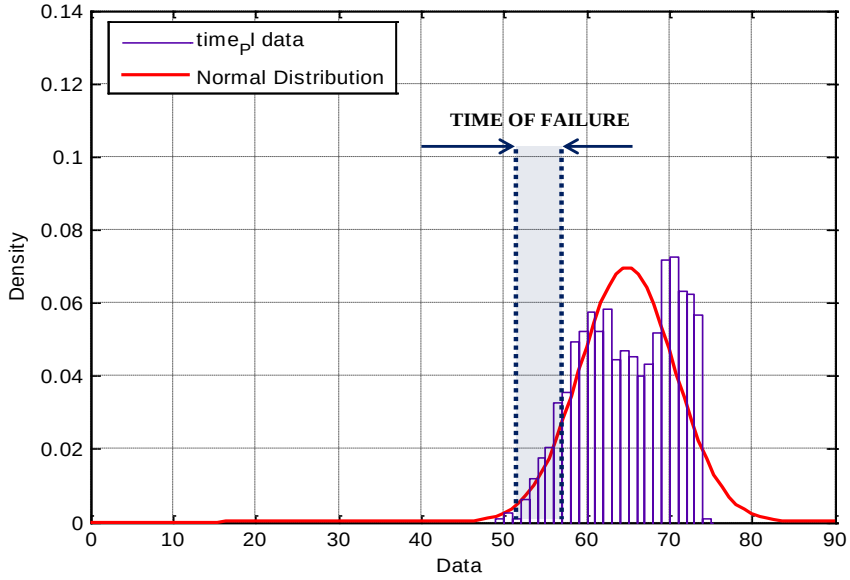

Fig. D. 7 – MT-4:Probability distribution of the time of failure for plastic instability.

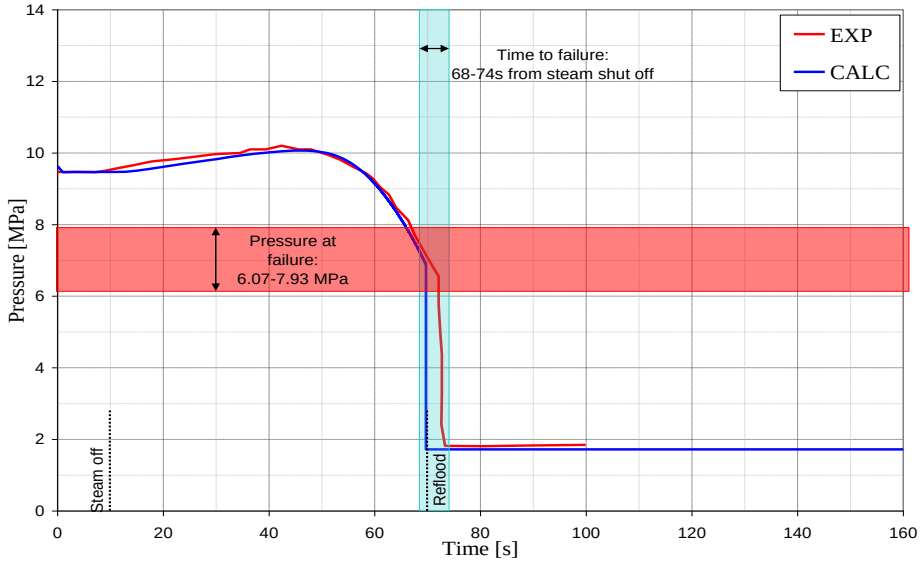

Fig. D. 8 – MT-6A: Fuel internal pressure as function of time: measured and calculated.

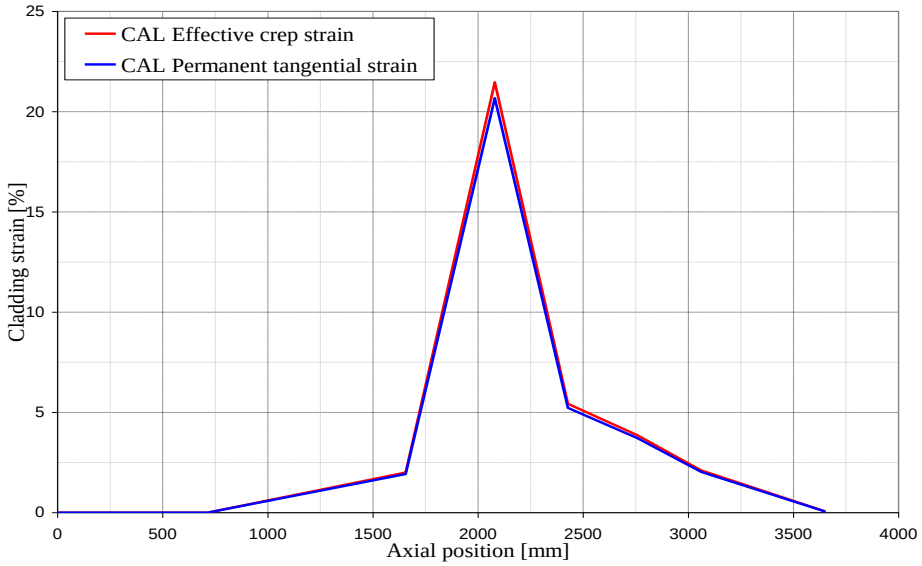

Fig. D. 9 – MT-6A: Effective creep and permanent tangential strains at end of irradiation.

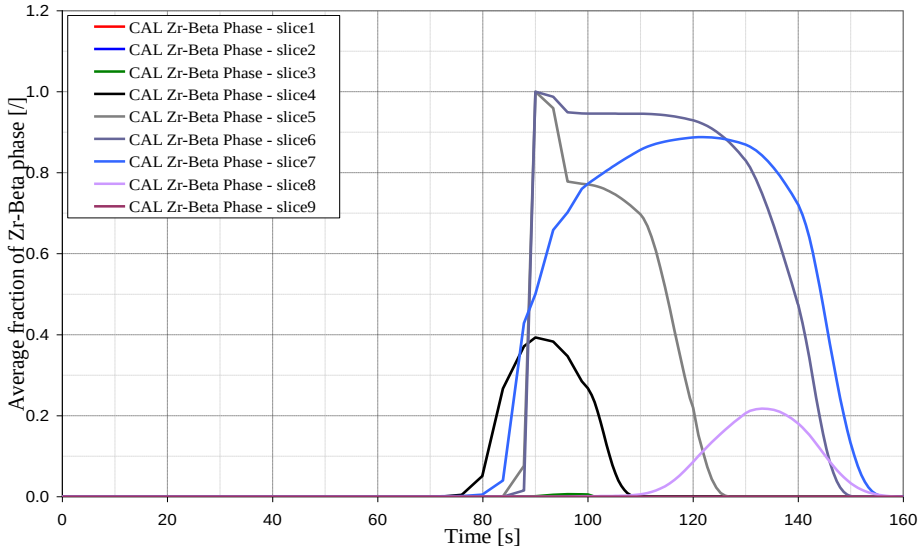

Fig. D. 10 – MT-6A: Zr beta phase as function of time, all axial elevations.

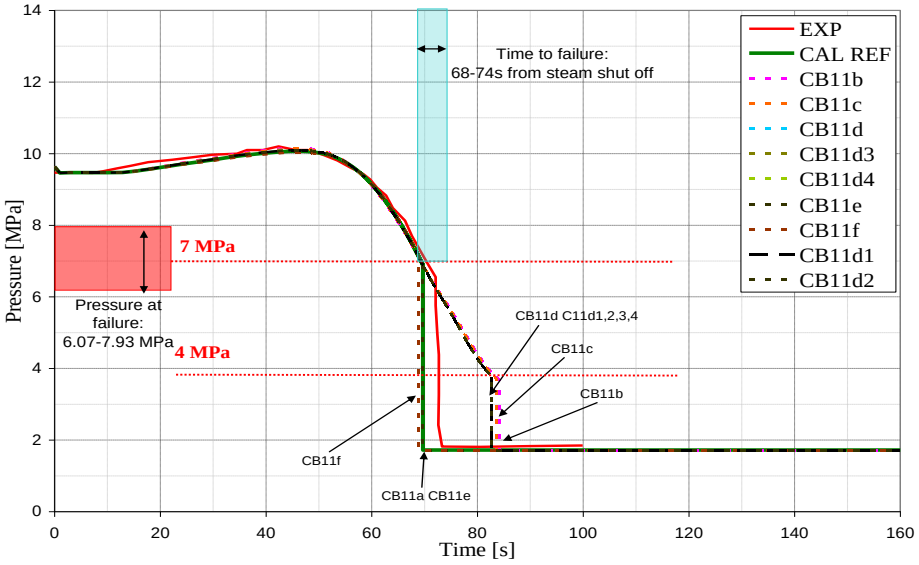

Fig. D. 11 – MT-6A: Initial free volume in the fuel UP sensitivities: fuel internal pressure as function of time, measured and calculated.

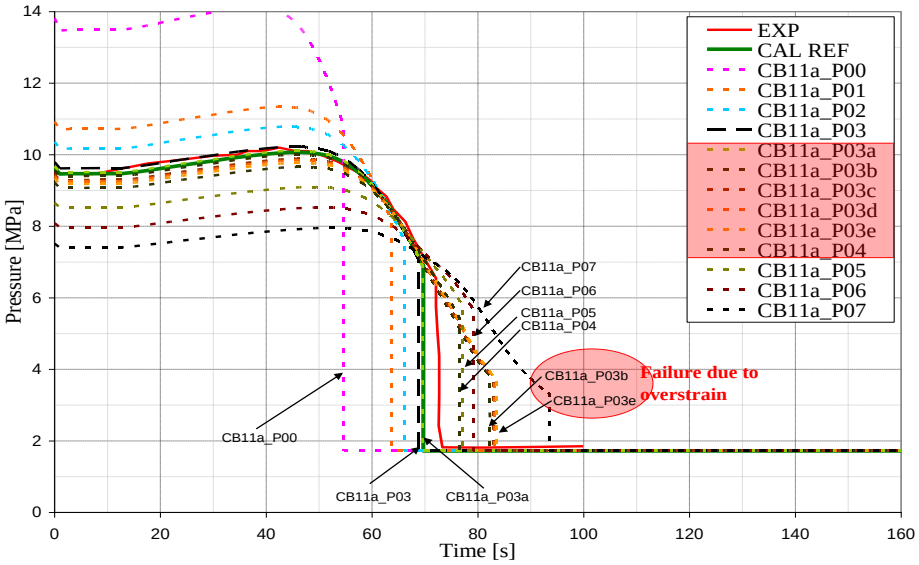

Fig. D. 12 – MT-6A: Fill gas pressure sensitivities: fuel internal pressure as function of time, measured and calculated.

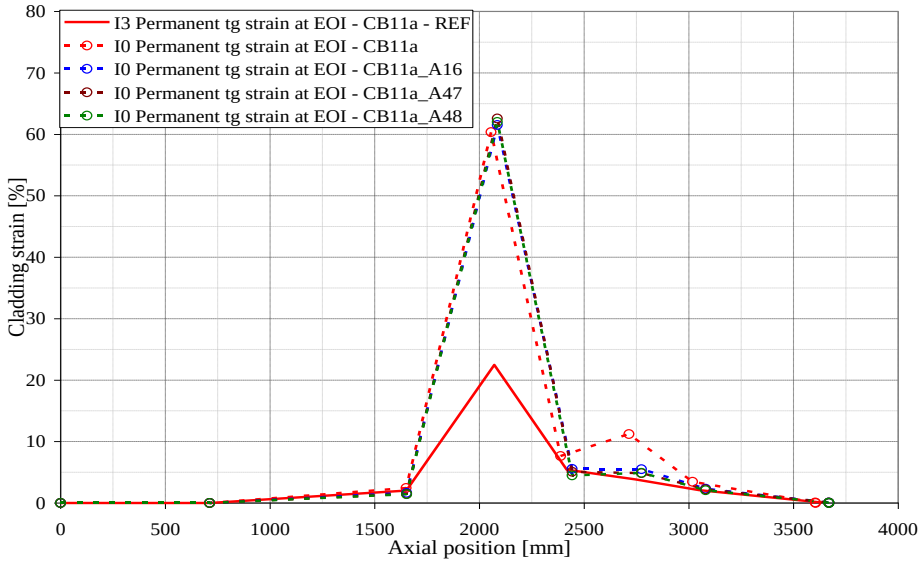

Fig. D. 13 – MT-6A: Summary permanent tangential strains at time of burst.

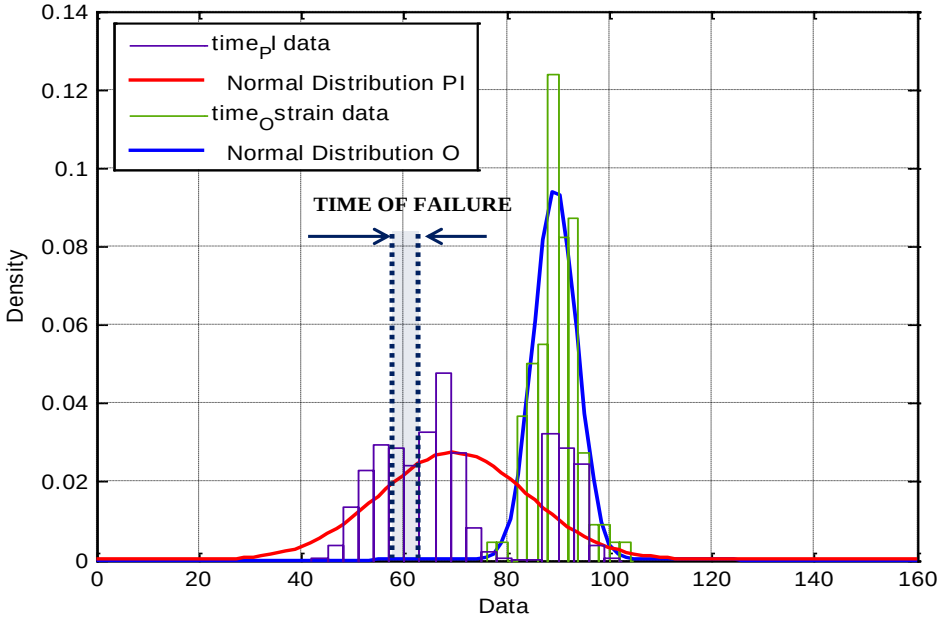

Fig. D. 14 – MT-6A:Probability distribution of the time of failure for plastic instability.

APPENDIX E. NON STANDARD APPLICATION OF TU CODE: FK-1 CASE

The present activity is focused on the behavior of the fuel rod, with the aim of studying the behavior of the fuel during RIA.

The analyses performed address the behavior of three BWR fuel rods. The rods FK-1, FK-2 and FK-3 were refabricated from irradiated segment fuel rods of BWR 8x8BJ (STEP I) design. The segments were irradiated to an assembly average burn-up of 30.4 MWd/kgU in Fukushima Daiichi Nuclear Power Station Unit 3. An irradiation history is available for each test section from the IFPE database,. (*Fuketa October 2000, Fuketa Aprol 2000, Nakamura 2002, Nakamura 2000*).

After the experiments, the test train was dismantled and several post irradiation examinations were performed The experimental data are used for assessing the TU capabilities in predicting phenomena related to RIA. Focus is given on the capabilities and limitations of the different model options available in the code and on the selection and interpretation of the boundary conditions. For a better understanding of the uncertainties involved and their technological consequences, the analysis is completed with the probabilistic calculations.

E.1.1 Objective of the activity

The objective of the activity is the validation of TRANSURANUS “v1m1j09” code in predicting fuel and cladding behavior under RIA conditions using the experimental databases FK-1, FK-2 and FK-3. It is pursued assessing the capabilities of the code models in simulating the phenomena and parameters involved, such as: pressure trend in the fuel rod, cladding creep, and geometry changes, (*Fuketa October 2000, Fuketa Aprol 2000, Nakamura 2002, Nakamura 2000*). The analysis is aimed at having a comprehensive understanding of the applicability and limitations of the code in the in the conditions of the experiments.

In addition, the code simulations are also used in order to improve the understanding of the phenomena involved in the experiments and on the boundary conditions, as well as for checking or completing the documentation and data provided within the OECD/NEA IFPE FK-1, -2, and -3 database. The objective of the activity is fulfilled developing three reference input decks, one for each experiment, suitable for the assessment of TU code versions “v1m1j09”.

The failure issue and the related calculation of the failure threshold it is out of the aim of the current analysis, due to the fact that no rods failed in the experiment here addressed.

E.2 Description of the experiments

Boiling water reactor (BWR) fuel rods with bumps of 41 to 45 GWd/tU were pulse-irradiated in the Nuclear Safety Research Reactor (NSRR) to investigate the fuel

behaviour during a reactivity initiated accident (RIA) at cold startup. BWR fuel segment rods of 8x8BJ (STEP I) type from the Fukushima Daiichi Nuclear Power Station Unit 3 were refabricated into short test rods, and they were subjected to prompt enthalpy insertion from 293 to 607 J/g (70 to 145 cal/g) within about 20 ms. The fuel cladding had enough ductility against the prompt deformation due to pellet cladding mechanical interaction. The plastic hoop strain reached 1.5% at the peak location. The cladding surface temperature locally reached about 600 °C. Recovery of irradiation defects in the cladding due to high temperature during the pulse irradiation was indicated via X-ray diffractometry. The amount of fission gas released during the pulse irradiation was from 3.1% to 8.2% of total inventory, depending on the peak fuel enthalpy and the normal operation conditions (*Fuketa 1997, Sugiyama 2004*).

E.2.1 Test fuel rods

The rods FK-1, FK-2 and FK-3 were refabricated from irradiated segment fuel rods of BWR 8x8BJ (STEP I) design. The segments were irradiated to an assembly average burn-up of 30.4 MWd/kgU in Fukushima Daiichi Nuclear Power Station Unit 3. Fig. E. 1 from (*Fuketa 1997*) shows a schematic diagram of the test rods and the location of the test sections as taken from the mother rod.

Fig. E. 2 from (*Fuketa 1997*) shows the base irradiation power history of the mother assembly in the commercial BWR. An irradiation history is available for each rod from IFPE database.

Before refabricating, the whole fuel rod was examined by:

- Visual observation.
- X-radiography.
- Eddy current testing.
- Dimensional measurements.
- oxide thickness measurement.
- Gamma scanning.
- Fission gas sampling.

Each test was conducted on sections of fuel stack ~106 mm long, chosen to have a flat axial burn-up profile. An iron core was placed in the top end fitting to measure fuel stack elongation and an internal pressure sensor was built into the bottom fitting. Hafnium disks were placed at both ends of the fuel column to prevent power peaking and the rods sealed with 0.3 MPa helium gas corresponding to the original filling conditions. Prior to the test, each rod was subjected to the following examination:

- Helium leak test.
- Visual observation.
- X-raydiography.
- Eddy current testing.
- Dimensional measurement.

- weight measurement.
- Gamma scanning.

Two sheathed thermocouples were attached to each sample and mounted 10 mm distant from the cladding to measure coolant temperature. Three small diameter thermocouples (0.2 mm) were spot welded to the outside cladding of FK-1 and FK-3 to measure clad temperatures.

E.3 Pulse irradiation in NSRR

The pulse irradiation of FK-1, FK-2 and FK-3 were carried out on 21 November 1996, 7 February 1997 and 18 March 1998 respectively. Power for the three tests are shown in Fig. E. 2 (a). The origin of the horizontal axis is the time of a "fire signal" for extracting control rods. The reactor power arose at about 0.20 s for FK-1 and -3, and about 0.22 s for FK-2. The pulse widths (full width at half maximum) are 4.4 ms for FK-l and -3, and 6.7 ms for FK-2.

The relationship between reactor power and rod power was evaluated by the SRAC/SWAT code system, in which a "coupling factor", i.e. fission number per unit fuel mass and unit reactor power, was derived. The values are $1.96X10^{11}$fissions/g/MJ for FK-1 and -2, and 2.23~1011 Fissions/g/MJ for FK-3. These values were confirmed to be reasonable by gamma-ray spectroscopy on pulsed fuel pellet samples prepared by the method described in (*Fuketa 1997*) for the tests FK1 and FK-3. The histories of rod linear heat rate derived from the reactor power histories and the coupling factors are shown in Fig. E. 2 (b). The peak of linear heat rate for FK-3 is higher than that for FK-1 despite the similar reactor power, because the rod FK-3 has lower burnup and thus more residual fissile materials than FK-1. The peak fuel enthalpies were evaluated to be 544, 293 and 607 J/g (130, 70 and 145 Cal/g) for the tests FK-1, -2 and -3, respectively.

A summary of the test conditions can be found in Tab. E. 1.

E.3.1 Post test PIE

After testing each rod was subjected to the following examination:

- Visual observation
- X-radiography
- Eddy current test
- Dimensional measurement
- Gamma spectrometry
- Rod puncture and gas analysis
- Fuel dissolution to determine energy deposition; FK-1 and FK-2 only.
- Immersion density determination
- Metalography
- Clad hardness measurement
- SEM and EPMA examination
- TEM of one sample from the periphery of a pellet from FK-1.
- X-ray diffractometry.

E.4 Main outcomes of the test

The main outcomes are listed below:

- The plastic deformation mainly due to the post-DNB deformation was observed in the tests FK-1 and -3 with peak fuel enthalpies of 544 and 604 J/g, respectively. These enthalpies were relatively high compared to the previous NSRR tests with irradiated rods, but the claddings had enough ductility against the PCMI and subsequent post-DNB deformation.
- The measurements of the cladding temperature transient and metallurgical examinations indicated that the peak cladding temperatures were considerably different depending on the axial and circumferential positions.
- The lattice constant measurement showed that the cladding temperatures during the pulse irradiation reached high enough levels for the recovery of irradiation defects.
- The amount of fission gas released during the pulse irradiation was correlated with the peak fuel enthalpy and that during the normal operation. The FP gas analysis and pellet EPMA indicated that the FP gas was released uniformly across the whole pellet or mainly from the center region of the pellet.

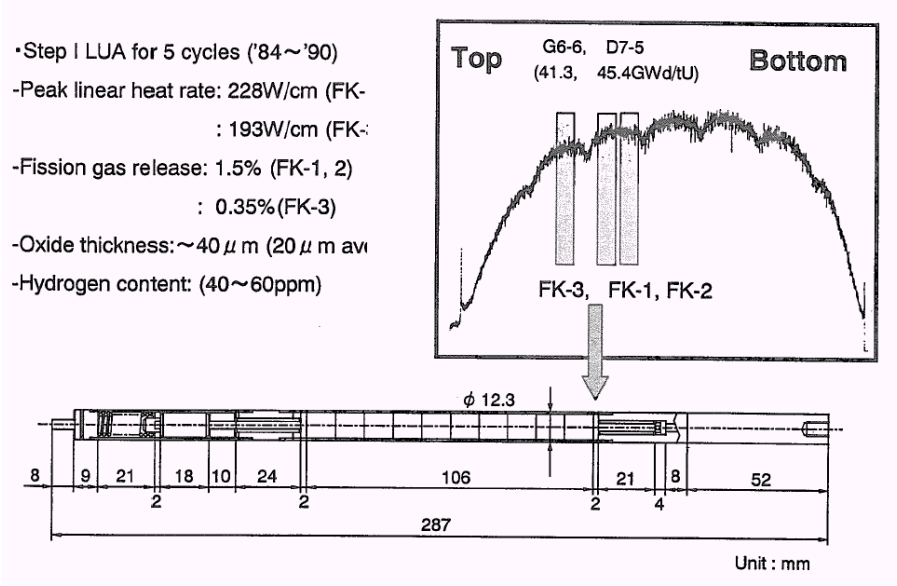

Fig. E. 1 – Configuration of test sections and their relation to the mother rod.

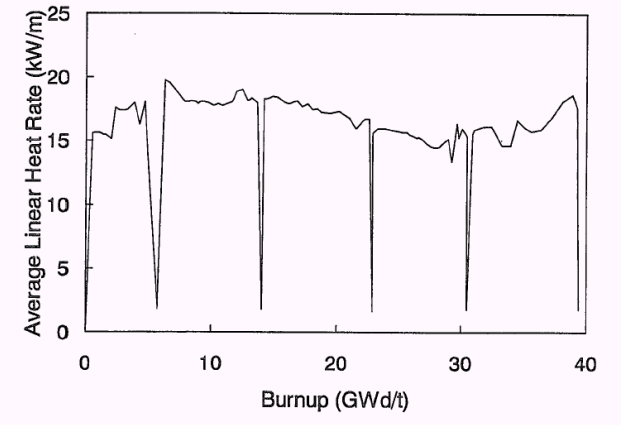

Fig. E. 2 – Base irradiation history for segmented fuel rod used to provide RIA test section.

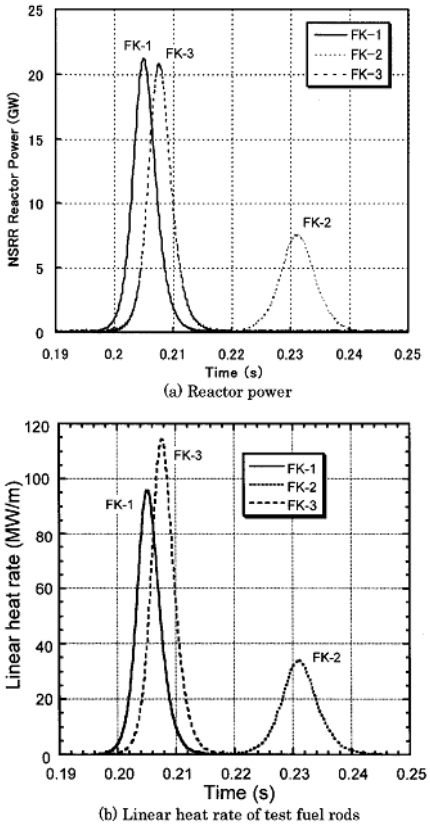

Fig. 16 Histories of reactor power and corresponding linear heat rate.

Fig. E. 3 – Power histories (Fuketa 1997).

Test ID		FK-1	FK-2	FK-3
Time and date of irradiation		15:18 Nov. 21, 1996	15:18 Feb. 7, 1997	14:38 Mar. 18, 1998
Capsule type		X-1V (double sealed)		
Initial coolant temperature		room temperature		
Initial capsule internal pressure		atmospheric		
Coolant flow rate		stagnant		
Inserted reactivity ($)	nominal	4.6	3.2	4.6
	bank [a]	4.52	3.14	4.50
Integrated reactor power within 1 s (#1 / #2) (MJ)		112.3 / 110.0 Ave. 111.2	62.3 / 62.0 Ave. 62.2	110 / 108.5 Ave. 109.3
Peak fuel enthalpy [b]	(cal/g)	130	70	145
	(J/g)	544	293	607

[a] Evaluated from the curve of regulation rod worth (bank operation).

[b] Expected from the measured integrated reactor power and the coupling factor which was estimated from fuel rod burnup and the NSRR core neutron calculations with SRAC/SWAT code system.

Tab. E. 1 – Pulse irradiation conditions.

E.4.1 TRANSURANUS models and cases analyzed

The restart optiond descrive in section 5.4.2 is used for the current analysis.

The activity is performed using TRANSURANUS code, version “v1m1j09”, with the deterministic and probabilistic options, thermal and mechanical analysis. The version of the manual is “v1m1j09”.

A conditioning irradiation is performed, up to the desired burnup. Then, the RIA transient starts.

The reference input deck for FK-1 test is prepared complying with the information available in the code manual (*Lassmann 2009*). The models selected are generally the ones standard. Only the active part of the fuel is accounted for the simulation. It is divided into 3 or five axial sections of different length, according to the experimental data available. For all the calculations, the nominal geometrical values are used when available, since tolerances are not specified.

The input deck of FK-2 and FK-3 rod differs from the FK-1 one for the boundary conditions of cladding temperatures and coolant pressure. The case FK-2 differ from the others also because the option for the determination of the heat transfer coefficient between fuel rod and coolant (IAPLHA=0 instead of 2).

All the BIC are prepared automatically though the preparation of ad-hoc programs. The complete list is reported in Tab. E. 2. The coolant temperature and linear heat rate for each test is reported from Fig. E. 4 to Fig. E. 9. The comparison with the data available from the IFPE database is reported as well.

The boundary conditions used for the analysis are:

- linear heat rate;
- fast flux;

- cladding temperature (except the case FK-2 in which coolant temperature is prescribed, together a zero mass flow);
- outer coolant pressure.

E.4.2 Selection of the cases to be analyzed

The set of calculations used for the analysis is described in this section. Only case F-1 is analyzed. A base irradiation calculation is preformed to condition the fuel before the test.

Sensitivity analyses are performed in order to address the influence of the options available in TU or to tests different interpretations of the boundary conditions on code results. The impact of selected parameters and/or code options on the results and the limits of the models implemented in the code are investigated. The analyses is subdivided in sensitivities for al the tests on model options, more detail can be found in (*Adorni 305/2010*). Probabilistic analyses are finally performed to complete the set of calculations. 50 runs are performed for each rod, using the boundary conditions reported in (*Adorni 305/2010*).

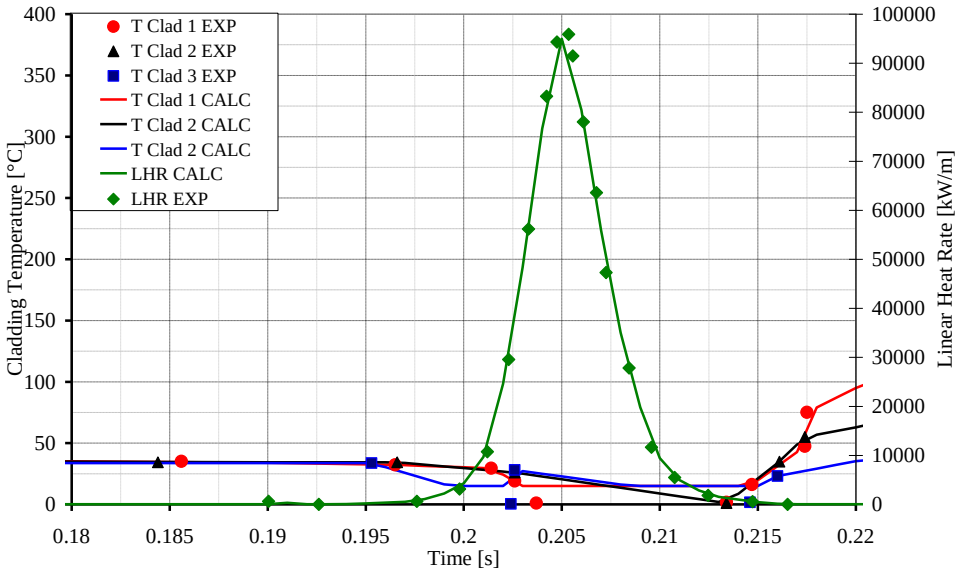

Fig. E. 4 – FK-1: Coolant temperature and linear heat rate, zoom on the power peak.

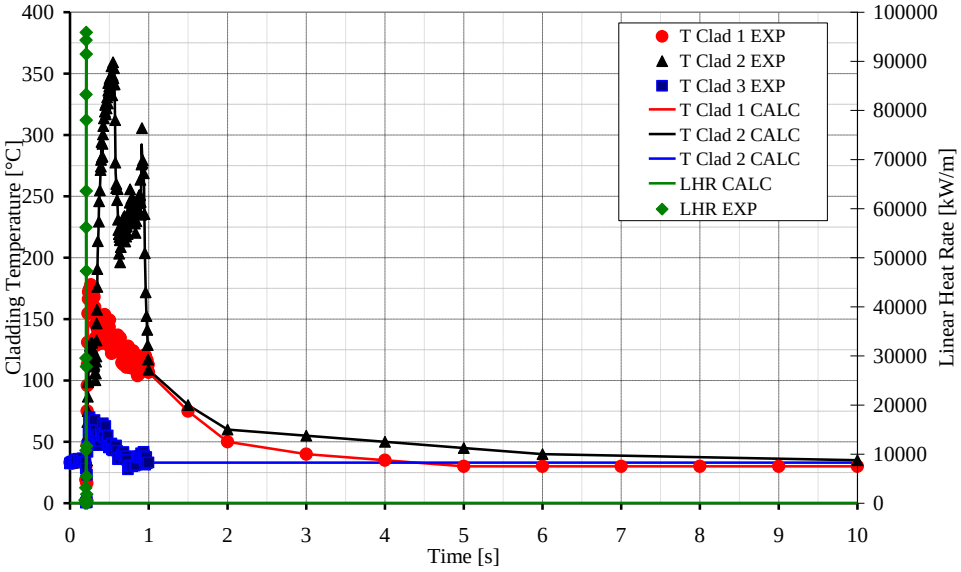

Fig. E. 5 – FK-2: Coolant temperature and linear heat rate, all the transient.

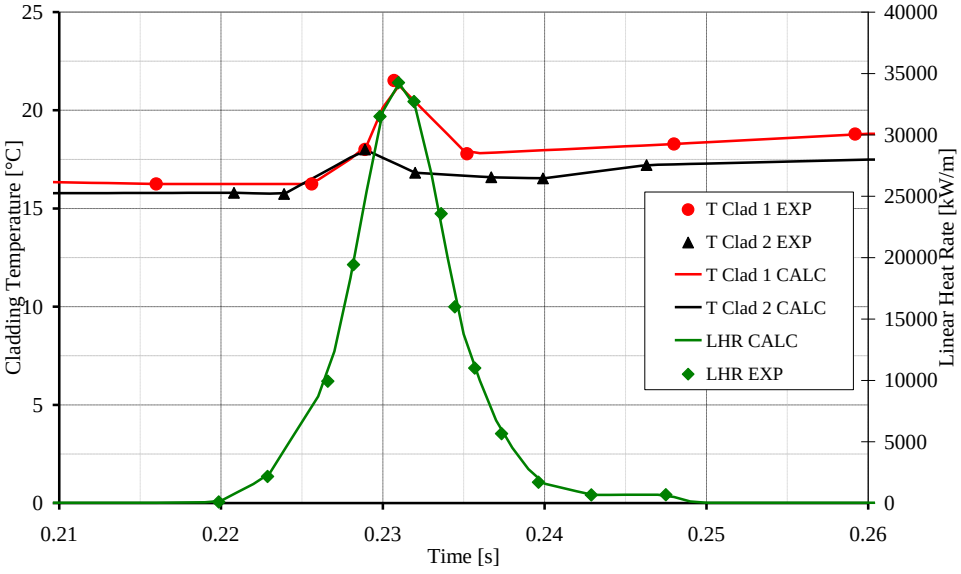

Fig. E. 6 – FK-2: Coolant temperature and linear heat rate, zoom on the power peak.

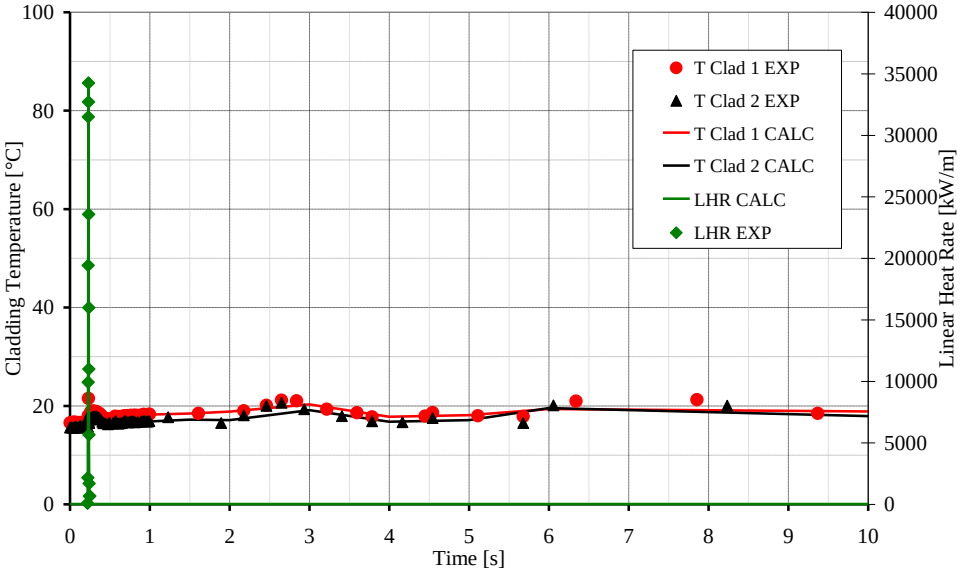

Fig. E. 7 – FK-2: Coolant temperature and linear heat rate, all the transient.

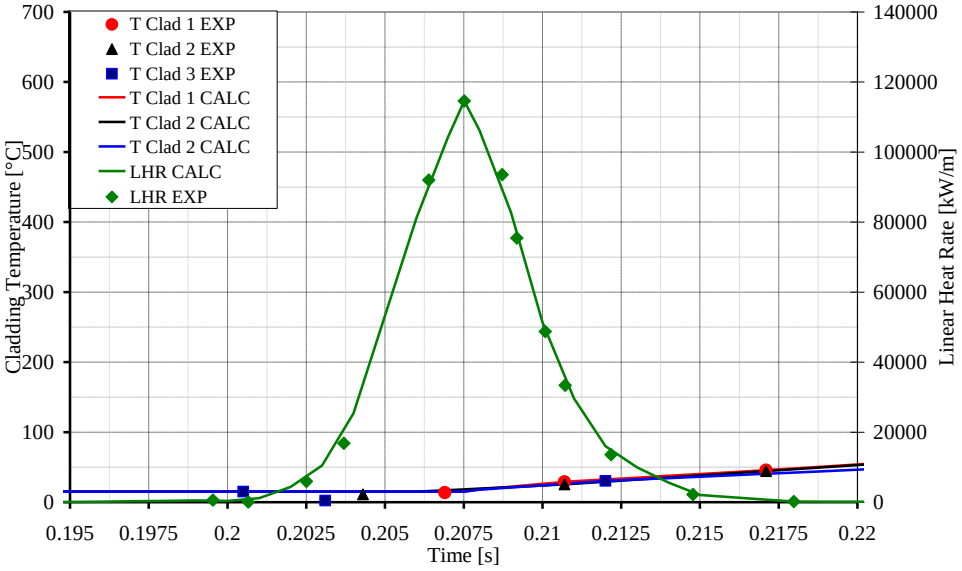

Fig. E. 8 – FK-3: Coolant temperature and linear heat rate, zoom on the power peak.

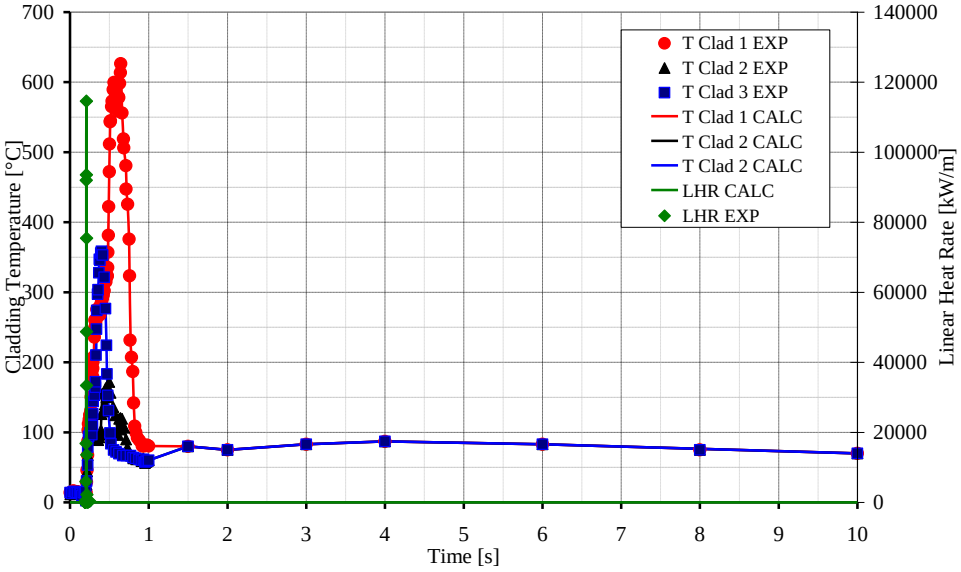

Fig. E. 9 – FK-3: Coolant temperature and linear heat rate, all the transient.

#	Program ID	D/P	Input file needed	Output/Note
1	Int_LHR_r0.m	D	FKX_LHR_Trans.txt	FKX_LHR_Trans_rev1.txt BIC_FKX.xls
2	Int_TCLAD_r0.m	D	FKX_TCLAD_Trans1.txt	FKX_TCLAD_Trans1_rev1.txt FKX_TCLAD_Trans1_rev2.txt FKX_TCLAD_Trans1_rev3.txt BIC_FKX.xls
3	MAIN_BIC_r0.m	D	FK-1_BIC_all_OK.txt	MACRO_trans.txt (BIC of TU)
4	run_FIG_r7d.m	D		Post-processing for the reference case
5	ENTHALPHY_DIFF_r1.m	D		Calculation of the enthalpy increase during RIA
6	run_REF_r4a.m	S	Channel_List.inp	
7	FAIL_MT_r0c.m	S	Channel_List.inp	Failure_list.dat
8	MAX_ALL_r0.m	S	Channel_List.inp	ZZZ_MAX_ALL.dat
9	FAIL_MT_r1b.m	P	standard.out	Failure_list.dat
10	Time_r0.m	P		

D Deterministic calculation
P Probabilistic calculation
S Sensitivity analysis

Tab. E. 2 – M-Programs developed to run the calculations and prepare the figures.

E.5 Results of FK-1 case

Relevant figures are reported from Fig. E. 10 to Fig. E. 17.

Measurements of the burnup were available at the end of the base irradiation. The predictions are very similar, that suggests the correctness of the linear heat rate boundary conditions for the base irradiations.

The pressure in the gap reported in Fig. E. 10. It should be noted that the modification of the restart option is evident here: the inner pin pressure is changed, as well as the gap con position, at the beginning of the transient. The reference case is identified by IDEN2.

Changes during RIA transient are evidenced by the cladding outer radius, Fig. E. 11. The maximum fuel temperature is exhibited at the time of the power peak, Fig. E. 12 and correspond also with the calculated maximum enthalpy value, Fig. E. 17.

The fission gas release calculated at the end of the base irradiation fits very well with the measured data, Fig. E. 13. Major differences are evidenced at the end of the transient. The comparison with the measured pellet stack and cladding elongation evidences a systematic under prediction, Fig. E. 14 and Fig. E. 15respectively. Finally, comparison with measured and calculated fuel radii, Fig. E. 16 evidences a good prediction.

E.5.1 Consideration on Fission Gas Release for the Restart Case

The issue fission gas release (FGR) needs special attention. FGR is defined as the fraction of released gas to the theoretically produced amount of fission gas. The produced amount is irradiation dependent, calculated directly from the actual burnup and constitutes therefore no problem by a restart. However, the released amount, together with the fill gas, i.e. the gas content in rod free volume (plenum, gap, open porosity), could be removed or changed by the restart operation. The question is now how TRANSURANUS considers the “artificial” removal of already released gas. It was confirmed that the amount of fission gases (e.g. Xe and Kr), released during the base run of TRANSURANUS, is stored and added to the amount of gas released after the restart (second run). The integral results in the “overview output”, commonly called OUTP22, related to fission gas, i.e.:

- Fission gas production (cm**3)”
- Fission gas release (cm**3)”
- Fission gas release (%)”

are therefore correct without any further adjustment. On the contrary, all numbers related to single gases (He, Xe, Kr etc.) in the detailed printout file, commonly called OUTP21, are reflecting the real gas content at every moment of the calculation. They must therefore, in order to suit with the FGR numbers by any detailed gas content analysis, be adjusted with the corresponding modifications of gas content, GASTOT(m,1), made by the restart with the RSTRTM.FOR file.

E.6 Conclusions

The capability of TRANSURANUS code version “v1m1j09” in predicting the fuel and cladding behavior under RIA conditions is assessed using the experimental database based of FK-1. The tests address the behavior of three refabricated rods, with the aim of studying the cladding behavior during RIA. FK-1, FK-2 and FK-3 databases are suitable the validation of fuel pin mechanic codes, thus enlarging validation domain to accident conditions and improving the level of understanding of the code capabilities and limitations.

The approach to the analysis was performed in this way for each test:

1. set-up and run of the reference input deck;
2. execution of sensitivity analyses;
3. execution of the probabilistic analyses;
4. comparison of the results of the reference calculation to the experimental data when available; and

More benchmarking would be required to assure the reliability of the capability of the code in simulating RIA accidents, also analyzing databases in which the fuel rods fail. This would help the development of a failure limit for the RIA analysis.

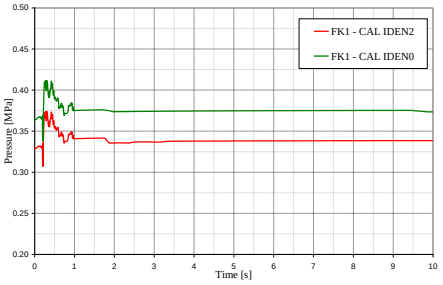

Fig. E. 10 – Calculated fuel pin pressure for two different code options.

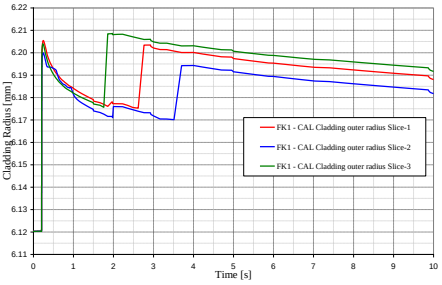

Fig. E. 11 – Calculated cladding outer radius for different axial positions.

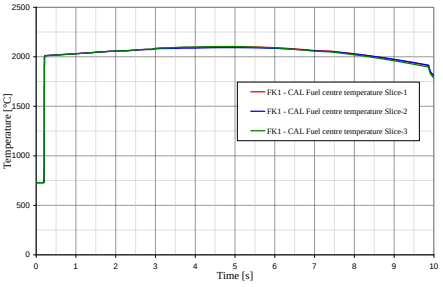

Fig. E. 12 – Calculated fuel centre temperature for different axial positions.

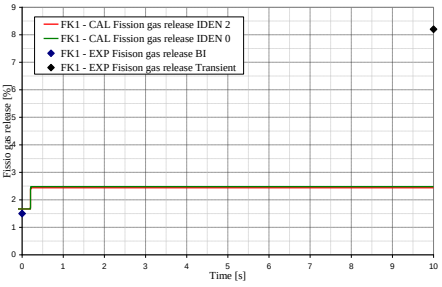

Fig. E. 13 – Calculated and measured fission gas release.

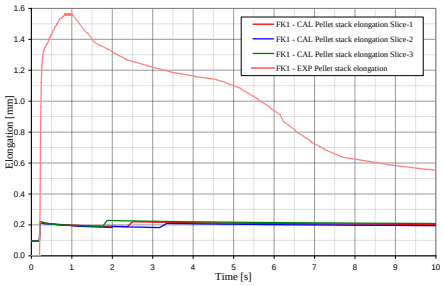

Fig. E. 14 – Calculated and measured pellet stack elongation.

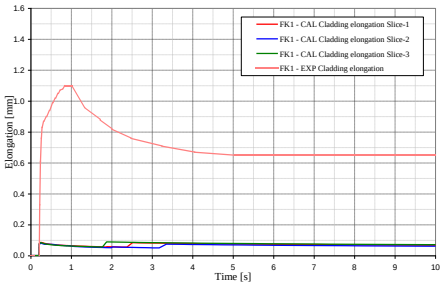

Fig. E. 15 – Calculated and measured cladding elongation.

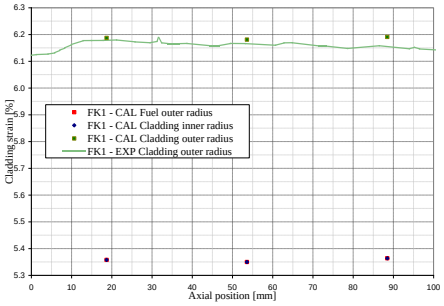

Fig. E. 16 – Calculated and measured cladding outer radius, and calculated fuel outer radius and cladding inner radius.

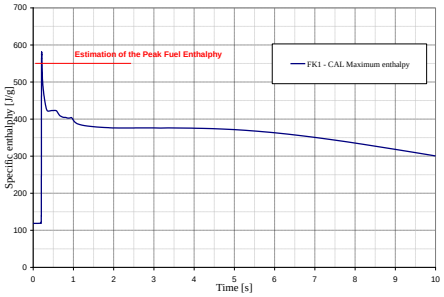

Fig. E. 17 – Calculated and estimate peak fuel enthalpy.

APPENDIX F. SUMMARY OF VALIDATION ACTIVITIES

The current section contains the summary table of the validation activities based on the data gathered from the IFPE database.

VALIDATION DOMAIN							
Main phenomenon	**Experiment**	**No. rods**	**Thermal modules**	**Mechanical modules**	**FGR modules**	**Burn-up modules**	**Validation documentation**
PCI/SCC	*CNEA MOX Experiments*	*5*	*X*	*X*	*X*	*X*	*FUEL/FUMEX-III/03(10)*

Range (parameters) of validity			Parameters for validation		
Parameter	**Unit**	**Values/ Descript.**	**#**	**CNEA MOX EXP**	**TU simulation**
Pellet material	--	**$U,Pu)O_2$**	*Burn-up*	●	X
Cladding material	--	**Zr-4**	*Cladding creep*	○	X
Enrichment	%	**1.25**	*Cladding expansion in ramp*	○	X
Pellet density	%	**95**	*Grain size after ramp (pellet centre)*	●	X
Pellet outer diameter	mm	**10.4**	*Gap final dimensions*	●	X
Diametric gap size	µm	**1300**	*Ridges height (avg. and max) after ramp*	●	--$
Clad outer diameter	mm	**12.9**	*Failure / Not Failure*	●	X
Active length	mm	**179-224**	● suitable for code assessment ○ limited suitability – not suitable		
Initial grain size	µm	**6.2**	**#**	**BACO simulation**	**TU simulation**
He filling pressure	MPa	**0.1**	*Fuel centerline max temperature*	■	X
Average burn-up	MW_d/kg_U	**0-15**	*FGR*	■	X
Operative pressure	MPa	**14.5**	*Cladding final radius*	■	X
Average LHR3 (BI)	kW/m	**23-28**	*Fuel final radius*	□	X
Average NFF4 (BI)	10^{15} n/cm^2s	**1**	*Fuel max enthalpy*	■	X
Ramp rate	kW/mh	**50-90**	■ suitable for code to code comparison ◘ limited suitability for code to code comparison □ not suitable for code to code comparison		
Ramp Terminal Level	kW/m	**39-45**			
LHR change	kW/m	**39-45**			
Holding time at RTL5	hrs	**0.3-6**			

1 BI: Base Irradiation
2 AR: After Ramp
3 LHR: Linear Heat Rate
4 NFF: Neutron Fast Flux (>1 MeV)
5 RTL: Ramp Terminal Level
$ Not predictable by 1½D code

Tab. F. 1 – CNEA MOX Experiments from (Rozzia 2010).

VALIDATION DOMAIN

Code version: TRANSURANUS v1m1j09

Main phenomenon	Experiment	No. rods	Thermal modules	Mechanical modules	FGR modules	Burn-up modules	Reference
PCI/SCC	*BWR Inter-Ramp*	*20*	*X*	*X*	*X*	*X*	*FUEL/FUMEX-III/02(10)*

Range (parameters) of validity			Parameters for validation		
Parameter	**Unit**	**Values/ Descript.**	**#**	**BWR IR EXP**	**TU simulation**
Pellet material	--	**UO_2**	*Burnup*	●	X
Cladding material	--	**Zr-2**	*Cladding creep down in two types of measures BI*[1]	●	X
Enrichment	%	**2.8-3.5**	*Cladding expansion in ramp (two types of measures)*	●	X
Pellet density	%	**93-95**	*Cladding corrosion after ramp*	○	X
Pellet outer diameter	mm	**10.4-10.5**	*Grain size after ramp (pellet centre)*	○	X
Diameter gap size	µm	**80-250**	*FGR after ramp*	●	X
Clad outer diameter	mm	**12.52**	*Elongation after BI and ramp in two axial positions for active length and rod*	○	X
Active length	mm	**403**	*Ridges height (avg. and max) in BI*	●	--$
Grain initial size (MIL)	µm	**8.3-10.9**	*Ridges height (avg. and max) after ramp*	●	--$
He filling pressure	MPa	**0.1**	*Clad ovality max BI and after ramp*	●	--$
Average burnup	MW_d/kg_U	**10-20**	*Active fuel weight change after BI and ramp*	●	X
Operative pressure	MPa	**7.2**	*Inner cladding oxidation after ramp*	○	--
Average LHR3 (BI)	kW/m	**26.5-35.5**	*Failure / Not Failure*	●	X
Average NFF4 (BI)	10^{13} n/cm^2s	**4-8**	*Iodine burst test (cracks dimension and stresses)*	○	--$
Ramp rate	kW/mh	**230-325**	● suitable for code assessment ○ limited suitability – not suitable		
Ramp Terminal Level	kW/m	**41-65.5**			
LHR change	kW/m	**10-30**			
Holding time at RTL5	hrs	**0.08-24**			

1 BI: Base Irradiation
2 AR: After Ramp
3 LHR: Linear Heat Rate
4 NFF: Neutron Fast Flux (>1 MeV)
5 RTL: Ramp Terminal Level
$ Not predictable by 1½D cod
e

Tab. F. 2 – BWR Inter-Ramp from (*Rozzia 2010*).

VALIDATION DOMAIN							
Main phenomenon	**Experiment**	**No. rods**	**Thermal modules**	**Mechanical modules**	**FGR modules**	**Burn-up modules**	**Validation documentation**
PCI/SCC	*PWR Super-Ramp*	*28*	*X*	*X*	*X*	*X*	*FUEL/FUMEX-III/01(10)*

Range (parameters) of validity		
Parameter	**Unit**	**Values/ Descript.**
Pellet material	--	**UO_2**
Cladding material	--	**Zr-2**
Enrichment	%	**3.19-8.26**
Gd content	%wt	**0-4**
Pellet outer diameter	mm	**8.19-9.14**
Diametric gap size	µm	**142-200**
Clad outer diameter	mm	**9.50-10.76**
Active length	mm	**311-977**
Initial grain size	µm	**5.5-22.0**
He filling pressure	MPa	**13.8-22.5**
Average burn-up	MW_d/kg_U	**28-45**
Operative pressure	MPa	**14-14.5**
Average LHR3 (BI)	kW/m	**14-23**
Average NFF4 (BI)	10^{13} n/cm^2s	**3.12-8.30**
Ramp rate	kW/mh	**360-660**
Ramp Terminal Level	kW/m	**35-50.5**
LHR change	kW/m	**10-25.5**
Holding time at RTL5	hrs	**0.02-12**

Parameters for validation		
#	**PWR SR EXP**	**TU simulation**
Burnup	●	X
Cladding max creep down in BI[1]	●	X
Cladding expansion in ramp (two types of measures)	●	X
Cladding corrosion after ramp	●	X
Grain size after ramp (pellet centre/pheriphery)	●	X
FGR after ramp	●	X
Elongation after ramp	○	X
Ridges height (avg. and max) in BI	●	--$
Ridges height (avg. and max) after ramp	●	--$
Clad ovality after ramp	●	--$
Inner cladding oxidation after ramp	●	--
Failure / Not Failure	●	X

● suitable for code assessment
○ limited suitability
– not suitable

1 BI: Base Irradiation
2 AR: After Ramp
3 LHR: Linear Heat Rate
4 NFF: Neutron Fast Flux (>1 MeV)
5 RTL: Ramp Terminal Level
$ Not predictable by 1½D code (outside TU code capabilities)

Tab. F. 3 – PWR Super-Ramp from (*Rozzia 2010*).

VALIDATION DOMAIN							
Main phenomenon	**Experiment**	**No. rods**	**Thermal modules**	**Mechanical modules**	**FGR modules**	**Burn-up modules**	**Validation documentation**
PCI/SCC	*BWR Super-Ramp*	*16*	*X*	*X*	*X*	*X*	*FUEL/FUMEX-III/04(10)*

Range (parameters) of validity			**Parameters for validation**		
Parameter	**Unit**	**Values/ Descript.**	**#**	**BWR SR EXP**	**TU simulation**
Pellet material	--	**UO_2**	*Burnup*	●	X
Cladding material	--	**Zr-2**	*Cladding dimensional change in BI*[1]	○	X
Enrichment	%	**2.84-3.02**	*Cladding expansion in ramp (two types of measures)*	●	X
			Cladding corrosion after ramp	●	X
Pellet outer diameter	mm	**10.6-10.9**	*Grain size after ramp (pellet centre/pheriphery)*	●	X
Diametral gap size	µm	**67-115**	*FGR after ramp*	●	X
Clad outer diameter	mm	**12.52-12.55**	*Elongation after ramp*	○	X
Active length	mm	**314-753**	*Ridges height (avg. and max) in BI*	●	--[$]
Grain size (initial diameter)	µm	**7.6-18.0**	*Ridges height (avg. and max) after ramp*	●	--[$]
He filling pressure	MPa	**0.1-0.12**	*Clad ovality after ramp*	●	--[$]
Average burnup	MW_d/kg_U	**27-38**	*Inner cladding oxidation after ramp*	●	--
Operative pressure	MPa	**7.2**	*Failure / Not Failure*	●	X
Average LHR3 (BI)	kW/m	**10-21**			
Average NFF4 (BI)	10^{13} n/cm^{2}s	**2.4 -6.8**			
Ramp rate	kW/mh	**540-600 0.198-0.336**	● suitable for code assessment ○ limited suitability ─ not suitable		
Ramp Terminal Level	kW/m	**30-44**			
LHR change	kW/m	**7-20**			
Holding time at RTL5	hrs	**0.0-24**			

1 BI: Base Irradiation
2 AR: After Ramp
3 LHR: Linear Heat Rate
4 NFF: Neutron Fast Flux (>1 MeV)
5 RTL: Ramp Terminal Level
$ Not predictable by 1½D code

Tab. F. 4 – BWR Super-Ramp from (*Rozzia 2010*).

VALIDATION DOMAIN							
Code version: TRANSURANUS v1m1j09							
Main phenomenon	**Experiment**	**No. rods**	**Thermal modules**	**Mechanical modules**	**FGR modules**	**Burn-up modules**	**Reference**
Ballooning	*MT-4 / MT-6A*	*2**	*X*	*X*			*FUEL/ITU312 63/01(10)*

Range (parameters) of validity		
Parameter	**Unit**	**Values/ Descript.**
Pellet material	--	**UO_2**
Cladding material	--	**Zr-4**
Enrichment	%	**2.93**
Pellet density	%TD	**95**
Pellet outer diameter	mm	**8.41**
Diameter gap size	µm	**150**
Clad outer diameter	mm	**9.63**
Active length	mm	**3660**
Grain pellet initial diameter	µm	**10**
He filling pressure	MPa	**4.62/6.03**
Average burnup	MW_d/kg_U	**0**
Operative pressure	MPa	**0.28 / 1.72**
Average LHR	kW/m	**1.2 kW/m**
Average NFF	10^{12} n/cm^2 s	**2**
PCT	°C	**875.6/898.9**
Time of PCT	s	**74/100-110**
Cladding max heatup rate	°C/s	**7.5/8.3**
Failure	--	**Y**
End of transient	s	**90/160**

Parameters for validation		
#	**MT-4/MT-6A**	**TU simulation**
Burnup	**--/--**	**--/--**
Failure / Non-Failure	**●/●**	**P/P**
Pressure trend during the test	**●/●**	**Q/P**
Time of failure	**●/●**	**Q/P**
Ballooning	**●/○**	**Q/Q%**
Gas flow	**--/--**	**N/N**
Cladding strain	**●/○**	**Q/Q%**
Geometry changes	**●/○**	**Q/Q%**
Coolability	**●/○**	**N/N**
Embrittlement	**--/--**	**--/--**
α to β-phase transformation	**○/○**	**Q/Q**
Oxidation	**○/○**	**Q/Q**
Fuel fragmentation and relocation	**--/--**	**--/--**
Fuel centerline temperature	**●/--**	**P/--**

● Suitable for code assessment
○ Limited suitability
-- Not suitable

P Predictable by the code
Q Qualitatively predictable
N Not predictable
-- Not addressed

* One average fuel rod for each test
% Partially predictable by 1½-D code
X Addressed in the validation process

Tab. F. 5 – MT-4 and MT-6A from (*Adorni 2010*).